

# **BIOMECHANICS OF THE LIGAMENTOUS STRUCTURES OF THE HUMAN FOOT**

by

**ANDREW W. DONN, MEng**

This thesis is submitted as partial fulfilment of the requirements for the degree of  
**Doctor of Philosophy** in the Bioengineering Unit.

**Bioengineering Unit  
University of Strathclyde  
Glasgow  
UK**

**March 1997**

**The copyright of this thesis belongs to the author under the terms of the United Kingdom Copyright Acts as qualified by the University of Strathclyde Regulation 3.49. Due acknowledgement must always be made of use of any material contained in, or derived from, this thesis.**

## ABSTRACT

The work reported in this thesis was carried out to investigate the mechanisms of ligamentous action in the human foot during the functions of standing and walking.

A comprehensive literature review of the relevant subject areas was presented and a need for further work demonstrated.

Ligament strain patterns in cadaveric feet were measured for a number of foot positions and static and dynamic loading patterns, including simulations of standing and gait. Levels of functional strain have been established for each ligament and it has been shown that the plantar ligaments of the tarsus are especially sensitive to the motions of inversion and eversion. Maximum strain levels were witnessed during the toe-off phase of the gait cycle where values of approximately 4 times those seen during standing were found. The action of the extrinsic musculature was able to supplement passive support mechanisms by reducing strain in the subject ligaments.

Uniaxial tension testing of isolated preparations of the subject ligaments was then carried out utilising measurements of local strain. In addition to providing a record of the load-deformation responses of the tissues tested, these experiments allowed derivation of a range of functional force estimates for intact normal feet. Stress-strain relationships were also derived and these were compared to contemporary models of ligament mechanics. Functional values of stress were also reported.

A mathematical model representing the foot during stance was developed. Force-deformation data and measured anatomical data provided the necessary information to solve the model for the stance condition. The effect of simulated ligament rupture through injury and the effects of surgical ligament release on the strain and force patterns of the unaffected ligament structures were identified.

The results of this investigation served as a record of the quantitative biomechanics of the ligaments in the human foot.

## ACKNOWLEDGEMENTS

The author would like to thank the following people who assisted in the work presented in this thesis:

- Dr A.C. Nicol for supervising the project and for providing much useful advice, enthusiasm and guidance.
- Professor J.P. Paul for additional guidance in the practical work and preparation of the text of the thesis.
- Professor J.C. Barbenel for advice on the protocols and interpretation of the results of the isolated ligament tests.
- D. Robb, J. McLean, D. Smith, W. Tierney, I. Tullis and R. Hay for construction of the experimental apparatus and assistance in developing the testing programmes.
- Dr. J. Shaw-Dunn for the use of the dissection facilities at Glasgow University Department of Anatomy and for his enthusiasm and interest in bioengineering.
- Dr. R. Reid and P. Kerr of the Department of Pathology at the Western Infirmary for the use of their X-ray facilities.
- D. Rand for help in debugging the model code.

I would like to make a special thank you to M. Butterfield for her unfaltering support and encouragement to me throughout the course of this investigation. Without her support, and typing skills, the completion of this work would have been infinitely more difficult.

Financial support for this investigation was provided by the Medical Research Council.

# CONTENTS

	Page
Title	i
Abstract	iii
Acknowledgements	iv
Abbreviations	viii
<b>CHAPTER 1 Introduction</b>	<b>1</b>
<b>CHAPTER 2 Basic functional anatomy of the foot</b>	
2.1 Introduction	4
2.2 Positions and motions	4
2.3 Bones and joints	5
2.4 Ligaments	8
2.5 Muscles	11
<b>CHAPTER 3 Review of the relevant literature</b>	
3.1 Introduction	14
3.2 Theories of foot function and experimental structural analysis	14
3.3 Experimental analysis of the biomechanics of ligaments	24
3.4 Mathematical modelling of the foot	36
5.5 Clinical disorders	43
5.6 Summary	44

## **CHAPTER 4 Mechanical testing of intact cadaveric feet**

4.1	Introduction	45
4.2	Material	45
4.3	Methods	46
4.4	Results	59
4.5	Discussion	62

## **CHAPTER 5 Mechanical testing of excised ligament specimens**

5.1	Introduction	69
5.2	Material	69
5.3	Methods	69
5.4	Results	76
5.5	Discussion	83

## **CHAPTER 6 Mathematical modelling of the foot**

6.1	Introduction	91
6.2	Model description	91
6.3	Results	101
6.4	Discussion	109

## **CHAPTER 7 Discussion and conclusions**

7.1	Introduction	116
7.2	Discussion	117
7.3	Conclusions	123
7.4	Recommendations for future work	126

<b>References</b>	129
-------------------	-----

## **Appendices**

<b>Appendix 1:</b>	<b>Transducer calibrations</b>	<b>143</b>
<b>Appendix 2:</b>	<b>LMSG performance assessment</b>	<b>145</b>
<b>Appendix 3:</b>	<b>LMSG placement parameters</b>	<b>150</b>
<b>Appendix 4:</b>	<b>Ligament strain data for intact foot tests</b>	<b>154</b>
<b>Appendix 5:</b>	<b>Stress-strain and load-strain relationships in the foot ligaments</b>	<b>169</b>
<b>Appendix 6:</b>	<b>Functional forces in the foot ligaments</b>	<b>179</b>
<b>Appendix 7:</b>	<b>Functional stresses in the foot ligaments</b>	<b>184</b>
<b>Appendix 8:</b>	<b>Isolated ligament test specimen dimensions</b>	<b>189</b>
<b>Appendix 9:</b>	<b>Anatomical input data for the foot model</b>	<b>192</b>
<b>Appendix 10:</b>	<b>Model program code</b>	<b>195</b>
<b>Appendix 11:</b>	<b>Ligament forces and strains predicted by mathematical modelling</b>	<b>209</b>

## ABBREVIATIONS

2D	Two-dimensional
3D	Three-dimensional
ACL	Anterior cruciate ligament
AH	Adductor hallucis
ATFL	Anterior talofibular ligament
BW	Body weight
CNL	Calcaneonavicular ligament
DF	Dorsiflexion
DFD	Dominant fibre direction
DIP	Distal interphalangeal joint
DOF	Degrees of freedom
EHL	Extensor hallucis longus
EMG	Electromyography
FDB	Flexor digitorum brevis
FDL	Flexor digitorum longus
FE	Finite element
FHL	Flexor hallucis longus
ICNL	Inferior calcaneonavicular ligament
IMT	Intermetatarsal joint
LMSG	Liquid metal strain gauge
LPL	Long plantar ligament
MET	Metatarsal
MIIL	Mean inter-insertion line
MTP	Metatarsophalangeal joint
PA	Plantar aponeurosis
PF	Plantar flexion
PIP	Proximal interphalangeal joint
PL	Peroneus longus
QLV	Quasi-linear viscoelasticity
RSA	Roentgenstereophotogrammetry

SPL	Short plantar ligament
TA	Tibialis anterior
TACH	Tendo Achilles
TC	Talocrural joint
TCN	Talocalcaneonavicular joint
TMT	Tarsometatarsal joint
TP	Tibialis posterior
TT	Transtarsal joint

## CHAPTER 1. INTRODUCTION

The foot is a highly complex structure composed of twenty six bones, over fifty ligaments, twelve extrinsic and eighteen intrinsic muscles (some of which have multiple insertions and tendons and cross several joints). As suggested by its intrinsic anatomy the function of the foot is highly specialised. It forms the primary interface between the body and the ground in locomotion, providing efficient and adaptable support allowing us to stand, walk, jump, run and cope with all manner of surface terrain.

Foot pathologies are both common in occurrence and varied in nature. Some of the more frequently encountered disorders include hallux valgus and rigidus, congenital malformations, e.g., talipes equinovarus (clubfoot), sports injuries, trauma, plantar fasciitis and static deformities such as flat feet. Treatment of the above conditions with surgery has its problems. There is often a long and painful rehabilitation period associated with many procedures. For some pathologies there exists a large number of different corrective procedures, perhaps indicating the lack of superiority of any of them. For example, in the treatment of hallux valgus many different types of osteotomy are used, and this is in addition to the types of arthroplasty techniques which are almost as numerous. More conservative management of foot disorders involving orthotics, physiotherapy and podiatry is often utilised for less serious complaints. The high incidence of foot disorders in the population is of significant clinical importance. Improvements in treatment would be of great benefit not only to patients but to the NHS who incur large costs in the provision of surgery, orthoses and rehabilitation services.

The mechanisms of load support in the foot have been the subject of investigation for many years. A central debate throughout this research has been the relative importance of the muscles and ligaments to the maintenance, or support, of the normal arched structure of the foot. Jones (1949), by performing experiments on cadaver feet and palpation of muscles in living subjects, concluded that there was limited or no muscle activity when standing statically and that the extrinsic muscles alone were not capable of restoring collapsed arches. He further concluded that the primary agents of arch support were the plantar ligaments and the short plantar muscles (long intrinsic) also contributed to arch support since they were mechanically better positioned to do so than the extrinsic musculature. Using electromyography (EMG)

Basmajian and Stecko (1963) investigated the role of six leg and foot muscles in arch support of the foot. By vertically loading the knee of a sitting subject it was found that there was little or no muscle activity below the applied force of 1800 N. It was concluded that the first line of defence of the arch was ligamentous, the muscles forming a dynamic reserve called upon reflexively during periods of excessive loading, e.g. the toe off phase of walking. These conclusions were further verified by the investigations of Mann and Inman (1964) and Walker (1991).

Investigations into the load bearing function of the plantar ligaments of the foot have been performed in a number of studies. Most of these have used a selective dissection process to explore the contributions of each ligament to the support of the longitudinal arches of the foot (Ker *et al*, 1987; Walker, 1991 and Huang *et al*, 1993). Although broad conclusions of the relative importance of each of the plantar structures can be drawn, the precise interrelationships of their function in the intact foot cannot be found from such tests. The results from these studies have, however, highlighted a number of passive structures important to the load bearing function of the foot, these being the plantar aponeurosis (PA), long and short plantar ligaments (LPL and SPL) and the calcaneonavicular or 'spring' ligament (CNL).

Few studies on the mechanical properties of the plantar foot ligaments have been carried out. Wright and Rennels (1964) performed tests on fresh PA specimens and estimated its elastic modulus to be approximately 568 MPa. Jacob (1989), in his work on the forefoot, performed similar tests and found a value of elastic modulus of 1236 MPa. All of the above investigations failed to address either the complex continuous geometry of the plantar ligaments and their insertions, or simplified the analysis of their mechanical behaviour to a linear response. Due to the frequency of their injury, the properties of ankle ligaments have been well documented (Attarian *et al*, 1985 and Siegler *et al*, 1988) but as yet the plantar ligaments of the foot, other than the PA, remain uninvestigated.

Various attempts at producing mathematical models of the foot have been made. Often these models are used to estimate joint reaction and muscle forces using an inverse dynamics approach. Procter (1980) estimated talocrural and subtalar joint reaction forces and extrinsic muscle forces, but essentially the foot was modelled as a single unit below the level of the ankle joint. Jacob (1989) modelled the forefoot and

obtained estimates of the metatarsophalangeal (MTP) joint reactions, intrinsic muscle and PA forces. Simkin (1982) made detailed measurements of the joint torsional stiffness for inclusion in his ligamentous foot model. His representation of the plantar ligaments, however, was based on the mechanical results of another study. Other models have included the action of the PA (in a simplified form) but for reasons of complexity have not considered the other plantar structures, since these inevitably introduce more indeterminacy into the analysis (Salathe *et al*, 1986; Morlock, 1990 and Scott and Winter, 1993).

Passive mechanisms have been shown to be the primary method of load support in the foot and vital to its normal function. Although qualitative information on the relative importance of several of the passive structures has been gathered, there has been no quantitative investigation of the entire system of plantar ligaments in the intact foot. In addition, no detailed measurements of the complex geometry, insertions, size, shape and tissues properties have been made and related to the structure of the foot as a whole. In the past this lack of knowledge has been reflected in attempts at modelling the foot where either gross simplification or omission of the details of structure and function of the plantar ligaments have been the norm. A detailed understanding of the biomechanics and function of the plantar ligaments and passive support structures of the foot would be a significant advance in knowledge. The information rendered by such a study would be of value not only to biomechanics researchers but to surgeons and other clinicians, orthotists, prosthetists and footwear designers.

**The aims of the present study were:**

1. To make quantitative measurements of the mechanics of the passive support mechanisms of the foot during functional activities, e.g. standing and gait.
2. To investigate the mechanical properties of the various plantar support structures and assess their role in the measured mechanics.
3. To represent the foot in a mathematical model in order to estimate ligament force and strain and to explore the effects of injury and surgical procedures.

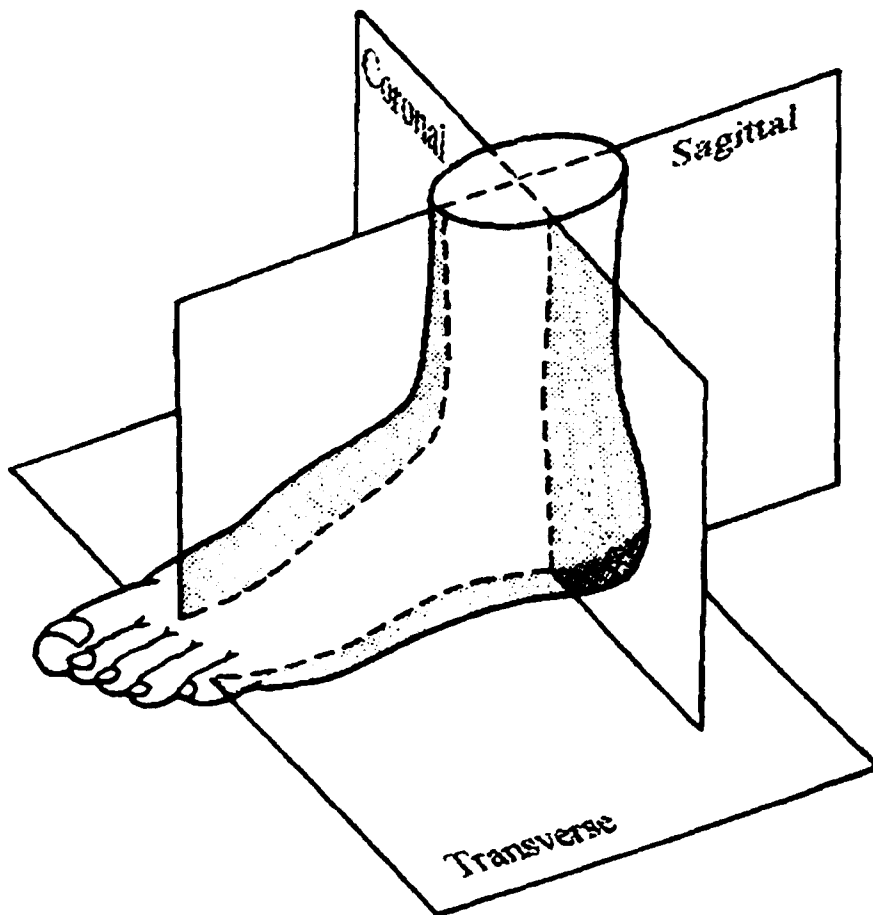


Figure 2.1 The coronal, sagittal and transverse anatomical planes of reference as they apply to the foot (adapted from Helal and Wilson, 1988).

## **CHAPTER 2. BASIC FUNCTIONAL ANATOMY OF THE FOOT**

### **2.1 INTRODUCTION**

This chapter gives a brief account of the anatomy of the foot with regard to the details of the musculoskeletal system under investigation in the present study. As might be expected of a highly specialised structure such as the foot its anatomy is correspondingly complex in nature. The intention here is to introduce to those readers new to the area of foot biomechanics or anatomy sufficient information to understand the analyses and arguments presented in this thesis. If a greater degree of understanding is sought or more detailed information is required then the reader should refer to one of the following texts: McMinn *et al*, 1982; Romanes, 1987; Sarrafian, 1983; Williams *et al*, 1989.

### **2.2 ANATOMICAL TERMINOLOGY OF POSITION AND MOTION**

When the body is in the standard anatomical position the foot differs from other limb segments in that its longitudinal axis lies in the horizontal, or transverse plane. As a result the terms used to describe motions and positions are notoriously confusing. The terms used in this thesis are consistent with those of Williams *et al* (1989) and are defined as shown in figures 2.1 and 2.2.

The three standard reference planes remain unchanged (fig 2.1). The following positional terms are defined with reference to the foot:

Anterior:	Toward the toes (front)
Posterior:	Towards the heel (rear)
Medial:	Towards the median plane
Lateral:	Away from the median plane
Dorsal:	Towards the upper surface
Plantar:	Towards the lower surface (sole)

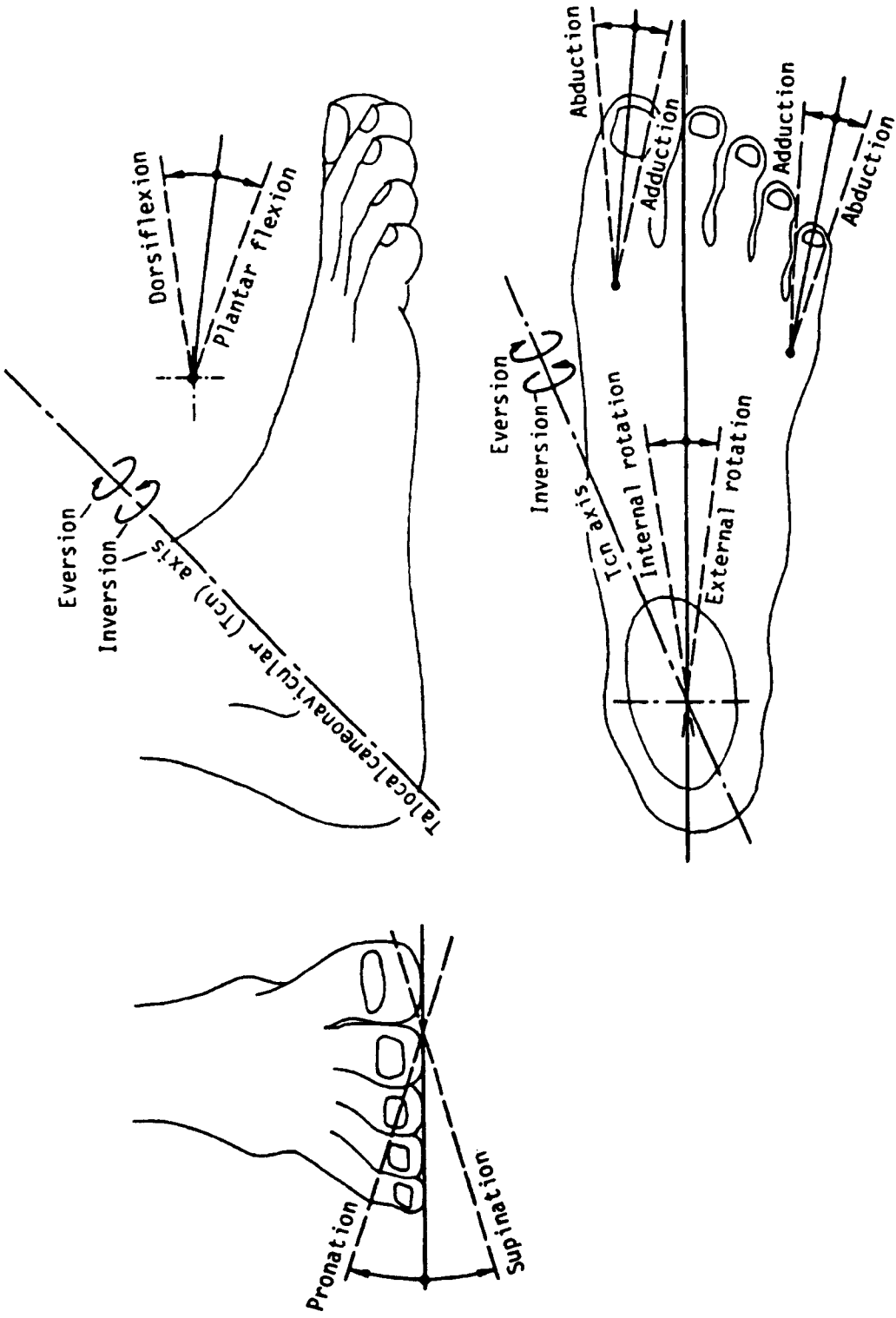


Figure 2.2 Terms of reference used to describe movement of the foot and toes (adapted from Jacob, 1989)

Superficial: Towards the skin

Deep: Towards the centre of the segment.

Special care must be taken when describing the terms of reference of motion of the lower leg and foot since confusion is easy. Motions occurring in the sagittal plane which tend to fold a limb (or move the distal segment anteriorly) are known as flexion, whilst those tending to straighten the limb (or carry it posteriorly) are referred to as extension. To avoid confusion at the ankle flexion and extension are commonly referred to as plantarflexion and dorsiflexion respectively. Abduction of the foot is movement away from the median plane and conversely adduction is movement towards it. Movements of the toes in the transverse plane are referred to a longitudinal axis running from the centre of the heel through the second toe, abduction and adduction of the toes being movements away from and towards this axis. External and internal rotations move distal portions away from and toward the median plane respectively.

Complex motions about an axis system, which will be discussed in the next section, are responsible for the movements of inversion and eversion. In inversion the medial border of the foot is raised bringing the sole round to face medially. Eversion involves the opposite motion where the sole is turned to face laterally (fig 2.2). The terms pronation and supination are very often used incorrectly in describing inversion and eversion. Pronation and supination are movements occurring around the longitudinal, anteroposterior axis of the foot. Pronation is a rotation where the medial portion (or the first ray) moves down towards the sole of the foot. Supination is the reverse of this. Pronation and supination are considered to be components of inversion and eversion and functional distinctions can be drawn. In this thesis pronation and supination will refer more specifically to motion tending to twist the forefoot with respect to the hindfoot as in forefoot adaptation during stance ( Hicks, 1953; Williams *et al*, 1989).

### **2.3 BONES AND JOINTS**

Twenty six bones, excluding sesamoid and accessory bones, comprise the skeleton of the foot (seven tarsals, five metatarsals and fifteen phalanges) and are shown

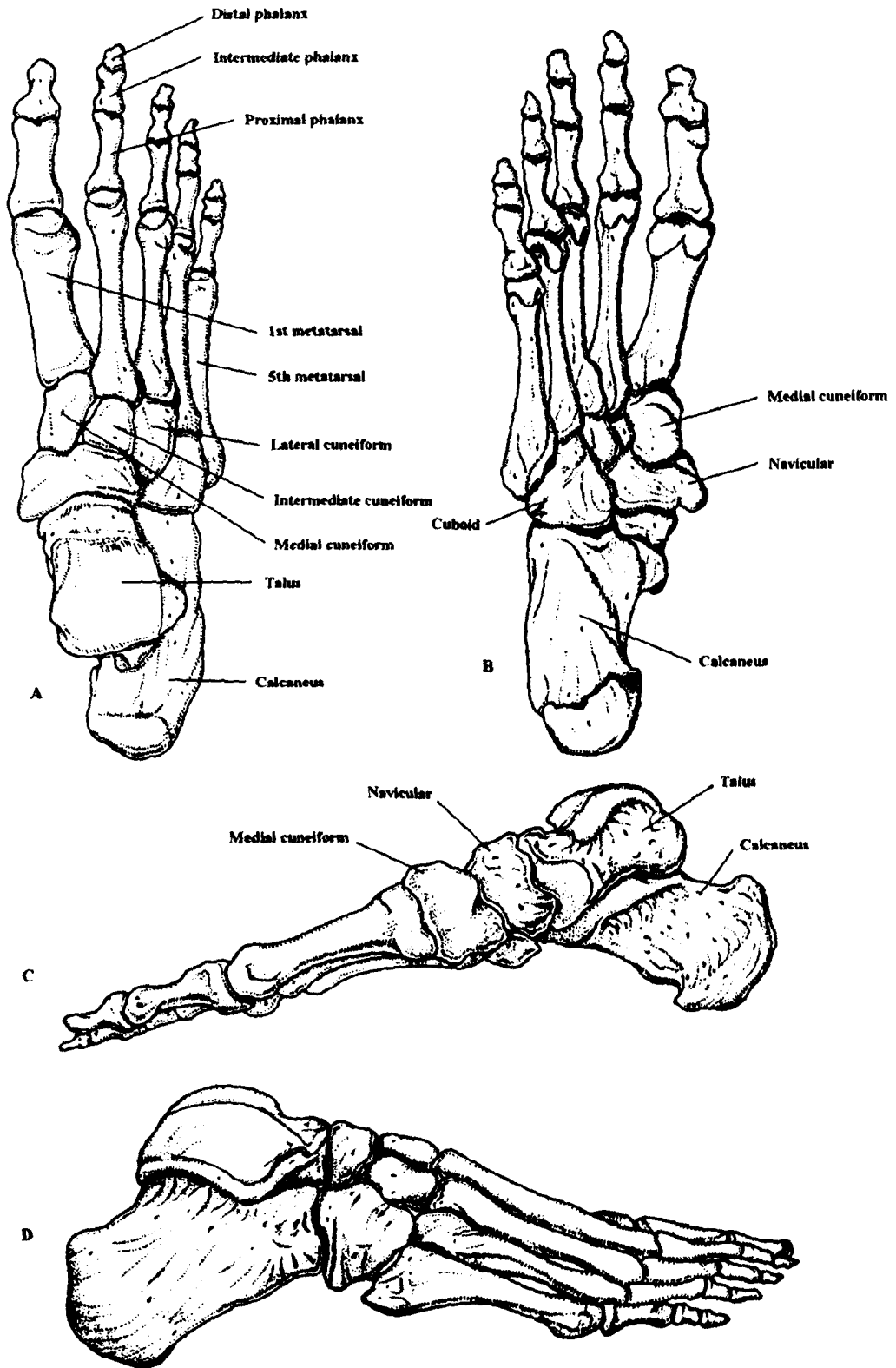


**Figure 2.3** The skeletal anatomy of the foot: (A) from above, (B) from below, (C) medial view and (D) lateral view (adapted from Helal and Wilson, 1988).

in figure 2.3. The many joints of the foot have varying geometries, types of articulation and ranges of motion. Some joints are very important in adaptation of the foot to various surfaces whilst others have very small movements indeed. The most functionally important joints are discussed below.

The foot articulates on the inferior concave surfaces of the tibia and fibula via the superior domed facet of the talus forming the talocrural (TC) joint. Motion at this joint is generally limited to the sagittal plane allowing plantar and dorsiflexion of the foot. The joint has been found to behave like a conical hinge where the axis of rotation is angled at approximately  $80^\circ$  to the long axis of the tibia sloping from the medial to the lateral and at  $96^\circ$  to the midline of the foot sloping rearwards from the medial to lateral as shown in figure 2.4 (Inman, 1976; Isman and Inman, 1969). The view that the TC joint acts with a single axis has been questioned by Hicks (1953) and Lundberg (1988) who proposed separate axes for plantarflexion and dorsiflexion.

The talus also has multifaceted joints with the calcaneus, which forms the major part of the skeleton of the heel, and the navicular. Anatomically two separate joints can be identified. The subtalar joint is formed by the largest and most posterior of the talocalcanean articulations, whilst the rounded head of the talus articulates with two smaller facets on the anterior portion of the calcaneus and the concave surface of the navicular forming the talocalcaneonavicular (TCN) joint. In addition the talar head also has an articulation with the superior fibrocartilaginous surface of the plantar calcaneonavicular (or spring) ligament. Combined movements about the subtalar and TCN joint allow inversion and eversion (previously described). The axis of rotation of the combined motion is angled obliquely to the anatomical reference planes as shown in figure 2.4.

Some confusion exists in the terms subtalar, talocalcanean and talocalcaneonavicular with respect to which joints they describe (Hicks, 1953; Inman, 1976; Isman and Inman, 1969; Langelan, 1983; Lundberg, 1988; Manter, 1941). The mix-up was acknowledged in both Williams *et al* (1989) and Brooks and Warwick (1989). The correct anatomical use of the term 'subtalar' is as described above. Some authors use the term subtalar to refer to all the talocalcanean articulations or indeed, all the articulations between the talus calcaneus and navicular. Since it is generally

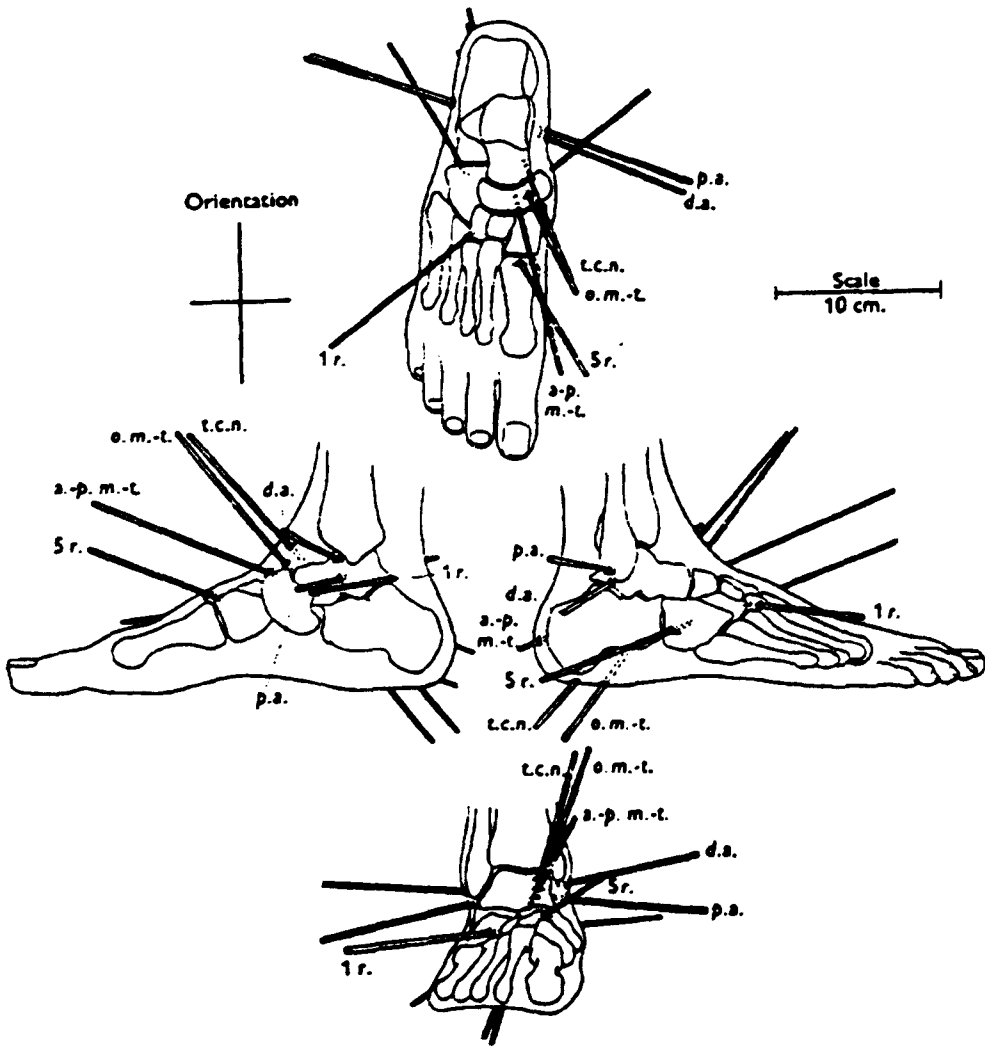


Figure 2.4 Joint axes of the foot and ankle (from Hicks, 1953).  
 (Note: pa = plantarflexion ankle, da = dorsiflexion ankle,  
 tcn = talocalcaneonavicular, apmt = anteroposterior midtarsal  
 and omt = oblique midtarsal).

accepted that the subtalar and TCN joints function together the more embracing term talocalcaneonavicular (TCN) joint will be used in the present study.

Two other functionally important joints of the tarsus are the calcaneocuboid and talonavicular joints. These joints lie in a similar transverse plane and act together to produce motions about the two axes of the mid-tarsal or transtarsal (TT) joint as shown in figure 2.4 (Elftman, 1960; Hicks, 1953; Manter, 1941). The transverse or oblique axis of the TT joint allows dorsiflexion/abduction and plantarflexion/adduction motion of the forefoot about the calcaneus and talus. Predominantly pronation/supination movements of the forefoot about the calcaneus and talus result around the second longitudinal axis. The remaining intertarsal joints, the cuneonavicular, intercuneiform, cuneocuboid and cubonavicular joints are small and allow only slight gliding motions of the bones relative to each other due to their rigid ligamentous ties.

The five metatarsals are similarly shaped, all taper distally and have a rounded head which articulates with the proximal phalanx of each ray. Proximally the first, second and third metatarsals articulate with the medial, intermediate and lateral cuneiforms respectively, while the fourth and fifth metatarsals articulate with the cuboid. Collectively these are known as the tarsometatarsal (TMT) joints. Movement at these joints are small, the first metatarsal being the most mobile while the second metatarsal being 'built-in' by the medial and lateral cuneiform has the least amount of independent movement.

The skeleton of the toes is made up of three bones, the proximal, intermediate and distal phalanges (in the great toe, and occasionally also in the fifth, the intermediate and distal phalanges are fused). Dorsiflexion/plantarflexion and abduction/adduction of the toes about the metatarsals takes place at the metatarsophalangeal (MTP) joints whilst the proximal and distal interphalangeal joints (PIP and DIP respectively) allow only relative flexion and extension movements of the phalanges. Two small sesamoid bones in the tendons of the extensor hallucis brevis muscle articulate in the grooves on the plantar surface of the first metatarsal head.

The skeletal structure of the normal human foot is arched in shape, a feature possessed by no other primate. The medial longitudinal arch consists of the calcaneus, talus, navicular medial, cuneiform whilst the lateral consists of the calcaneus cuboid and fifth metatarsal. The medial arch is higher and more deformable giving rise to the

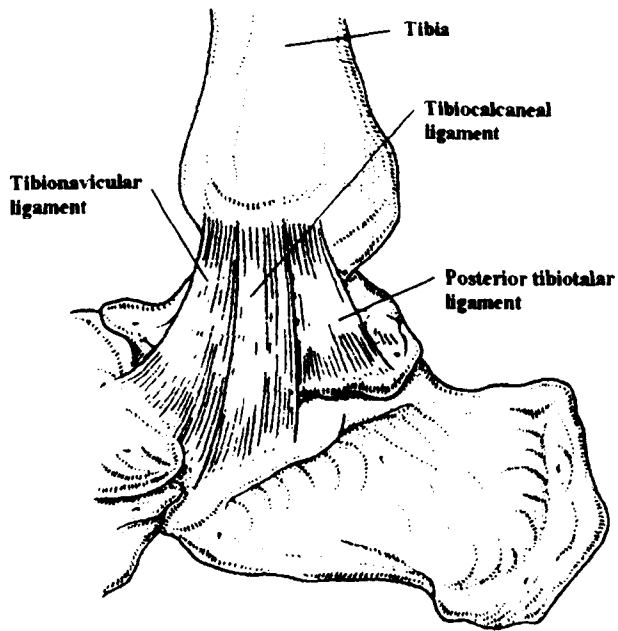


Figure 2.5 Medial ligaments of the ankle (adapted from Helal and Wilson, 1988).

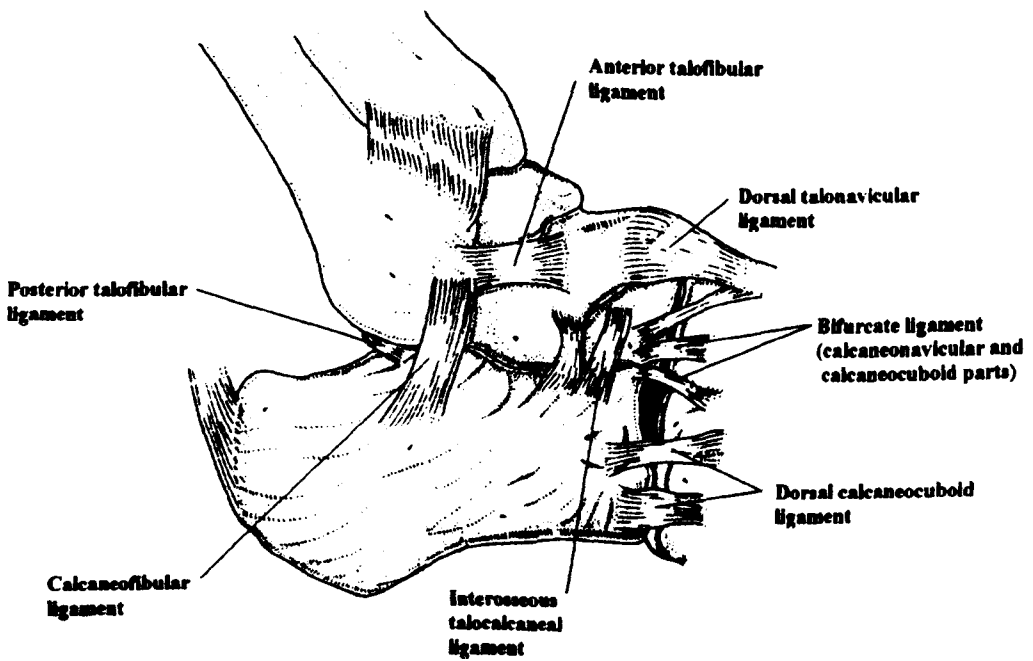


Figure 2.6 Lateral ligaments of the ankle and tarsus (adapted from Helal, 1988).

concave sole of the foot and the characteristic human footprint. Both longitudinal arches have a complex system of ligamentous and muscular support. The transverse arch refers to the general curved arrangement of the bones across the foot, the curve becoming shallower when moving from the distal tarsal bones to the heads of the metatarsals.

Analogies of the arched pedal skeleton to static architectural structures and forms are common and sometimes misrepresentative. The arched structure of the foot is dynamic in nature and support and loading conditions vary widely throughout the range of foot function. A detailed discussion of the functional aspects of the arched structure of the foot is presented in section 3.2.

## **2.4 LIGAMENTS**

Not surprisingly the complex osteology and arthrology of the foot is accompanied by a similarly complicated and rather poorly understood system of over 50 ligaments (Alexander, 1992). Descriptions of the ligaments that were investigated in the present study together with an overview of the remaining important structures are given below.

Two groups of ligaments act at the TC joint on the medial and lateral sides of the joint capsule. The medial (or deltoid) ligament is triangular in shape with three superficial bands (tibionavicular, tibiocalcanean and posterior tibiotalar) and two deep bands (anterior and posterior tibiotalar) which all attach to the apex of the medial malleolus (fig 2.5). Three separate structures make up the lateral ligament complex namely the anterior and posterior talofibular and calcaneofibular ligaments. These ligaments are prone to rupture in forced inversion injuries of the foot, the most frequent affected being to the anterior talofibular ligament (fig 2.6). As well as restraining the TC joint from dislocation laterally and medially the ligaments also play roles in limiting dorsiflexion and plantar flexion and in controlling articulation of the talus on the tibia and fibula.

The talus has multiple ligamentous connections to the calcaneus and navicular, some of which are associated with separate fibrous joint capsules of the subtalar and TCN joints. The short lateral talocalcanean ligament descends posteriorly from the

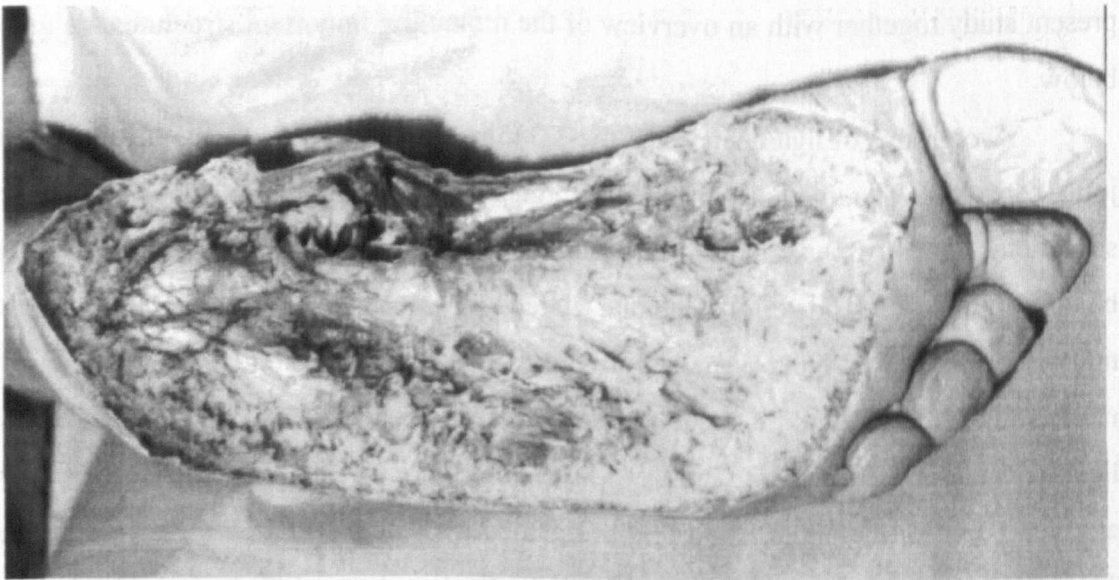
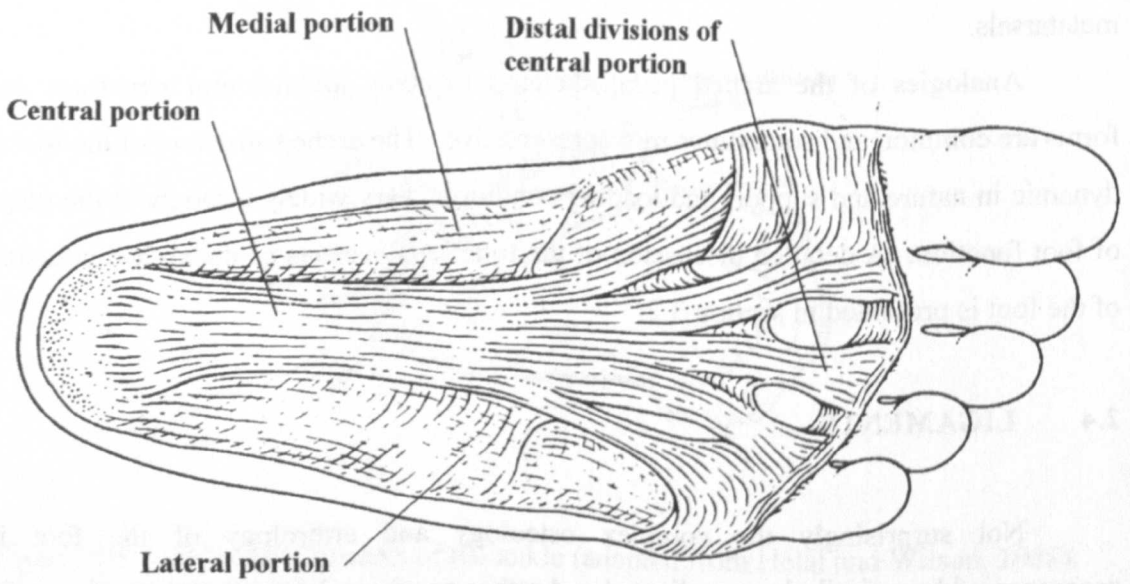


Figure 2.7 The plantar aponeurosis (drawing adapted from Helal and Wilson, 1988).

lateral talar surface to the lateral calcanean surface where it is attached anterosuperiorly to the calcaneofibular ligament. The medial talocalcanean ligament joins the medial tubercle of the talus to the medial surface of the calcaneus, in the region of the sustentaculum tali, the most posterior fibres residing in the groove for the flexor hallucis longus tendon. The strong interosseous talocalcanean ligament lies in the tunnel between the talus and calcaneus (sinus tarsi) attaching the neck of the talus to the superior calcanean surface. The broad talonavicular ligament connects the dorsal surfaces of the talus and navicular.

The remaining ligaments on the dorsum of the tarsus, thickened joint capsules, are flat or sheet like in form and bind their respective bones tightly together. These are the dorsal cuneonavicular and cubonavicular ligaments. Three small ligaments act on the lateral sides of the calcaneonavicular and calcaneocuboid joints namely the calcaneonavicular and calcaneocuboid parts of the bifurcate ligament and the dorsal calcaneocuboid ligament.

The plantar aponeurosis (PA) is a thick specialised layer of fascia located subcutaneously in the sole of the foot (fig 2.7). Although it is often described as being composed of medial, central and lateral portions the central portion is the most important functionally (the medial and lateral parts are very much thinner and are often incomplete). The central portion is well defined and triangular in shape, with its origin at the medial calcanean tuberosity. Distally the aponeurosis broadens until near the heads of the metatarsals where it diverges into five longitudinal segments which proceed towards the toes. Distally to the metatarsal heads each of these segments have superficial connections to the skin whilst two vertical slips go deep to attach to either side of the fibrous flexor sheath, plantar ligaments of the metatarsophalangeal joint and the deep transverse metatarsal ligaments. The distal insertions of the PA provide attachments to each of the proximal phalanges. This arrangement is functionally important since dorsiflexion of the toes tends to increase the tension in the PA, an effect known as 'Hicks Windlass' (Hicks, 1954). In addition the position of the PA close to the sole spanning almost the whole length of the foot gives this structure a great mechanical advantage in its important role of maintaining the arched structure of the foot.

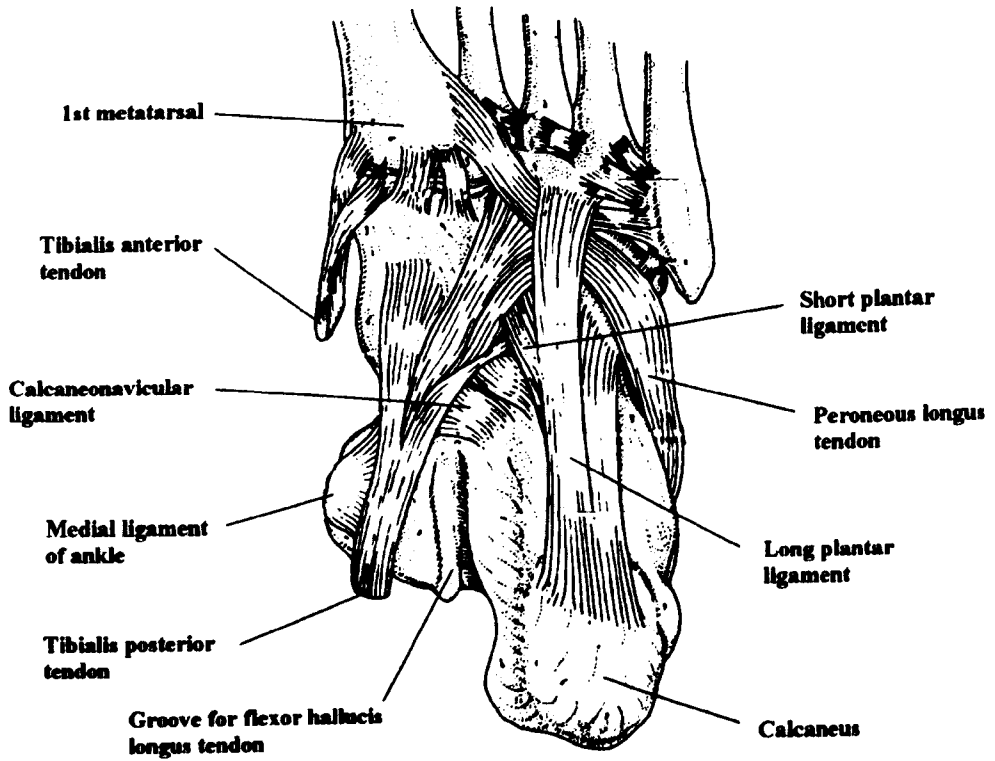


Figure 2.8 Plantar ligaments of the foot (adapted from Helal and Wilson, 1988).

Several plantar ligaments of the tarsus have important load support functions. The long plantar ligament (LPL) is long, strong and originates from a wide insertion on the plantar surface of the calcaneus in front of the medial lateral processes of the tuberosity. The main body is usually 1.5 - 2.0 cm wide and approximately 2.5 cm long. Its fibres pass over the calcaneocuboid joint and split into deep and superficial components. The deep fibres (the majority of the ligament) insert on the oblique crest of the cuboid. The thinner, more superficial layer of fibres passes over and forms a tunnel for the peroneus longus tendon and divides into four thinner slips inserting in the bases of the metatarsals 2-5 (fig 2.8). The plantar calcaneocuboid, or short plantar ligament (SPL) originates from the anterior tuberosity of the calcaneus. The fasciculated fibres (in bundles) fan out anteriomedially and insert over the entire triangular surface located posteriorly to the crest of the cuboid. The lateral edge is partly under cover of the LPL. The LPL and SPL act primarily at the calcaneocuboid joint limiting its movement and helping to maintain the longitudinal arched structure. The LPL has further minor functions in preventing dorsiflexion at the TMT joints, through its slips that are sent forward to meet the metatarsal bases.

The plantar calcaneonavicular ligament (CNL), or spring ligament, is trapezoidal in shape stretching from the anterior margin of the sustentaculum tali to the plantar surface of the navicular. The ligament is thick and fibrous at its medial border and its dorsal surface articulates with the portion of the talar head otherwise unsupported by articular surfaces. The lateral edge of the ligament is more fasciculated occasionally having two components while the medial border is continuous with the deltoid ligament of the ankle and is in close contact with the tibialis posterior tendon. The CNL has an important role in helping to maintain the form of the medial longitudinal arch. The four ligaments described above, PA, LPL, SPL and CNL form the main primary support for the longitudinal arches (Basmajian and Stecko, 1963; Huang *et al*, 1993; Ker *et al*, 1987; Walker, 1991)

Dorsal, plantar and interosseous ligaments bind the remaining tarsal joints (intercuneiform, cuneocuboid, cuneonavicular and cubonavicular joints) firmly together allowing very little relative movements of the bones. The tarsometatarsal (TMT) and intermetatarsal (IMT) joints are also bound rigidly together with dorsal, plantar and interosseous ligaments. The first TMT joint has the greatest range of motion while the

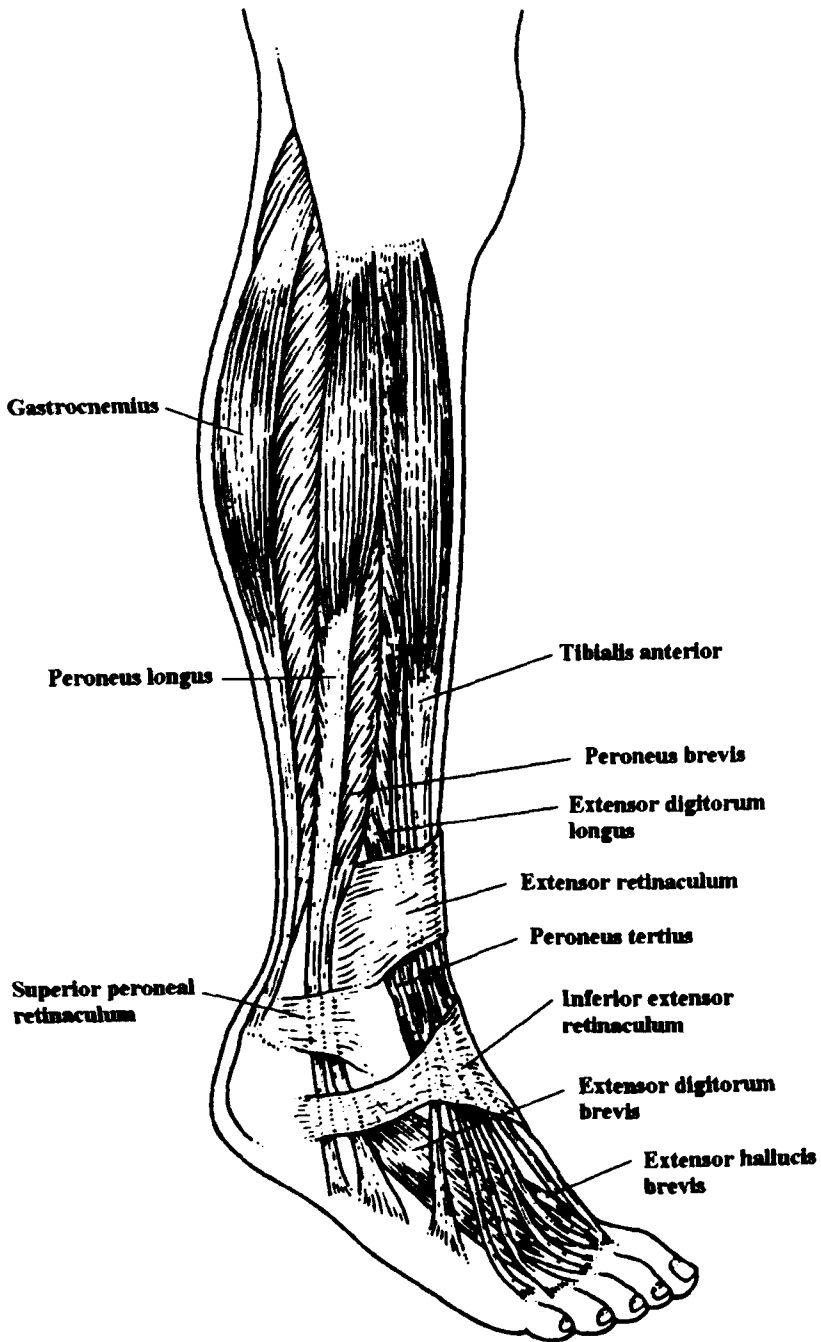


Figure 2.9(a) Extrinsic muscles of the foot (lateral view).

second is the least mobile of all due to its substantial ligamentous restraint and 'built-in' bony geometry. The distal ends of the metatarsals are joined by the deep transverse metatarsal ligament which connects the plantar ligaments of the metatarsophalangeal (MTP) joints. This ligament prevents spreading of the metatarsal heads and also limits independent movement of the individual metatarsals.

The MTP joints have a fibrous capsule surrounding them, the sides and plantar surface of which are thickened to form the collateral and plantar ligaments. The plantar portion is attached to other ligamentous structures such as the PA and deep transverse metatarsal ligaments as mentioned above. The proximal and distal interphalangeal joints have similar ligamentous structures to those of the MTP joints but their movements are limited to flexion and extension only by bony and ligamentous restraints.

The superficial fascia on the sole of the foot has an important function in the transfer of vertical and horizontal shear forces into the remaining foot structure. In the region of the main weight bearing areas, the heel and metatarsal heads, it is particularly thick and well attached to both the skin and to the deeper structures through strong fibrous bands which divide the fatty tissue.

## **2.5 MUSCLES**

The numerous muscles that have functions in the foot may be broadly subdivided into those which originate outside the foot, the extrinsics, and those which exist uniquely within the structure of the foot itself, the intrinsics. The intrinsic muscles are classically described as existing in a succession of layers which are subsequently revealed when dissecting inwards from the sole of the foot. A more functional classification is described below which also includes the extrinsic musculature. The reader should note that the muscular anatomy of the foot, like the anatomy of the bones and ligaments, is once again highly intricate. Lines of action of the foot muscles are rarely straight, many of the extrinsic muscle tendons move through large angles when entering the foot (in the region of the ankle, the tendons of extrinsics are restrained by fibrous band-like thickenings of the deep fascia called retinacula). Multiple muscle

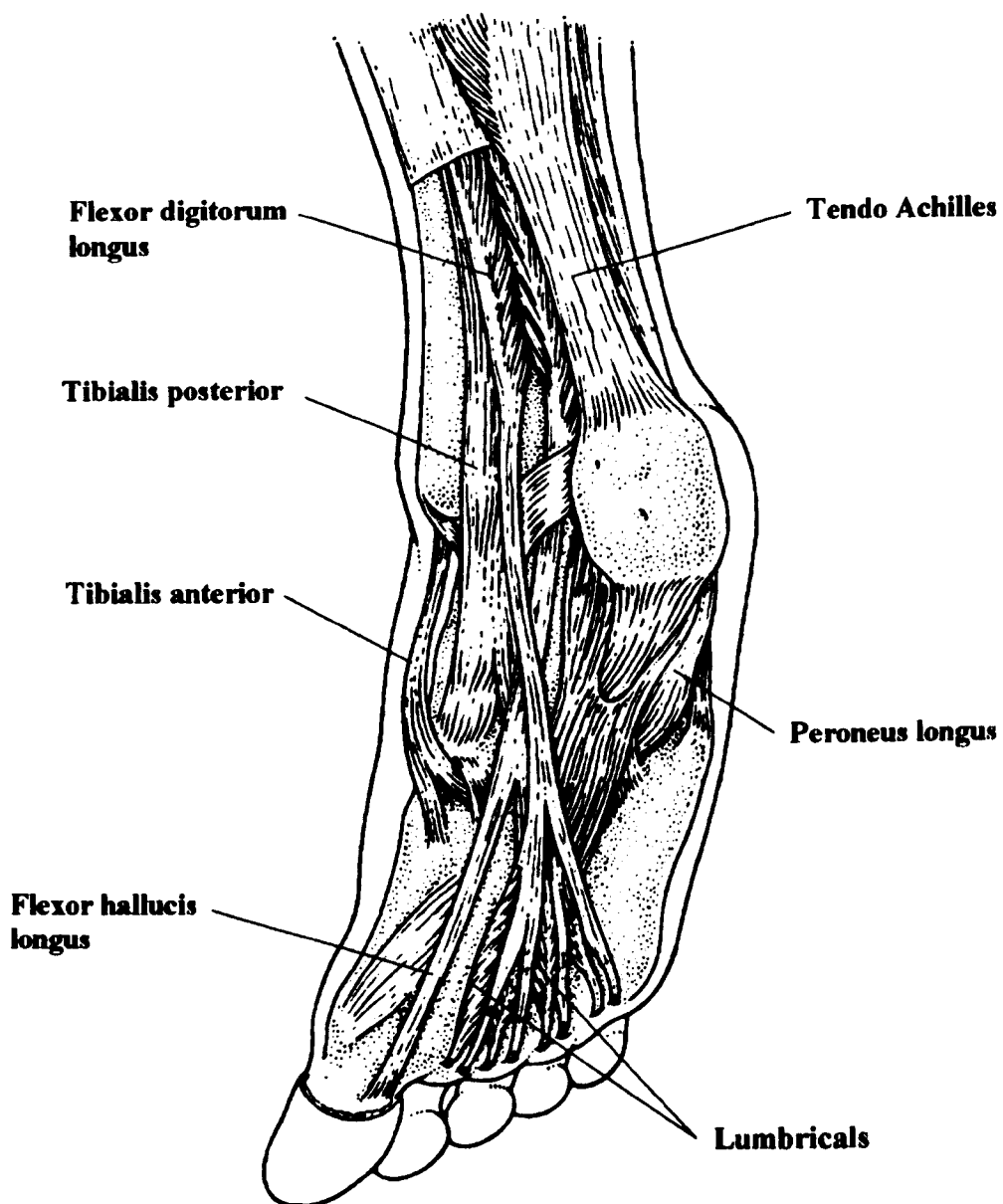


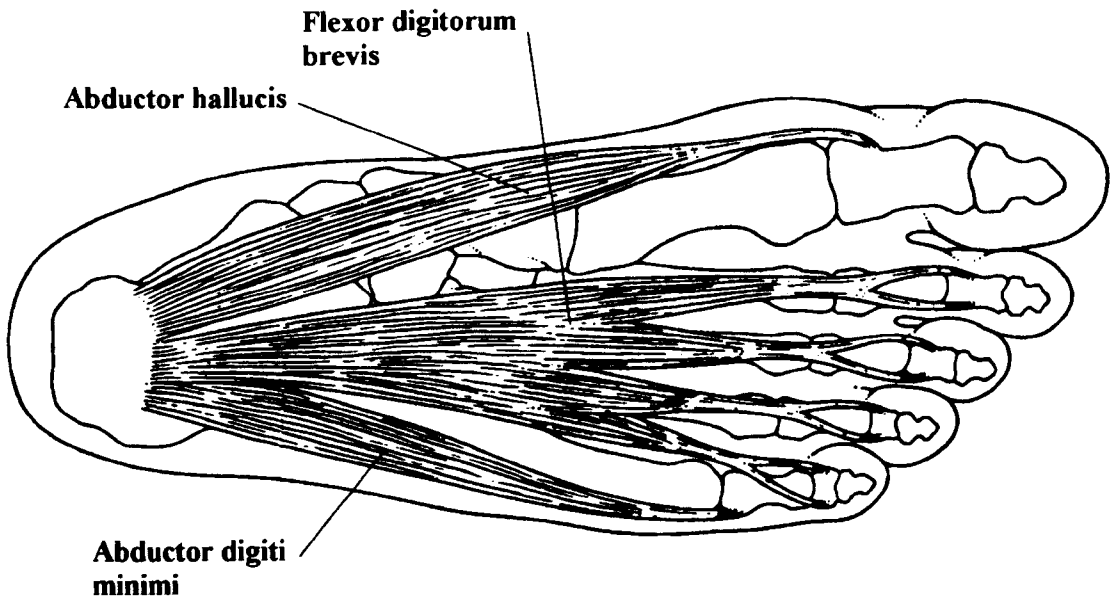
Figure 2.9(b) Extrinsic muscles of the foot (medial view)(adapted from Helal and Wilson, 1988).

heads, multiple tendons and insertions are features common to many muscles of the foot.

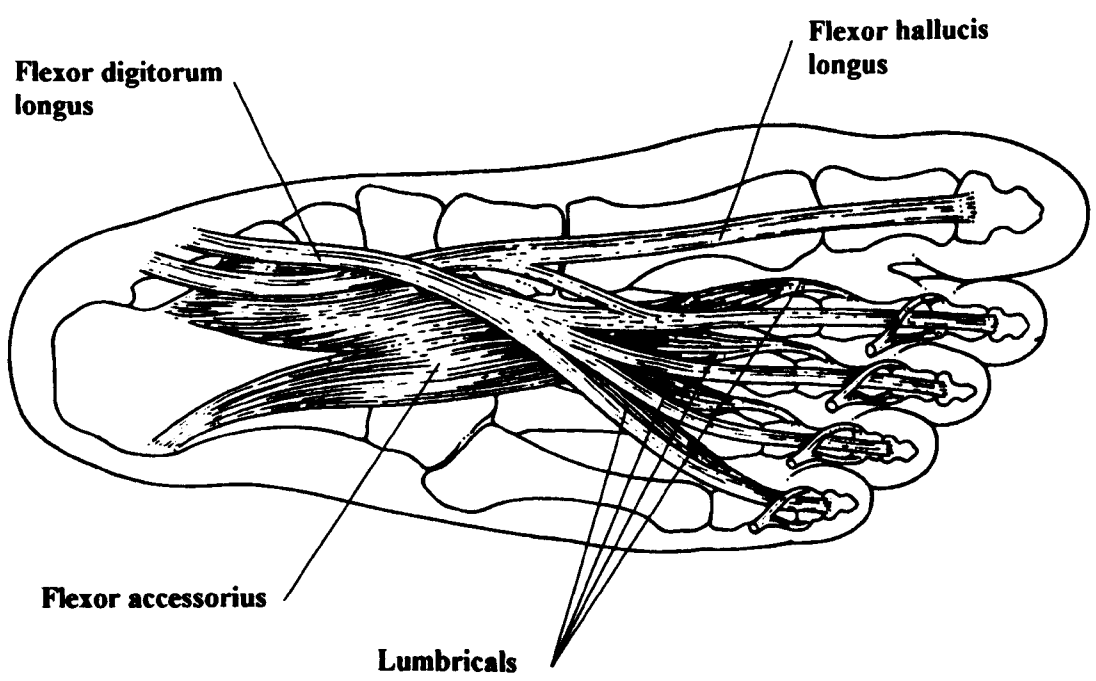
The extrinsic muscles in general move the foot relative to the lower limb and also have roles in movement of the toes and maintenance of the longitudinal arched structure of the foot. The long extrinsic muscles exist over a large proportion of the length of the foot and are involved with the functions of flexion/extension of the toes and abduction of the first and fifth toes. The short extrinsics are responsible for flexion\extension movements of the MTP joints and also adduction of the hallux. The remaining muscles, the interossei, provide abduction\adduction movements of the toes. The origins, insertions and major functions of the muscles of the foot are listed in tables 2.1 to 2.3. Illustrations of the major muscles having actions in the foot are shown in figures 2.9 and 2.10.

<b>Name</b>	<b>Origin</b>	<b>Insertion</b>	<b>Action</b>
Gastrocnemius (Medial and lateral heads)	Femur, medial and lateral condyles	Posterior calcaneus (via tendo Achilles)	Ankle PF Knee Flexion
Soleus	Posterior tibia (middle 1/3) and fibula( upper 1/3)	Posterior calcaneus (via tendo Achilles)	Ankle PF
Tibialis posterior	Posterior, interosseous membrane, upper 1/2 of tibia and fibula	Navicular tuberosity, medial cuneiform and slips to other tarsals	Ankle DF Arch support Foot inversion
Flexor hallucis longus	Posterior fibula, lower 2/3	Base of distal phalanx of hallux	Ankle PF Hallux flexion
Flexor digitorum longus	Posterior tibia, middle 2/4	Bases of distal phalanges of toes 2-5	Ankle PF Toes 2-5 flexion
Tibialis anterior	Lateral tibia, upper 1/2	Medial base of 1st metatarsal and medial cuneiform	Ankle DF Foot inversion Arch support
Extensor hallucis longus	Anterior fibula, middle 1/3	Base of distal phalanx of hallux	Ankle DF Hallux extension
Extensor digitorum longus	Anterior fibula, upper 1/3	Bases of intermediate and distal phalanges of toes 2-5	Ankle DF Toes 2-5 extension
Peroneus longus	Lateral fibula, upper 2/3	Base of 1st metatarsal and medial cuneiform	Ankle PF Foot eversion
Peroneus brevis	Lateral fibula, lower 2/3	Base of 5th metatarsal	Ankle PF Foot eversion

Table 2.1 Extrinsic muscles of the foot (DF = Dorsiflexion, PF = Plantarflexion).



(a)



(b)

Figure 2.10 Intrinsic muscles of the foot: (a) long intrinsic and (b) short intrinsic (adapted from Helal and Wilson, 1988).

<b>Name</b>	<b>Origin</b>	<b>Insertion</b>	<b>Action</b>
Abductor hallucis	Medial process of calcanean tuberosity and PA	Medial proximal phalanx of hallux	1st MTP abduction and flexion Arch support
Abductor digiti minimi	Both processes of calcaneaneal tuberosity and PA	Lateral base of proximal phalanx of toe 5	5th MTP abduction
Flexor digitorum brevis	Medial process of calcanean tuberosity and PA	Intermediate phalanges of toes 2-5	2-5 MTP and PIP flexion Arch support
Extensor hallucis brevis	Anteriosuperior surface of calcaneus	Proximal phalanx of hallux	1st MTP extension
Extensor digitorum brevis	Anteriosuperior surface of calcaneus	Intermediate and distal phalanges of toes 2-4	2-4 MTP and PIP extension

Table 2.2 Long intrinsic muscles of the foot.

<b>Name</b>	<b>Origin</b>	<b>Insertion</b>	<b>Action</b>
Flexor hallucis brevis	Plantar cuboid	Proximal phalanx of hallux	1st MTP flexion
Adductor hallucis (transverse and oblique heads)	Bases of metatarsals 2-4 and plantar ligaments of MTP 2-4	Lateral base of proximal phalanx of hallux	1st MTP adduction Accentuation of anterior transverse arch
Flexor digiti minimi brevis	Base of 5th metatarsal	Lateral base of proximal phalanx of toe 5	5th MTP flexion
Flexor accessorius	Plantar and medial calcaneus	Lateral border of FDL tendon	Assists action of FDL
Lumbricals (four)	Tendons of FDL	Bases of proximal phalanges and extensor expansions of toes 2-5	2-5 MTP flexion 2-5 PIP extension
Dorsal interossei (four)	Adjacent sides of pair of metatarsals	Proximal phalanges, lateral side of toes 2-4 and medial side toe 2	2-4 MTP abduction
Plantar interossei (three)	Medial side of metatarsals 3-5	Medial side of proximal phalanges 3-5	3-5 MTP adduction

Table 2.3 Short intrinsic and interossei muscles of the foot.

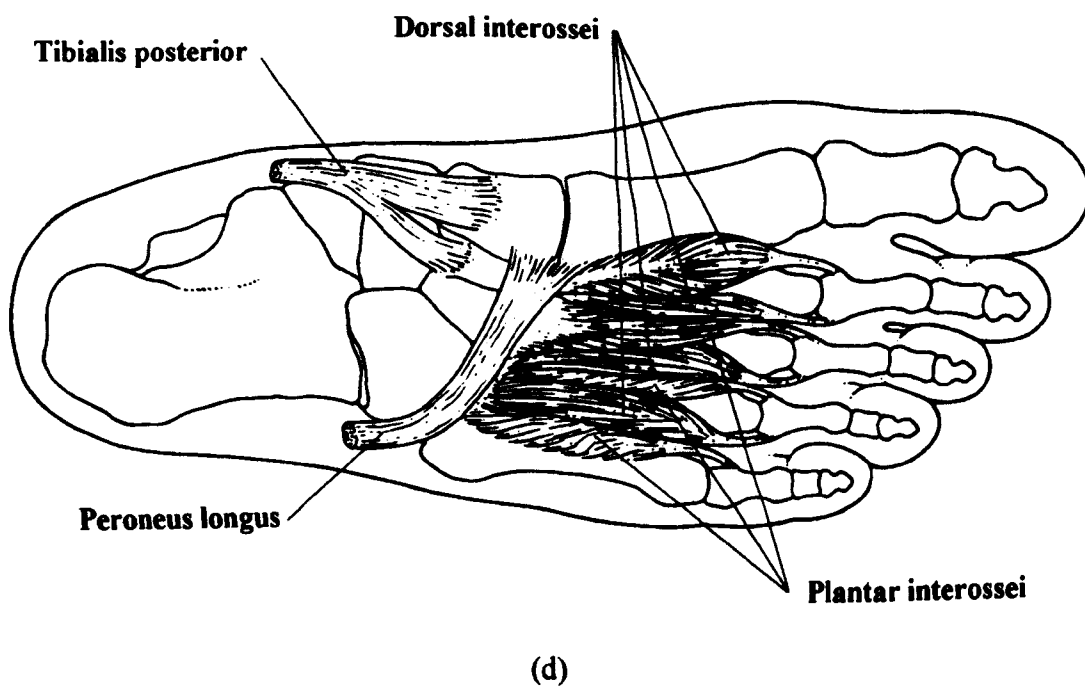
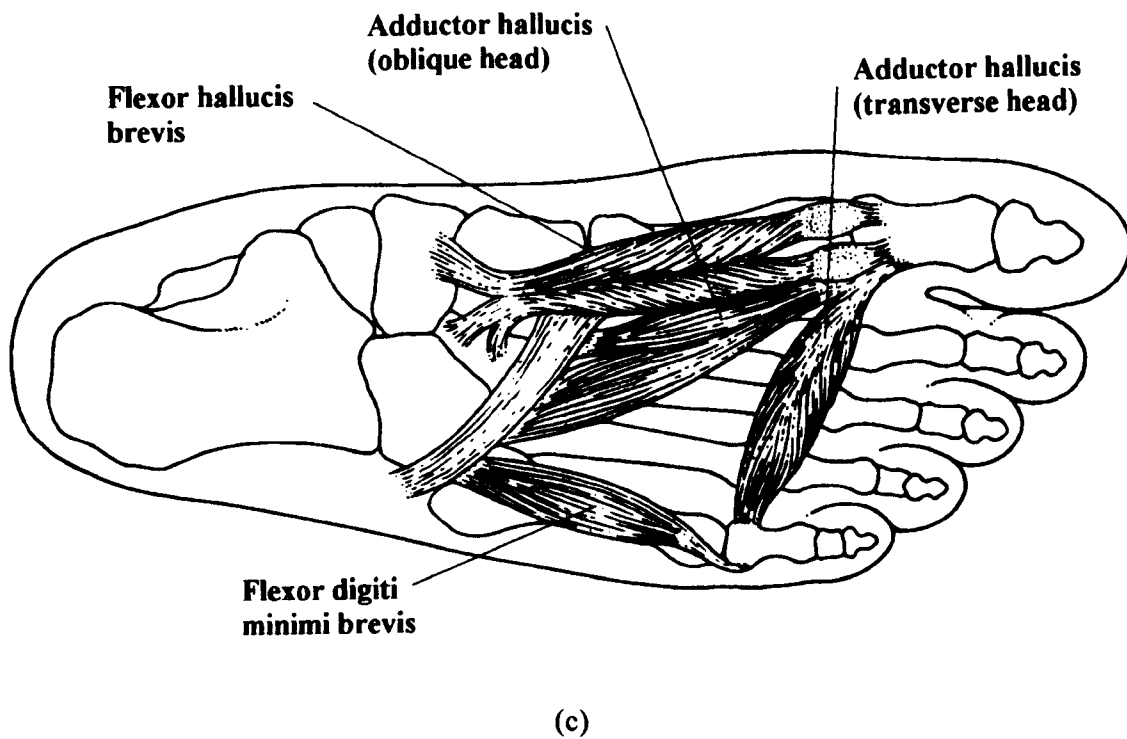


Figure 2.10(cont.) Intrinsic muscles of the foot: (c) short intrinsic and (d) interossei (adapted from Helal and Wilson, 1988).

## **CHAPTER 3. REVIEW OF THE RELEVANT LITERATURE**

### **3.1 INTRODUCTION**

In this chapter the biomechanical literature of relevance to the present study is critically reviewed. The areas of experimental structural analysis, ligament mechanics and testing, ligament strain and force measurement and modelling of the foot have been covered. A short section on the clinical disorders of the foot ligaments has also been included. After summarising the conclusions of the literature the need for further investigation was identified. This formed the basis for the work conducted in the present study.

### **3.2 THEORIES OF FOOT FUNCTION AND EXPERIMENTAL STRUCTURAL ANALYSIS**

The foot's ability to provide the adaptive, efficient and sustained support necessary for bipedal locomotion is unique in nature. As suggested by its intricate anatomy the foot's function is highly specialised. Debate over contributions of individual structures in the mechanisms of load support has long existed. The letter of Humphry (1867) illustrates the themes under discussion between doctors and surgeons of the day. Argument over whether the talus or the navicular was "the keystone of the arch" was typical of the concept of the foot as a static architectural structure. The relative contributions of the muscles and ligaments (PA and CNL) were also mentioned, the ligament's function being simply described as "responding to demands made upon them". Debate of the above points continued until the 1940's based on personal opinion rather than scientific evaluation.

The work of Lapidus (1943) marked the end of the non-technical era, however it still retained a rhetoric of opinion based conclusions. Based on simple mechanics and observations from nature and of patients with muscular deficiencies Lapidus concluded that the ligaments provide the primary means for support of the foot which was likened to a truss structure. Experimental work was neglected in favour of a simplified

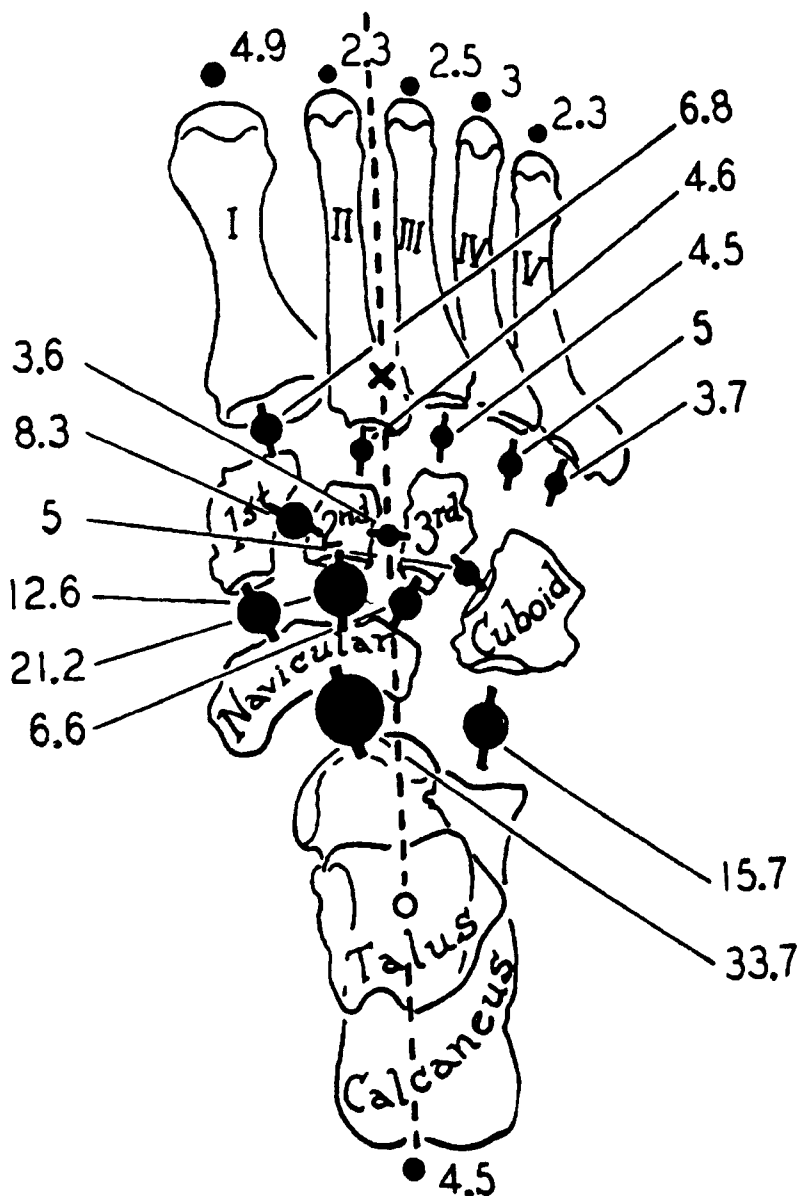


Figure 3.1 Compressive forces in the joints of the foot, shown graphically in pounds force, found from loading experiments in cadaveric specimens (from Manter, 1946).

mechanical analysis to arrive at the incorrect conclusion that the foot was a rigid structure, possessing “no springiness”.

During the 1940's and '50's experimental work by three investigators made important advances in foot biomechanics. Jones (1941) loaded dissected foot specimens in an apparatus which measured forces on the forefoot. By measuring the reaction force produced under the forefoot with applied tibial and extrinsic muscle forces, a measure of ‘mechanical advantage’ was obtained for each muscle after further comparison with cross sectional area measurements. Tests on the specimens where the ligaments were then cut revealed that simulated muscle action alone was not able to maintain normal arch shape or restore collapsed arches. The extrinsic muscles of live standing subjects were palpated and found to be relaxed. From these observations Jones concluded that the ligaments, and to a lesser degree the intrinsic musculature, were responsible for the primary mechanism of support. From measurements in cadaver specimens and live subjects, Jones also suggested that the medio-lateral force distributions under the metatarsal heads were controlled reflexively by extrinsic inverter and everter muscles. This study was the first attempt at a quantitative structural analysis of the foot.

Manter (1946) made measurements of compressive stresses in the joints of cadaveric feet. Thirteen joints of the tarsus and metatarsals were instrumented with lead sheets and small steel balls. When a vertical force was applied to the feet, the joints compressed and the force in each was measured by examining the areas of lead indented and comparing to calibrated plates. Similar arrangements were used to measure contact forces under the heel and metatarsal heads. The largest compressive forces were found in the talonavicular and intermediate cuneonavicular joints, whilst transverse forces were also found between the cuboid and cuneiforms. Slight lateral shifts in loading greatly altered the reaction forces under the metatarsals heads but it was found that ligamentous support alone could produce normal plantar force patterns as seen in living subjects. The results of Manter are shown in figure 3.1.

In the mid 1950's Hicks conducted three investigations into different aspects of foot biomechanics (Hicks, 1953; 1954 and 1955). After first finding positions of the joint axes of the foot, figure 2.4, Hicks then turned his attention to the internal loading of the foot structures. Hicks (1954) observed both in cadaveric and living subjects that

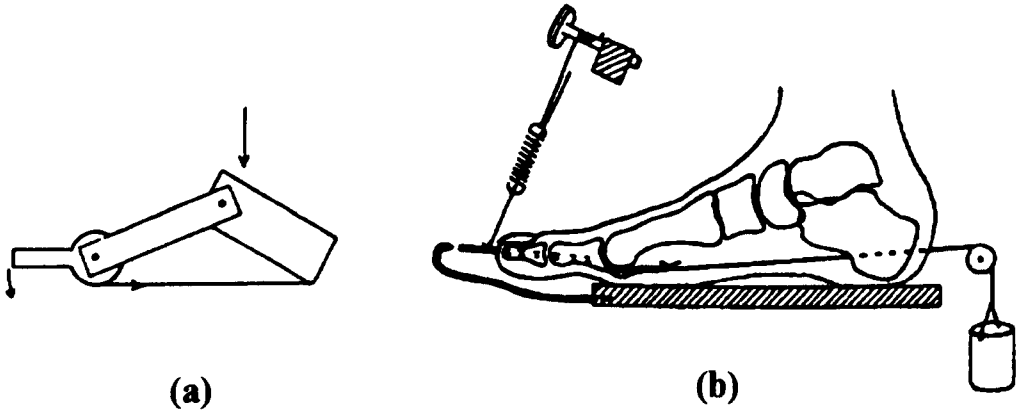


Figure 3.2 The spring balance apparatus used by Hicks to measure PA forces in loaded cadaver feet: (a) The action of the windlass mechanism and (b) calibration of the force measuring method (from Hicks, 1955).

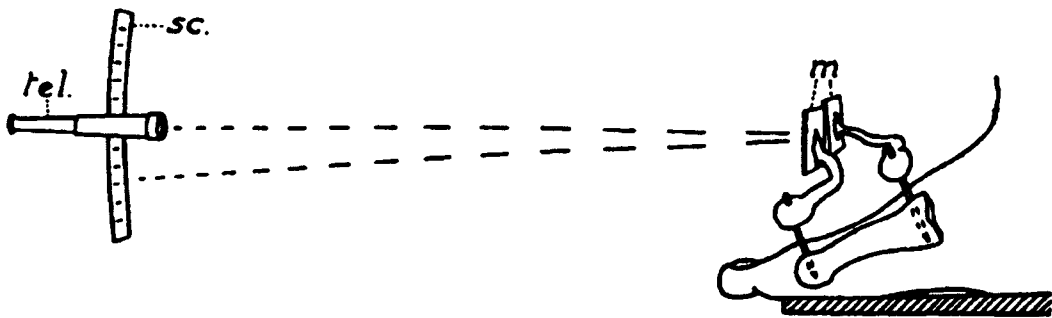


Figure 3.3 The optical lever used by Hicks to assess metatarsal bending in loaded cadaver feet: sc. = scale, tel. = telescope, m = mirror (from Hicks, 1955).

dorsiflexion of the toes produced tension in the PA and subsequent movements of the metatarsals that produced raising of the arches. The observations were confirmed with radiographic data and cinematic records of standing and walking subjects. A preliminary mechanical analysis was conducted where the PA was cut in loaded cadaveric specimens and tension tests were performed on isolated PA specimens. Hicks suggested that the effects of toe dorsiflexion would be particularly important during the thrust phase of gait where the heel is raised. In describing the mechanism Hicks likened the tightening of the PA around the metatarsal heads to that of a 'windlass' winding a cable, a term which is still used today.

Hicks (1955) further developed his experimental analysis to explore two proposed mechanisms of loading in the foot. Six cadaveric feet were instrumented with spring balances on the toes to measure PA forces, and an optical arrangement to record bending in the metatarsals (figures 3.2 and 3.3). The feet were loaded in a jig to physiological levels whilst simulated Achilles tendon forces were used to move the centre of pressure,  $x_{cp}$ , in the sagittal plane. The importance of the two mechanisms was assessed by severing the PA and noting the altered effects on metatarsal bending for the same loading conditions. It was found that PA force had a linear relationship with force applied to the ball of the foot. Both mechanisms were found to operate in the intact, foot flat position. When the PA was severed the bending action in the metatarsals was increased. A simple formula developed to assign applied load to each mechanism was used to demonstrate that toe dorsiflexion induced PA tension and reverse bending of the metatarsals. The load unaccounted for by this formula was attributed to 5th metatarsal base loading only; forces in other plantar ligaments was not considered. The ability of the metatarsals to carry bending forces independently was noted. Hick's work constituted an advance in foot mechanics due to the quantitative investigation of theoretical ideas and also the introduction of the concept of the 'windlass' mechanism.

The importance of the PA to foot function has a sound anatomical basis which has been well documented. The complex distal attachments which terminate on the proximal phalanges, transverse ligaments and skin of the distal sole have been particularly well described by Bojsen-Møller and Flagstad (1976) and Sarrafian (1983). Jacob (1989) in his work on the biomechanics of the forefoot was obliged to carry out loading tests on cadaveric feet to examine the loading of the PA and metatarsals.

Conventional strain gauges bonded to the metatarsals 1-3 were used to measure the bending forces in each of these bones in simulated standing experiments (340N vertical force). The importance of the PA was assessed, after Hicks, by cutting and noting the altered bending states in the metatarsals. Bending deformation of the metatarsal was confirmed and when the PA was cut the strain levels increased with varying amounts. Force values for the PA and deformation of the skeletal structures were not presented. Some problems may have existed with the experimental technique e.g. one specimen tested, thermal effects and non-linearities of gauged bone were not quantified, the PA was removed and then reattached at the heel before testing. On the basis of these results Jacob concluded that the role of the PA was overestimated by Hicks, a claim which is perhaps unfounded given additional evidence available for the importance of the PA (Huang *et al* 1993; Ker *et al*, 1987 and Walker, 1991).

The actions of the PA have also been shown to be affected by pronation and supination of the foot induced by external and internal rotation of the tibia. Sarrafian (1987) described this mechanism by likening the foot to a twisted plate where pronation caused loading of the PA and lowering of the medial arch and supination caused raising of the arch and unloading of the PA. These movements were also described by Hicks (1953).

Advances in electronics enabled the role of the muscles in the structural mechanics of the foot to be investigated, using electromyography (EMG) techniques. In simple terms this procedure measures the inherent electrical activity accompanying muscle contraction, or force generation, using surface or intramuscular electrodes. Basmajian and Stecko (1963) used intramuscular EMG to directly assess the role of muscles in the support of the foot arches (four extrinsic and two intrinsic muscles of twenty subjects). Vertical forces of up to 1780N were applied to the knees of seated subjects while measurements of muscle activity were made (the feet were loaded in five positions). No muscle activity was recorded below a level of 890N and even at full loading only slight activity was noted. Although the EMG readings were not normalised nor muscle forces estimated it was concluded that the ligaments alone could provide complete support in the foot at levels of force seen during standing. It was proposed that the muscles formed a dynamic reserve, called upon reflexively during excessive loading such as the toe-off phase of gait.

Mann and Inman (1964) used fine-wire EMG in six intrinsic foot muscles. Again the results were not normalised to maximum activity levels and instead were presented as temporal records for the functional activities studied; namely walking, standing and standing with the heel raised. It was observed that although the timing and duration of the activity of the intrinsic musculature varied with the activity, the muscles functioned together as a unit. Activity was noted in all the intrinsics when standing on the toes but in agreement with Basmajian and Stecko (1963) it was seen that during quiet standing the muscles were inactive.

Suzuki (1972) conducted EMG of extrinsic and intrinsic foot muscles in subjects with normal and flat feet. The subjects performed a range of standing and weight shifting activities in addition to tests similar to those of Basmajian and Stecko (1963). The normal subject's muscles again showed no significant activity during standing or applied tibial loading of up to 500N. In flat footed subjects 100-300N forces elicited activity in some muscles (PL, AH and FDB). In weight shifting experiments muscle activity was witnessed in both types of feet.

Using EMG and comparative evolutionary anatomy techniques, Reeser *et al* (1983) studied patterns of muscle function in order to clarify the roles of the intrinsic toe flexors and adductor muscles. The EMG analysis was augmented with simple motion analysis and force platform measurements. In addition to reconfirming the inactivity of the muscles during standing, Reeser *et al* also noted intrinsic muscle activity during pronation/supination. This was compared to observed functional anatomy in primates. It was suggested that this mechanism was a remainder of the adaptation of the prehensile functions of the foot in early hominids to the role of standing.

Walker (1991) was the first to conduct fatigue resistance studies, combined with a properly normalised analysis, on the intrinsic foot muscles (4 extrinsics, 4 intrinsics on 6 subjects). The effects of wearing shoes on muscular activity levels were also studied. Each subject performed a wide range of gait and forefoot support activities. Muscle activity levels were normalised to the maximum voluntary contraction level whilst muscle fatigue was assessed by examining changes in the frequency density components of the EMG signals. The observations of the previous investigators were re-affirmed. Forefoot standing, the wearing of shoes and weight shifting during standing all caused increased levels of activity in the intrinsic muscles. Shoes also increased the variability

in results between subjects. Walker's results for fatiguing of the intrinsic muscles showed a curious phenomenon. Significant fatigue of the intrinsic muscles was seen to occur after only 30s of forefoot standing. After 60s the intrinsics recovered slightly to a stable level while the extrinsics continued to fatigue. Walker suggested that the intrinsics may have been operating in a duty cycle, temporarily unloading one another to give a more fatigue resistant behaviour overall.

Little direct work exists on proprioceptive mechanisms in the foot although proprioceptive feedback paths between ligaments and muscles have been suggested (Basmajian and Stecko, 1963 and Valenti, 1988). The proprioceptive mechanisms are believed to function in unconscious adaptation to changing terrain, loading and movements and the necessary neurological apparatus, mechanoreceptors, have been found in histological studies. Valenti (1988) identified modified chondrocytes in the adipose tissue of the sinus tarsi and Michelson and Hutchings (1995) confirmed the existence of mechanoreceptors in human ankle ligaments, similar to those discovered at the knee. Freeman (1965a and 1965b) postulated that articular nerve fibres terminating in mechanoreceptors in the joint capsules and ligaments of the ankle had a role in proprioceptive control. It was further suggested that sprain injuries or ligament rupture were responsible in de-afferenting the joints leading to impaired reflex control of the ankle (chronic lateral instability). Treatment methods focusing on retraining of the neuromuscular pathways were described and were found to have a greater degree of success when compared to conventional physiotherapy and immobilisation.

Several investigators have examined the movement or deformation of the foot skeleton during load-bearing activities in an attempt to quantify patterns of motion. Carlsöö and Wetzenstien (1968) used multiplane X-ray techniques on normal subjects performing weight shifting during standing. The authors concluded that no significant deformation of the foot skeleton occurred during standing and in the absence of muscle activity, as suggested by Basmajian and Stecko (1963), the non-linear properties of the ligaments were responsible for the results witnessed. Sherref *et al* (1990) conducted similar experiments on normals and subjects with bilateral hallux valgus. Unfortunately the measurements were arbitrary with respect to the biomechanics and did not reveal the overall patterns of deformation. Lengthening and widening, of the forefoot, were

identifiable in 90% of cases. This study demonstrated the difficulties associated with simple multi-view radiographic techniques.

Winson *et al* (1994) overcame many of the systematic errors of previous approaches by using Roentgenstereophotogrammetry (RSA). In short this technique involves implanting small radiopaque markers into the bones to be studied and taking simultaneous biplanar X-rays. The relative positions of the bones as well as rotational axes can be found and the method can be used, as it was in this study, in living subjects. In particular heel raising and forefoot support activities showed that the talonavicular joint had the largest degree of motion of the tarsal joints with up to 19° flexion. The values of motion for the living subjects was higher than that of cadaveric specimens and a large variation in results between subjects was noted.

Motion of the joints of the midfoot, intertarsal and tarsometatarsal, was explored by Ouzounian and Sherref (1989). Test motions were applied to whole prepared cadaveric feet and individual joint deflection was measured with pins inserted into the bones. In dorsiflexion/plantarflexion maximum motion occurred at the 4th and 5th tarsometatarsal joints (9.6° and 10.2°) followed by the talonavicular (7.0°) and intermediate and medial naviculocuneiform joints (5.2° and 5.0°). Supination/pronation movements were found to occur primarily at the talonavicular (17.7°) and 4th and 5th tarsometatarsal joints (11.1° and 9.0°). Although the applied movements and loading were unphysiological, this study served to show the relative movements within the midfoot joints and would seem to agree with earlier results of Inman (1976) and Hicks (1953).

Dynamic changes of the foot structure during walking were made by Yang *et al* (1985) and Kayano *et al* (1978) using skin mounted linear extensometers on the transverse and longitudinal arches. In normal subjects the patterns of deformation were found to be repeatable and showed distinct forms. The medial longitudinal arch lengthened during mid-stance and shortened during toe flexion implying operation of the windlass mechanism (average total range of motion of 16mm). Similar patterns of deformation were recorded for the transverse arch (average total range of motion of 4mm). Tests on a subject with painful flat feet showed a noticeably different pattern of arch deformation.

As an alternative to radiographic procedures Hennig and Cavanagh (1985) used an ultrasound technique to measure vertical deformation of the dorsal surface of subjects with normal, planus and cavus feet. Normalised deflections between the groups showed significant differences (3.3% cavus, 5.9% normal and 7.8 planus). It was suggested that this type of evaluation would be a more reliable method of classifying foot type than methods based on footprint analysis.

Several investigators have explored the contributions of individual ligaments to the mechanics of the foot by conducting what the author describes as 'serial sectioning' tests (Huang *et al* 1993; Ker *et al*, 1987 and Walker, 1991). All these investigations applied vertical forces to cadaveric specimens and monitored deflections of the skeletal structures. By progressively cutting the ligaments believed to be carrying load and repeating the tests, the contribution of each ligament was analysed. Ker *et al* (1987) cyclically loaded six specimens to a constant amplitude simulating the forces occurring during running. After cutting of the ligaments the force response from the foot for each subsequent cycle was reduced. Lateral X-rays were also used to confirm the levels of skeletal deformation. The four test ligaments were the PA, LPL, SPL and CNL. This study was the first to clearly demonstrate that variation in the integrity of the ligaments could drastically alter the load-deformation relationship of the foot.

Walker (1991) conducted similar tests in six cadaveric feet however the experiments were more refined in that measurements of force under the sole, applied muscle forces and different foot positions were used. Under dynamically applied load the reaction forces under four areas of the sole were monitored and load shifts recorded when each of the ligaments were cut. Walker considered the skin as a force carrying structure in addition to the PA but failed to make a functional distinction between the LPL and SPL. The results of Walker's study illustrated the problem with tests of this type in that the required information, i.e. the function of the ligaments, has to be inferred qualitatively from secondary measurements, in this case localised reaction force. When the number of test variations increases the analysis and comparison of results becomes difficult and the potential impact of the conclusions drawn is reduced.

Huang *et al* (1993) used additional extensometer instrumentation to measure vertical arch deflection in another set of serial sectioning tests (fig 3.4). Effects of cutting the PA and LPL were seen to have the greatest effects on foot mechanics further

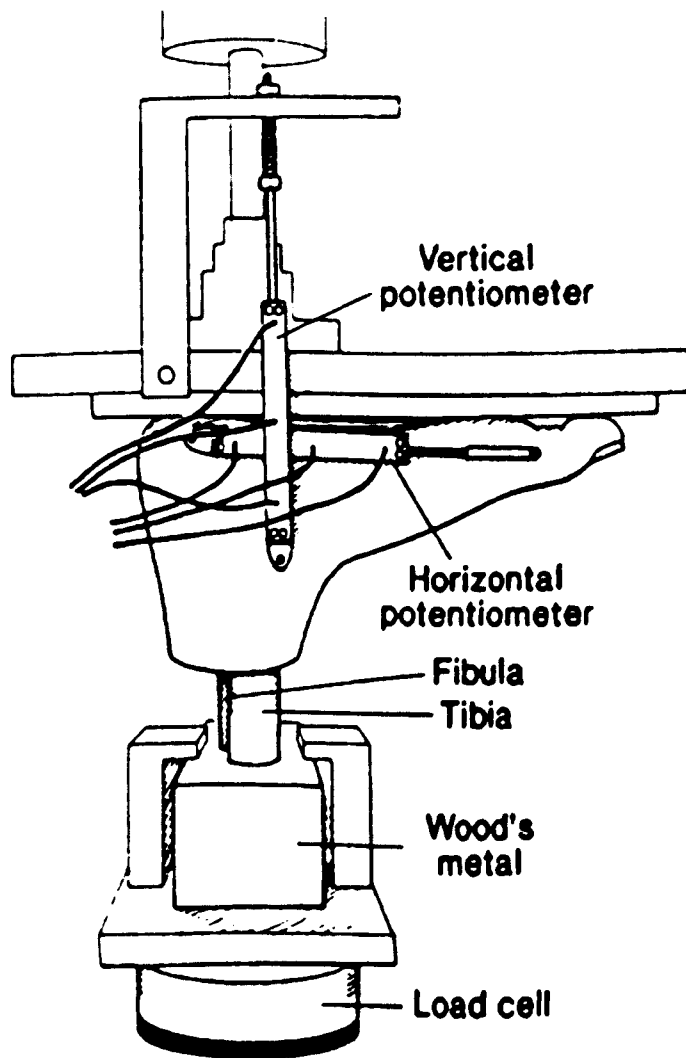


Figure 3.4 The apparatus used by Huang *et al* to measure arch deformation in loaded cadaver feet (from Huang *et al*, 1993).

confirming the results of previous tests. Again Huang *et al* failed to make a functional distinction between the LPL and SPL. The order of ligament cutting and the age of the specimens were shown not to be significant to the outcome of the tests.

Ottevanger *et al* (1989) presented details of apparatus for measuring forces on cadaveric foot specimens undergoing applied motions *in vitro*. Preliminary data was presented but this was carried out on embalmed specimens and the results are such that they do not reveal any details of internal loading.

The structure of the foot itself, usually referred to as arch height or shape, has been shown to have an effect on its biomechanics. Simkin *et al* (1989) investigated the relationship between arch shape, orthosis use and the incidence of stress fractures in 295 army recruits. Statistical analysis of the results revealed that the incidence of femoral and tibial stress fractures was significantly higher in subjects with a large calcaneal angle (arch height). The incidence of metatarsal fractures was higher in subjects with a low calcaneal angle. It was concluded that the energy absorbing role of the foot structure, as affected by arch shape and the orthosis was important to the incidence of stress fractures although it was correctly stated that the exact aetiology was multifactorial.

The effects of arch height on the reaction forces and kinematics of the foot were explored by a group from the University of Calgary (Nachbauer and Nigg, 1992 and Nigg *et al*, 1993). Influenced by aetiological studies, Nachbauer and Nigg (1992) examined the effects of arch height and flattening on selected variables in the ground reaction forces of running subjects. It was found that arch height and flattening could not accurately be used to predict changes in the reaction force profiles. As discussed by the authors the ground reaction forces are largely influenced by movement of the centre of mass of the whole body, which could have possibly masked effects due to small changes in foot structure. Nigg *et al* (1993) investigated whether arch height influenced kinematic variables suggested to be related to injuries in running e.g. forced eversion on heel strike and related axial rotation of the tibia. Using 3D motion analysis it was found that eversion and internal rotation were highly correlated. Only 27% of the variance in the coupling of the two movements was explained by arch height. Arch height must be considered along with other, as yet unidentified variables, when assessing predisposition to foot injury.

An often used clinical measuring tool is a simple foot print, analysis of which is used to classify foot types into high, normal and flat arches (Cavanagh *et al*, 1987). The reliability and applicability of this type of measurement to the biomechanics field is however strictly limited (Hawes *et al*, 1992).

Experimental analysis of joint contact forces has progressed since the investigation of Manter (1946). Both studies reviewed below used pressure sensitive film (Fuji Photo Films, Ltd) which has been shown to produce reliable and accurate measurements of contact area in comparison with other methods when used with precaution (Ateshian *et al*, 1994). Calhoun *et al* (1994) performed a detailed study on the three facets of the talocrural articulation in cadaveric specimens. Maximum contact area was found when a combination of inversion/eversion and dorsiflexion was applied. Wang *et al* (1995) made *in vitro* measurements of contact forces and areas in two talocalcaneal articulations of the TCN and subtalar joints, of loaded cadaver feet. The subtalar joint was found to transmit 75-80% of the total compressive load applied with a maximum contact stress of 5MPa for an applied 600N load. Higher applied tibial forces were seen to concentrate the contact stress on an anterioinferior portion of the subtalar joint which was suggested as an initiation site for compressive calcaneal fractures. Both these studies showed the patterns of contact area and stress in joints of the ankle complex were affected significantly by the magnitude of the applied force and more importantly the position of the foot during loading.

Although not investigated directly in the present study, the plantar fascia and fat pads in the sole of the foot have been found to have a vital function, particularly in dynamic interaction with support surfaces during locomotion (Donn, 1992; Ker *et al*, 1989 and Kim *et al*, 1994). Numerous studies have documented the anatomy of this part of the foot. In short, strong fibrous bands bind the skin to the underlying skeletal structures dividing the fatty pads of the sole into tightly formed globules. The attachments are particularly strong in the areas of greatest load bearing. Strong attachments help transmit shear forces whilst properties of the constrained fat globules are important in dynamic impact attenuation. Dynamic loading of the foot is influenced by foot-shoe-surface interactions, an area which has attracted a large degree of biomechanical research in recent years especially with increased activity in the area of sports biomechanics and commercial interests in the development of athletic footwear.

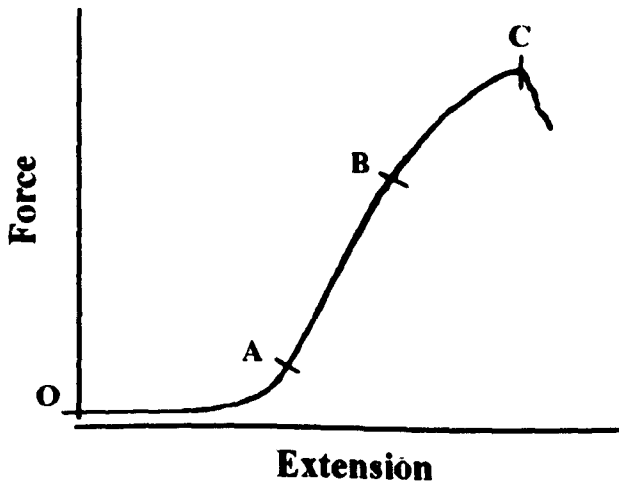


Figure 3.5 Typical force-extension curve for a specimen of ligament or tendon (see description in text).

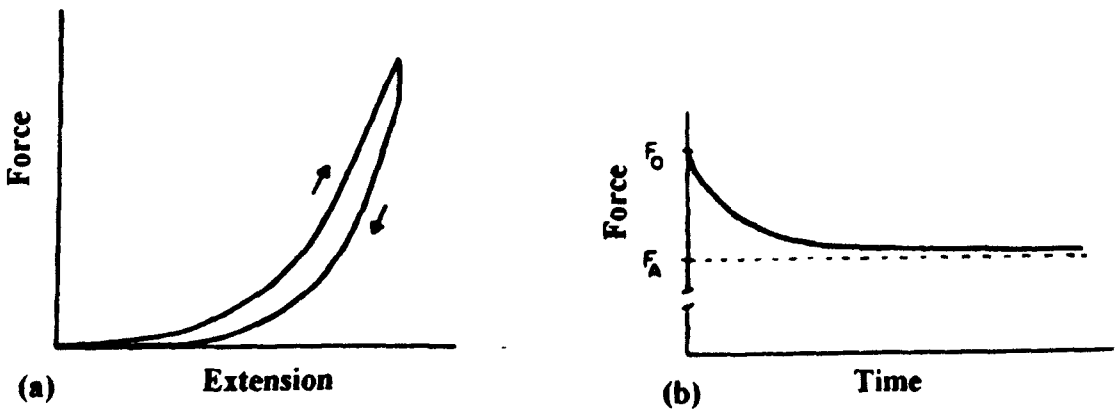


Figure 3.6 Aspects of ligament tensile behaviour: (a) Force-extension curve for a loading and unloading cycle, showing hysteresis and (b) load relaxation response.

### **3.3 EXPERIMENTAL ANALYSIS OF THE BIOMECHANICS OF LIGAMENTS**

#### **3.3.1 Testing of Excised Ligament Specimens**

Ligaments and tendons are composed of a biological composite-like tissue containing a matrix of fibrous proteins of collagen and elastin and a fluid component, or ground substance, composed mainly of glycosaminoglycans, glycoproteins and water. The collagen fibres are arranged, from a molecular level upwards, in long chain helical arrangements resulting in a number of identifiable structural fibre subdivisions of different diameters. At the fibril level the collagen fibres form a wave like pattern. This phenomenon is called crimping and is thought to have an important influence on the mechanical behaviour of parallel fibril collagenous tissue. A full account of the details of the microstructure of parallel fibred collagenous tissue and its inter-relationships with its mechanical properties is given by Viidik (1980a). As a result of the complicated micro-structure and multi-phase composition, the mechanical properties of ligaments and tendons are complex.

In tissues where the collagen component is highly orientated, as in ligaments and tendons, the mechanical properties have been well characterised experimentally and are described below (Fung, 1993). A typical load-extension curve for a tendon undergoing uniaxial tension at a constant strain rate is shown in figure 3.5. A flat “toe” region, can be seen, corresponding to the normal physiological functioning range, in which the load increases exponentially with strain (O-A). In the second portion a more linear relationship between load and extension is seen (A-B) and finally the curve becomes non-linear as the ligament approaches rupture (B-C). If a ligament is loaded to a level below failure and unloaded at a constant rate, a load-extension curve of the form seen in figure 3.6(a) results. Note that there is hysteresis on unloading. If, however, the ligament is loaded to a finite extension and held the load will approach an asymptotic level as shown in figure 3.6(b). This phenomenon is known as stress relaxation. If a specimen of ligament is loaded repeatedly to the same force level the load-extension curve will be seen to shift with each cycle. If the cycling is repeated continuously,

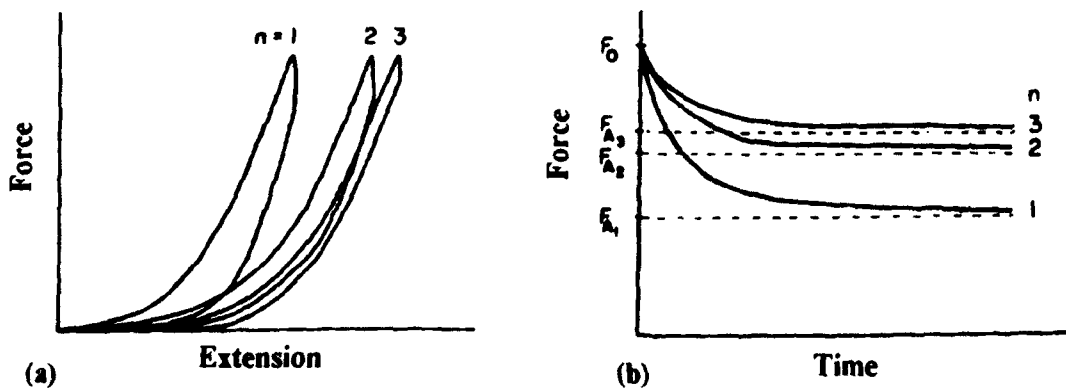


Figure 3.7 Preconditioning effects in ligamentous tissue when subjected to (a) repeated cyclic loading and (b) stress relaxation tests.

without giving time for the specimen to recover, the difference between cycles will disappear and the material may be described as being preconditioned. Preconditioning also causes an increase in the asymptotic load achieved in stress relaxation tests as seen in figure 3.7.

A great many studies have been carried out in the mechanical testing of different types of ligaments and tendon, both in animals and humans. The information yielded from such investigations is of interest, not only to biomechanics researchers, but to those interested in the mathematical modelling of tissues themselves. Reviews of the general issues involved in testing and modelling ligamentous and tendonous tissues have been compiled by Viidik (1987) and Fung (1993).

Aside from pure biomechanical interests in the properties of ligaments, a major thrust in the reasoning for conducting mechanical testing is the clinical relevance of the results. One particular example is in the area of ligament replacement where most attention has been focused at the knee joint. Crucial to the design and use of ligament reconstructions is an understanding of the mechanical properties of the natural ligaments that are being repaired as compared to those being used as the prosthesis (Grood and Noyes, 1976; Kennedy *et al*, 1976; Noyes and Grood, 1976; Noyes *et al*, 1984 and Race and Amis, 1994).

Studies characterising the mechanical properties of the ligamentous tissue of the foot have been, by comparison with the knee, rare. Most clinical interest has been focused at the ankle, a commonly injured joint complex (Hølmer, 1994). Attarian *et al* (1985) conducted tensile tests on 20 specimens of 3 lateral and 1 medial bone-ligament-bone specimens. The specimens were tested at varying rates of deflection and a strain rate dependence was observed, especially at high extension rates of 1000 mm/min. Maximum failure loads and extensions, stiffness values and energy to failure were reported ( table 3.1). In testing to failure at high strain rates, to simulate injury, avulsion fractures were seen to occur in 50% of cases. No correlation of data to age, sex, height or weight was performed and no measurement of area, and thus stress, was conducted. The ATFL seemed to be the weakest and have the lowest energy to failure of all structures, a result which would tend to support the high clinical incidence of injury to this ligament. Siegler *et al* (1988) studied 20 specimens of 3 medial and 3 lateral ankle ligaments prepared as bone-ligament-bone specimens. In this investigation, the area of

the ligaments was measured using a modified micrometer and thus stresses were calculated. Strain of the ligaments was calculated from the grip deflection and averaged bone-to-bone measurements under a standard level of pre-load. Incremental loading was applied to the ligaments to fully characterise the load-deflection response and ultimate properties of the specimens were determined to estimate the propensity for failure during injury. The ATFL was again shown to have the lowest failure load of all the ligaments, however, when ultimate stresses are compared it was seen that the posterior tibiotalar ligament was the weakest in terms of stress (table 3.1). Since a larger number of specimens was tested, and a more thorough experimental protocol seems to have been used, the values of Seigler *et al* (1988) would appear more representative. Seigler did not explore strain rate dependence, opting to test at a standard slow extension speed of less than 30% per minute. Seigler found a high incidence of bone avulsion failure, as did Attarian *et al* (1985).

Study	Ligament	Failure load (N)	Failure strain	Stiffness ( $10^5 \text{Nm}^{-1}$ )	Elastic modulus (MPa)
Attarian <i>et al</i> (1985)	ATFL	139	0.53	4.00	-
	CFL	346	0.38	7.05	-
	PTFL	261	1.00	3.98	-
Seigler <i>et al</i> (1988)	ATFL	222	0.14	1.42	256
	CFL	289	0.13	1.27	512
	PTFL	400	0.16	1.64	217
Nigg <i>et al</i> (1990)	ATFL	130	-	-	-
	CFL	296	-	-	-
	Deltoid	244	-	-	-
Davis <i>et al</i> (1996)	CNL	477	0.87	0.56	10.2

Table 3.1 Mechanical properties of selected ankle ligaments (mean values shown).

Nigg *et al* (1990) carried out tension tests on 3 ankle ligaments as part of a study investigating loads in ankle ligaments at different positions. Ligament extensions, measured during motion of cadaveric feet through a range of movements, were compared to extensions measured during isolated testing of specimens. A force value for each ligament in each position could then be calculated. Problems of fibre re-

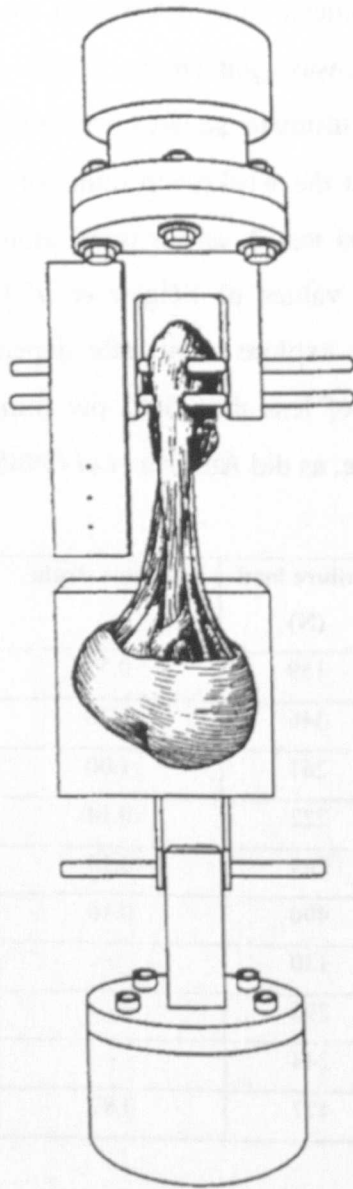


Figure 3.8 Plantar aponeurosis specimen mounted for tensile testing. The calcaneus (uppermost) has been fixed with steel rods while the forefoot has been embedded in PMMA bone cement (from Kitaoka *et al*, 1994).

orientation and establishment of a zero extension reference were experienced when testing the isolated specimens. Failure loads were found for each structure and are presented in table 3.1.

The postulated importance of the PA has led to investigation into the biomechanics of its structure. Wright and Rennels (1964) conducted simple tension tests on isolated cadaveric PA specimens and made measurements of the elastic modulus and ultimate failure load. Testing procedures were, however, not of the standardised form used today and some aspects of the methodology were unsatisfactory e.g. poor low load accuracy of the testing machine, only loading curves were presented, the tests were not dynamic in nature and the tissue was not preconditioned. A modulus for the PA in the linear region of 344-827 MPa was found. Similar tests by Jacob (1989) on one specimen indicated a higher modulus of elasticity but this study again used non-standard testing methods. Jacob calculated the PA modulus in the linear region as 1236MPa with a cross-sectional area of 27.3mm<sup>2</sup>. Kitaoka *et al* (1994) overcame some of the technical shortcomings of the above studies when testing 9 PA specimens as bone-ligament-bone preparations (fig 3.8). The stiffness of the specimens was found using extension from a video marker system and was found to be insensitive to changes in loading rate. A stiffness of 209N/mm was noted for the structure but the exact method of derivation was not given. Failure loads were also found to be significantly higher in men than in women (1540N in men, 1002N in women). The pattern of failures close to the calcaneal insertion was seen to mimic *in vivo* injury mechanisms and symptoms of plantar fasciitis.

Davis *et al* (1996) conducted an anatomical, histological and biomechanical examination of the CNL ligament inspired by clinical interest in acquired pes planus disorders of the foot. Detailed dissections showed there to be an anatomical subdivision of the CNL into two portions, a large sheet like portion - the superomedial CNL (SMCNL), and a smaller inferior band like structure - the inferior CNL (ICNL). Eight specimens were tested ultimately where a two stage failure pattern was observed with the ICNL failing first. Whilst area measurements were taken the specimens were not preconditioned and were only loaded once to failure and, hence, a full biomechanical analysis of the tissue properties was not possible.

Testing of foot ligaments, particularly the plantar ligaments of interest in this study, have not previously been tested utilising stress-strain relationships, nor have the tissues been characterised with respect to a mathematical model of their material properties.

Much work has concentrated on characterising the mechanical responses, of the types mentioned above, and of suggesting models for the behaviour of ligament and tendon tissues. A review of the main elastic and viscoelastic models of ligaments and tendons was carried out by Woo *et al* (1993). Frisén *et al* (1969) formulated an elastic model where the non-linear behaviour of the tissue was modelled as a series of viscous, dry friction and elastic elements of different length, representing the collagen fibrils in the tissue which were recruited progressively when the material was stretched. As elongation continues a greater proportion of the fibres were loaded and a more linear response resulted. A constitutive equation relating load and deformation was derived for the tissue and this was found to adequately describe the behaviour of rabbit anterior cruciate ligaments, from which the constants in the constitutive equation were calculated. The crimping of the collagen fibrils in the un-strained condition was modelled by Lanir (1980) to account for low load behaviour of the tissue. Crimps in the collagen fibres were assumed to be maintained by elastin fibres under tension attached randomly at points along their lengths, causing the collagen fibres to form buckled loops (or crimps). Despite rigorous development of the mathematics of the tissue behaviour, terms in the constitutive equation could not be determined experimentally although the forms of the tissue responses were seen to resemble those obtained empirically.

One of the most widely used viscoelastic models is that which was described by Fung (1967). This quasi-linear viscoelastic (QLV) model incorporated terms which could account for the elastic and time dependent components of the tissue response. The constitutive equation, as proposed by Fung (1972), is as follows:

$$\sigma(\lambda, t) = G(t)\sigma^e(\lambda) \quad (3.1)$$

Stress was described as a function of both strain and time in the above expression where  $G(t)$  is a function of time,  $t$ , called the reduced relaxation function and  $\sigma^e(\lambda)$  is the elastic response, a function of  $\lambda$  only.  $\lambda$  is the stretch ratio where  $\varepsilon = (\lambda^2 - 1)/2$ . The

stress at any time,  $t$ , is given by:

$$\sigma(\lambda, t) = \int_{-\infty}^t G(t - \tau) \frac{\partial \sigma^e}{\partial \lambda} \frac{\partial \lambda}{\partial \tau} d\tau \quad (3.2)$$

A form of  $G(t)$  was proposed as:

$$G(t) = \frac{1 + \int_0^{\infty} S(\tau) e^{-t/\tau} d\tau}{1 + \int_0^{\infty} S(\tau) d\tau} \quad (3.3)$$

Where  $S(\tau)$  is a continuous relaxation spectrum and has the following special form:

$$S(\tau) = \frac{C}{\tau}, \quad \tau_1 \leq \tau \leq \tau_2 \quad (3.4)$$

$$S(\tau) = 0, \quad \tau < \tau_1, \tau > \tau_2 \quad (3.5)$$

Where  $C$ ,  $\tau_1$  and  $\tau_2$  are constant parameters.

Woo *et al* (1981) used Fung's relationship to describe the behaviour of canine medial collateral ligament. Experimental data was used to find constants in the expressions for the reduced relaxation function elastic response. Woo rearranged Fung's expression for  $G(t)$  as follows:

$$G(t) = \frac{1 + C [E_1(t/\tau_2) - E_2(t/\tau_1)]}{1 + C \ln(\tau_2/\tau_1)} \quad (3.6)$$

Where  $E_1(y)$  is the exponential integral:

$$E_1(y) = \int_0^{\infty} \frac{e^{-t}}{t} dt \quad (3.7)$$

Using the values of  $G(\infty)$ ,  $G(120)$  and the slope of the relaxation curve,  $dG(t)/d(\ln t)$ , values of  $C$ ,  $\tau_1$  and  $\tau_2$  were determined. An elastic response of the form:

$$\sigma^e = A(e^{B\epsilon} - 1) \quad (3.8)$$

was used in a non linear least squares curve fit to constant strain to find the terms A and B. In cyclic tests on the same ligament tissue, used as a validation of the model, stress predicted from the calculated relationships agreed well with experimental data.

Haut and Little (1972) used the same reduced relaxation function as Woo *et al* (1981) and an elastic response of the form:

$$\sigma^e = B\epsilon^A \quad (3.9)$$

to model the mechanical behaviour of rat tail collagen. Although the model accurately predicted the hysteresis on unloading of the tissue, sinusoidal cyclic loading gave a

poorer agreement with experimental results. Jenkins and Little (1974) used a QLV expression similar to that of Haut and Little to successfully model the mechanical properties of bovine ligamentum nuchae. Once again the model was less valid when predicting stress during cyclic loading of the tissue.

Padras and Calleja (1990) developed a non-linear viscoelastic model to characterise the creep behaviour of human hand flexor tendons. The constitutive equation they derived included terms to account for previous stress history in a very similar fashion to QLV. A more complex form of elastic response was used than Fung (1972) and Woo (1981 and 1983) which was found to over estimate the values obtained from experiments, whilst the reduced creep function was correspondingly underestimated. Working from a basic assumption of progressive recruitment of individual viscoelastic fibres, the authors were able to derive the quasi-linear constitutive equation and concluded its validity in modelling parallel fibred collagenous tissue.

Barbenel *et al* (1973) used a viscoelastic phenomenological viscoelastic model to model the torsional load response of skin. Load relaxation experiments were used to establish constants in an expression for load incorporating a continuous logarithmic relaxation spectrum. Whilst the model accurately predicted the viscoelastic behaviour of the experimental results the non-linear elasticity of the tissue was not addressed, the model only being valid for strains similar to those of the experiments used to derive the spectral constants.

When conducting mechanical testing on ligamentous tissue there are several factors of the experimental protocol that must be carefully considered e.g. donor age, storage method, temperature when testing, isolated versus bone-ligament-bone preparations, method of area measurement and preconditioning of the specimen. Technical issues in ligament testing have been comprehensively reviewed by Butler *et al* (1978) and also by Viidik (1987).

The biochemical and histological changes in connective tissue associated with maturation and ageing have been shown to cause changes in the mechanical properties of these tissues (Viidik, 1982). Experiments on animal tissues have revealed that during maturation significant increases in the modulus of elasticity, stress at failure, strain at failure and energy to failure occur (Viidik, 1982; Vogel, 1983 and Woo *et al*, 1986). As

ageing progressed in the above studies a decrease in certain mechanical properties was noted, particularly in ultimate stress and the required energy to failure. The effects of antemortem activity levels have also been shown to have an important effect. Viidik (1966) compared the mechanical properties of tendon and ligaments in rabbits half of which had undergone a training cycle. The failure energy and failure load in both the trained tendons and ligaments were higher than the control group. The trained tendons were also found to have a higher modulus in the linear region, but ultimate failure was unaffected by the training regime. Woo *et al* (1980) found that the porcine flexor tendons of animals that had undergone training showed significant differences from a control group. Again, increases in failure load stiffness in the linear region and energy to failure were found in the exercised tendons whilst the ultimate strain was found to decrease. Analysis of the excised tendons also revealed that weight and cross sectional area increased with training as did the concentration of collagen in the tissue. The strength to percentage weight of collagen and stiffness to percentage weight of collagen ratios increased with training suggesting that exercised tendon tissue may have undergone microscopic and macroscopic strengthening changes.

Noyes and Grood (1976) studied the relationship between age and mechanical properties in human ACL specimens taken from young trauma victims (in which antemortem effects were excluded), amputees and cadavers. Large differences were found in the material properties between the older and younger age groups. The values of elastic modulus, maximum stress, strain energy to failure and strain at failure were all found to be larger in the younger group by factors of 1.7, 2.8, 3.3 and 1.2 respectively. Statistically significant correlation of the above parameters with age were found and the mode of failure was also seen to differ between the groups; ligament failure in the young and bone avulsion in the older specimens. Noyes and Grood accounted for the differences in the results from the above animal studies by suggesting that the human specimens had undergone true ageing with many associated factors affecting the tissue properties e.g. degenerative processes, disuse effects related to inactivity level and superimposed disease changes. Since older cadaveric specimens tend to be used, as they are most commonly available for testing, the authors recommended caution when extending the results of this type of tissue to that of a younger, more active and healthier population.

### **3.3.2 Evaluation of Ligament Function Using Strain and Force Measuring Devices**

Direct instrumentation methods have been widely used in biomechanical investigations of ligament function. Within the primary classification of strain and force measuring devices a diverse range of technologies have been employed to examine many aspects of ligament function, e.g., force and strain in prepared isolated specimens, strain and force in intact structures *in vitro* and *in vivo*, performance of ligament grafts and designs of orthoses.

Buckle transducers have been successfully used to measure tendon and ligament forces and by the nature of their design are suitable for *in vivo* investigations. Komi (1990) and Komi *et al* (1992) used an 'E' shaped strain gauged buckle to measure the Achilles Tendon forces in live normal subjects during walking, running, jumping and cycling of 3.6, 12.5, 2.6 and 0.8 body weight respectively. In a further study Fukashura *et al* (1993) used the same transducer to validate estimates of Achilles Tendon forces calculated from an inverse dynamics model of the ankle during jumping. An *et al* (1990) reported details of a modified one-piece design of buckle which reduced the problems of slippage and temperature compensation of the older 'E' shaped, two-piece transducers. The application of buckle transducers to measuring ligament forces is made more difficult by problems of access (usually associated with ligaments deep inside joint capsules), ligament shortening affecting load sharing in other ligaments of the same joint complex and impingement of the transducer on neighbouring bony structures giving false results. These problems were assessed by Lewis *et al* (1982) when measuring cruciate ligament forces in cadaveric knee ligaments. It was concluded that with careful placement and suitable transducer geometry the effects above could be minimised to acceptable levels, although only functional subdivisions, and not whole ligaments, could be instrumented. Barry and Ahmed (1986) reported design and calibration details of a miniaturised buckle transducer, specifically for use in small ligamentous structures, which they used to measure ligament forces in the anterior cruciate ligament *in vitro*. They highlighted the fact that slight stiffening of the ligament occurs when the transducer is in place and that a strict preconditioning regime of the

ligament-transducer system is important in maintaining a consistent transducer response between testing and calibration.

Several designs of tendon and ligament force transducers have also been developed that could be implanted *in vivo* into the required structures. Xu *et al* (1992) has reported on the performance of deformable metal foil with a curved geometry whilst Platt *et al* (1994) designed a flat device with a central angled portion to measure forces in the flexor tendons of ponies. Holden *et al* (1994) used a modified pressure transducer to make estimates of ACL forces in goats, at various flexion angles and when walking. Whilst all of the above devices used conventional strain gauge techniques, transducer-structure interactions lead to non-linearities in transducer response which necessitate calibration in isolated specimen configurations. In addition precautions have to be taken when implanting these types of transducer since their response is sensitive to their position and orientation, and also dimensions of the structure under study. As with buckle transducers a small amount of local shortening of the ligaments is unavoidable.

Strain measuring techniques have also been widely used to examine ligament biomechanics. Arms *et al* (1983) reported details of a design of transducer based on the Hall-effect. In this device, displacement of a miniature magnet relative to a Hall-effect semiconductor device produces a varying voltage that can be calibrated to strain when attached to a ligament. Whilst the resulting device, 10 mm long and 1.5 mm wide, is small enough to be implanted onto most ligamentous structures, fixation of this type of device is typically achieved with barbed spikes and suturing.

Arms *et al* (1983) successfully used this device to measure strain in the medial collateral knee ligaments of human autopsy specimens. Hall-effect displacement transducers have also been used in studies of lateral ankle ligaments *in vitro* (Cawley *et al* 1991 and Renström 1988). Fleming *et al* (1994b) used a Hall-effect transducer in conjunction with an implantable force transducer to determine zero strain references during *in vitro* mechanical testing of human ACL specimens. The force reading in this investigation was used as a switch to establish the zero-load length of the transducer, thereby establishing an absolute reference for strain measurements as opposed to relative measurements such as those used by Arms *et al* (1983). More recently, Hall-effect transducers have been used to investigate ligament mechanics *in vivo*. Beynnon *et al* (1992a) and Howe *et al* (1990) made measurements of human ACL strain *in vivo*.

The same group extended their analysis to the biomechanics of patellar tendon grafts used in ACL replacement. Beynnon *et al* (1994) measured strain in newly implanted ligament grafts during passive flexion tests. Although flexion strain behaviour similar to the normal ACL was found, the graft responses displayed an initial settling period on functioning. In a further study, measurements of ACL isometry measured intra-operatively were not well correlated with elongation of the graft measured directly during applied passive flexion movements due to altered kinematics of the ACL deficient knee (Fleming *et al*, 1994a). Measurements of isometry are used routinely prior to positioning of ACL grafts, but limitations in such techniques were identified by direct strain measurement in the ligament.

Hall-effect transducers have also been used to assess the performance of orthoses by measuring their effectiveness in reducing ligament strain, and therefore potential injury, during functional activities. Beynnon *et al* (1992b) evaluated seven designs of knee brace by measuring ACL strain in live subjects whose knees were subjected to varying known states of loading (anterioposterior shear, tibial torsion, etc.). These results show that even the most effective orthoses were found to have small strain shielding effects and no significant differences were found between cheaper ‘off the shelf’ and more expensive custom made devices.

Kogler *et al* (1995a and 1995b) measured strain in the plantar aponeurosis of cadaveric feet subjected to applied loads simulating standing. The average value of strain in the posterior PA was 2.62% with an applied vertical load of 450 N during simulated standing. The effects of different footwear and arch support orthoses in reducing PA strain were investigated. Designs of arch orthoses that supported the bony structures along the medial arch in the region of the navicular were found to be most effective in reducing PA strain, and thus were recommended for conservative treatment in cases of plantar fasciitis. Interestingly some designs of everyday footwear were found to give increases in PA strain when compared to the barefoot condition.

Hall-effect transducers are commercially available, however, they require specialist instrumentation and are, as a result, very expensive. Problems have also been identified when implanting them in areas where access is restricted (Kogler, 1995a and Colville, 1990) and the barbs used to attach them may not be suitable for flat, sheet like ligaments.

Mercury-in-rubber strain gauges or liquid-metal strain gauges (LMSGs) have been used to measure ligament strain. Originally developed for use in the automotive industry to monitor tyre deformation, these devices which can measure large strains and have a linear response soon found use in medical applications (Cobbold, 1974 and Janssen and Walter, 1971). Although slight modifications in design have been used by various investigators the principles of construction and operation are the same. A small length of microbore tube, usually of rubber, is filled with mercury and plugged at both ends with a metallic electrode. Lead wires soldered to the end electrodes connect the gauge to a strain gauge amplifier. Applied extension of the mercury column produces an increase in electrical resistance which can be measured and correlated to length.

In the medical field rigorous evaluation of the performance of LMSGs has been carried out. Stone *et al* (1983) compared the theoretical and experimental behaviour of gauges and found them to be in very close agreement. Brown *et al* (1986) conducted extensive static and dynamic calibrations, and also investigated effects due to misalignment of the implanted gauge and temperature drift. It was found that the gauges remained linear up to approximately 30% strain, dynamic response was unaltered below 50 Hz and misalignment of 15° produced approximately 1% change in output. An average temperature induced apparent strain of 0.185%/°C was found.

Youidin and Reich (1976) showed through theoretical analysis that the temperature drift in LMSGs was due to temperature induced changes in resistivity of the component materials and presented equations to compensate for these effects. They also described details of how to incorporate temperature compensating circuitry into the experimental instrumentation.

While the majority of LMSGs have been used in a quarter Wheatstone bridge circuit configuration, Meglan (1988) reported details of an alternative series circuit arrangement. Although absolute gauge length was easier to measure and the need for amplification was eliminated, the gauge output from such a circuit was non-linear and temperature effects were similar to that in conventional circuitry.

LMSGs have been used to measure knee ligament strain *in vitro* in humans (Edwards *et al* 1970; Kennedy *et al*, 1977 and Kurosawa *et al* 1991) where limited function was simulated by simple flexion and extension. A similar study was carried out *in vivo* in dogs where various forces and moments were applied to the lower limb

(Monahan *et al*, 1984). Colville *et al* (1990) simulated functioning human cadaveric ankles in which the lateral ligaments had been instrumented with LMSGs. Using ligament strain as an indicator to possible injury this study confirmed the clinically observed situation where the anterior talofibular ligament has a high propensity to injury. Ankle ligament strain was also measured by Albert *et al* (1992) in an investigation into possible detrimental effects of distraction conducted during arthroscopy of the ankle joint.

LMSGs have been used in both animals and humans to estimate *in vivo* ligament and tendon forces. This was usually done in two stages: 1. The ligament tendon strains were measured in the live subject, 2. After sacrifice or death the tendon or ligament specimen was tested in isolation and the tensile force estimates were obtained by matching the previously measured strains in each case. Riemersma and Lammertink (1988) described details of such a technique used to express tendon forces in terms of strain for tests on the digital flexor tendons of horses. Their methods included compensation for temperature effects and shifts in the tendon load-strain relationship when remounting the specimen for isolated testing, by matching secondary measurements of load using a buckle transducer. The shift in the tendon-load relationship was attributed to slight rearrangements of the tendon fibres on mounting for the isolated tendon tests. Jansen (1995) used these techniques to measure *in vivo* tendon forces in ponies during walking. These results were further verified by a kinematic and force plate model of the joint in question and good agreement between measured and computed tendon force was obtained. Due to inherent toxicity of mercury, LMSGs have not found common use *in vivo* in humans. Lamontange *et al* (1987 and 1993) used isolated tension tests on instrumented patellar tendon specimens to provide the necessary force-strain relationship to measure quadriceps force in living subjects. Although attempts were made to match the sizes of the live and cadaveric tendons, errors would have been introduced in assuming that the responses of each were identical.

Other methods of strain and force measurement in ligaments and tendon have found favour in the literature. Röntgenstereophotogrammetry (RSA) has been used to measure strain and force in human wrist ligaments *in vivo* during prescribed motions (Savelberg *et al*, 1991 and 1993). This technique uses biplane X-ray photographs to

measure the distances between ligament insertions marked with radio-opaque pellets. The distances are then reproduced in isolated tension tests to obtain estimates of force.

Conventional strain gauges bonded to bone in the vicinity of ligament insertion points have provided a method of indirect measurement of force, a secondary isolated force-strain calibration procedure being required in order to quantify the forces. This technique has been used to measure human knee ligament forces *in vitro* and tendon forces in horses *in vivo* (Barnes and Pinder, 1974 and France *et al* 1983). There is some question of the stability in the behaviour of foil strain gauges when bonded to an inhomogeneous material such as bone and also temperature drift is a major source of error in such experiments.

Optical methods of measuring local strain in ligaments and tendons has been widely used *in vitro* (Butler *et al*, 1984 and 1990; Derwin *et al*, 1994; Lanir and Fung, 1974; Noyes *et al*, 1984 and Woo *et al*, 1983). When using this method local strain of the tissue was monitored by measuring the distance between markers attached to the ligament surface as the material was loaded either in uniaxial or biaxial tension.

Video measurement of ligament strain has identified that the load strains are consistently and considerably less than those measured by grip to grip measurements of deflection by a factor of 0.4 - 0.5 (Butler *et al*, 1984 and 1990; Woo *et al*, 1983). Strain at the bone ligament interface was correspondingly higher than that in the mid-substance of the ligament. In addition, tensile strains have also been found to vary along the length of ligament specimens (Butler *et al*, 1990 and Woo *et al*, 1983). Optical access limitations have restricted video measurements of strain to *in vitro* use only. Recently Fujie *et al* (1995) have used a six-degree of freedom load cell to measure ACL forces *in vitro*. With this technique no contact with the ligament was necessary although severing of the other knee structures was required since the ACL forces were found by superposition.

### **3.4 MATHEMATICAL MODELLING OF THE FOOT**

Many attempts at explaining the structure and function of the foot using mathematical models have been made. The resulting models range from the very simple to the highly complex, although one may argue that no model of the foot could be

detailed enough. Zittlperger (1960) introduced the concept of representing the foot as an indeterminate space frame. Dissatisfied with the traditional architectural analogies of foot function relating to descriptions of 'arches', he attempted to introduce an analysis of internal loading and interpret this accordingly. In what was essentially a 3D graphical technique, he measured the positions of the centroids of area in the joints of an assembled foot skeleton with respect to local co-ordinate systems of the bones. A wire frame was then assembled to represent the 'paths' of stress in the bones. No muscles or ligaments were represented nor quantitative data presented. An inconclusive analysis of the framework only served to highlight the complexity of the modelling task but did, however, reveal some oversimplifications of previous analyses.

The most comprehensive mathematical analysis to date is that of Simkin (1982), who constructed a 3D model of the ligamentous foot in standing. Positional data of joint centres, points of load application, ligament insertion sites were obtained from dissections of cadaveric feet after conducting RSA to establish local co-ordinate systems for each bone. The non-linear load-deflection relationships for each joint studied were determined *in vitro* for 6 degrees of freedom (DOF). The model itself was solved incrementally using a matrix structural analysis program where the vertical input load was stepped 20 times to a value of 500N. The PA and LPL and deep transverse metatarsal ligament were modelled separately from the joint capsules as linear elastic members using the material constants of Wright and Rennels (1964) ( $E = 400\text{Mpa}$ ,  $\nu = 0.3$  and  $G = 0.4E$ ). Results included foot reaction forces at 6 points, bone excursions under load, ligament forces and 6 DOF joint loading data. Although the ligament strains were not presented directly they could be deduced from the bone movements. At 360N vertical loading, approximately 0.5 BW, forces of 260N and 67N were found for the PA and LPL respectively.

Morlock (1990) and Morlock and Nigg (1991) produced a model of the foot with 10 muscles, 5 ligaments and variable number of DOF from 1 to 18 (fig 3.9). The model was constructed around measurements made on a cadaveric foot specimen and was solved using the inverse dynamics approach. The loading in the PA was calculated from a formula suggested by Hicks (1953), which was an over simplification due to the other plantar ligaments being neglected. The model was applied to an athletic side-step movement of a subject when wearing different footwear. Maximum PA forces of

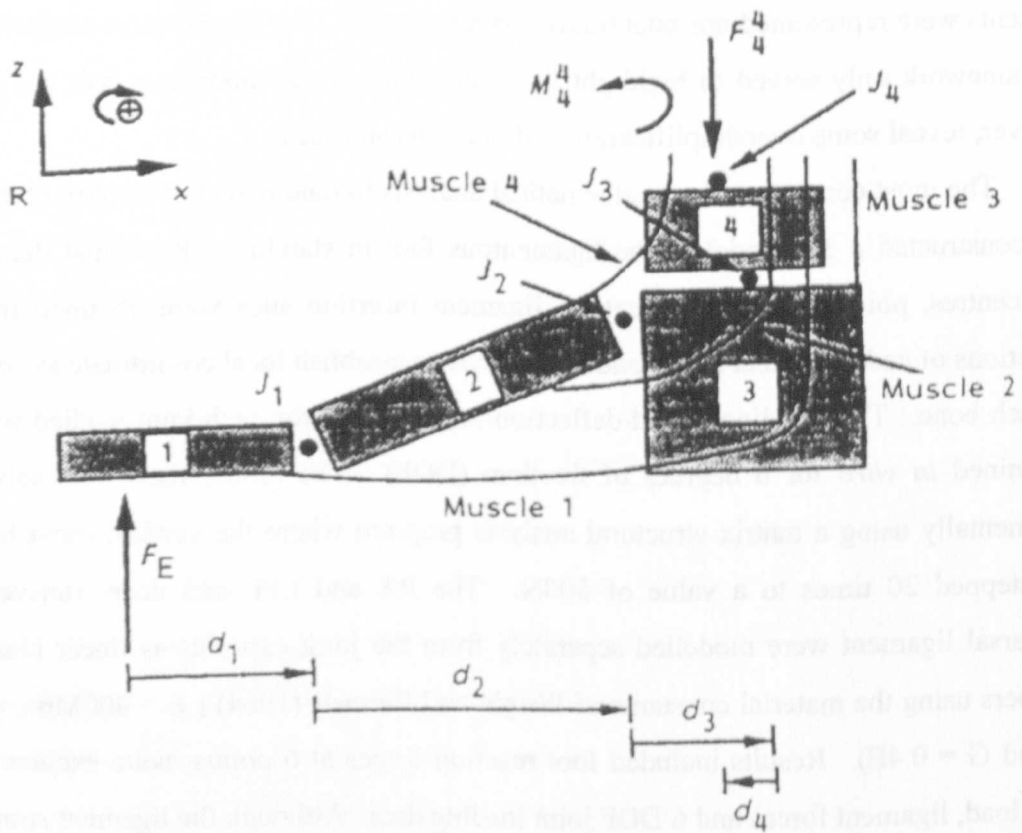


Figure 3.9 Schematic diagram of a model used to estimate forces in the joints, muscles and one ligament of the foot for an athletic side-step activity:  $F$  = forces,  $M$  = moments,  $J$  = joint reactions and  $d$  = joint positions (from Morlock and Nigg, 1991).

2200N for a 'stiff' shoe and 2400N for a 'torsion' shoe were calculated. Muscle forces, joint moments and reactions and length changes in the ankle ligaments were also presented. The effect of model complexity and sensitivity to input variables was explored well. The 4 segment 6 DOF model with maximum muscle force optimisation was suggested to be the most suitable representation.

Salathé *et al* (1986) produced a 3D indeterminate model to investigate PA loading and metatarsal bending. The metatarsals were treated mechanically as curved beams whilst the PA was modelled as a linear elastic member. The model included the facility to examine the effects of inversion/eversion during forefoot loading and the windlass mechanism. Some of the input data however was taken liberally from the literature ( $E_{PA} = 250\text{mpa}$  from Woo *et al* (1981)) whilst the remainder was estimated. Normalised metatarsal reaction forces and PA tensions were calculated. Although actual results could not be taken directly due to the unrealistic tissue parameters used, the model proved useful in comparing the patterns of loading for different foot orientations. PA forces of 2.1 times the applied load were found in the heel raised position and the 1st and 5th metatarsal heads were found to be the most highly loaded. Salathe *et al* (1990) adapted the above model to study the shock absorbing properties of the foot during running, where extensor muscle tendons were added to the anatomical description of the model. Constitutive relationships for the tendons and ligaments were taken as proposed by Fung (1972) and Woo (1981). The model was solved numerically using tissue properties not specifically derived for the foot. Impact force values predicted by the model were too high due to the gross simplification of omitting the tissue properties of the heel pad from consideration in the reaction dynamics.

Scott and Winter (1993) included the properties of the plantar soft tissue in a 3D kinematic model of the foot. Motion analysis and force plate measurements for 3 walking subjects provided the kinetic and kinematic input to the model. Properties of the plantar fascia and joint positions were taken from the literature. The model was used to produce estimates of loading at 7 support points, angles and moments at the joints. No internal structures, passive or active, were represented.

Modelling of the ankle joint complex was conducted by Allard *et al* (1985) in a kinematic analysis comprising 14 bones and 60 ligaments. RSA analysis and subsequent dissection was used to find the positions of the ligament insertions and joint

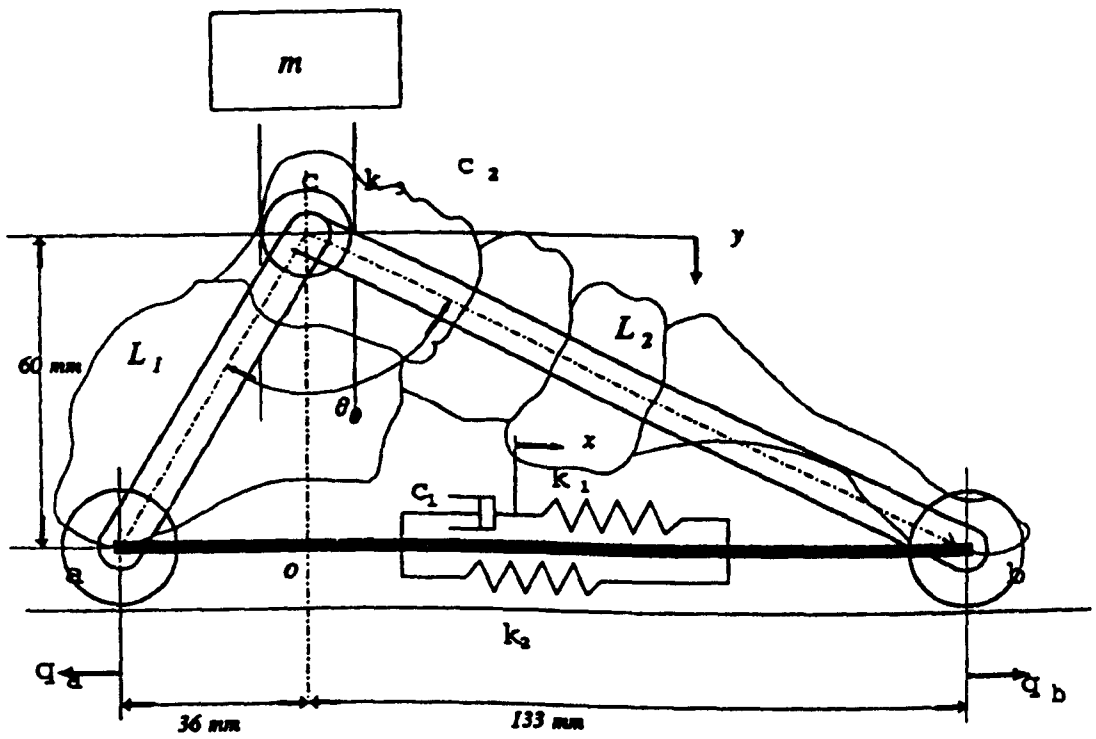


Figure 3.10 Two dimensional model used to investigate the shock absorbing properties of the plantar aponeurosis:  $m$  = mass,  $k$  = stiffness elements,  $c$  = viscous damping elements,  $q$ ,  $x$ ,  $y$ ,  $\theta$  = displacements (from Kim and Voloshin, 1995).

axes in 3D. A simulation program was written to compute excursions of the ligament insertion sites for applied passive joint rotations. Results were presented for strain values in the ankle ligaments for 20° dorsiflexion and 50° plantarflexion of between 0.6% and 29%. Important shortcomings of the model were that no forces were applied to the foot and that the RSA technique was only applied at one position i.e. the test movements were truly simulated.

Procter (1980) devised a model of the ankle joint complex to estimate internal forces during walking. The TC and TCN joints were modelled in detail but the foot was assumed to be rigid below this level. Muscle lines of action and joint surface profiles were determined from cadaveric data and force plate data and motion analysis was used to provide the remaining inputs to the model. The indeterminacy was reduced by grouping the muscles and assigning weighting factors based on tendon cross sectional areas. Estimated peak joint reaction forces in the TC, TCN and subtalar joints of 3.2-4.6, 1.4-2.9 and 2.2-3.3 times body weight respectively were found. Although the ankle ligaments were not represented in the model, the implications and anticipated consequences of their inclusion on the results were discussed.

Modelling of the specific function of the PA in foot biomechanics has received some attention in the literature. In a recent study by Kim and Voloshin (1995) the effects of clinical PA severing on the dynamic load bearing properties of the foot were investigated. Experimental data from impact tests on a living subject were used to solve a 2D model using Lagrangian mechanics and a numerical technique (quasilinearisation). The PA was modelled as a viscoelastic Kelvin solid (fig 3.10). Stiffness of the PA was found to be  $8.1-11.5\text{kNm}^{-1}$  and a PA force of 14% of the applied vertical load was found. Sectioning of the PA increased the vertical ankle deflection by 20% from 3.8 to 4.5mm. PA release was not found to have a significant effect on shock absorption, as measured by changes in acceleration of the tibia. Although viscoelasticity of the tissues was addressed the assumed elastic response was linear unlike that of real tissue.

A simple 2D model was used by Simkin and Leichter (1990) to explore the effects of calcaneal inclination on the energy storing capacity of the foot. The PA was represented by linear and exponential springs and the foot was exposed to 4000N vertical loading. Both models showed a distinct peak energy storage at a calcaneal angle of 21.3°. The model, however, vastly overestimated the actual amount of energy

stored by the foot at 80-160J (compared to 10J in Ker *et al* (1987)), because complete collapse of the structure took place. The value of stiffness taken for the PA of  $100\text{kNm}^{-1}$  was unjustified.

Forces in the forefoot were obtained from a simple model by Stokes *et al* (1979). The geometry was obtained from cadaveric data and measurements on living subjects and the force data was obtained using modified force plates to measure load under the metatarsal heads. The PA was not modelled, perhaps an over assumption considering toe-off was being modelled (windlass mechanism). Jacob (1989) carried out a similar analysis for the first two rays of the foot and calculated muscle forces, joint reaction forces in the MTP and PIP joints and bending of the metatarsals. After inspection of the results of the experiments Jacob decided not to model the effect of the PA since he considered the metatarsal bending to be the predominant force carrying mechanism.

Models have been used to examine the effects of orthoses and footwear on the internal loading of the foot. Veres (1977) used a 2D graphical analysis of a simple 2 segment model of the foot containing 1 idealised plantar ligament. The effects of varying the static support conditions, shoe sole type and heel shape were investigated. The internal loading of the ligament was shown to vary markedly in some of the modelled conditions e.g. introduction of a rocker on the sole of the shoe produced a 40% reduction in the plantar ligament force. Despite the simple nature of the model Veres was able to show how an orthotist could deliberately alter the internal forces by inducing subtle changes in the external loading.

Li and Ladin (1992) used a 2D model of pronation/supination to explore the effects of different combinations of compliance under the foot at heel strike. Lagrangian mechanics were used to solve the model whilst motion analysis data was used for verification. Results confirmed that a more compliant lateral portion controls pronation by effectively shifting the centre of pressure medially, i.e. closer to the TCN joint axis, thus reducing the pronating moment. Simplifications of the model included the omission of muscle forces, a linear subtalar joint stiffness and the static nature of the analysis.

Nakamura *et al* (1981) used a 2D non-linear finite element (FE) model of the foot and shoe to study how the pressures at the foot-shoe interface varied with elastic stiffness of the sole (clinically significant to the treatment of diabetic feet). The sole

stiffness was seen to have a significant effect and non-linear sole materials gave values close to optimum.

Lam *et al* (1987) also used an FE model in the assessment of designs of polypropylene ankle-foot orthoses. A 2D linear FE mesh representing the soft plantar tissue, bone and orthosis was constructed. A variety of loading conditions was applied to the model and stress in the orthosis and ankle joint were used as criteria to optimise the orthosis design. The model was recognised by the author as being an over simplification of the foot structure and no ligaments were represented. The model of Patil *et al* (1993) was even more simplified. The authors computed stresses in bone using FE analysis, where the foot was modelled as one single piece of material. The type of model described above may be suitable for continuous media such as the plantar fascia, but is of very limited use in representing an assembled structure of discrete mechanical elements as a homogeneous mass of idealised material.

A more applicable use of the FE method was demonstrated by Yettram and Camilleri (1992) in an investigation of internal stresses in the calcaneus. Ligamentous and muscular forces acting on the calcaneus were estimated using optimisation techniques. A cadaveric calcaneus was sectioned and digitised to give accurate 3D bone geometry. A mesh was set up and solved to obtain the internal stress patterns which correlated well with patterns of trabeculae seen in bone sections from the literature. Another successful application of the FE method, combined with optimisation techniques, was demonstrated by Goel *et al* (1993) when modelling the spine. A detailed structural analysis was performed which was able to include muscular and ligamentous elements to reveal the nature and effects of postural forces in the lumbar vertebrae.

Recent advances in computer technology have made processing power more readily available. Complex graphics based numerical models of the musculoskeletal system have been developed. As in other models, the inverse dynamics approach is used along with optimisation algorithms to solve the equations giving force values in the structural elements. One of the main advantages of this technique is that through a developed user interface, data visualisation is now more immediate and the effects of introducing changes in variables can be directly witnessed through graphical animation. Using this type of model the effects of surgical procedures have been investigated and

detailed motion of the lower and upper limbs have been animated (Chao *et al*, 1993; Delp *et al*, 1990 and Kepple *et al*, 1994).

### **3.5 CLINICAL DISORDERS OF FOOT LIGAMENTS**

Foot pathologies are both common in occurrence and varied in nature. The high incidence of foot disorders in the population is of significant clinical importance. Conditions affecting the ligaments of the foot include injury, overuse syndromes, neurological trauma and congenital deformities.

The high incidence of lateral ankle ligament injury has been well documented and may be as high as 7/1000 population per year (Hølmer *et al*, 1994). Depending on the severity of the injury conservative or surgical reconstruction may be necessary to prevent chronic lateral instability of the ankle in the long term (Karlsson *et al*, 1995 and Jackson, 1988). The plantar ligaments are also affected by injury, most notably the PA. Plantar fasciitis is a condition whose mechanism has been linked to repeated overloading and micro-tearing of the PA and is a common over-use syndrome in athletics (Andrews, 1983 and Torg *et al*, 1987). Symptoms include pain and swelling on the plantar surface of the calcaneus in the region of the medial calcaneal tuberosity (the insertion site of the PA). Often a calcaneal bone spur in this region is visible on X-rays in cases of late development. Conservative management of plantar-fasciitis such as rest, arch orthoses, strapping, anti-inflammatory drugs and local steroid injections have a high success rate (Campbell and Inman, 1974; LeMelle *et al*, 1990 Newell and Miller, 1977 and Roy, 1983). Only in intractable cases is surgical release of the PA used as a therapeutic procedure. Although good clinical results are achieved by PA sectioning it has been shown that this leads to flattening of the longitudinal arches (Daly *et al*, 1992). Rupture of the PA in athletes, due to trauma, has also been reported in the literature (Ashstrom, 1988 and Leach *et al*, 1978). Rupture and injury to the tarsometatarsal ligaments are less common and are almost always the result of violent trauma to the forefoot (Meyer *et al*, 1994 and Shapiro *et al*, 1994).

Disruptions in the normal functioning of the extrinsic musculature of the foot can have secondary effects on the ligaments. Traumatic rupture of the tibialis posterior tendon has been shown to cause progressive onset of flat-foot deformities and associated

stretching of the plantar ligaments (Cozen, 1965; Mann, 1983; Mann and Thomson, 1985 and Funk *et al*, 1986). Surgical intervention by means of a tendon transfer procedure is often carried out in cases of severe deformity. Tendon transfers are also performed in cases of muscle imbalance caused by peripheral nerve damage, muscle loss or neuromuscular disorders (polio, stroke) and congenital malformations such as club foot (Mann and Plattner, 1988). The complex biomechanics of transferring otherwise healthy tendons away from their natural point of action to replace diseased or damaged tendons and the effects of sudden loss of muscle function have not been investigated.

### **3.6 SUMMARY**

Experiments on both cadaveric and live feet have shown that the plantar ligaments are vital to the normal load bearing function of the foot. Due to the nature of previous experimental methods, little quantitative data exist on ligament function in the foot other than for the PA. In addition there has been scant biomechanical testing of the ligamentous tissue of the foot and force estimates in the plantar ligaments for functional activities have not been made. While simplification of the foot structure is inevitable when modelling, no model of the deeper plantar ligaments has been formulated. Also the modelling of surgical procedures and injury to the plantar ligaments has not been attempted to date.

# CHAPTER 4. MECHANICAL TESTING OF INTACT CADAVERIC FEET

## 4.1 INTRODUCTION

The mechanics of load support in the foot have been the subject of investigation for over 100 years. EMG experiments have revealed that the principal mechanisms of load support are ligamentous, the muscles forming a dynamic reserve called upon during periods of excessive loading (Basmaijan & Stecko, 1983 and Walker, 1991). Several investigators have used a selective dissection process to explore the relative contributions of the plantar ligaments of the foot to normal weight bearing function (Ker *et al*, 1982; Haung *et al*, 1994 and Walker, 1991). While such tests provided broad conclusions of the relative importance of each of the plantar structures, the precise functional interrelationships in the intact foot could not be found. These studies were also limited in terms of the range of test activities carried out. The aim of the experiments described below was to gain a detailed, quantitative understanding of the biomechanics of the plantar ligaments and passive support mechanisms. Methods of direct instrumentation of the ligaments of cadaveric feet subjected to simulated functional loads, positions and movements were adopted.

## 4.2 MATERIALS

All experiments were performed on cadaveric foot specimens which were made available from the pathology department of a Glasgow hospital. The feet were removed at the time of post-mortem examination, frozen as soon as possible afterwards and then were stored at -20°C in a dedicated tissue freezer until time of testing. Numerous previous investigations have shown that freezing tissue specimens at -20°C and subsequent thawing prior to testing has an insignificant effect on the measured mechanical properties, provided precautions are taken against tissue dehydration

The mechanics of foot support in the laboratory

for over 100 years. The mechanical

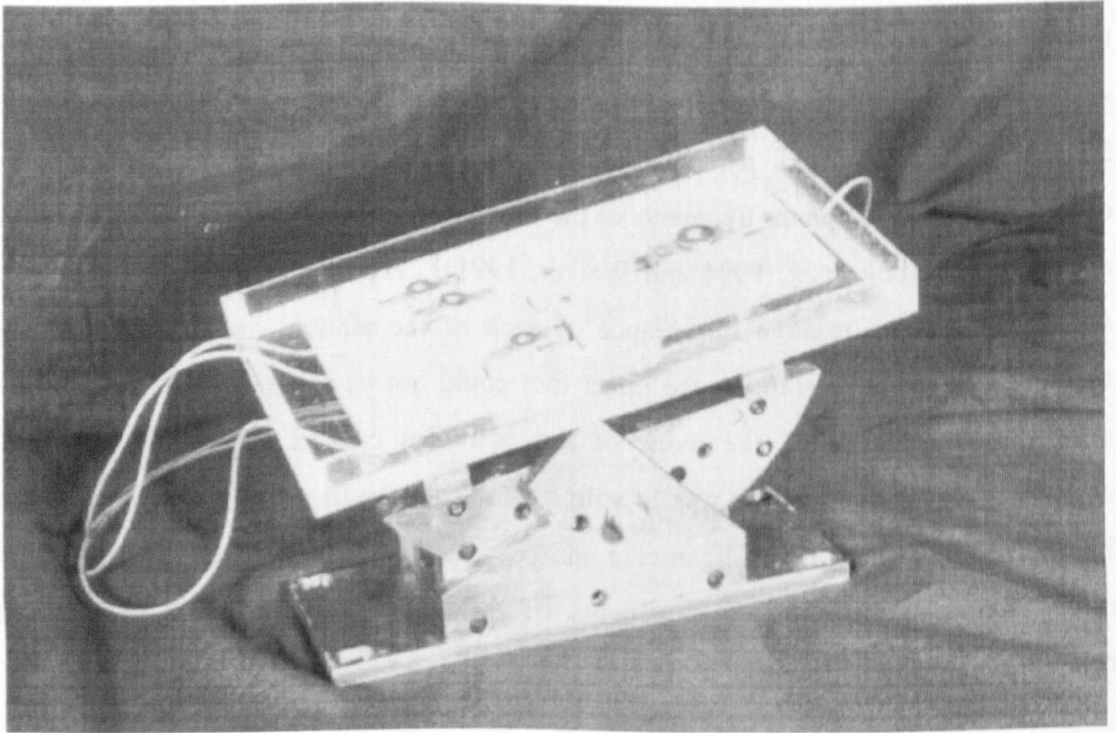


Figure 4.1 Adjustable foot support platform and plantar load cells.

All experiments were performed on laboratory foot pressure measurement  
equipment from the pathology department of a Glasgow hospital. The test was repeated  
in the time of post-menstrual examination. Forces were measured at various angles and  
were stored in a 256-bit digital data base. The time of testing (10 minutes)  
previous investigations have shown that foot pressure measurement at 20°C and  
independent showing that the testing has an important effect on the measurement  
techniques provided. The test results are shown in the following table.

Galante, 1967; Noyes and Grood, 1976; Rigby, *et al*, 1959; Viidik and Lewen, 1966 and Woo *et al*, 1986).

Test No.	Subject No.	Side	Sex	Age	Height	Cause of death	Ambulatory before death
1	107	L	M	67	-	Heart failure	✓
2	104	R	M	90	-	Bronc. Pneum.	✓
3	113	L	M	53	-	Heart failure	NK
4	108	L	M	82	-	Pneum.	NK
5	107	R	M	67	-	Heart failure	✓
6	131	L	M	62	5'9"	NK	NK

NK = Not known.

Table 4.1 Details of the foot specimens tested

Although more than 6 feet were made available during the time of testing some specimens were rejected as being abnormal due to pathological changes, e.g. hallux valgus, pes cavus. Time constraints also limited the number of feet tested. Only limited patient data were disclosed and are presented in table 4.1. To limit the effects of inactivity, attempts were made to find out whether the subjects were ambulatory before death. Where this was not possible, feet displaying visible signs of muscle wasting were rejected from consideration in the study. The average age of the specimens was 70 years. Only in one case was any information on the height and weight of the donor obtained. The specimens used in tests 2 - 6 underwent all experimental permutations whilst foot number 107L was not tested under conditions of applied tibial torsion.

### 4.3 METHODS

#### 4.3.1 Loading System

An Instron® 4505 load frame was used to apply vertical compressive forces to the prepared foot specimens. A computer control system was used to drive the load



Figure 4.2 A foot specimen mounted in the Instron® test machine. Muscle forces were simulated using static weights applied to tendons with wire traces.

frame with a variety of deflection or force profiles depending on the nature of the test. Cross head speeds of up to a maximum of 1000 mm/min (16.6 mm/s) allowed physiological rates of loading to be applied although dynamic overshoot of the cross head occurred at higher speeds. An Instron<sup>®</sup> 10 kN load cell was used to measure forces applied to the tibia of the feet tested. This load cell was accurate to within  $\pm 0.25\%$  of the maximum reading and was insensitive to off axis loading. Extension measurement was performed with an automated digital encoder circuit on the cross head drive mechanism which was accurate to  $\pm 0.02$  mm over 0 - 10 mm, and  $\pm 0.03$  mm from 10 - 99.9 mm. Calibration of the load and extension systems was carried out at regular intervals by a qualified service technician.

The tests took place below the cross head and so the load cell was mounted to its underside. Loads were applied into the foot via a set of specially designed multi-functional couplings. These could provide complete universal motion of the foot in two planes or restricted motion in one plane, or completely rigid fixation. The toe - in/toe - out angle was adjustable and a roller thrust bearing, incorporated into the design, allowed tibial torsion to be applied during loading with minimal friction. The configuration of coupling used varied with the function being simulated (see section 4.3.5).

The platform of Walker (1991) was used to provide adjustable support of each foot specimen (fig 4.1). This platform, made of steel, allowed the foot to be tilted in the transverse and sagittal planes in 5° increments. The support plate in contact with the foot was modified to make the area of the contact larger, to cope with larger specimens, and more rigid to reduce deflections during high loading. A tray to catch any blood or contaminated water was also incorporated into the design.

Four load cells, as used by Walker (1991), for measuring forces under selective regions of the foot were incorporated into slots in the support surface. Spaces between the load cells were filled in with small blocks of polyethylene to ensure a continuous support surface. Details of the design, construction, and calibration of these transducers have been described elsewhere (Walker, 1991). Measurements of plantar force were used in this study only in the set-up of the experiments to highlight areas of uneven loading. Inclusion of the measurements into the results would have served only to



Figure 4.3 Foot mounted in the Instron® during the gait experiments. The foot is shown in the toe-off position with the pulley system attached to the Achilles tendon

repeat the results of Walker, (1991). Measurements of the plantar force cannot give quantitative conclusions of ligament mechanics directly.

Muscle forces in the foot were applied with either static weights or a pulley arrangement directly attached to prepared muscle tendons. Apparatus was specially designed to support the weights and pulley arrangements. This consisted of a 420 mm diameter aluminium plate with a central hole which was bolted onto the underside of the crosshead over the load cell. Moveable guide blocks fitted in two circular grooves to hold the wires used to attached the weights to wires fastened onto the tendons. The guide blocks were adjustable to any angle around the tibial axis and were positioned so as to approximate physiological lines of tendon action. Forces were applied by adding calibrated 50 N weights to the tendons wires, where rollers incorporated into the guide blocks minimised frictional effects.

To apply larger muscle forces to the TACH and TA tendons during gait simulation a load-measuring pulley system was designed. This consisted of two couplings for interfacing the tendon and the upper load plate, a load cell in series with both, and a 5:1 purchase pulley block. The tendon load cell interface was of a 'double see-saw' design in order to distribute force equally in the four cords used to attach it to the tendon. The load cell was of the standard ring design (inside diameter = 30mm, outside diameter = 40mm, width = 15mm), was made from stainless steel and had a rating of 2000 N. Calibration of the tendon load cell was performed before each test run (see section 4.3.3). The tendon load cell was mounted in grips designed to allow only the application of tensile forces. The pulley block was attached to the load cell and then to the upper load plate with a high-strength bolted fastening. Again, the position of the bolt on the load plate was adjustable to allow physiological lines of force action to be reproduced. The assembled test set-up, with weights applied to two muscle tendons, is shown in figure 4.2. Figure 4.3 shows the pulley system being used to simulate toe-off, where the heel is raised above the support platform.

## **4.3.2 Development of Strain and Force Transducer System.**

### **4.3.2.1 Ligament strain gauge construction.**

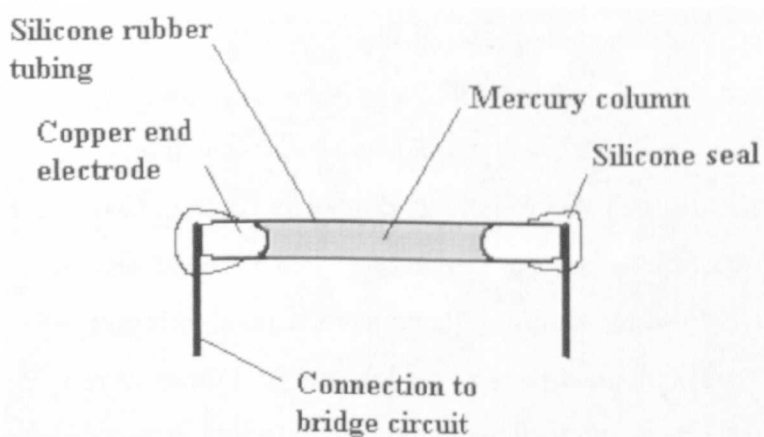


Figure 4.4 Schematic drawing of LMSG construction.

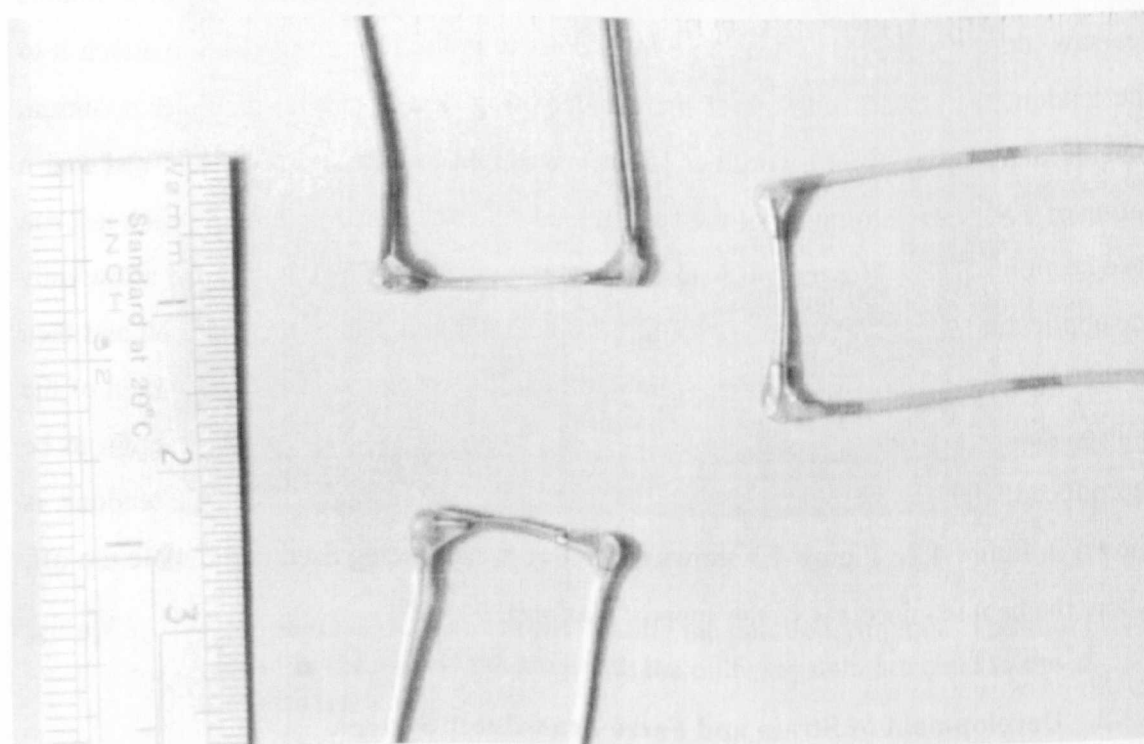


Figure 4.5 LMSGs of different sizes.

Commercially available ligament strain gauge transducers are based on either Hall-effect or LMSG technology. To overcome the disadvantages of fixed size, implantation problems, possible non-linearities and prohibitive cost of commercial transducers it was decided to design and manufacture purpose built ligament strain transducers. The simplicity of construction and the ability to use existing strain gauge circuitry with LMSGs were major factors in selecting this design of transducer for development.

Considerable effort was expended on refining the methods of construction used in order to obtain gauges with a stable and reliable function. The basic methods of construction were adapted from Meglan *et al* (1988). Each gauge is composed of: (1) a piece of silicone rubber tube, 0.51mm ID by 0.91mm OD of desired length for the gauge body (Sani-Tech, Lafayette, NJ, Part Number STHT-C-020), (2) purified mercury inside the tube, (3) solid copper end electrodes, 0.711 mm x 3 mm long pushed into the ends of the silicone tubing, (4) Insulated 7 x 0.2 mm multi-core copper wire soldered to the end electrodes and (5) a small amount of clear air-curing silicone rubber to seal the gauge ends (Silastic<sup>®</sup>, Dow-Corning<sup>®</sup>, Michigan, USA). A diagram of a completed gauge is shown in figure 4.4.

The construction procedure was as follows: The gauge body was cut to a length of 6 mm longer than the required gauge length of the transducer. Transducers with five sizes of gauge length were made, namely 14, 9, 8, 6 and 4 mm (figure 4.5). Copper wire, used for the end electrodes, was filed to a rounded end and cut to the required 3 mm in length. The insulated wires were then carefully soldered to the square end of the electrodes at right angles. Ultra-pure mercury was then taken up in a small syringe fitted with a blunted size 22 needle which was gently pushed into one end of the silicone tube. Mercury was injected into the tube until full, any over spill being caught in a plastic tray. In order to get the end electrodes into the tube without damage or trapping air, dipping in a bath of xylene was carried out to expand the silicone tube. When dilated, the silicone tube was carefully gripped with tweezers while the electrode was gently inserted. When the xylene evaporated the silicone shrank back to its original dimensions thus sealing the mercury. This process was repeated for the opposite end when removed from the syringe. Finally a small amount of liquid silicone rubber was placed around each tube end to ensure a good seal. Due to the toxicity of mercury and

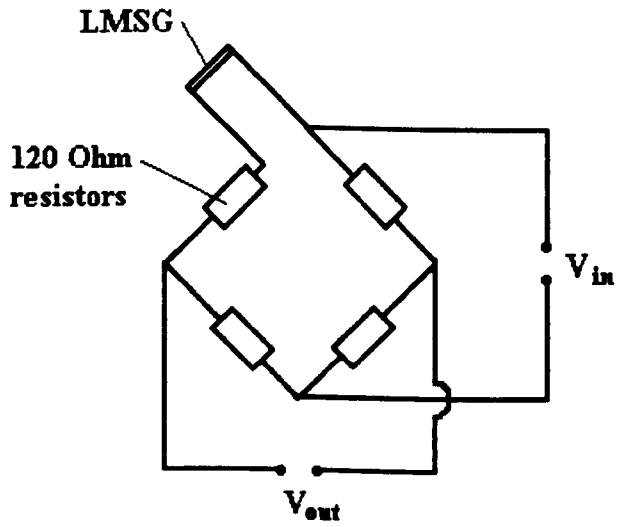


Figure 4.6 LMSG and Wheatstone bridge circuitry.

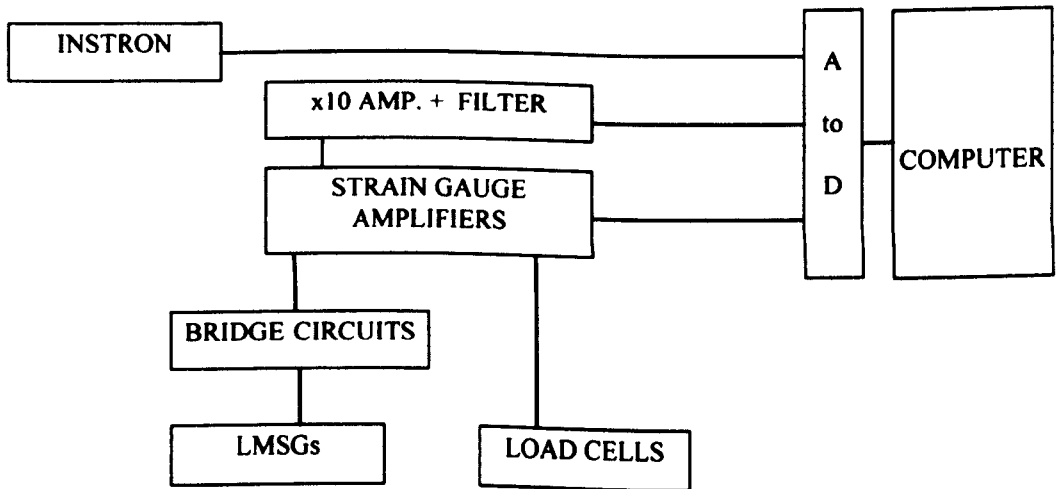


Figure 4.7 Schematic diagram of transducer instrumentation and data acquisition system.

xylene this whole process was carried out in a fume cupboard and suitable protective clothing was worn.

In the finished gauges the mercury was under pressure as a result of the xylene expansion process. This was favourable in a number of ways: (1) on stretching of the gauge the chance of pressure drops giving rise to voids in the mercury column was reduced, (2) the oxidation of the mercury was reduced since oxygen could not diffuse across the pressure gradient between gauge and atmosphere and (3) the pressure was able to overcome the high surface tension of mercury to ensure good electrical contact with the end electrodes.

Some problems had to be overcome during development. In early attempts contamination from mercury migrating towards the end electrodes dissolved the soldered joints resulting in gauge failure. To overcome this a thin film of epoxy was applied to the soldered area under a magnifying lens. To further prevent migration of mercury under the tube, the silicone rubber sealing process was introduced. Some of the prototype gauges showed signs of localised leaking through the tubes near the end electrodes. It was found that the tweezers used to handle the tubes were causing damage. This was remedied by placing soft PVC sleeving over the gripping area of the tweezers. Due to an amalgamation reaction between the copper of the electrodes and the mercury, voids in the mercury column and subsequent gauge failure did eventually occur after 12 - 15 weeks. The option of eliminating this by using platinum or silver electrodes was rejected on the grounds of cost. Gauges were manufactured for each test two days before hand and were used only once, hence the problem of deterioration of gauge performance with time did not arise (see appendix 1).

Pertinent features of the finished design included: miniature construction (diameter of  $\approx 1$  mm), manufacture in a range of sizes, lead wires at right angles for implantation in areas of restricted access and excellent leak resistance.

#### **4.3.2.2 Amplification circuitry**

Each gauge was used in a quarter bridge arrangement in a conventional Wheatstone bridge circuit. This enabled conventional strain gauge amplifiers to be used in conjunction with the transducers. Since the actual resistance of each LMSG is low

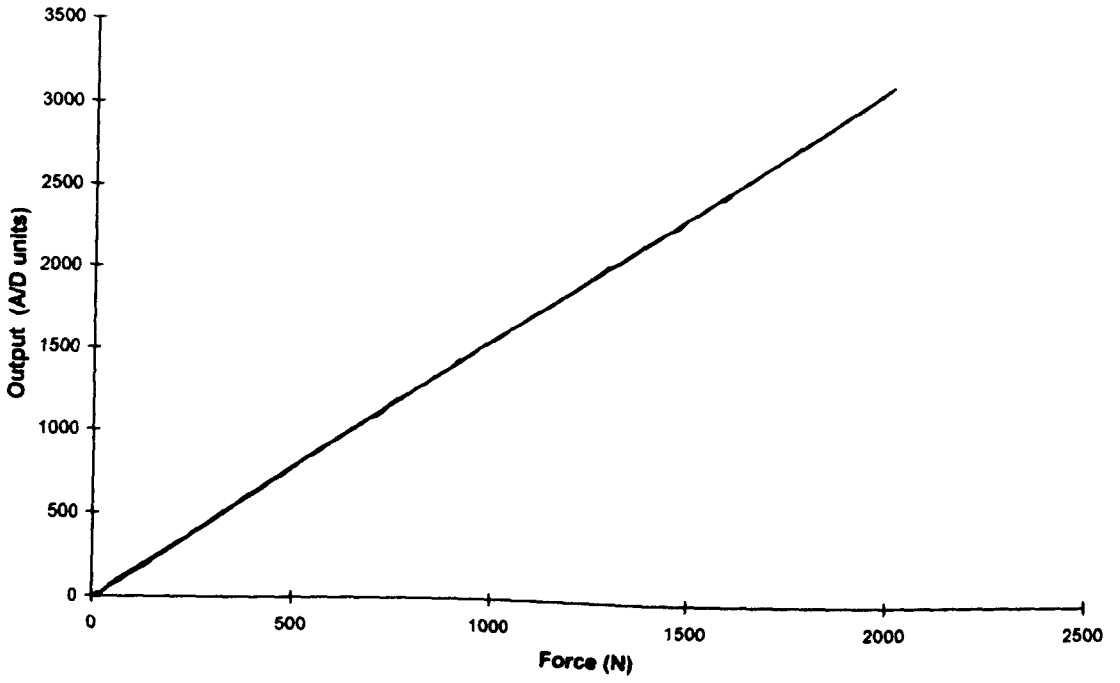


Figure 4.8 Calibration curve for tendon load cell (loading and unloading)

( $0.6\Omega$ ) compared to the nominal  $120\Omega$  for a metal foil strain-gauge, each LMSG was placed in series with a  $120\Omega$  resistor in a dummy full bridge circuit (fig 4.6). An enclosing box was designed to hold this circuitry for three overriding reasons: (1) thermal drift in the  $120\Omega$  resistors was reduced by having all of them encapsulated in a sealed environment, (2) remote implantation of the LMSG's necessitated removal of the gauges whilst the circuit remained functioning (a switch was incorporated to facilitate temporary removal of the LMSG from the circuit) and (3) prevention of contamination from fluids. The gauges were interfaced with the bridge box on a long lead cable fitted with a 24-way D connector. All cables were screened to reduce noise.

The five channels from the bridge box were connected to the strain gauge amplifiers where bridge voltages of 3V and gains of 500 - 2k were used. Further  $\times 10$  amplification of the signals were then performed with a separate amplifier which had a 20 Hz low-pass filter built in to reduce stray noise in the system. Identical strain gauge amplifiers were used to provide signal conditioning for the other strain gauged transducers, i.e. tendon load cell and plantar force transducers.

#### **4.3.2.3 Data acquisition system**

The signals from the LMSGs, other force transducers along with the analogue signals of extension and load from the Instron® test machine were all sampled with a data acquisition system. This consisted of a personal computer fitted with a 12 bit A/D conversion card running in-house data acquisition software (Philips, 1989). The layout and connections of all the electronic circuitry and data acquisition system can be seen in figure 4.7.

#### **4.3.3 Calibration of Transducers**

Calibration of the plantar load cells and tendon force transducers were carried out using the Instron load frame to apply a known force cycle. Calibration procedures of the plantar load cells were conducted as described by Walker (1991). The tendon load cell was calibrated to a tensile force of 2000 N before each test. Five loading and unloading force cycles were applied and linear regression analysis was used to find an

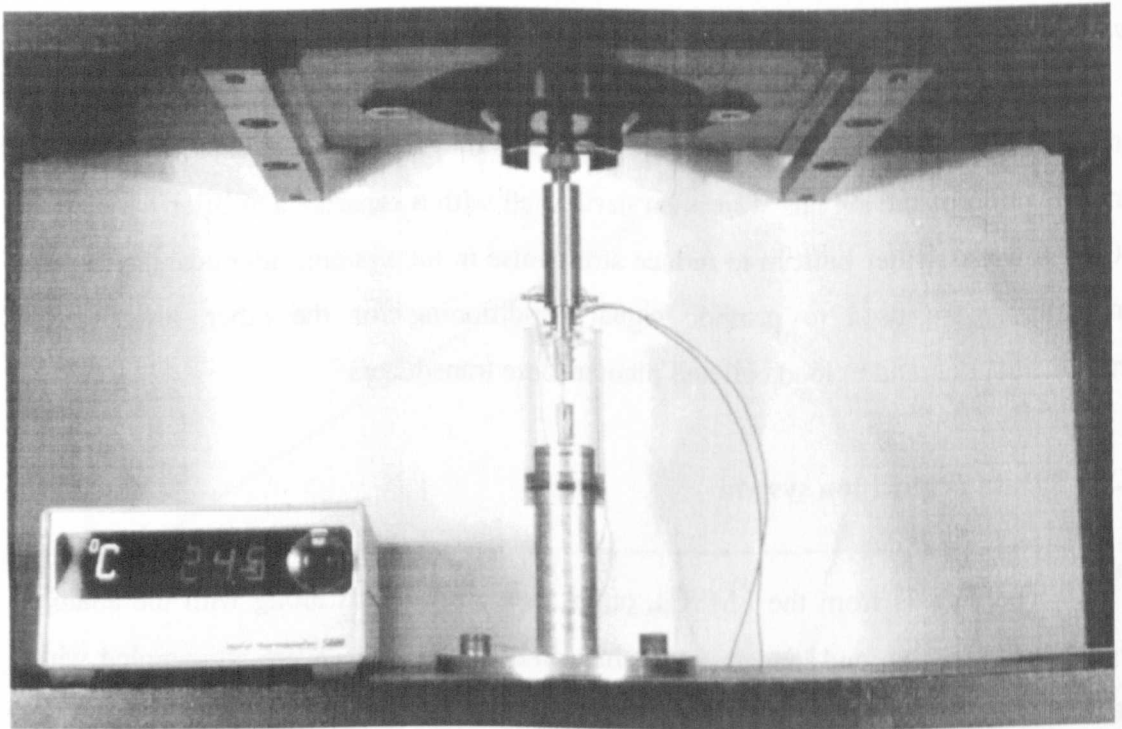


Figure 4.9 Calibration of an LMSG in the Instron® load frame. The LMSG is held in the grips located inside the perspex chamber. The 100N Load cell is shown at the top of the picture.

average calibration factor. The transducer was seen to have a stable and highly linear response ( $R^2 = 0.993$ ). Details of the calibration coefficients can be found in appendix 1. A transducer response curve used to derive this information can be seen in figure 4.8. Calibration was conducted in the Instron as this method was semi-automated and provided more than acceptable accuracy (0.25% of reading).

Rigorous calibration and performance evaluation was carried out on the LMSG transducers. Details of the calibration procedures are given below, while an assessment of other performance criteria such as temperature effects and forces required to deform the LMSGs are presented in appendix 2.

Calibration of LMSG's was conducted in the Instron® for a number of reasons: (1) extension of the LMSG's was possible to an accuracy of  $\pm 0.02$  mm, (2) the semi-automatic nature of the test provided a fast calibration, (3) specified rates of extension could be applied, (4) the force required to deform the gauge could be measured and (5) digital sampling of the Instron® signals and gauge output allowed calibration to a larger number of data points than conventional methods. The LMSGs were mounted in specially made grips in the Instron that held the gauges straight by the end electrodes. A retractable perspex chamber was incorporated to provide secondary containment in case of mercury spillage and to maintain the temperature of the calibration approximately constant (reduce effects due to convection and draughts). The calibration apparatus is shown in figure 4.9. After first allowing to settle the temperature of calibration was recorded to the nearest 0.1 degree using a thermocouple installed in the perspex chamber in the vicinity of the LMSG body. Starting from a small pre-strain of approximately 5% the LMSGs were extended cyclically by 20% at a rate of 4% per second. Data were sampled at 10 Hz and 5 cycles were applied giving a total of approximately 500 data points for calibration. This process was repeated 5 times for each LMSG and the calibration results were averaged.

From Ohm's Law it can be shown that the voltage increase in the Wheatstone bridge circuit is given by:

$$\Delta V = \frac{GV_b}{R_b} \Delta R \quad (4.1)$$

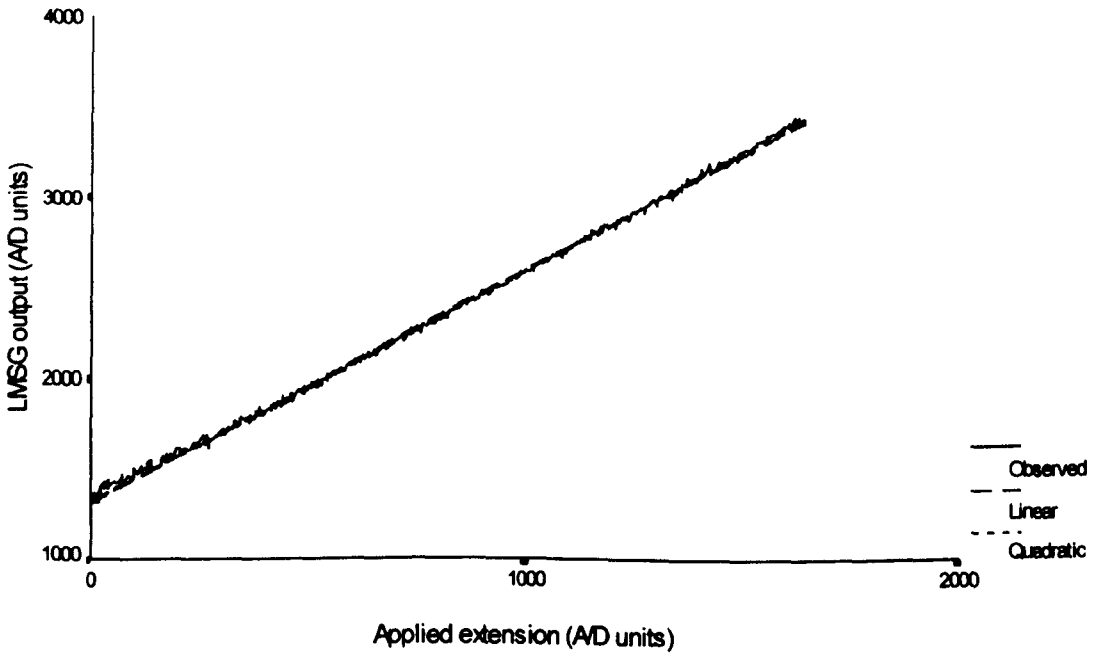


Figure 4.10 Calibration curve for 14mm LMSG (No.55) showing linear and quadratic regression lines.

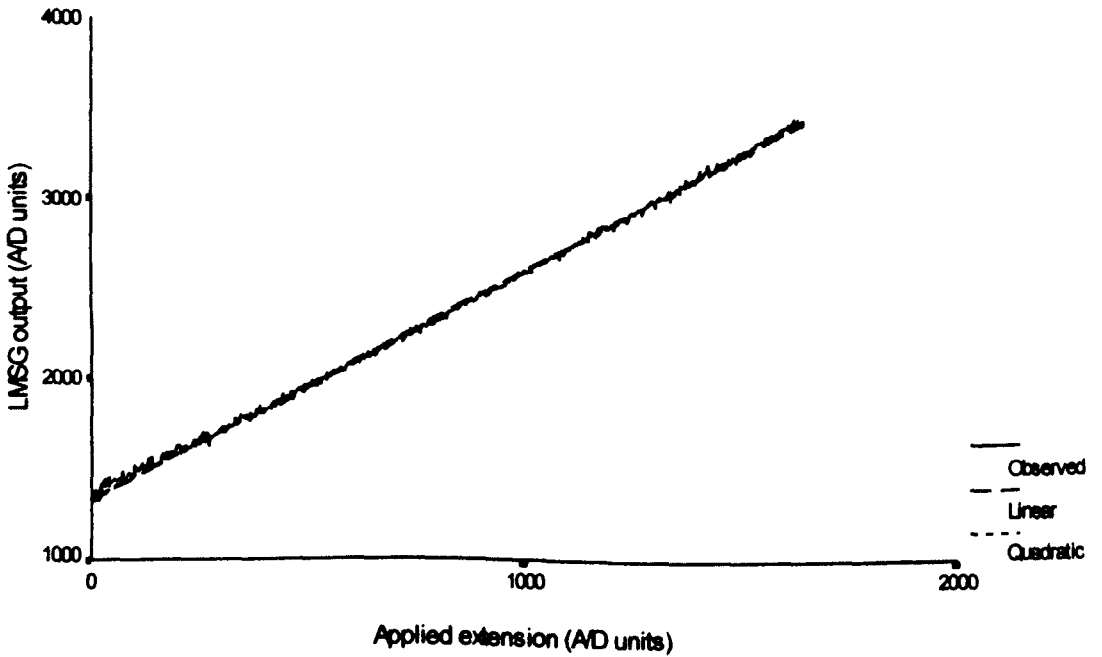


Figure 4.11 Calibration curve for 4mm LMSG (No.41) showing linear and quadratic regression lines.

Where  $\Delta V$  = change in voltage,  $G$  = amplifier gain,  $V_b$  = bridge voltage,  $R_b$  = nominal bridge resistance, and  $\Delta R$  = change in resistance of the LMSG. It may be shown from first principles that the change of resistance of the LMSG is related to length in the following relationship (Stone *et al* ,1983 and Cobbold, 1974):

$$\frac{\Delta R}{R_0} = 2\left(\frac{\Delta L}{L_0}\right) + \left(\frac{\Delta L}{L_0}\right)^2 \quad (4.2)$$

Where  $\Delta L$  is the change in length and  $R_0$  is the resistance at the initial length  $L_0$ . Rearranging and substituting (4.2) into (4.1) the result gives:

$$\Delta V = C_1\Delta L + C_2\Delta L^2 \quad (4.3)$$

Where constants  $C_1$  and  $C_2$  are determined from curve fitting of the calibration data. It has been shown that for small strains the effect of the second (squared) term in (4.3) can be neglected, resulting in a linear relationship between LMSG output and strain  $\varepsilon$  (Cobbold, 1974, Stone *et al*, 1983 and Youdin and Reich, 1976):

$$\Delta V = C_c \varepsilon \quad (4.4)$$

Where  $C_c$  will be termed the ‘calibration constant’ for the LMSG.

The raw calibration data were subjected to both linear and quadratic regression to test the above hypothesis using a computer statistics package (SPSS for Windows®, Version 6.1). The calibration data were found to be very repeatable, free from hysteresis effects and highly linear ( $0.946 < R^2 < 1.000$ ). Although the quadratic curve fitting procedure gave a slightly better fit in some cases the  $R^2$  values were not significantly closer to unity to warrant calibration using the non-linear analysis. Calibration curves for two gauge sizes are presented for both linear and quadratic regression in figures 4.10 and 4.11.

The calibration coefficients were found for each LMSG using the following expression:

$$C_c = \frac{4096 e}{p \varepsilon_A} \quad (4.5)$$

Where  $e$  = extension during calibration,  $p$  = pen setting on the Instron<sup>®</sup> console and  $\varepsilon_A$  = applied strain compensated for 5% pre-strain (i.e. 19%). The value 4096 was the resolution of the 12 bit A/D converter in A/D units. Calibration data for the gauges used during the tests is presented in appendix 1.

It has been shown that temperature has an effect on LMSG output which can be accurately described by temperature induced changes in the resistivity of mercury (Jansen 1994, Meglan *et al* 1994, Riemersma and Lamertink 1988 and Youdin and Reich 1976). The temperature dependence of the LMSG output is given by:

$$\Delta V = C_c \varepsilon (1 + \alpha(T_i - T_0)) \quad (4.6)$$

Where  $T_i$  is the test temperature,  $T_0$  the temperature of calibration and  $\alpha = 89.10^{-5} \text{ }^\circ\text{C}^{-1}$ , the temperature coefficient of the resistivity of mercury. Equation 4.6 was used to conduct temperature compensation of the test results. For further details on temperature compensation see appendix 2.

#### 4.3.4 Preparation of Cadaveric Foot Specimens

Each foot specimen was thawed overnight at room temperature before testing. A dissection protocol was followed to prepare each foot for mounting into the Instron<sup>®</sup> test machine. The tibia and fibula were exposed and cleared of muscle to a level of 5 cm above the ankle joint centre. This ensured minimum disruption to the lines of action of the tendons as they entered the foot below the ankle joint. The TA, TP, PL and FDL tendons were folded over to form loops, glued with cyanoacrylate adhesive and whipped with cotton and more adhesive to form a strong bond. Steel wire traces, used to apply static forces to the tendons, were then attached to the loops with braided polyester cord (breaking force = 256 N). The pulley arrangement was attached to the TACH using four double figure-of-eight stitches through and around the structure of the tendon with the polyester cord. The double see-saw device ensured that equal tension was applied in all

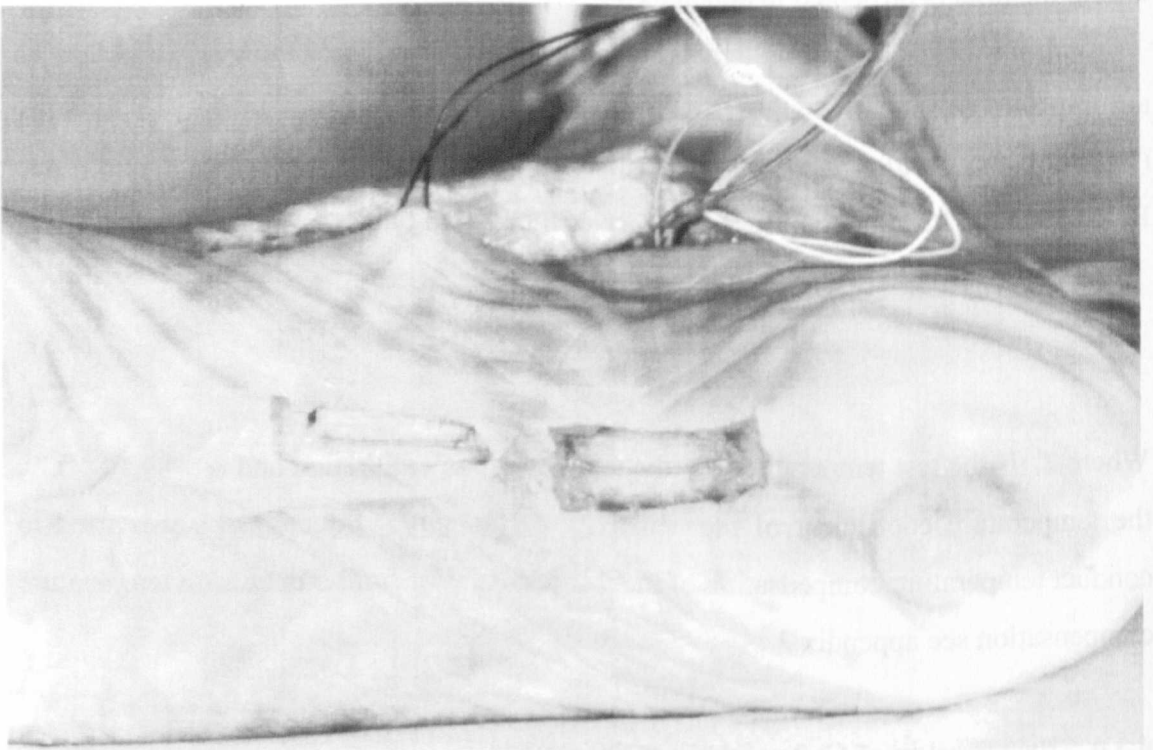


Figure 4.12 LMSGs implanted on the plantar aponeurosis. Windows were cut in the skin and plantar fascia to access the ligament. LMSG wires were routed subcutaneously to the medial incision.

eight cords thus reducing the risk of breakage. With eight cords the breaking force of the attachment was approximately 4 kN, allowing physiological force levels to be applied. The tibia and fibula were cut to a length 200 mm from the ankle joint centre and potted in a brass collar using bone cement. A specially made coupling on the top of the collar provided an attachment site to the Instron<sup>®</sup> load-cell. Great care was taken to align the collar parallel with the tibia in both the sagittal and coronal planes.

The techniques used to implant the LMSGs were assessed and tested using embalmed cadaveric material made available by the Department of Anatomy at the University of Glasgow. The work of Haung *et al* (1993), Ker *et al* (1989) and Walker (1991) have established that the PA, LPL, SPL, and CNL are important to the biomechanics of the foot. Anatomically these ligaments are the most prominent on the plantar aspect of the foot. Dissection of three cadaveric feet and inspection of numerous prepared dissections confirmed that the structures were separate and clearly identifiable. A qualitative assessment of anatomical variations of the ligaments was also performed at the same time, e.g. presence of medial and lateral portions of PA, differences in ligament shape and fibre density.

During implantation of the LMSGs attempts were made to keep the structure of the foot as intact as possible. Access to the PA was achieved through small windows in the plantar fascia in the sole of the foot. Due to the length and shape of this structure it was decided to implant two LMSGs in tandem along the longitudinal axis of the foot. Access to the LPL, SPL and CNL were made through a medial incision along the bony margins separating the abductor hallucis muscle from the bony extremities. With a limited amount of further dissection and retraction of the incision good access to the deep plantar ligaments was achieved. Since no structures were divided and only a very small amount of tissue was removed the anatomy of the foot was left essentially intact. The intrinsic musculature was not sacrificed and hence the passive support properties were preserved.

The size of gauge used and the position of implantation on the ligament was determined using a set of reproducible normalised placement parameters derived from dissections of embalmed foot specimens (Note: For the derivation of these see appendix 3). After first marking the position of implantation of the LMSG on the ligament using a fine indelible ink pen, each LMSG was cemented onto the ligament using a small

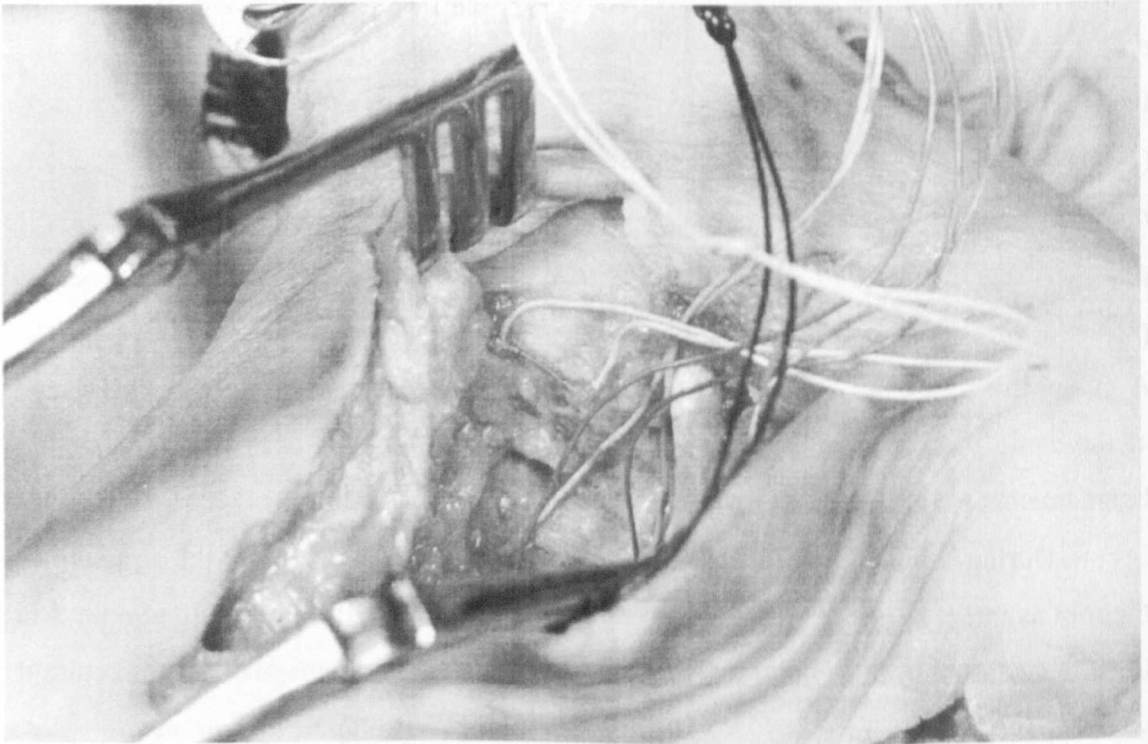


Figure 4.13 LMSG implanted in the calcaneonavicular ligament as seen through the medial incision. Note also the retractors and the wires leading to the LPL and SPL transducers.

amount of cyanoacrylate adhesive (Loctite® Prism 406) (figs 4.12 and 4.13). The use of an adhesive in preference to suturing was again established from trial implantations conducted on embalmed specimens. The following disadvantages were found with the suturing technique: (1) difficult and time consuming to complete on the LPL and SPL due to space limitations, (2) loosening of sutures occurred with time, (3) Rotation and subsequent 'snaking' of the LMSG at the suture, (4) inability to accurately determine the depth of the suture in the ligament and (5) disruption and crushing of the ligament fibres. The adhesive technique offered an instant fixation solution and had the advantage of attaching the gauge to several ligament fibre bundles, thus potentially averaging the strain in each and hence reducing the effects of uneven fibre recruitment. Although the local properties of the ligament were altered at the attachment site, the diameter of adhesive patch used was small compared to the length of the ligament and the distance between insertions. The following additional precautions were taken to ensure an effective bond: (1) the ligament surface was carefully cleaned of loose connective tissue, (2) the ligament surface was lightly dried at the attachment site using cotton and (3) a primer was used to ensure a strong bond with the silicone rubber gauge end material (Loctite® Prism 770 Polyolefin Primer). Great care was taken to align the ends of the LMSG's so as to eliminate apparent strains due to lateral shifts and fixed rotations. The foot specimen was palpitated to ensure that the ligaments were unloaded and the LMSG's were implanted with a small pre-strain of approximately 5%. This was done to reduce the chance of the LMSG becoming slack during testing and giving a false strain reading. The lead wires of each electrode were bent to conform to the interior of the incision to minimise any movements and routed out of the foot through the medial incision. The wires from the PA gauges were routed subcutaneously in the sole to the medial incision. Finally retraction was removed and the skin flap of the medial incision was closed over the wires.

During testing the foot specimen was enclosed in a polythene cover to prevent dehydration and was lightly sprayed with a 0.9% buffered saline solution at regular intervals. After the test had finished the foot was removed from the rig and the integrity of LMSG fixation was inspected. No incidence of gauge loosening was witnessed during the six tests. The gauges were then removed by peeling off the by lead wire, some of which were re-calibrated (see appendix 2). After removal of the tendon

apparatus and bone pot the specimens were moistened with saline, sealed in airtight bags and re-frozen to  $-20^{\circ}\text{C}$  in the neutral position.

### **4.3.5 Test Activities**

#### **4.3.5.1 Introduction**

Dynamic loading cycles were applied to the foot specimens to simulate the functions of standing and walking. Additional aspects of the tests examined the effects of foot position, tibial rotation and toe dorsiflexion on ligament strain. Each of the loading patterns was repeated five times per test to examine the reproducibility of the ligament strains and also to precondition the tissues. An additional preconditioning loading cycle was also applied before data were collected. Although the dynamic response of the Instron<sup>®</sup> load frame was not suitable for applying very fast rates of loading, near physiological rates were usually attainable. When the cross head was moved a constant rate of displacement was always prescribed, i.e. the test machine was operating in displacement control mode with load limits. A zero reference loading and position arrangement for ligament strain was established for each separate set of activities (20N vertical load in the neutral position with no applied muscle forces). A thermocouple placed into the lateral incision monitored the temperature of the specimen used to correct the LMSG outputs.

#### **4.3.5.2 Standing**

Each foot specimen was tested in five positions, namely neutral,  $5^{\circ}$  inverted,  $5^{\circ}$  everted,  $10^{\circ}$  dorsiflexed and  $10^{\circ}$  plantarflexed. In the absence of specific body weight data for each specimen a constant body weight of 700 N was assumed. Force was assumed to be equally distributed between each foot and so a 350 N force was applied to simulate standing on both legs. To explore ligament strains at higher loading 700 N force was also applied to the specimens in each of the five positions (equivalent to a subject standing with only one foot in contact with the ground). To account for the slight anteroposterior muscle forces due to the continuous postural adjustments seen in

live subjects a 50 N force was applied to the TA and TACH tendons. An additional vertical force of 20 N was applied to the specimen to act as a reference load. This level of force corresponded to the approximate weight of the specimen and was used because the true zero-loading position was difficult to obtain reliably in a laboratory set-up. The foot is rarely completely unloaded in nature in any case, e.g. when sitting some of the weight of the lower limb is supported by the feet resting on the floor. The rate of loading was chosen to simulate a subject rising from a sitting position to reach standing in under 2 seconds. This corresponded to a crosshead speed of between 100 and 200 mm/min. Ligament strains in the neutral position with 20 N load applied were used as the zero strain references for this set of activities. The reference position was reproduced after every increment in position of the foot.

The effects of tibial torsion were explored as follows: The Instron<sup>®</sup> load frame was programmed to apply a constant level of force of firstly 350 N and then 700N while the tibia and fibula were rotated externally and internally by 10°. This was achieved using the thrust bearing coupling described in section 4.3.1. Five full cycles of rotation were applied. The ligament strain reference was taken when the foot was loaded with 20 N in the neutral position with zero applied tibial torsion.

With the foot in the neutral position 50 N and 100 N simulated extrinsic muscle forces were applied with calibrated weights. The tendons were loaded in the order TA, TP, PL and FDL. To simulate true standing five 350 N vertical load cycles were applied using the same rates as in the first set of tests. Again, a small 20 N load was used at the start of the test. The zero strain reference for this set of activities was, again, the foot placed in the neutral position with 20 N applied and with zero applied muscle force.

To fully explore the effects of the windlass mechanism on the foot ligaments toe extension (dorsiflexion) was applied with the foot in a simulated standing position. With constant 350 N and 700 N vertical loads applied, approximately 45° toe extension was introduced using a thin metal plate to articulate the toes in unison. Five cycles of extension were applied. Once more a force of 20 N applied to the foot in the neutral position was used as the zero strain reference position.

#### **4.3.5.3 Gait**

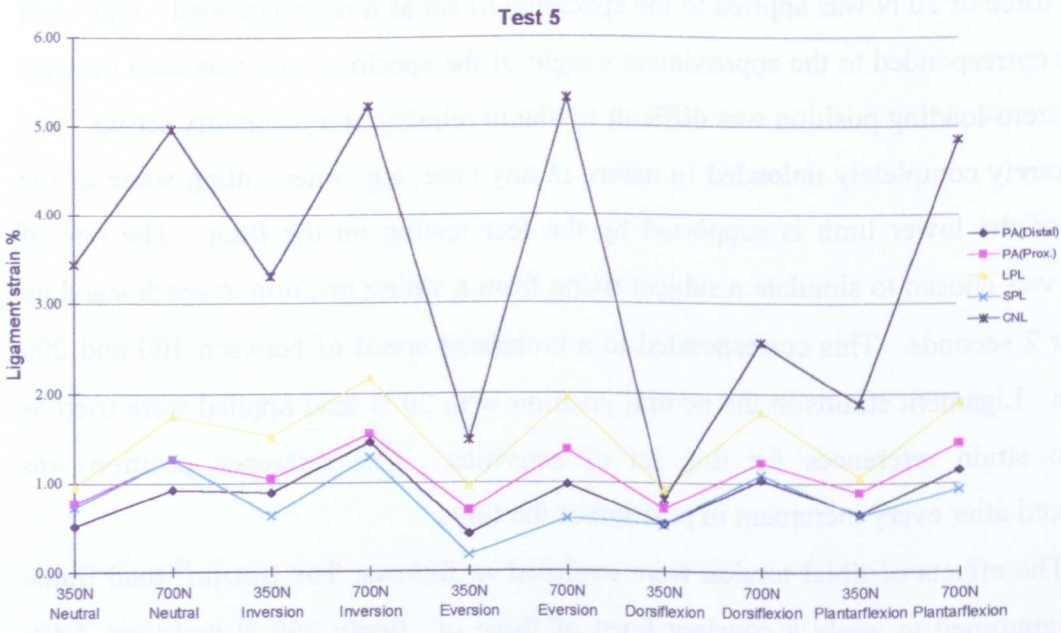


Figure 4.14 Strains in the foot ligaments during standing in test No.5. The specimen was loaded in five different positions.

In order to simulate gait it was necessary to apply physiological levels of tendon force whilst moving the position of the centre of pressure,  $x_{cp}$ , along the longitudinal axis of the foot. Due to practical limitations the gait cycle had to be simulated in three stages: (1) toe-off, (2) mid stance and (3) heel strike. To avoid overshoot a crosshead speed of 100 mm/min was used. This gave a cycle time of 2 seconds maximum, approximately a third of the physiological rate for these activities.

With the foot in the plantarflexed position, simulating toe-off, the tendon load cell was attached to the TACH. The length of the tendon apparatus was adjusted to give a net 700 N force at the ball of the foot when the heel was just above the surface of the support platform, and the load cell force was noted. Load cycling from 20 N to the above predetermined force was carried out five times (Note: This effectively simulates toe-off activity in reverse). A coupling hinged in the sagittal plane eliminated bending forces due to mal-alignment being transmitted to the load cell (fig 4.3). The ligament strain reference position described earlier was used for all the gait simulations, i.e. 20 N load in the neutral position with zero muscle force.

For simulation of mid stance the tendon apparatus length was adjusted so that half the maximum toe-off TACH force was applied with the foot in the neutral position. The load cell force was noted and used as a mean value around which the applied force was cycled, simulating the oscillatory nature of the vertical force in mid stance. A cyclic net force of  $700 \pm 140$  N was applied five times to the specimen starting from a 20 N reference load.

Heel strike was simulated by attaching the tendon apparatus to the TA tendon and loading the foot in a dorsiflexed position. The length of the tendon apparatus was adjusted to give a net force of 700 N at the heel with the forefoot just above the support platform. The vertical load was cycled five times from 20 N to 700 N (heel strike action was simulated in reverse).

## **4.4 RESULTS**

### **4.4.1 Introduction**

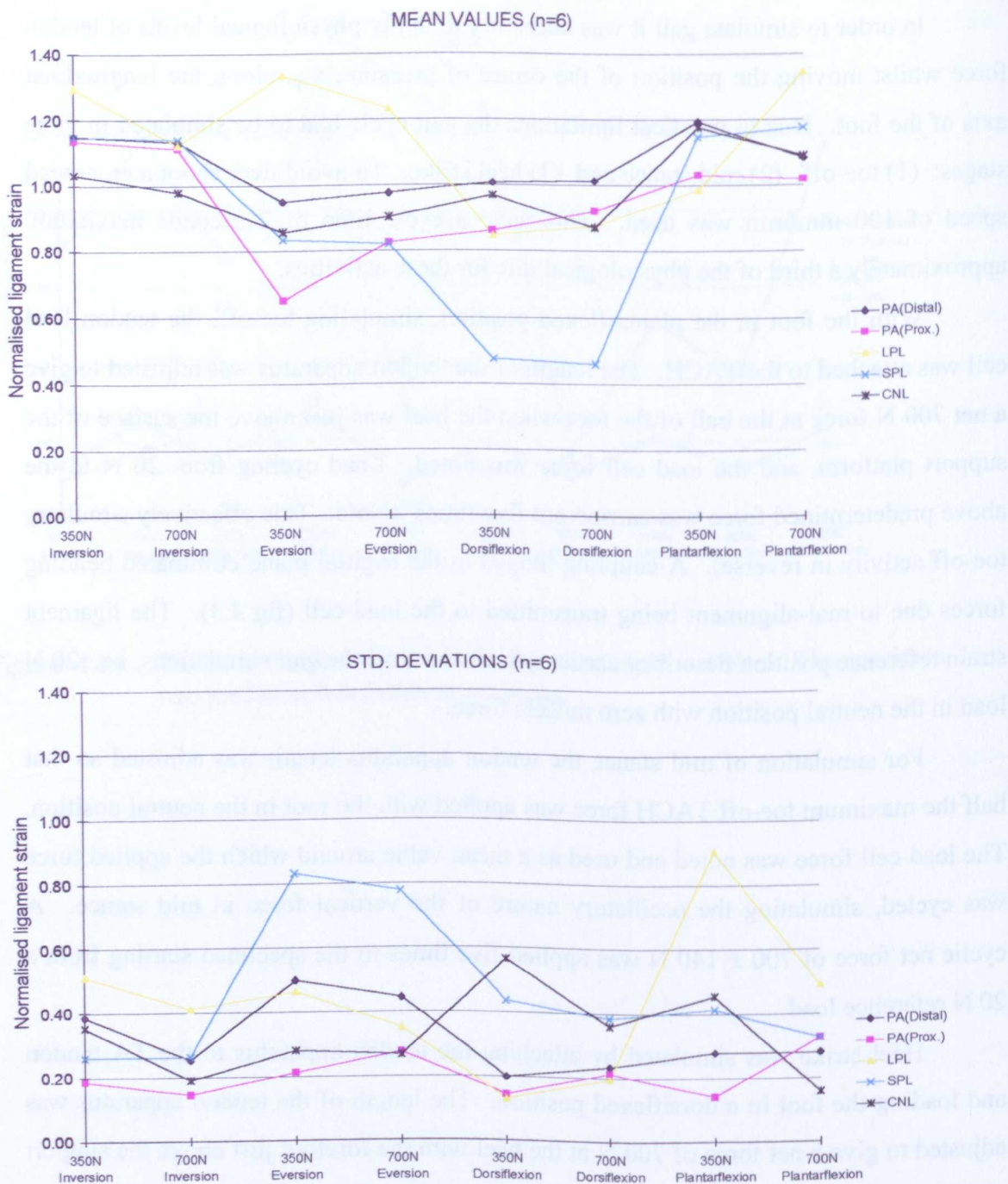


Figure 4.15 Means and standard deviations of the normalised ligament strains of feet loaded in different positions (n=6).

Due to the small number of specimens tested, only limited statistics were performed on the test results. The raw results are presented as line graphs showing ligament strain versus test condition for each of the five groups of tests, i.e. foot position, tibial torsion, muscle forces, toe extension and gait. The strain values were also normalised with respect to specific reference states, to quantify the natural spread of the data, to highlight trends and aid interpretation. Averaged normalised strain results will be presented in the main body of the text along with a typical sample of raw data for one of the specimens. The reader is directed to appendix 4 where the entire set of raw data is graphically presented.

The reader should note that negative strain values do not represent compressive loading in the ligaments. By definition negative strain values merely represent a reduction in length of the ligament with respect to the reference position. No negative strains in excess of -5% were noted and hence these results retained their validity within the data set (LMSGs were implanted with approximately 5% pre-strain).

Ligament strain was manually noted from the test records using the data acquisition software previously described. Processing, calibration, temperature compensation and presentation of the data was performed with spread sheet software (Microsoft<sup>®</sup> Excel 5.0). In all tests it was noted that maximum strain values, and minimum values where appropriate, were always coincident with maximum levels of applied force and it was these values that were presented. A full discussion of the test results follows in Section 4.5.

#### **4.4.2 Foot Positions**

Actual ligament strains in each foot position at the 350 N and 700 N loading levels are presented for test N<sup>o</sup>. 5 in figure 4.14. On inspection of the results it was seen that the levels of strain in each structure contained a wide spread between specimens. It is suggested that this was due to natural variation within 'normal' population as seen in many biologically related measurements and as a result of the localised nature of the strain being measured. In order to compensate for these effects the ligament strains were normalised with respect to the strains in the neutral position at 350 N and 700 N

Test 5

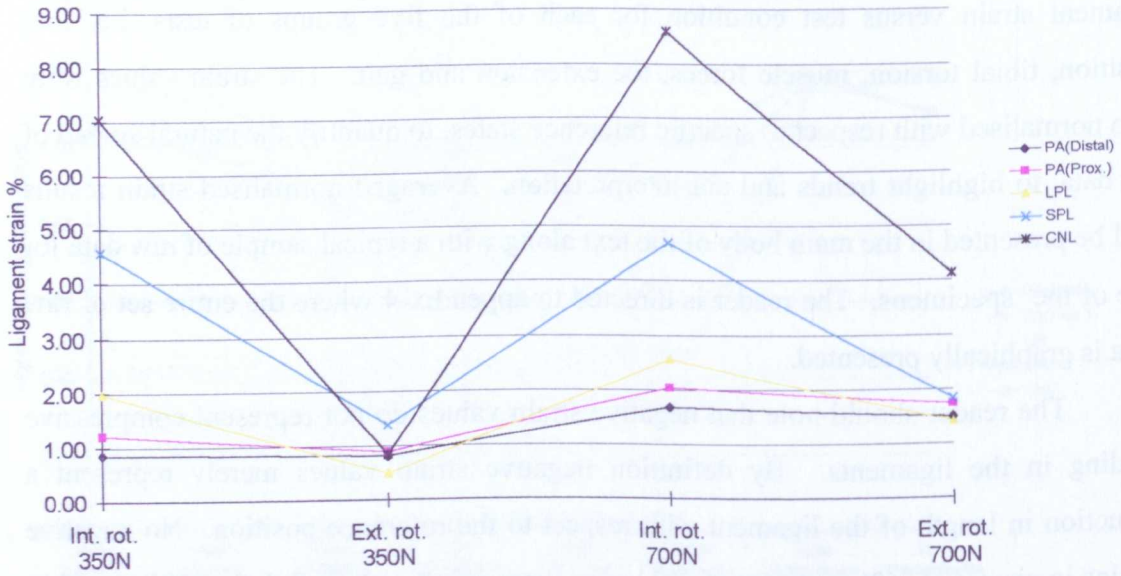


Figure 4.16 Strains in the foot ligaments with applied tibial torsion during standing (test No.5).

load levels. The mean and standard deviations for the averaged normalised tests are presented in figure 4.15.

#### **4.4.3 Tibial Torsion**

Ligament strains were seen to vary considerably when the tibia was externally and internally rotated under vertical loading. External rotation tended to put the foot into inversion whilst internal rotation moved the foot to an everted position. Consistent patterns of ligament strain were noted for each specimen as shown below for specimen N<sup>o</sup>. 5 (fig 4.16). External rotation produced lower strains than internal rotation in every test case and in all ligaments. On inspection of the results it was seen that the rotations caused strains to vary about a resting position approximating the mean of the two results (internal and external rotations respectively). The results for this activity were normalised by dividing the difference of the two values by the sum of the values (Note: the sum of the values is twice the average value). This gave a figure between 0 and 1 which reflected the sensitivity of each structure to the applied test movements. The averaged normalised results for the tests, numbers 2 - 6, are shown in figure 4.17.

#### **4.4.4 Muscle Forces**

Ligament strains affected by extrinsic muscle force during simulated standing were calculated and presented as below for test N<sup>o</sup>. 5 (fig 4.18). Repeatable patterns of change in strain were witnessed for various combinations of ligament and muscle force. The strain results were normalised with respect to the zero muscle force condition (fig 19). It was found that applied muscle forces were able to reduce the strain levels in all ligament structures (especially TA and TP forces).

#### **4.4.5 Toe Extension**

The strains occurring as a result of applied toe extension, during simulated standing, were measured to explore the mode of operation of the windlass mechanism. The strains in some structures behaved according to theory, however, phase differences

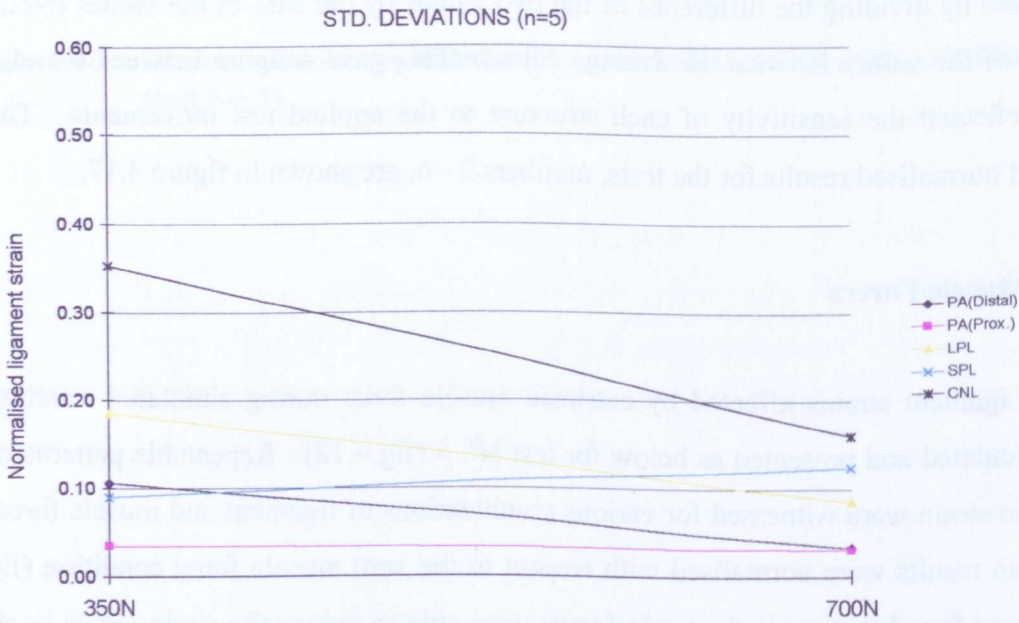


Figure 4.17 Means and standard deviations of the normalised ligament strains of feet subjected to applied tibial rotation during standing (n=5).

in some of the ligaments strains were identified. The test data is presented below again for specimen No. 5, in figure 4.20. The values of strain in the extended position were normalised with respect to the values at zero extension. The average normalised results are shown in figure 4.21. Strains in the PA were seen to increase in every case however the strains in the plantar tarsal ligaments were on average not affected by toe extension.

#### **4.4.6 Gait**

The strain levels for each of the three simulated stages of gait are presented together in figure 4.22, again taking the results of specimen No. 5 as a typical example. Although distinct patterns of strain were demonstrated in the raw strain results normalisation of the data was performed with respect to the strains occurring during standing (in the neutral position at the 350 N load level in the position tests) (fig 4.23). This neutral position was considered to represent most closely the actual standing condition since small forces were applied to the TA and TACH tendons to represent the slight muscle activity occurring *in vivo* during intermittent postural adjustments. Both the raw and normalised results showed that the largest strains occurred during toe-off in all ligaments. Average normalised values of strain during gait were greater than those during simulated standing.

## **4.5 DISCUSSION**

### **4.5.1 Positions**

Only one previous study has made calculations of functional strain in the foot ligaments. Kogler *et al* (1995) found mean levels of strain of  $2.62 \pm 1.78$  % and  $3.54 \pm 2.02$ % in the PA of cadaveric foot specimens subjected to 450 N and 675 N vertical force respectively (n = 7). In the present study mean PA strains of  $1.08 \pm 0.20$  % (distal) and  $1.14 \pm 0.68$ % (proximal) were found at the 350N loading level with no applied muscle force (n = 6). At the 700 N loading level, although with small TA and TACH forces of 50 N, strains of  $1.22 \pm 0.48$ % and  $1.40 \pm 0.50$ % were calculated for the distal and proximal PA respectively. Given the inherent sensitivity of the measurements to

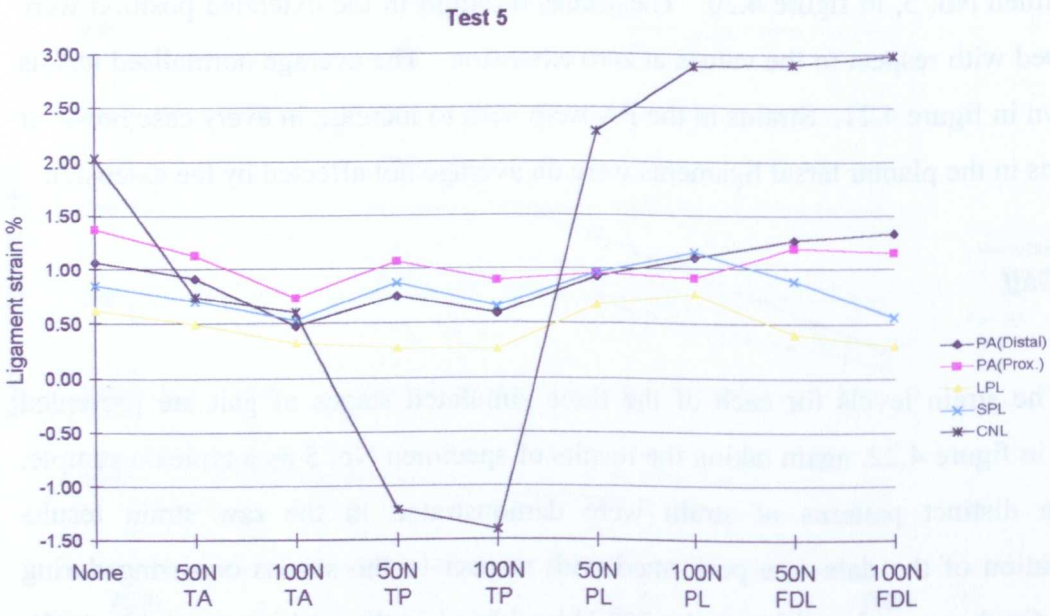


Figure 4.18 Strains in the foot ligaments with applied extrinsic muscle forces during standing (test No.5).

local variations in strain the results of the two studies compare favourably. The slightly higher values found by Kogler *et al* may have been a result of the different measuring position, close to the calcaneal insertion, used in that investigation. The PA strains during gait of  $3.02 \pm 0.62\%$  (distal) and  $4.05 \pm 1.77\%$  (proximal) are in agreement with the value of  $4.29 \pm 2.20\%$  found by Kogler *et al* at 900N vertical loading.

Pseudo-functional strains have been measured in other ligaments using similar techniques to the present study. Levels of strain in the lateral ankle ligaments of cadaveric feet, subjected to applied movements and loading, have been found between 3% (Cawley and France, 1991 and Renstrom *et al*, 1988) and 15% (Colville *et al*, 1990) maximum. Strains in the medial collateral ligament of cadaveric knee specimens of 4% have been measured at 120° of flexion (Arms *et al*, 1983). *In vivo* strains in the anterior cruciate ligament of  $3.7 \pm 0.8\%$  (n = 10) were found when a Lachman test was performed on the subjects whose ligaments had been instrumented with a Hall-effect device (Beynon *et al*, 1992). The ligament strain values of the present study are in agreement with the range of strain magnitudes reported in other structures in the literature.

On examination of the raw data it was observed that the higher load level of 700N always gave greater strain, or more negative strain where this was witnessed, than the 350 N force. Shifts in strain between pairs of values at each position accounted for the differences in shape of the strain graphs between specimens. Normalised values of strain in both PA positions increased, on average, by a factor of 1.17 during inversion. Increased strains of 1.02 and 1.20 for the distal and proximal PA respectively during plantar flexion were also observed. Averaged normalised eversion and dorsiflexion values of distal PA strain remained close to 1.0 while the proximal PA was seen to be more affected by position causing decreases of between 0.64 (36%) and 0.93(7%). It was observed that the PA (distal)/PA(proximal) strain ratio was altered from that occurring in the neutral position to varying degrees as seen in both raw and normalised averaged data (particularly during eversion and plantar flexion).

The differences in the ratios of the PA strains may be difficult to account for, on initial inspection, given the logical assumption that an approximately constant ratio should be obtained when considering that strains within one continuous structure, subject to uniform tensile loading, are being measured. Two factors, however, could

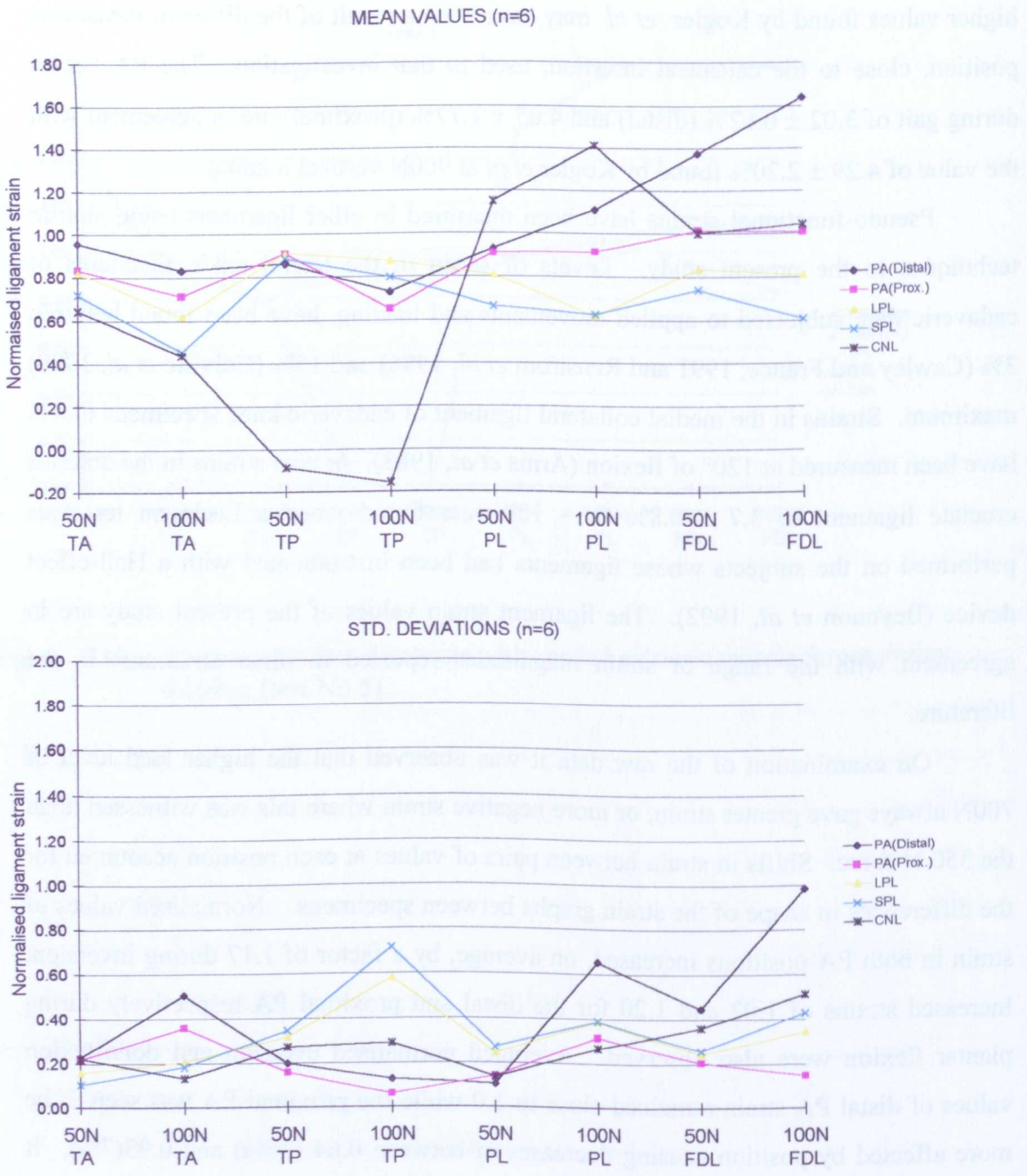


Figure 4.19 Means and standard deviations of the normalised ligament strains of feet with applied extrinsic muscle forces during standing (n=6).

perceivably produce varying PA strain ratios with applied foot position. In the first instance the central PA is connected laterally and medially to deep septa which compartmentalise the foot structure, superficially to different areas of the skin and also deeply to structures such as the flexor digitorum brevis muscle and ligamentous structures of the forefoot. The uniaxial force within the PA may be disrupted by the high probability of these insertions carrying a small portion of the force that would otherwise be borne by the PA in isolation. Also it must be remembered that the strain measurements are localised in nature and as such strain will inevitably not be measured in the same functional groups of fibres along the ligament. This gives rise to the possibility that altered forefoot loading conditions may give rise to differing fibre recruitment, resulting in alterations of the relative strain values measured in the two PA transducer positions. Changes in the PA strain ratios were also witnessed in the muscle force experiments which supports this hypothesis.

On inspection of the raw strain data varying patterns of strain for the tarsal ligaments were observed. Patterns identifiable from both the raw and normalised averaged data included a clear reduction of strain in the SPL during dorsiflexion of 0.44 (66%) with respect to the neutral position, on average, and an average increase in strain in the LPL during eversion by a factor of approximately 1.25.

Normalised average values of strain for the CNL did not vary beyond 0.8 to 1.2 times the values obtained in the neutral reference position. The lack of more identifiable trends in the strain data with varying position were attributed to: (1) natural variation between specimens in keeping with the biological nature of the measurements; and (2) the fact that each specimen assumed a unique position under loading due to the altered support conditions between each foot position.

#### **4.5.2 Tibial Torsion**

When torsional rotations were applied to the tibias of the foot specimens under constant load, a very definitive pattern of ligament strains resulted. In general, external rotation caused strains in all structures to decrease from the resting neutral position and internal rotation had the opposite effect. The actual strains in the neutral position were higher than in the previous tests due to slight internal rotation during loading (the tibia

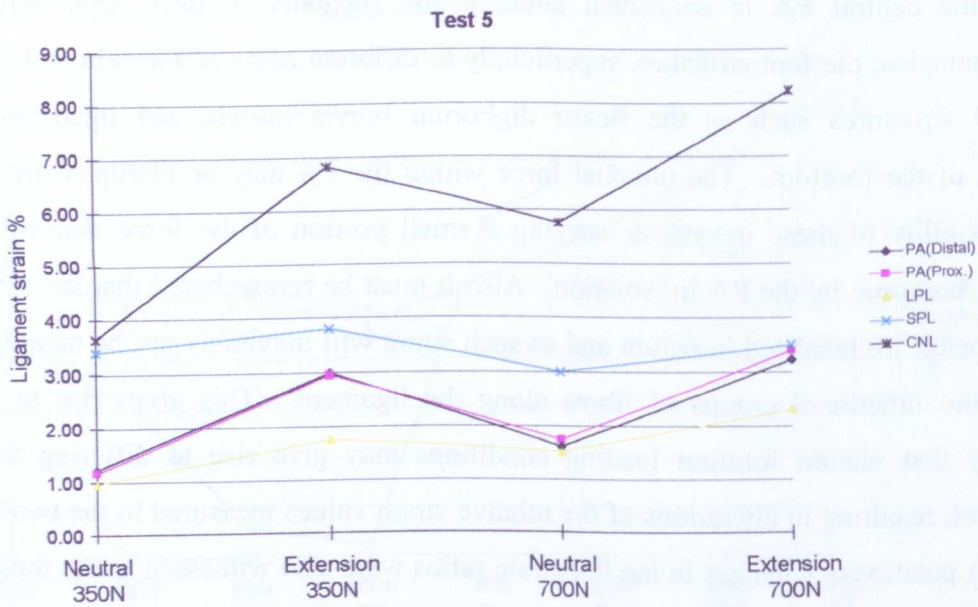


Figure 4.20 Strains in the foot ligaments with applied toe extension during standing (test No.5).

was free to rotate in this test). On inspection of the raw strain data it is immediately apparent that the PA (distal) and PA (proximal) are much less sensitive to these movements than the plantar ligaments of the tarsus. This observation was supported by the averaged normalised results which were specifically designed to highlight those ligaments most affected by this type of movement. From these results it was seen that the order of sensitivity of the ligaments was CNL, SPL, LPL, PA(proximal) and PA (distal). The lower levels of change in the PA strains may be explained by the fact that the induced rotations in the tarsal bones are more remote from forefoot insertions of this structure. It may be deduced, however, from the above results that internal rotation of the tibia does induce slight lengthening of the arched skeletal foot structure, seen as increased PA strain values. It was noted that at the higher loading levels the relative change in strains caused by the test movements was smaller than at the lower force level of 350 N. This was most likely due to the increased load levels causing a more rigid foot structure less prone to deformation by the applied tibial rotations. On inspection of the standard deviations of the normalised data it is seen that the spread of data follows approximately the same relationship as the mean results, i.e. PA strains have the lowest spread with the CNL having the highest. This confirms the observation made when inspecting the raw data that the largest variation in strain changes occurred for the plantar ligaments of the tarsus, i.e. LPL, SPL and CNL. The measured patterns of ligament strain confirm previous observations on foot ligaments. Hicks, 1953; Sarrafian, 1987 and Williams *et al*, 1989 have all described longitudinal twisting, pronation and supination movements, induced by tibial rotation resulting in loading and unloading of the plantar ligaments of prepared anatomical specimens. The results of the present study supersede mere observation by providing a quantitative measure of the strain levels in the plantar foot ligaments during external and internal rotation of the tibia.

### **4.5.3 Muscle Forces**

With a few notable exceptions it was seen that in general the application of extrinsic muscle forces decreased the strains in the test ligaments. Forces applied to the TA were seen to be able to reduce the strains in all the test structures but the effects

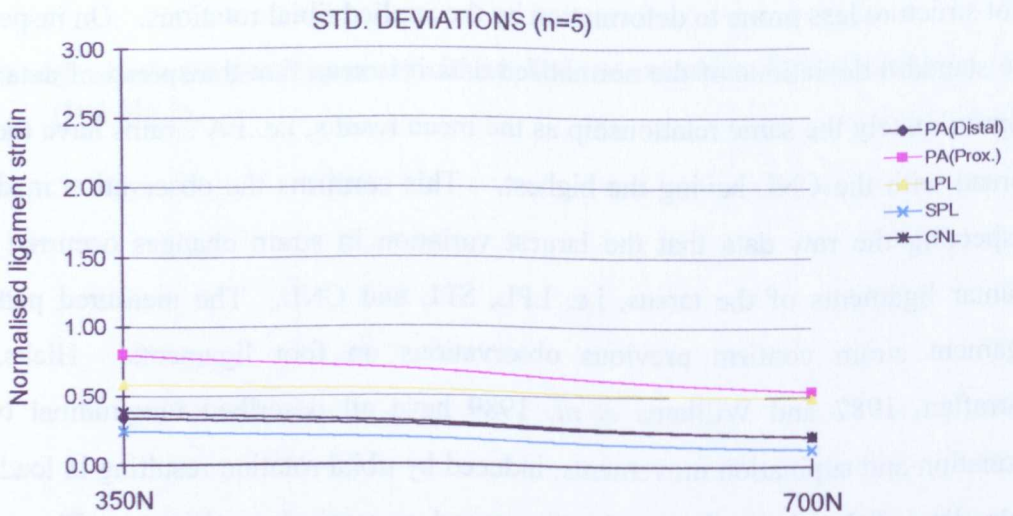
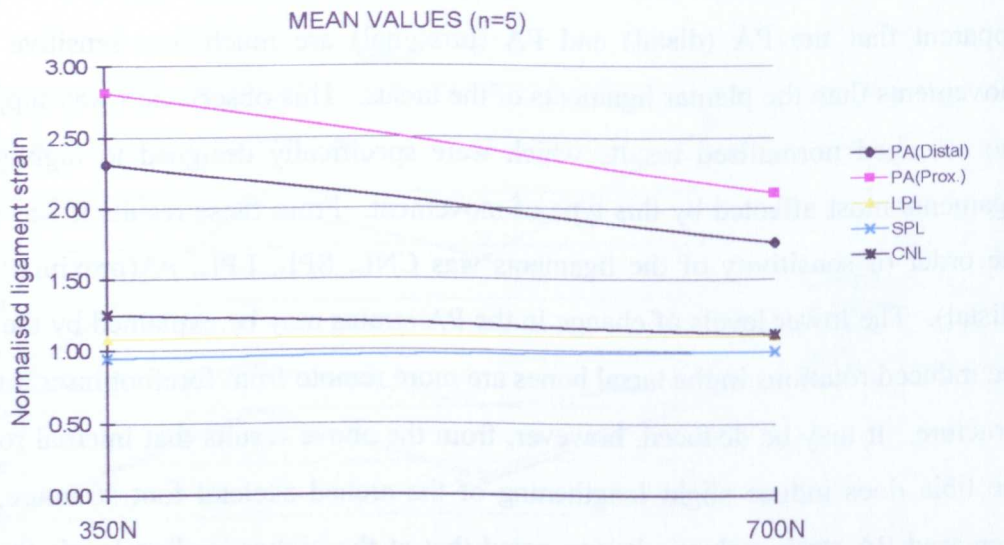


Figure 4.21 Means and standard deviations of the normalised ligament strains of feet with applied toe extension during standing (n=5).

were greatest for the tarsal ligaments where reductions of 0.61(39%) (LPL) to 0.42 (58%) (CNL) were found on average. In addition the effects were found to be progressive, i.e. higher levels of muscle force gave bigger reductions of strain in all cases.

Forces applied to the TP tendon also had a progressive reducing effect on the strains in all ligaments. On average the PA strains were smaller than with TA forces although the attenuating effect was reduced for the LPL and SPL. The greatest reduction was achieved in the CNL where negative strain values were recorded on average (-0.1% at 50 N and -0.18% at 100 N). On inspection of the raw data the effects of the TP force on the CNL strain were clearly seen as a reproducible pattern.

The changes in ligament strain caused by TA and TP forces may be explained by considering the normal action of these muscles. Both insert on the medial border of the foot and tend to cause inversion and raising of the medial arched structure. As shown in the previous set of experiments these movements cause unloading of the ligaments and a resulting decrease in the measured strain. The large reduction in the CNL strain with the application of TP forces occurs as a result of the insertion and line of action of the TP tendon. Inserting on the inferiomedial aspect of the navicular and acting posteriorly, forces in the TP muscle will tend to move the navicular rearwards thus unloading the CNL. Clinical manifestations of the above phenomena have been commonly observed where disruptions in the normal functioning of the TA and TP tendons, either due to trauma or disease, caused overloading of the ligaments eventually leading to flat foot deformities (Cozen, 1965; Mann, 1983; Mann *et al*, 1985 and Fink *et al*, 1986).

Applied PL forces caused more complex patterns of ligament strain. Progressive loading of this structure produces changes in the average PA (distal)/PA (proximal)ratio implying that an altered forefoot loading condition was being created (see section 4.5.1) Values of LPL and SPL strain were again reduced to levels of approximately 60% of the 'no-force' condition. The PL tendon is in close anatomical proximity to the distal end of the LPL as it runs obliquely across the underside of the mid-foot to its insertion on the base of the first metatarsal. Forces in the PL may be responsible for reducing strain in the calcaneocuboid ligaments by providing a posterior component of force on the cuboid thus unloading the LPL and SPL. The PL muscle is also an everter of the foot, a

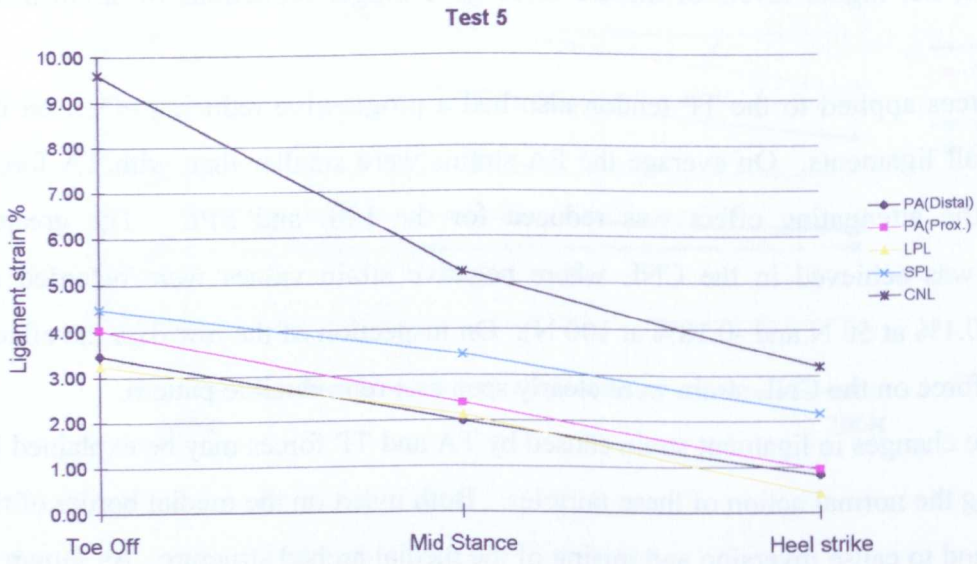


Figure 4.22 Strains in the foot ligaments during 3 stages of simulated gait.

fact that accounts for the increased strain levels produced in the CNL when this muscle is loaded (on average 1.4 times that during the 'no-load' condition).

FDL muscle forces were seen to continue the trend in the difference in PA (distal)/PA (proximal) ratio by further altering the forefoot loading condition. It is highly likely that the insertion and routing of this tendon, in close proximity to the PA in the forefoot, is the root cause for the increase of the distal PA strain with respect to the strain in the proximal region. Whilst the proximal PA values remain close to 1.0 during FDL loading, the strain in the distal PA rose progressively to an average of 1.62 of the 'no-load' condition. FDL loading was seen to have little or no effect on the strain levels of the CNL on average, but decreases of between 0.80 (20%) and 0.60 (40%) were noted for the calcaneocuboid ligaments, LPL and SPL.

#### **4.5.4 Toe Extension**

On inspection of the strain data for the two PA positions it was seen that the established theory of the windlass mechanism as applied to this structure was valid, i.e. toe flexion caused increased loading of the PA, manifested as a rise in strain in all of the tests. Additionally, the applied test movements had greatest effect on the proximal PA giving strain increases of 2.8 at 350 N load level compared to 2.3 in the distal PA on average. The relative increases in PA strain were lessened in both positions at the higher, 700 N, load level. The likely cause of this observation is that the additional strain caused by toe flexion was masked by the overall increased levels of strain produced when doubling the vertical load on the specimen.

Whilst the effects of toe extension with respect to the PA confirmed previous theories of windlass mechanism function, the strains produced in the LPL, SPL and CNL were less predictable. In formulating the theory of the windlass mechanism Hicks (1954) suggested that the combined movements of the foot bones occurring as a result of toe extension would cause similar effects to inversion of the foot, as achieved through external rotation of the tibia, resulting in reduced loading in the plantar ligaments of the tarsus. Inspection of the results reveals this to be at least partly true. The raw strain data showed that strains decreased in the SPL in three specimens, in the LPL in two specimens and in the CNL in one specimen, with applied toe flexion. The averaged

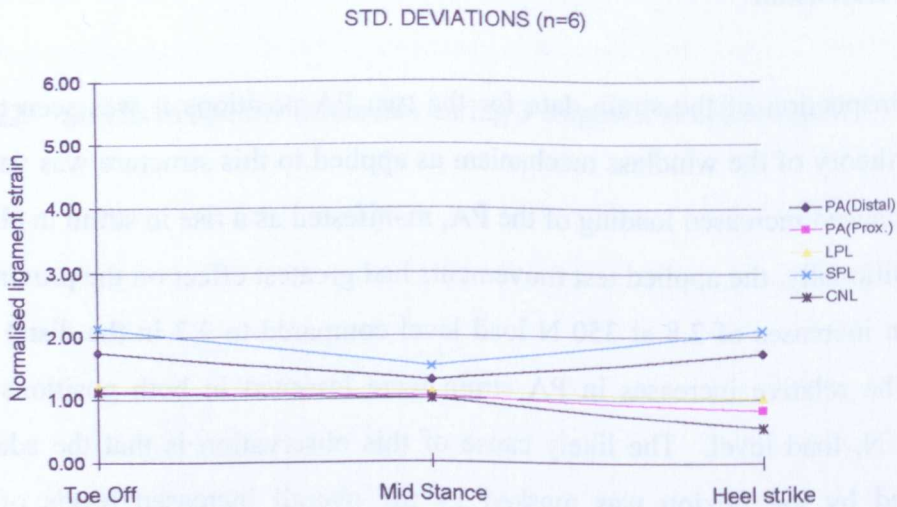
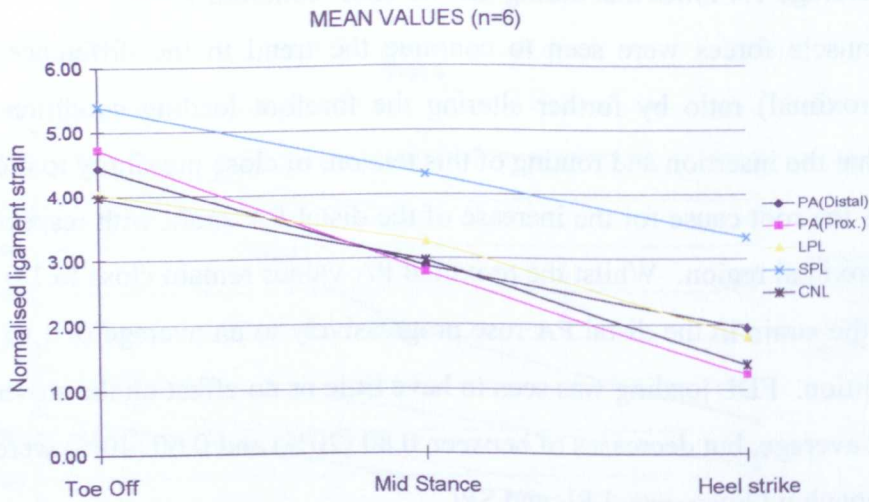


Figure 4.23 Means and standard deviations of the normalised ligament strains of feet during 3 stages of simulated gait (n=6).

normalised results for these ligaments show that the strains remain close to those of the zero-extension case at both levels of load indicating that in this simulated functional case, toe extension does not alter strain levels in the tarsal ligaments in the same manner as those in the PA. Although this simulated test does not accurately represent the true *in vivo* functional situation where toe extension occurs, toe-off during gait, the tests did however serve to confirm and quantify the effects of windlass mechanism on the strain patterns of the foot ligaments.

#### **4.5.5 Gait**

In simulating gait, in three positions, physiological levels of tendon force and altered foot position were necessary to alter the position of the centre of pressure under the foot. In the absence of the naturally occurring extrinsic and intrinsic muscle activity accompanying gait it is highly likely that the strains measured during these tests over estimated the ligament strains occurring *in vivo*. Although these tests are most contentious in terms of the accuracy of simulation with respect to the natural case, the results could conceivably constitute upper bounds or ‘worst-cases’ for the ligament strain values during gait.

The raw data for the six tests conducted clearly revealed that the largest strains in each structure were witnessed during simulated toe-off. Average values of strain ranged from 4.0 for the CNL to 5.4 for the SPL when normalised to the values found during standing. Mid stance strain values were the next greatest with the lowest values of strain during gait being found during simulated heel strike. The average strain values during heel strike were greater than the standing condition for all test structures as revealed by normalisation of the results.

# **CHAPTER 5. MECHANICAL TESTING OF EXCISED LIGAMENT SPECIMENS**

## **5.1 INTRODUCTION**

This chapter details experiments designed to explore the biomechanics of the ligaments of the human foot prepared as isolated specimens. The small number of previous studies of this type have either used non-standard testing methods or have not investigated the normalised mechanics of the tissues. Local measurements of strain were used to calculate specific stress-strain relationships which were characterised using a non-linear viscoelastic model. The strain in the isolated tests was matched to that in the intact tests of the previous chapter to give estimates of functional forces and stresses in the test ligaments.

## **5.2 MATERIALS**

The experiments described below were conducted on eight ligaments of two cadaveric foot specimens which had previously undergone testing as described in chapter 4. Donor details for these specimens, numbers 107R and 131L, are given in table 4.1. A third specimen, number 108L failed prematurely during testing, probably due to osteoporotic changes in the bone. Results for this test are incomplete, cannot be considered normal, and are therefore not presented.

## **5.3 METHODS**

### **5.3.1 Preparation of the Test Material**

On completion of the intact tests the whole specimens were re-frozen at  $-20^{\circ}\text{C}$  in airtight bags in the neutral position. Prior to testing, as described below, the specimens were thawed overnight at room temperature.

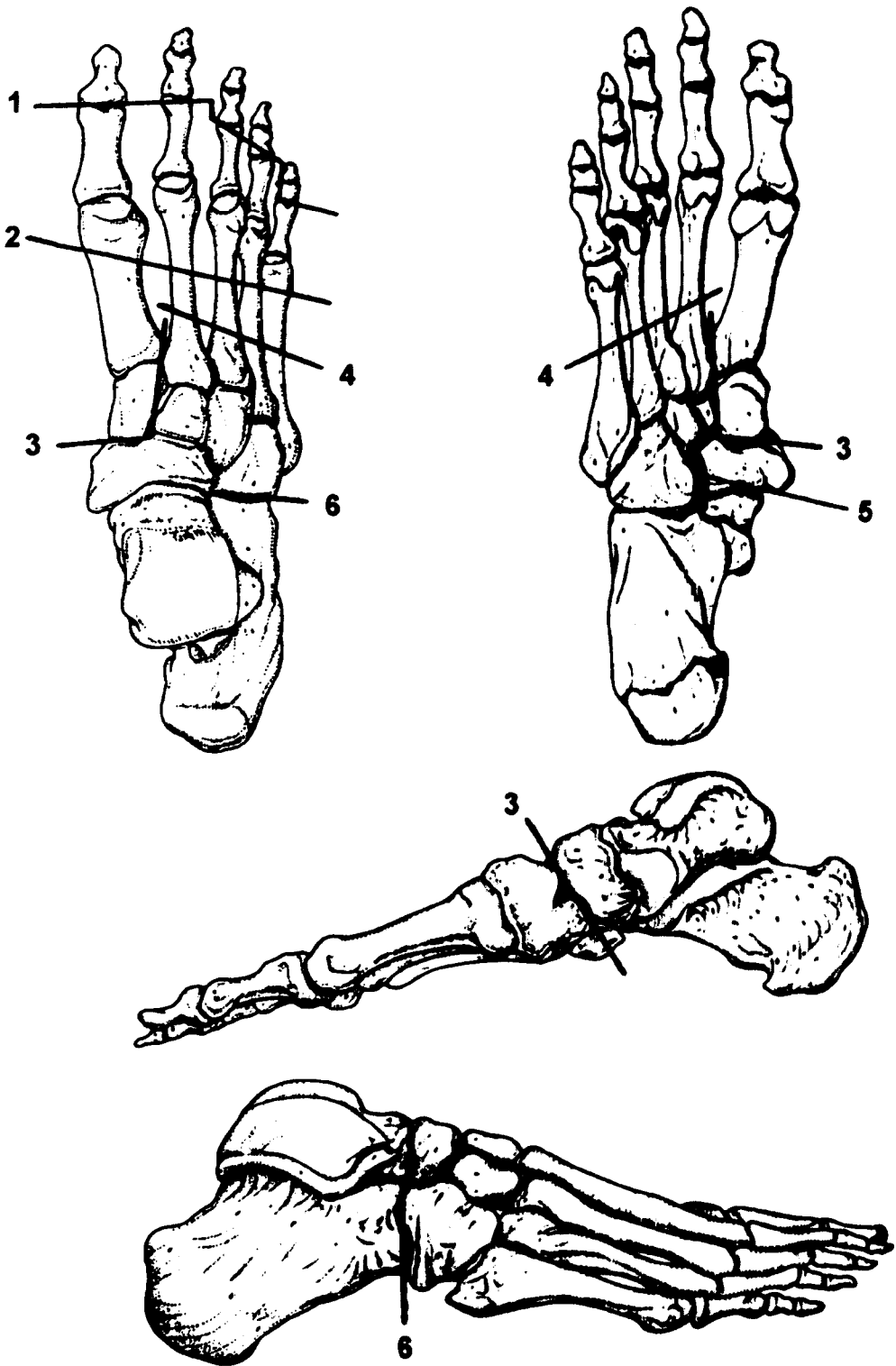


Figure 5.1 Dissection protocol for bone-ligament-bone preparations (talus was removed prior to incisions 1-6 marked on foot skeleton).

Each ligament specimen was tested as a bone-ligament-bone preparation in a uniaxial tensile test configuration. A dissection procedure was applied to both the specimens resulting in isolated preparations of the PA, LPL, SPL, and CNL. The major divisions made are shown in figure 5.1. First the tibia, fibula and talus were separated from the remainder of the foot. The distal and intermediate phalanges were then removed (incision 1, fig 5.1). All skin and fascia were also removed except the plantar skin distal to metatarsal heads (a PA insertion site). A transverse cut was made just proximal to the line of the MTP joints, dividing the metatarsals and freeing a portion of the forefoot containing the distal PA insertions (incision 2, fig 5.1). Next the first metatarsal and medial cuneiform were removed (incision 3, fig 5.1) whilst the metatarsals 1-4 were trimmed near their bases. Finally the interosseous, dorsal and lateral ligaments of the tarsus were divided to leave the LPL, SPL and CNL as the only ligamentous connections between the remaining bone units (incisions 5 and 6, fig 5.1). Note that the distal insertions of the LPL on the bases of the metatarsal heads were preserved on the bone unit composed of the cuboid, intermediate and lateral cuneiforms and metatarsal bases 1-4. During each stage of the dissection dimensions of the foot and individual ligaments, before isolation, were made. Measurements of the bone to bone insertion lengths of the ligaments were made to assist in establishing first estimates of strain for the initial testing parameters. Details of these measurements are given in appendix 8.

To help give rigid fixation of the bones during testing stiff steel wires, of diameter 1.5 mm, were inserted through drilled holes in the bones. The bones were potted in the test fixtures using bone cement and the protruding ends of the wire ensured that the irregularly shaped bone units were securely mounted. During testing the specimen was kept moist by periodic light spraying with a buffered 0.9% saline solution and a removable polythene sleeve prevented dehydration and also helped to dampen any shifts in temperature.

In order to conduct a normalised analysis of the mechanical properties of the ligaments it was necessary to make measurements of stress and strain. Local strain measurements were made with the LMSGs implanted in the same, previously marked, positions as the intact tests. The same size LMSGs were attached using the methods

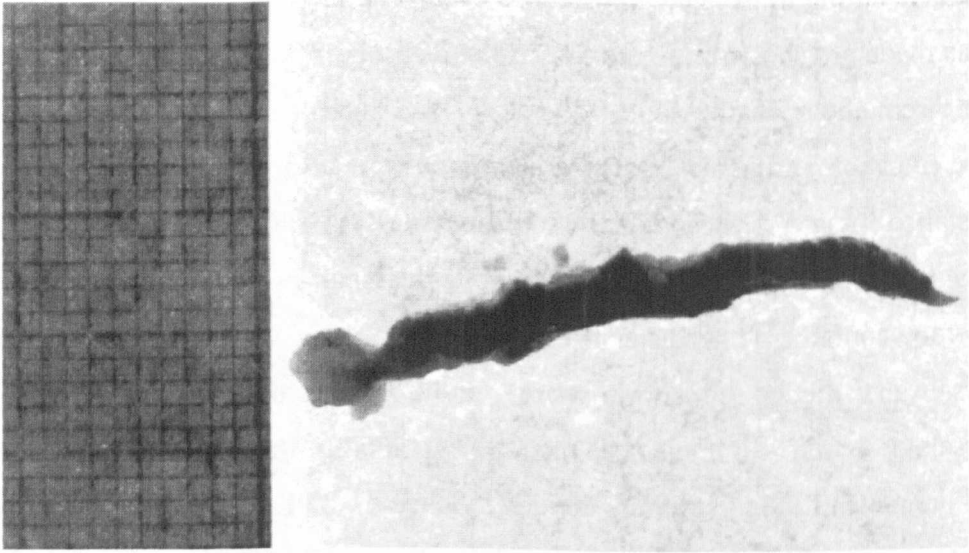


Figure 5.2 Section of proximal PA. Image was calibrated with graph paper on left.

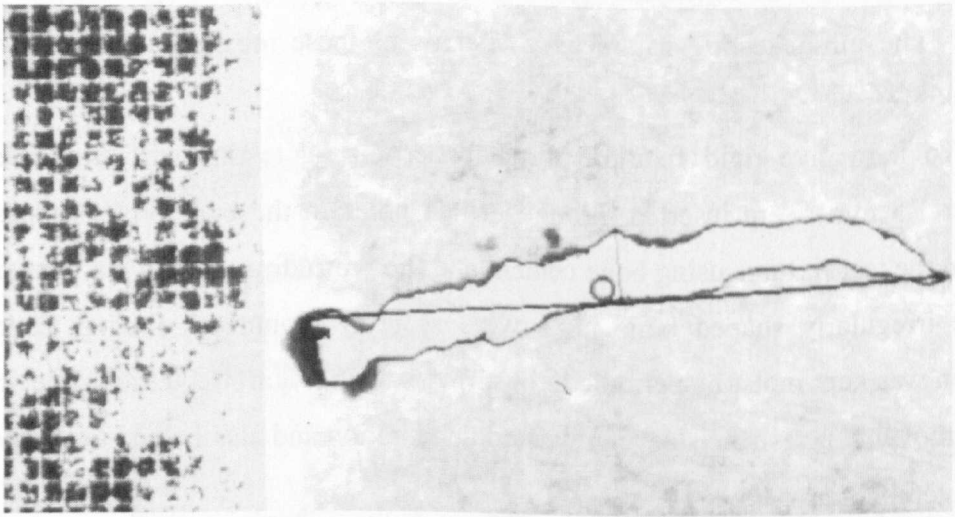


Figure 5.3 Section of proximal PA undergoing area measurement with image analysis.

described in chapter 4 after the ligament specimen had been mounted in the Instron® load Frame.

In order to derive the stress in the ligaments it was necessary to measure the cross-sectional area of the specimens. The method used was chosen after careful consideration of the specific practical issues involving testing of the foot ligaments. Since a measure of local area was required the use of gravimetric methods, e.g. wet weight per unit length, were immediately rejected. Although the use of area micrometers have proved successful in previous investigations, Butler *et al* (1978) and Ellis (1969), access limitations and the low aspect ratio of the ligament cross section prevented their use in the present study. It was decided to use planimetry of ligament cross sections to determine the area, a method which has been found to be accurate but which has rarely been used (Blanton and Briggs, 1970; Cronkite, 1936). When the specimens were mounted in the test rig a line was lightly drawn on the ligament surface normal to, and bisecting, the body of the LMSG. This line was assumed to represent the location of the stress corresponding to the strain being measured by the LMSG. After removal of the specimen from the rig a 1mm section of ligament, centred about the drawn line, was prepared using a dermatome blade. Care was taken not to crush the fibres or otherwise disrupt the structure of the ligament. The sections were then placed on a light box and photographed next to a piece of 1mm graph paper to calibrate the image (fig 5.2). The developed pictures were digitised on a flat bed scanner (Hewlett Packard, HP Deskscan III) and the areas were measured using thresholding procedures of a computer image analysis software package (Microscale TC/TM, Version 2.10, Digithrust Ltd, UK) (fig 5.3). The calculated areas are shown in table 5.1. Since the areas were measured in the absence of load it is likely that recovery of the tissue produced slight over estimation of the area values. Damage to the ligament structure during testing, and potential interference with the area measurements, could not be tolerated and so the ligament specimens were not tested to failure.

When the specimens were mounted into the loading rig care was taken to align the bone unit ends so as to prevent uneven recruitment of fibres across the width of the ligaments. Momersteeg *et al* (1995) have shown that in tests of human knee cruciate ligaments the stiffness of the specimens was significantly affected by changes in relative orientation of the end mountings. In the present study the angle of the distal bone pot

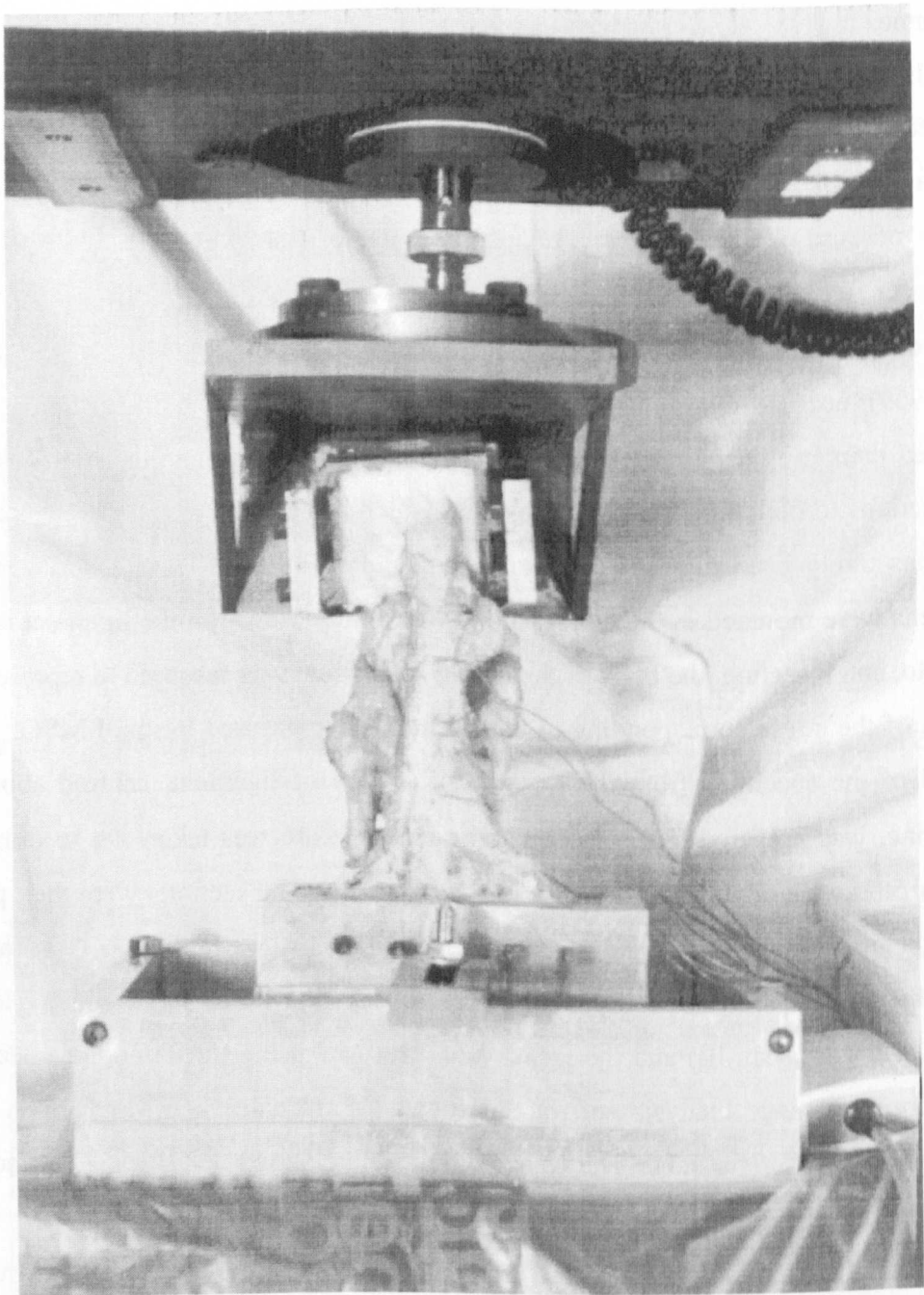


Figure 5.4 Tensile testing of a PA specimen. The calcaneus is mounted uppermost, near the load cell. The dissected portion of the forefoot was fixed in the lower pot. The LMSGs can be seen implanted on the ligament.

was adjusted using shims until equal recruitment of fibres was achieved, as assessed by visual inspection and palpation of small areas of the ligament. It is likely that this configuration, was however, different from the *in vivo* orientation of the ligament insertions and hence a degree of inaccuracy of testing, with regard to the natural ligament physiology was introduced (see also section 5.3.4).

Specimen	Ligament	Area(mm <sup>2</sup> )	Specimen	Ligament	Area(mm <sup>2</sup> )
131L	PA (distal)	71.2	107R	PA (distal)	56.7
	PA (prox)	67.6		PA (prox)	52.4
	LPL	66.6		LPL	48.9
	SPL	43.8		SPL	45.9
	CNL	106.3		CNL	100.5

Table 5.1 Ligament cross sectional areas measured by planimetry.

### 5.3.2 Loading Rig and Test Apparatus

The Instron<sup>®</sup> load frame was used to apply forces to the ligament specimens. The area above the crosshead was used and the forces were measured with a 10kN load cell. As the load cell was used at or below 10% of its rated load the load accuracy and resolution were verified by calibration with weights (from 0 to 10kg in 100g increments). The sensitivity of the load cell was maximised using the Instron<sup>®</sup> gain settings during each test. Resolution was found to be ultimately limited by noise in the load cell amplifiers but was calculated to be better than 0.1% of the maximum force measured. To maximise the accuracy of the force and crosshead deflection measurements noise was reduced in the Instron<sup>®</sup> analogue output signals with the use of a specially constructed low pass filter (20 Hz cut off frequency and -6dB/octave frequency response).

The rig used to mount the ligament specimens was composed of the following components: (1) Bone pots for the cuboid, navicular and forefoot bone units, (2) a 5 way adjustable coupling to interface the calcaneal bone pot with the load cell and (3) a fixture to secure the distal bone pots to the Instron<sup>®</sup> crosshead. Primary fixation of the bones in the pots was achieved using pointed screws. Bone cement was poured around the bones to provide final rigid fixation. All load-bearing rig parts were designed and

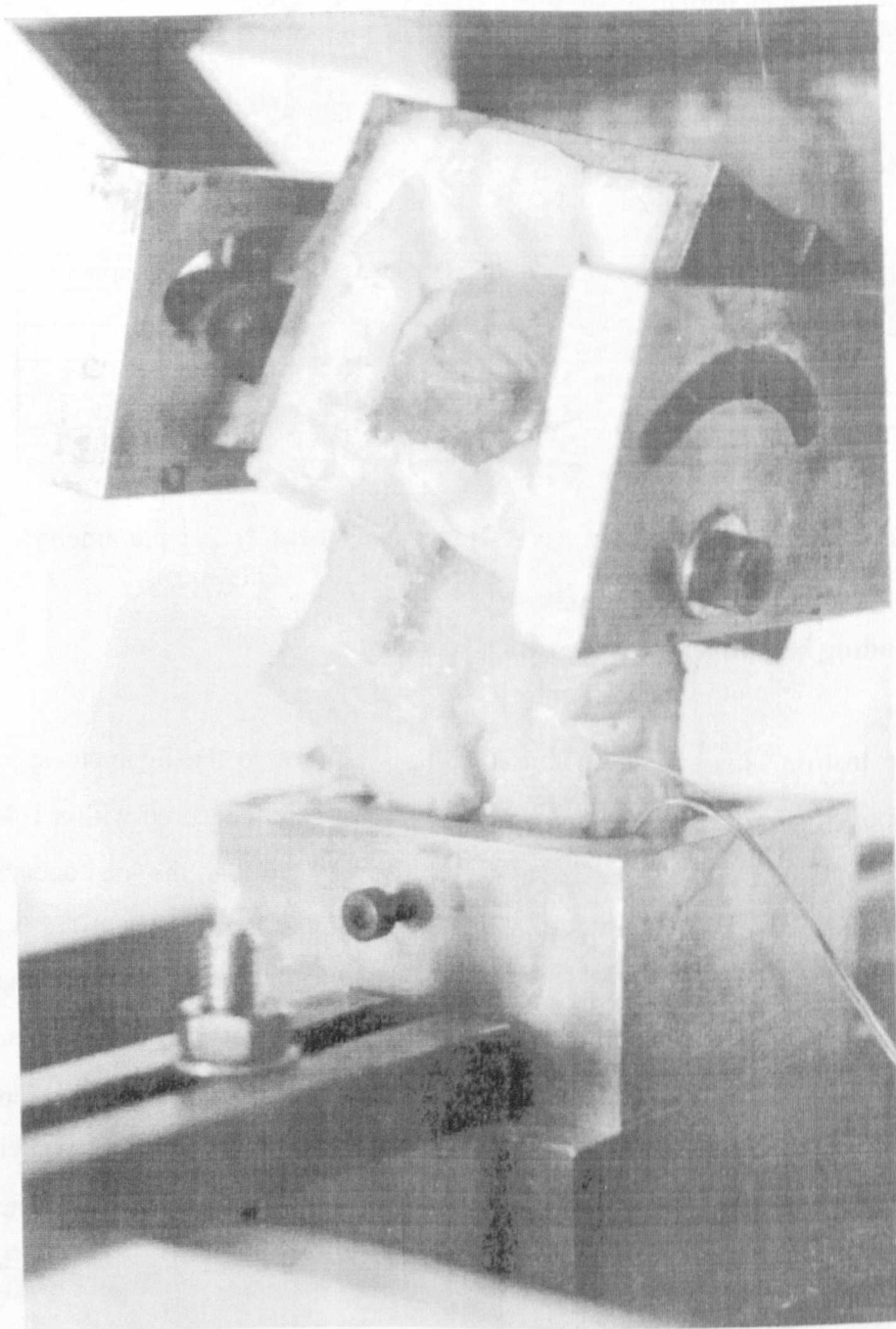


Figure 5.5 Close up of a tensile test of the CNL. The navicular is mounted in the lower bone pot. The angle of the calcaneus has been adjusted to allow the MIIL and test machine axes to be aligned. The LMSG can be seen in the right of the picture.

constructed for minimal deflection under applied load. The test set up can be seen for two ligament configurations in figures 5.4 and 5.5.

The MIIL of each ligament specimen was manually aligned with the test axis of the machine using a guide constructed for this purpose. The upper adjustable coupling was designed so that the centre of rotation was located near the plantar surface of the calcaneus in the region of the proximal insertion sites. Only one distal bone was attached at a time, thus the specimen was removed after each test in order to mount the next bone unit. Once the LMSG was attached to the ligament a final check of alignment was made.

Test data were sampled with the acquisition system described in chapter 4. Calibration of the LMSGs was performed as in the intact tests. Calibration data for the gauges used in the isolated tests are presented in appendix 1. The test temperature was recorded using a thermocouple placed in the substance of the ligament specimen near the implanted LMSG.

### **5.3.3 Test Modalities**

The tensile tests were all carried out at constant rates of crosshead deflection. In the first set of tests a loading rate of 200 mm/min caused over shoot of the crosshead and subsequent overload and failure of the specimen at the calcaneal insertion. For safety, therefore, the testing rate was kept below this value. Since the true strain rate could not be calculated quickly at the time of testing, fixed extension rates of 100 mm/min and 50 mm/min were used for the specimens. To explore the rate dependency of the force in the tissues, viscoelasticity, each specimen was tested at a slower rate of either 10 mm/min or 5 mm/min. As all the specimens were open to atmosphere simultaneously, the duration of testing had to be kept to a minimum to avoid tissue degradation effects. For this reason the ligaments could not be tested at speeds of lower orders of magnitude and stress relaxation tests, requiring up to 16 hours, could not be conducted.

Since the failure load of the specimens was unknown the maximum load of each cycle was incremented to a value where the experimental strain levels were of the same magnitude as those measured in the intact tests. In a small number of cases the strains

in the isolated tests did not reach the magnitudes measured in the intact tests. In these cases extrapolation of the load-strain curves was used to estimate functional forces and stresses in the ligaments. The shapes of the load/extension curves were also checked at the time of testing to ensure that at the highest force level the tissue had been loaded well beyond the 'toe' region. Preconditioning of the specimens was carried out at each load increment (20 cycles of loading and unloading) to ensure a stable and repeatable tissue response.

The zero load reference was taken when the specimen was first mounted onto the load cell. The force on the specimen at this point was therefore the weight of the distal bone pot. This same zero force was used as the lower force cycling limit for the tensile tests. The use of a small pre-load as the lower limit was justified by the fact that this was very small compared to the maximum force applied and that return to this load was more repeatable than using the true zero load of the specimen. During preconditioning the stability of the crosshead position corresponding to the zero load reference was verified. The values of the small zero-loads were found by weighing the distal bone pots and bone unit plugs on completion of the tests, and are shown in table 5.2.

Specimen	Bone unit weight (N)		
	Forefoot	Cuboid	Navicular
131L	14.3	10.6	8.4
107R	14.4	10.4	8.5

Table 5.2 Bone pot weights used as the zero-force references.

Testing of the PA and CNL was carried out between two load limits as described above. A different procedure was required for the LPL and SPL. During evaluation of the dissection procedures it was found that separate cuboid bone plugs could not be cut for the LPL and SPL without damage to the ligament structure (Note: Both ligaments insert on the cuboid and are in very close proximity, i.e. partially overlap). In addition, potting of the very small bone plugs arising from such a procedure was not practicable. A sectioning technique, described below, was used to measure the force in each ligament. First the angles between the MIILs of the two ligaments,  $\theta$  and  $\delta$ , were

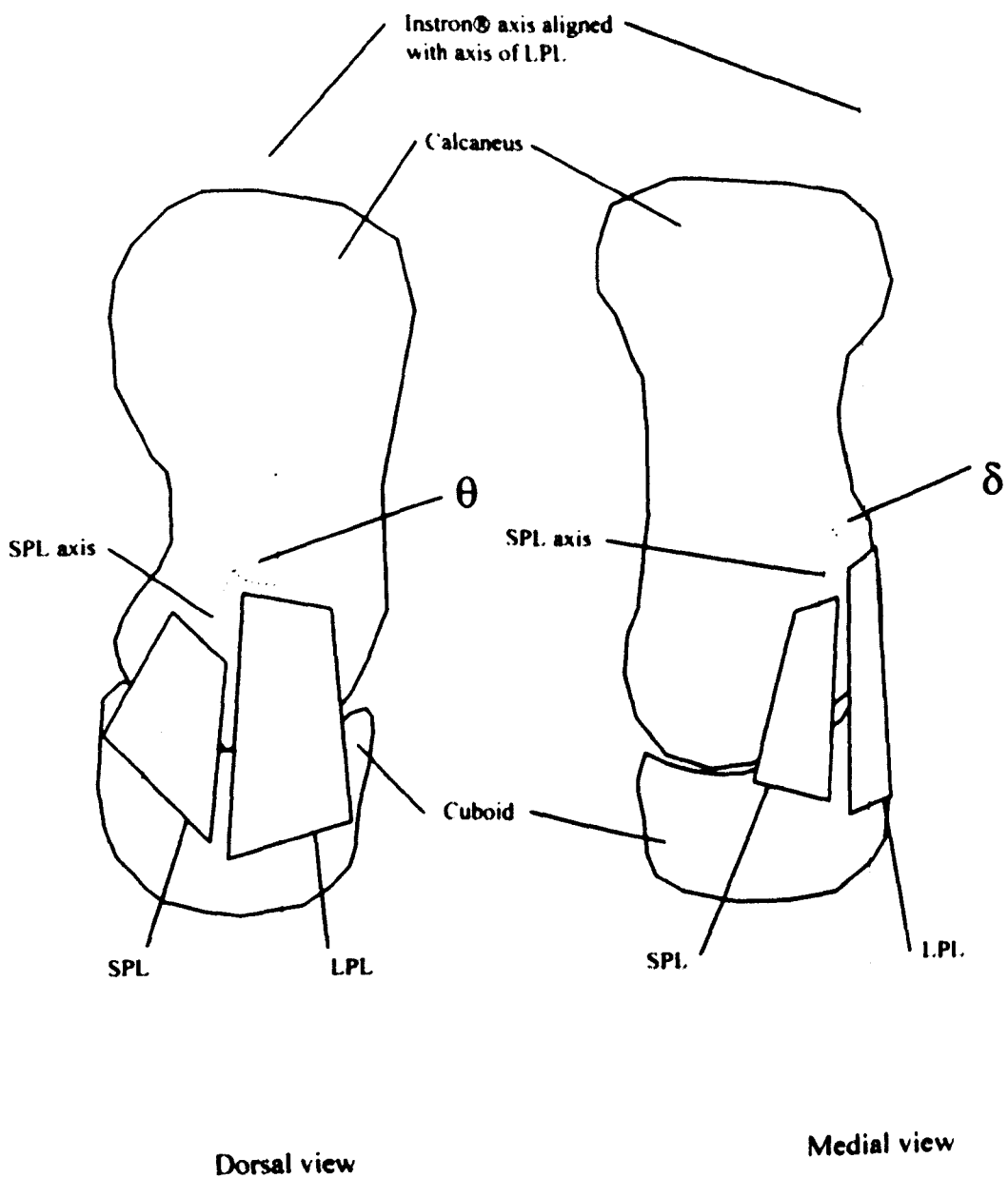


**Figure 5.6** Definition and measurement of the angles between the SPL and LPL in the sagittal and transverse planes ( $\delta$  and  $\theta$ ) during isolated ligament tensile testing.

measured in the two planes to the nearest  $0.5^\circ$  using a protractor placed on the upper loading rig (fig 5.6).

Tensile testing was performed from a zero load position where a finite deflection was applied with the LPL in line with the axis of the Instron<sup>®</sup> load frame. Strain in both ligaments was recorded. The SPL was then severed from its calcaneal insertion and the tests were repeated at the previous levels of extension and extension rate. Values of force in the SPL for the first set of tests were calculated using superposition as follows. At any given extension the total force measured,  $F_T$ , is given by:

$$F_{T_{INTACT}} = F_L + F_S \cos\theta \cdot \cos\delta \quad (5.1)$$

where both structures are intact and by :

$$F_{T_{CUT}} = F_L \quad (5.2)$$

for the LPL in isolation.

Where  $F_L$  and  $F_S$  are forces in the LPL and SPL respectively. Combining 5.1 and 5.2 gives the expression used to find force in the SPL at a finite level of extension:

$$F_S = \frac{F_{T_{INTACT}} - F_{T_{CUT}}}{\cos\theta \cdot \cos\delta} \quad (5.3)$$

The following assumptions were made when using equation 5.3: (1) the ligament extensions are small, (2)  $\theta$  and  $\delta$  do not change appreciably as the ligaments are loaded, (3) forces and moments generated in other planes are small compared to those along the MIIL of each ligament and (4) the rig was sufficiently rigid to ensure accurate reproduction of ligament extension between the intact and cut cases. Analysis of the test results for a number of extensions allowed the force-extension and stress-strain curves to be plotted for the SPL.

### **5.3.4 Force/Strain Matching**

Estimates of force and stress in the ligament during the simulated function tests were found by matching the strains in these tests with those during the isolated tensile tests.

In estimating force and stress as above it was assumed that the reference state adopted during the intact tests, 20 N in the neutral position, was approximately equal to the zero strain condition used in the isolated tests. Two potential sources of error could have been responsible for nullifying the above assumption: (1) differences in the two zero strain conditions between the two test types and (2) induced strain due to the small tensile forces used as the zero strain references in the isolated tests. On examination of the raw strain data it was seen that only very small changes in strain were induced between zero and 20 N applied vertical force as used for the reference in the intact tests. Levels of possible error due to the non-zero reference in the isolated tests were assessed and are presented in section 5.4.3. The above effects of differing reference position would tend to under estimate the ligament forces and strain during the intact tests. Quantification of any anatomical pre-stress existing in the ligaments of unloaded intact foot specimens was not possible. Functional forces and stresses were calculated using matching algorithms and linear interpolation between pairs of data points to improve accuracy of the estimation process. Data manipulation and analysis was carried out using spreadsheet software (Microsoft®, Excel , Version 5.0).

In a small number of cases the strain in the intact tests was greater than the strain induced during isolated tests. When this occurred force and stress estimates were found by extrapolation of the stress strain relationship found by curve fitting procedures (see section 5.4.2). Negative values of strain in the intact tests were assigned zero values of force by definition.

## **5.4 RESULTS**

### **5.4.1 Stress-Strain and Force-Strain Relationships**

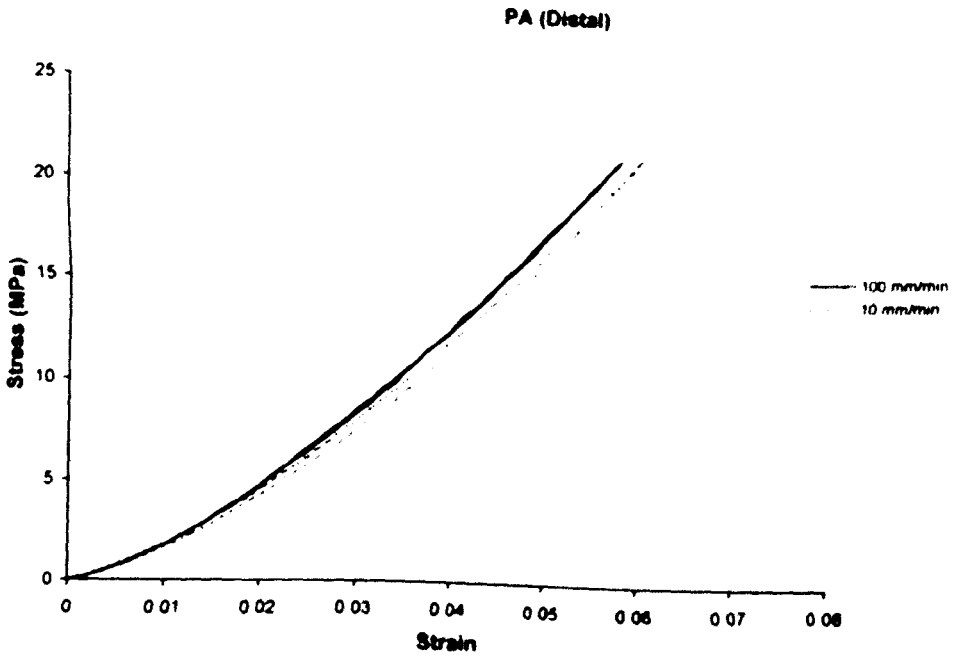


Figure 5.7 Stress-strain response of the PA in tension at two different extension rates (specimen 107R).

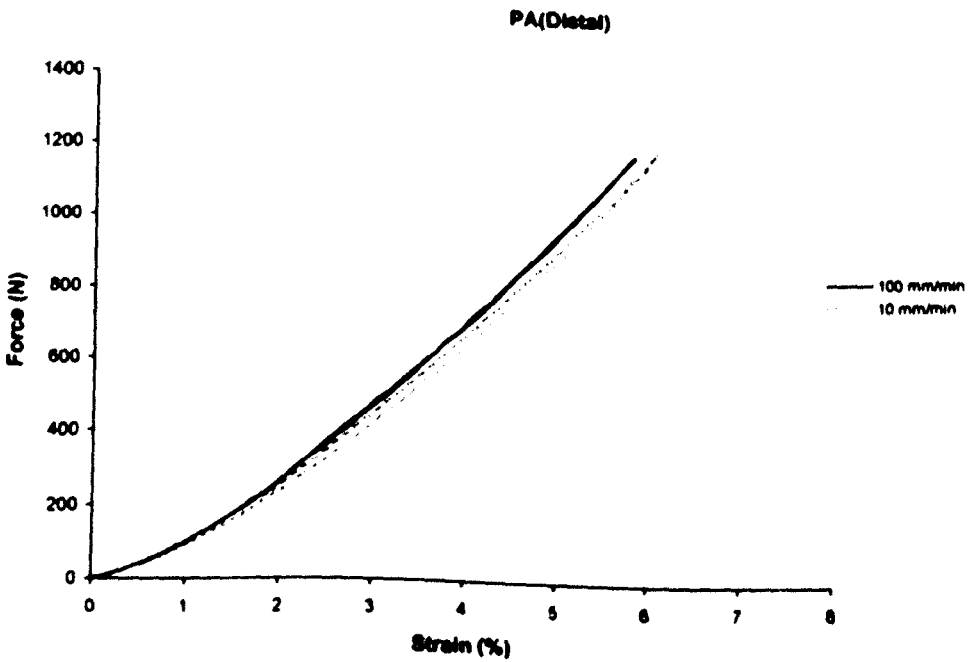


Figure 5.8 Force-strain response of the PA in tension at two different extension rates (specimen 107R).

The mechanical behaviour of the ligaments in simple tension was expressed in terms of the force-strain and normalised stress-strain responses. The force-strain curves provided the means of estimating functional forces during the intact tests and allowed evaluation of the specific mechanical properties of each ligament with respect to their force carrying potential, e.g. stiffness. The stress-strain curves gave the information necessary to assess aspects of the normalised tissue behaviour. This allowed the mechanical properties of each ligament specimen to be compared directly as well as providing a means to estimate the functional levels of stress in the intact tests.

Both the stress-strain and load-strain curves were produced from the final loading and unloading cycle taken during testing at the highest loading increment. After preconditioning of the tissue the load-strain response was found to be stable and highly reproducible.

The general shapes of the curves were of the form expected of biological material of this sort with a characteristic non-linear shape. The ligaments exhibited hysteresis when unloaded and slight rate dependency, viscoelasticity, was demonstrated. Examples of stress strain and load strain responses are given in figures 5.7 and 5.8. The stress-strain and load-strain curves for the SPL differed from those of other ligaments in that a more variable response was noted, marked apparent hysteresis when unloaded and low levels of force and stress with applied strain (fig 5.9). The characteristic shape of the SPL curves may have been due to off axis shear loading and the unique methodology used to derive the mechanical properties of this ligament. The complete set of stress-strain and force-strain results are presented in appendix 5.

#### **5.4.2 Modelling of the Tissue Mechanics**

Quasi-linear viscoelasticity has been successfully used to model the tensile behaviour of parallel fibred collagenous tissue (see section 3.3.1). Although experimental constraints prevented measurement of the stress relaxation properties of the ligaments in the present study, the elastic response of the tissues,  $\sigma^e$ , was calculated and compared to models previously proposed in the literature. The following forms of elastic response have been proposed and have been found to adequately describe the mechanical behaviour of ligaments and parallel fibred collagenous tissues. Recalling equations 3.8 and 3.9 from chapter 3:

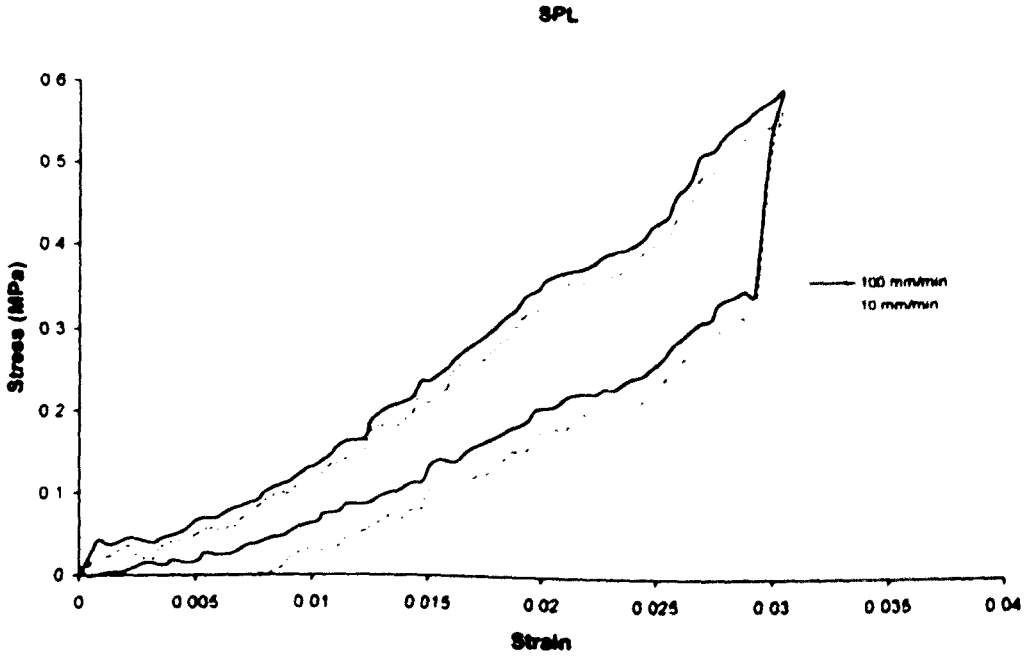


**Figure 5.9** Stress-strain response for the SPL in tension at two different extension rates (specimen 107R).

Jenkins and Little (1984)  $\sigma^e = A(e^{B\varepsilon} - 1)$  (5.4)  
Woo *et al* (1981)

Haut and Little (1972)  $\sigma^e = B\varepsilon^A$  (5.5)

On inspection of the experimental results it was seen that the stress-strain relationships for the ligaments were not sensitive to a ten-fold change in strain rate. Since the faster testing speeds were more representative of the physiological strain rates these values were taken for modelling (Note: By definition  $\sigma^e$  is the tissue response at infinite strain rate). Values of the loading cycle for the stress-strain data for each ligament were fitted to the above relationships using least squares regression curve fitting procedures of a statistical analysis package (SPSS®, Version 6.1). To simplify the computational effort equation 5.4 was expanded as a Taylor series giving:

$$\sigma^e = A \left( B\varepsilon + \frac{B^2\varepsilon^2}{2} + \frac{B^3\varepsilon^3}{6} + \dots + \frac{B^n\varepsilon^n}{n!} \right) \quad (5.6)$$

This allowed experimental data to be fitted to linear, quadratic and cubic polynomial expressions of the form:

$$\sigma^e = b_0 + b_1\varepsilon + b_2\varepsilon^2 + b_3\varepsilon^3 \quad (5.7)$$

The effects of inclusion of higher terms was explored with respect to the accuracy of the fit by inspection of the  $R^2$  values, i.e. the least order of polynomial required to effectively model the data. The ability of the model to describe the data was assessed by looking at the constant value,  $b_0$ , and the ratio of the coefficients of the strain terms, i.e.:

$$B_2 = 2 \frac{b_2}{b_1} \quad , \quad B_3 = 3 \frac{b_3}{b_2} \quad (5.8)$$

Where  $B_2$  and  $B_3$  were estimates of B from the quadratic and cubic terms respectively.

Ligament	Method	R <sup>2</sup>	b0	b1	b2	b3	B <sub>2</sub>	B <sub>3</sub>
PA (Distal)	Linear	0.986	-1.39	280.79	-	-	-	-
	Quadratic	0.999	-0.43	163.12	2283.47	-	28.00	-
	Cubic	1	-0.11	84.78	6143.71	-49757.00	144.94	-24.30
	Power	0.993	855.78	1.40	-	-	-	-
PA (Prox.)	Linear	0.989	-1.06	249.88	-	-	-	-
	Quadratic	0.999	-0.24	154.75	1636.11	-	21.14	-
	Cubic	1	-0.05	110.26	3588.58	-22067.00	65.09	-18.45
	Power	0.998	491.52	1.26	-	-	-	-
LPL	Linear	0.915	-0.94	117.74	-	-	-	-
	Quadratic	0.998	0.18	-15.96	2637.32	-	-330.47	-
	Cubic	1	0.01	29.25	336.48	30690.70	23.01	273.63
	Power	0.975	590.22	1.60	-	-	-	-
SPL	Linear	0.938	-0.10	29.02	-	-	-	-
	Quadratic	0.996	0.11	0.92	616.46	-	1339.39	-
	Cubic	0.997	0.07	10.23	100.03	7573.91	19.56	227.14
	Power	0.866	13.77	0.86	-	-	-	-
CNL	Linear	0.977	-0.16	13.58	-	-	-	-
	Quadratic	1	0.02	5.56	58.97	-	21.22	-
	Cubic	1	0.00	7.15	29.57	143.40	8.27	14.547
	Power	0.991	19.48	1.23	-	-	-	-

Table 5.3 Stress-strain curve fit parameters for specimen 131L.

Ligament	Method	R <sup>2</sup>	b0	b1	b2	b3	B <sub>2</sub>	B <sub>3</sub>
PA (Distal)	Linear	0.99	-1.89	366.89	-	-	-	-
	Quadratic	1.00	-0.37	199.93	2900.60	-	29.02	-
	Cubic	1.00	-0.10	139.01	5580.07	-30886.00	80.28	-16.61
	Power	0.998	910.09	1.34	-	-	-	-
PA (Prox.)	Linear	0.99	-2.33	355.02	-	-	-	-
	Quadratic	1.00	-0.61	194.28	2435.66	-	25.07	-
	Cubic	1.00	-0.11	100.74	6017.13	-36162.00	119.46	-18.03
	Power	0.996	1017.86	1.41	-	-	-	-
LPL	Linear	0.94	-1.13	125.27	-	-	-	-
	Quadratic	1.00	0.06	7.79	1945.84	-	499.71	-
	Cubic	1.00	0.07	6.27	2009.29	-705.43	640.56	-1.05
	Power	0.975	348.74	1.45	-	-	-	-
SPL	Linear	0.98	-0.04	19.24	-	-	-	-
	Quadratic	1.00	0.01	10.55	286.28	-	54.28	-
	Cubic	1.00	0.02	6.87	592.42	-6729.20	172.43	-34.08
	Power	0.908	11.28	0.92	-	-	-	-
CNL	Linear	0.95	-0.48	22.23	-	-	-	-
	Quadratic	1.00	0.05	3.23	111.15	-	68.75	-
	Cubic	1.00	0.00	6.75	58.80	204.52	17.43	10.44
	Power	0.975	29.05	1.29	-	-	-	-

Table 5.4 Stress-strain curve fit parameters for specimen 107R.

The data were also modelled using the power law given below:

$$\sigma^e = b_o \varepsilon^{h_1} \quad (5.9)$$

Results of the curve fitting analysis are given for the two specimens in tables 5.3 and 5.4.

### 5.4.3 Functional Force and Stress Estimates

Magnitudes of functional force and stress were calculated for two of the foot specimens previously subjected to standing and gait simulations. The results were presented graphically as histograms for each of the groups of activities in a similar fashion to the strain results in the intact specimens. Due to the small number of specimens tested statistical analysis of the results of this procedure was not viable. The entire set of data for the two foot specimens is presented.

Errors in the force estimates were caused by use of the weight of the bone-pots as the non-zero references. The above errors were expressed as percentages of the maximum force estimates for each of the ligaments of the two specimens in table 5.5.

Specimen	107R	131L
PA(D)	2.4%	2.0%
PA(P)	2.5%	2.4%
LPL	9.0%	0.8%
SPL	26%	24%
CNL	6.3%	6.0%

Table 5.5 Percentage errors introduced when using the weight of the bone pots as the zero force reference. Values as normalised to the maximum measured force or stress in each ligament.

Samples of relevant data are presented below, the full data sets are contained in appendices 6 and 7. (Note: Values extrapolated from curve fits of the experimental data are marked with an asterisk). Since values of functional force and stress in the foot

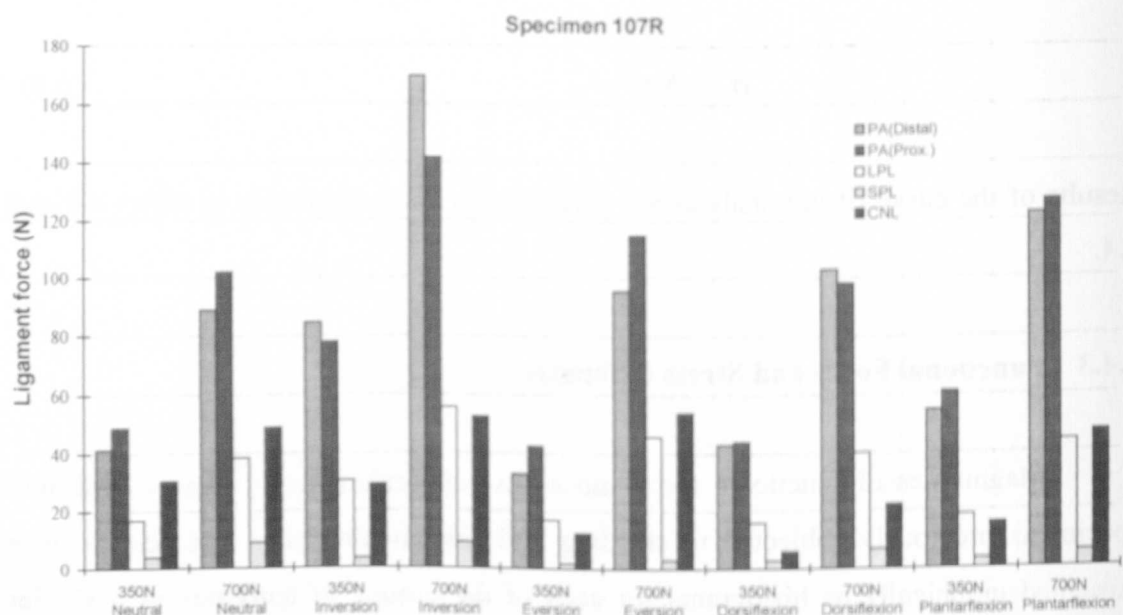


Figure 5.10 Functional forces in the foot ligaments with the foot placed in different positions during standing (specimen 107R).

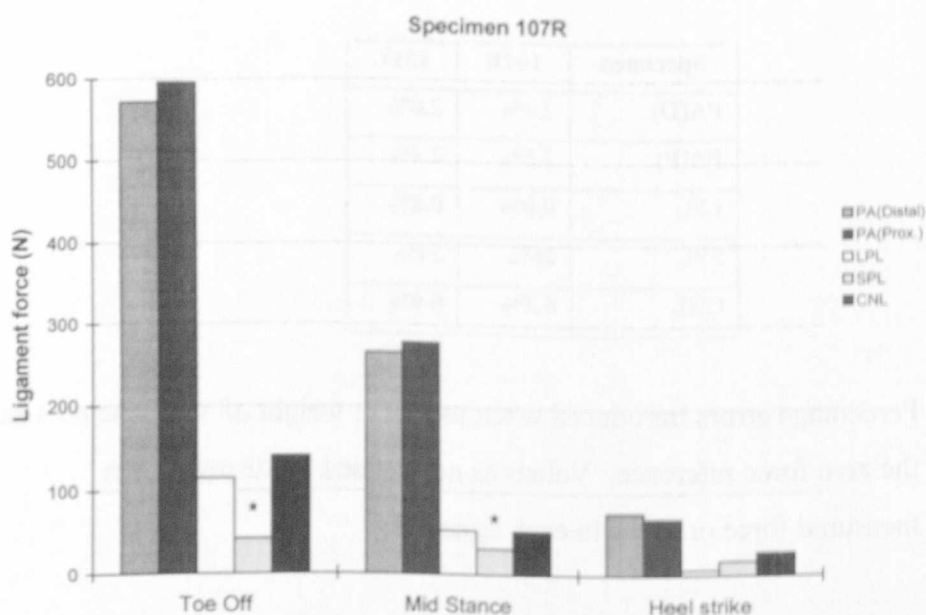


Figure 5.11 Functional forces in the foot ligaments during 3 stages of simulated gait (specimen 107R). Note: \* = interpolated value.

ligaments were derived directly from measured strain values, similar trends were observed in these data sets. Of primary interest were the levels of force and stress in the ligaments between activity types. From the simplest of functional viewpoints values of force and stress during quiet standing and simulated gait are of immediate importance. Values for these quantities are given in tables 5.6 to 5.9. In standing, in the neutral position, it was found that the PA was the most highly loaded structure with estimated forces of between 40 and 160 N. The SPL was very lightly loaded with forces of under 10N in both specimens. The SPL was also the least stressed of all the ligaments during standing with levels of 0.15 and 0.08 MPa. Stress levels in standing for the remaining ligaments ranged from 0.25 and 0.3 MPa for the two CNLs to 2.22 and 0.93 MPa for the PA. Values of ligament force during simulated gait were correspondingly greater than those during standing. PA forces were greatest during simulated toe-off where values of approximately 600 N were calculated. The forces in the remaining ligaments were also increased with respect to standing but the SPL was once again the most lightly loaded. The LPL of specimen 131L was noted as being heavily loaded during toe-off with a force of 1375 N. The PA and LPL were the most highly stressed ligaments during gait (10 MPa of stress at toe-off for the PA). Forces and stresses for specimen 107R during standing and gait are shown in figures 5.10 and 5.11.

Ligament	Force (N)	
	Specimen 131L	Specimen 107R
PA(Distal)	158.17	41.49
PA(Prox.)	69.82	48.92
LPL	41.90	16.77
SPL	6.57	4.03
CNL	27.01	30.52

**Table 5.6** Ligament forces during standing in the neutral position.

Specimen 107R

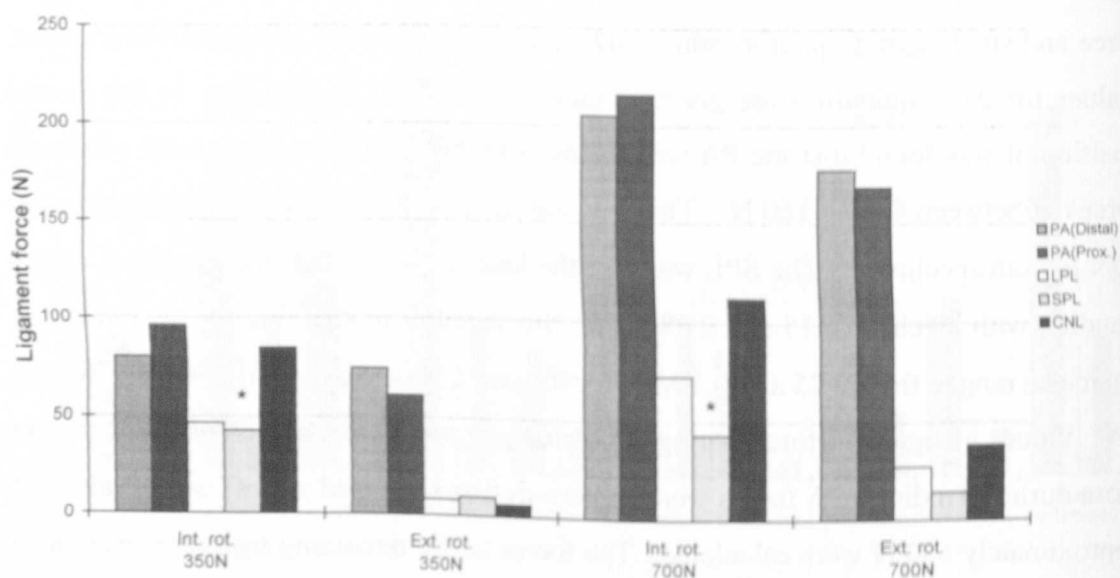


Figure 5.12 Functional forces in the foot ligaments with the foot subjected to applied tibial rotation during standing (specimen 107R). Note: \* = interpolated value.

Specimen 107R

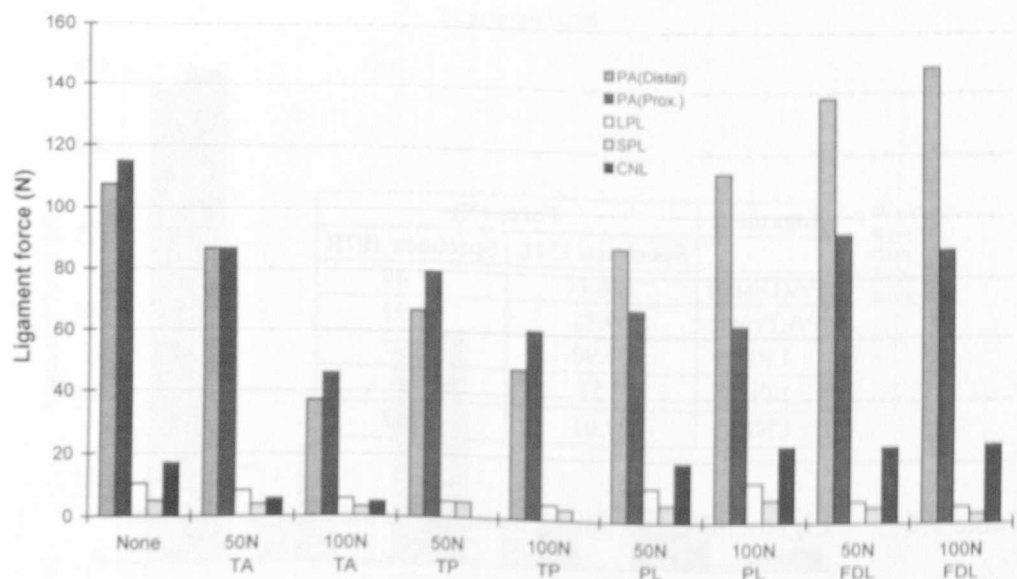


Figure 5.13 Functional forces in the foot ligaments with applied extrinsic muscle forces during standing (specimen 107R).

Ligament	Stress (MPa)	
	Specimen 131L	Specimen 107R
PA(Distal)	2.22	0.73
PA(Prox.)	1.03	0.93
LPL	0.63	0.34
SPL	0.15	0.09
CNL	0.25	0.30

Table 5.7 Ligament stresses during standing in the neutral position.

Ligament	Force (N)					
	Specimen 131L			Specimen 107R		
	Toe Off	Mid Stance	Heel strike	Toe Off	Mid Stance	Heel strike
PA(Distal)	664.9	337.8	94.7	571.1	264.9	76.0
PA(Prox.)	570.6	328.2	205.3	596.0	277.5	68.7
LPL	1375.9	1026.3	374.1	115.0	53.3	7.0
SPL	37.6	24.3	43.9	41.8	31.5	17.1
CNL	225.8	121.1	27.3	141.1	52.9	27.9

Table 5.8 Ligament forces during gait.

Ligament	Stress (MPa)					
	Specimen 131L			Specimen 107R		
	Toe Off	Mid Stance	Heel strike	Toe Off	Mid Stance	Heel strike
PA(Distal)	9.33	4.74	1.33	10.08	4.67	1.34
PA(Prox.)	8.44	4.85	3.04	11.37	5.29	1.31
LPL	20.66	15.41	5.62	2.35	1.09	0.14
SPL	0.86	0.55	1.00	0.91	0.69	0.37
CNL	2.13	1.14	0.26	1.40	0.53	0.28

Table 5.8 Ligament stresses during gait.

Applied tibial torsion had the greatest effect on the forces and stresses in the LPL and CNL in both test specimens. Internal rotation caused increased loading in these and other ligaments (fig 5.12).

In line with the strain results, applied muscle forces produced large changes in the levels of force and stress in the tarsal ligaments (LPL, SPL and CNL). The force and stress ratios in the distal and proximal PA were also altered by differing applied muscle forces (fig 5.13).

Specimen 107R

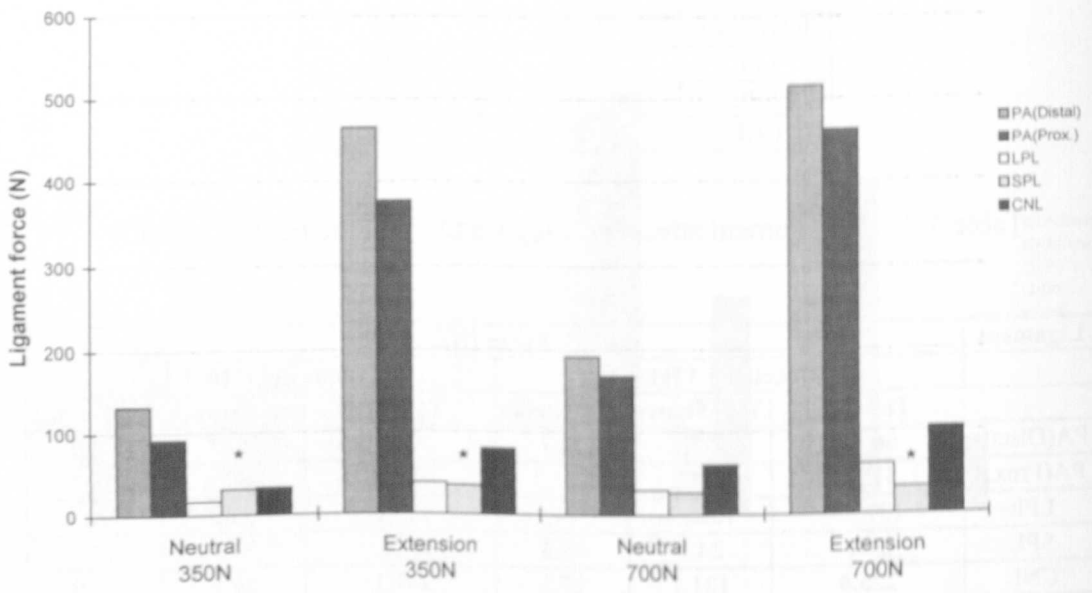


Figure 5.14 Functional forces in the foot ligaments with the foot subjected to toe extension during standing (specimen 107R). Note: \* = interpolated value.

Condition	PA(Distal) (N)	PA(Prox.) (N)	LPL (N)	SPL (N)	CNL (N)
Neutral 350N	130	90	20	35*	40
Extension 350N	470	380	45	40*	85
Neutral 700N	195	170	35	30	65
Extension 700N	520	470	70	45*	115

Applied toe-extension increased the levels of force and stress in both specimens by a factor of approximately 4 - 5, confirming the function of the windlass mechanism (fig 5.14).

Other points of note for the force/stress data set were identified. Dorsal and proximal PA forces were not in general calculated as being equal, an interesting observation since the PA is a single continuous ligament. Ratios in the two PA forces and stresses did not remain constant over the range of tests, a result requiring further interpretation. Force and stress in the SPL were consistently found to be the lowest of the test ligaments. High levels of force and stress were found in the LPL of specimen 131L during gait and on the application of TP forces. Reasons for, and the implications of these final observations are discussed in section 5.5.3.

#### **5.4.4 Other Findings**

Measurements of local strain, made with LMSGs, and strain derived from the crosshead extension and measured lengths of the ligaments were compared at the highest testing rates. When plotted against each other a linear relationship between the two quantities was found, however the gradients, other than for the PA, were not equal to 1.0, i.e. the effective gauge length of the ligaments derived from extension strain measurements were not equal to the measured length of the ligaments (fig 5.15). The gradients, greater or less than 1, revealed non-uniform strain distributions along the length of the ligaments. The patterns of relative gradient between the ligaments were similar for the two test specimens.

### **5.5 DISCUSSION**

#### **5.5.1 Mechanical Properties of the Foot Ligaments**

The shapes of the stress-strain and force strain curves for the foot ligaments in general fitted the form of tissue response of parallel fibred collagenous tissue, i.e. non-linear relationship with a flat toe region at small strains and a more linear portion at higher loading. Hysteresis and slight rate dependency were also exhibited.

**Specimen 107R**

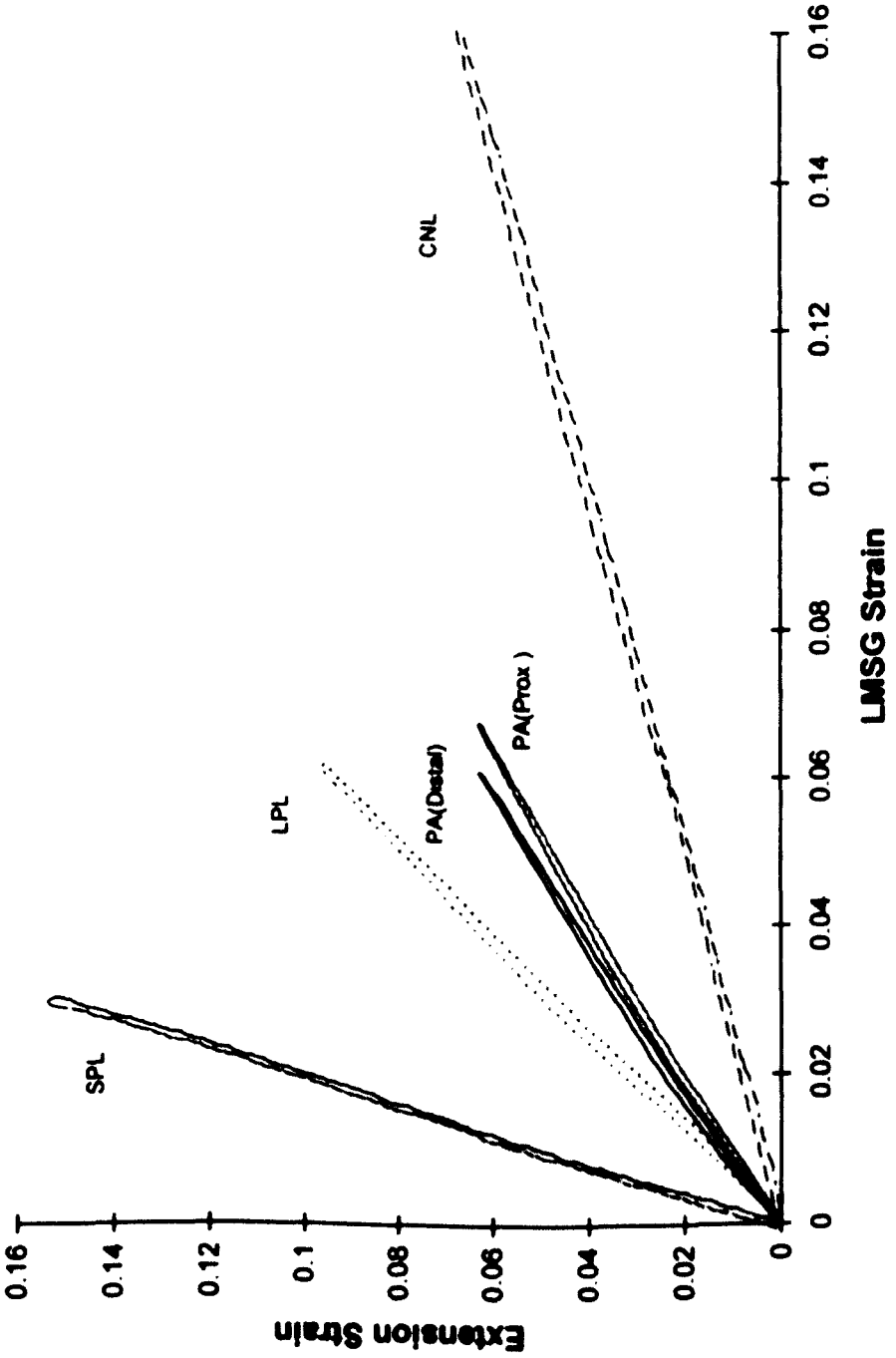


**Figure 5.15(a)** Extension strain vs. LMSG strain in the tension tests for specimen 107R. Data presented were taken from the loading curve at the highest extension rate.

The form of the SPL stress-strain relationship was, however, noticeably different from the remaining ligaments and had the following features: (1) short high gradient section at the beginning of loading, (2) marked hysteresis with rapid unloading on reversal of extension, (3) a greater apparent strain rate dependency and (4) overall low levels of force and stress. Possible reasons for this could have been due to aspects of the testing and analysis protocol or tissue response itself. Alignment uncertainties during set up of the isolated tests may have been introduced given the difficulty in reproducing the exact bone ligament geometry of the intact foot (SPL and LPL join the same two bones). It is also likely that the tensile nature of the tests would not have accurately reproduced details of physiological motion, i.e. the LPL was likely to be loaded in flexion/extension movements of calcaneocuboid joint while rotations about the longitudinal axis of the joint, as in pronation/supination, would have caused loading in the SPL in the intact foot. Despite the low levels of force witnessed in the SPL, strains of 3-4.5% were recorded that were of a similar magnitude to those during activities in the intact tests, implying that function was being simulated.

Errors introduced by the subtraction process in the SPL force derivations were seen as undulations in the SPL stress and force graphs, i.e. a greater degree of noise was present in this data than for the other ligaments. By definition the SPL was not loaded during testing in a direction parallel to the fibre direction as part of the prescribed technique. This would have introduced an element of shear loading in the ligament and may have caused abnormal fibre recruitment and loading at the bone-ligament insertion. Alternatively backlash effects due to slight laxity in the loading rig may have been responsible for the steep reduction of force on strain reversal.

The remaining ligaments, PA, LPL, and CNL showed similar mechanical responses characterised by a small amount of hysteresis (always returning to the zero stress/strain condition) and a slight strain rate dependency, or viscoelasticity. The largest difference between the maximum forces at the two testing speeds was 5% found for the distal PA of specimen 107R.

There have been few previous studies of the foot ligaments to which the results of the present study can be compared. Most interest has been focused at the PA where values of elastic modulus and stiffness have been calculated. (Elastic modulus: 344 - 827 MPa, Wright and Rennels (1964) and 1236 MPa, Jacob (1980); Stiffness: 209

Specimen 131L

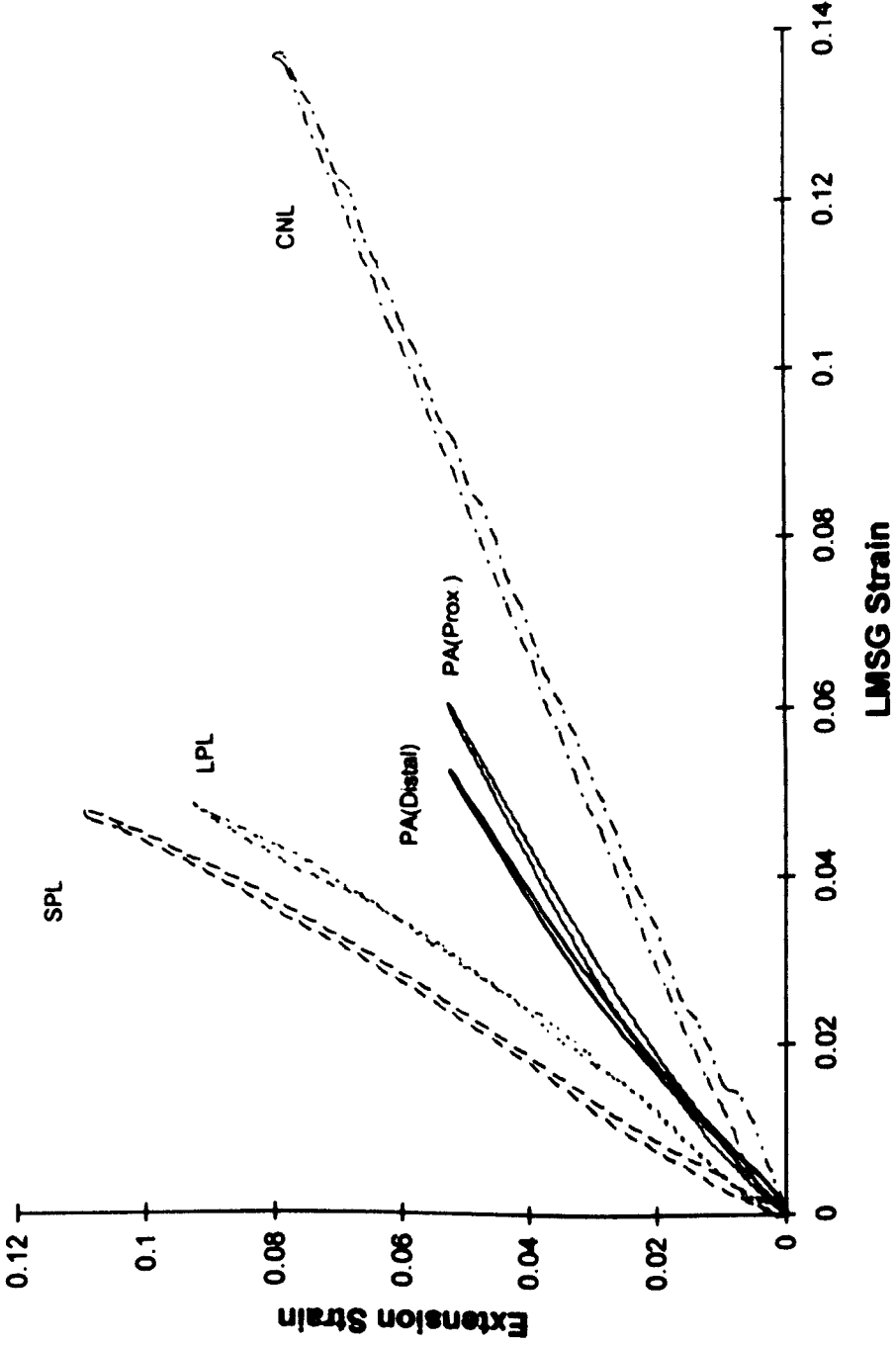


Figure 5.15(b) Extension strain vs. LMSG strain in the tension tests for specimen 131L. Data presented were taken from the loading curves at the highest extension rate.

N/mm Kitoaka *et al* (1994)). Estimates of the PA elastic modulus and stiffness in the present study were taken from the latter portion of the curves for the four PA measurements, and averaged ( $E = 352$  MPa,  $k=224$  N/mm). Kitoaka (1994) found that the stiffness of the PA was not significantly affected by a hundred fold change in the extension rate. Results of the present study, therefore, were seen to agree closely with the results of previous studies of PA mechanics.

Davies *et al* (1995) calculated the modulus of the CNL as 9.0 MPa which is smaller than the average value of 28 MPa found in the present study. Differing methods of strain and area measurement were used in the derivation of these two results.

Translation of the tissue response to a linear relationship is a convenient method of description and comparison of the tissue mechanics as a whole. The linear portion of the tissue response, however, cannot be considered in isolation since the stress-strain relationship is clearly not of this type. Linear treatment of the tissue mechanics is useful in analysis or modelling of situations where it is known that the ligaments are functioning in this condition. This was not the case in the present study hence the full extent of the mechanical behaviour of the tissue was considered.

### **5.5.2 Modelling of the Tissue Mechanics**

The stress-strain responses of the ligaments were modelled to four different relationships (linear, quadratic, cubic and power) suggested by previous tissue modelling investigations in the literature, the results of which are presented in tables 5.3 and 5.4.

On inspection of the correlation coefficients,  $R^2$ , it was seen that inclusion of higher polynomial terms increased the accuracy of the fit, as expected. Modelling the data to a quadratic relationship gave values of  $R^2$  approaching 1.0, while the cubic form gave  $R^2$  values of 1.0 in all but one ligament. For conformance of the data to the relationship  $\sigma^e = A(Be^e - 1)$ , values of  $b_0$  equal to zero and consistent ratios of polynomial coefficients were required. Inspection of these values in table 5.3 and 5.4 revealed that the above criteria were not displayed for any of the test ligaments. The CNL of specimen 131L was the closest approximating case. It was unlikely that inclusion of quartic and higher order terms would have increased the quality of the data

fit such that  $b_0$  and the coefficient ratios would have converged to satisfy the above relationship. The cubic model was considered to give an accurate description of the empirical results. The derived relationships may be of use in future investigations where linear representation of the tissue mechanics is not satisfactory. The cubic relationships were used to extrapolate to strain values just beyond the test range when estimating functional values of force and stress in the foot ligaments.

Modelling of the stress-strain data to the power expression gave moderately accurate agreement in most ligaments ( $0.866 < R^2 < 0.998$ ). Applying the power law model to the PA, LPL and CNL revealed a good fit for these ligaments ( $R^2 = 0.975 - 0.988$ ). It was concluded that the power law adequately described the experimental stress-strain results for the above structures. It was found that fitting only values of data away from zero gave a better adherence to the suggested relationship, i.e. the stress-strain values close to zero were responsible for the errors in the data fitting analysis. Fitting data using this particular relationship involved first linearising the expression using logarithms, a process which was sensitive to errors in values close to zero in the data set.

### **5.5.3 Functional Force and Stress Estimates**

Values of functional force in foot ligaments in the present study were made by matching functional strains to the specific measured mechanical responses of the ligaments. Estimates of foot ligament force made using other methods are compared to the results of this study in table 5.10. Values of force found in the present study during standing are within the range of the values found by other investigators. LPL forces in standing compare with the only previous estimates of this quantity. Values of ligament force during gait have not been previously calculated. It is likely that the PA force value of 2200N found by Morlock (1990) during a side-step movement was too high in view of the results of Kitoaka *et al* (1994) who found a breaking force for the PA of  $1189 \pm 244$ N. Morlock (1990) assumed only one plantar ligament, the PA, carried force in the foot. This assumption was very probably the cause of the over estimation. Assuming the data of Kitoaka *et al*(1994) to be correct it was found that the maximum PA force (618N), during toe-off, was approximately 0.5 times the breaking force (1189N) of the

PA. In the absence of intrinsic muscle activity present in the normal foot this value of PA force constituted a ‘worst’ case estimate.

Investigation	Ligament	Force (N)	Activity	Method
Simkin (1982)	PA	260	Standing	Modelling
	LPL	67	Standing	
Morlock (1990)	PA	2200	Athletic Side-Step	Inverse dynamics
Kim & Voloshin (1995)	PA	50	Standing	Inverse dynamics
Wright & Rennels (1964)	PA	164	Standing	Modelling
Present Study Mean values(n = 2)	PA (Distal)	99	Standing	Instrumented cadaver specimens
	PA (Prox.)	59	Standing	
	LPL	29	Standing	
	PA (Distal)	618	Gait (Toe-off)	
	PA (Prox.)	583	Gait (Toe-off)	

Table 5.10 Functional force estimates in the foot ligaments.

Forces and stresses in the SPL were small, by comparison with the other ligaments, and hence the effects of systematic errors in the force calculation techniques had a correspondingly greater effect on the force and stress values in this ligament. Possible errors of 25% in the SPL forces and stresses were introduced as a result of the non-zero force references used during the isolated tensile tests (tending to underestimate both quantities). In light of the above considerations, in addition to errors arising from the derivation techniques, less emphasis should be placed on the validity of the SPL force and stress values. Induced errors in the PA, LPL and CNL were of a much smaller magnitude (<6%).

A complex array of changing ligament forces was observed with position of the foot under load. Inversion and eversion movements resulted in changing distal and proximal PA force and stress ratios, indicating that forefoot twist alters the internal loading of the PA in the intact foot. Other results of functional importance were noted. At the highest applied load level, 700 N, CNL force was increased during eversion and plantarflexion by an average of 25%. This result may have implications in the live

subject for active eversion and incurred rearfoot motion during gait and running. Minimisation of this type of movement is an important consideration in the design of athletic footwear since excessive rearfoot motion is thought to be a factor in injury of soft tissue structures on the medial side of the foot (Nigg, 1986 and Li and Ladin, 1992).

Internal rotation, and induced eversion, was observed to increase the loading in all the ligaments of both specimens reaffirming the above conclusion. This result also confirms the traditional anatomical explanation of forefoot pronation causing the tarsal ligaments to become taught. This result also serves to show that the foot cannot be viewed in mechanical isolation from the rest of the lower limb. It was demonstrated that the torsion angle of the tibia with respect to the foot greatly affects the load bearing function of the foot and the mechanics of the ligaments. This angle is not commonly used or considered of interest in kinematic analysis during gait studies or biomechanical investigations of the lower limb.

Applied muscle forces were seen to be able to decrease the force in the foot ligaments. Forces in the TA decreased the forces in all ligaments in both specimens. TP forces gave the greatest reduction in the CNL, eliminating force altogether in one specimen. These observations confirm the published clinical experience of TP tendon rupture which has been shown to lead to acquired flatfoot deformity if left untreated (Cozen, 1965; Mann, 1983; Mann and Thomson, 1985 and Funk *et al*, 1986). It may also be surmised that acquired extrinsic muscle dysfunction may lead to increased ligament strain and eventual injury with repeated overloading, based on the above evidence.

Applied toe extension was seen to increase the force in the PA by a factor 4 to 5. The pattern of changes in force in the tarsal ligaments was less reproducible with increases and decreases recorded, although the relative changes were not as marked as in the PA. Whilst the result of toe extension confirmed the primary function of the windlass mechanism as one that increased the force in the PA, its function with respect to the other ligaments remained less clear (see also section 4.5.4). It was noted throughout the data set that the distal and proximal PA force and stress estimates were not equal in most cases. Also it was found that variations in forefoot loading altered the distal/proximal PA force and stress ratios between different activities. Possible reasons

for this have already been described in section 5.4.1 (insertions with other anatomical structures cause a varying force distribution along the length of the PA).

Large forces and stresses were noted in the LPL during gait and with applied TP forces. It is unlikely that a 100 N muscle force and 700 N applied vertical force could have actually caused forces of approximately 1000 N in the LPL. In the toe-off phase of gait the value of force reached 1400 N. It was probable that the LPL strain during these activities was increased due to local concentrations induced by the particular conditions of testing in these cases, i.e. strain in the instrumented ligament fibres was sensitive to the applied forces and the position of the foot in this particular case. In a large sample population these local variations would tend to be averaged out, but since only small numbers were tested in the present study large variations in the data were readily revealed. This result also highlights some of the inherent difficulty in measuring strain effectively in ligamentous tissue. Deriving strain from extension and overall length measurements is not a suitable method for ligaments with complex geometry and cannot reveal details of fibre recruitment patterns. Strain measurements taken using direct instrumentation methods, e.g. LMSGs, are prone to localised variations in the overall bulk strain in the ligament.

#### **5.5.4 Other Findings**

As validation of the LMSG technique, and in order to explore the possibilities of concentrations in the strain being measured, the LMSG strains and strain derived from crosshead extension and measured ligament lengths were compared. The results are presented graphically in figures 5.15a and b. Both specimens gave similar patterns of curvature and slope. The graphs of extension strain vs. LMSG strain were of a linear form indicating that LMSG response to strain was constant over the range of applied extension. The gradients in the distal and proximal PA were close to unity indicating that local and bulk strain were closely related for this structure. In the LPL and SPL the gradient was greater than 1.0 implying a greater portion of strain in the ligament was occurring beyond the limits of the gauge length of the transducer, i.e. near the ligament insertions. This supports the findings of previous studies that have described this effect when testing bone-ligament-bone preparations (Butler *et al* , 1984 and 1990; Noyes *et*

*al.*, 1984 and Woo *et al.*, 1983). Further evidence that the above result was an ‘end effect’ at the insertion site was given by the fact that the gradient in figure 5.15 increased with decreasing ligament length, i.e. the end effects became more dominant in smaller ligaments.

The CNL did not obey the above hypothesis displaying gradients of less than 1.0 in both specimens. This indicated that strain in this ligament was concentrated in mid-substance unlike the LPL and SPL. A possible reason for this strain distribution may have been the unique histology of this ligament. The area of the CNL that articulates with the head of the talus has been found to consist of fibrocartilage with a less orientated collagen structure than the deeper portions of the ligament (Davies *et al.*, 1996). Since the articular facet was in the centre of the ligament, away from the insertion sites, an area of more compliant collagenous tissue may have existed in this region.

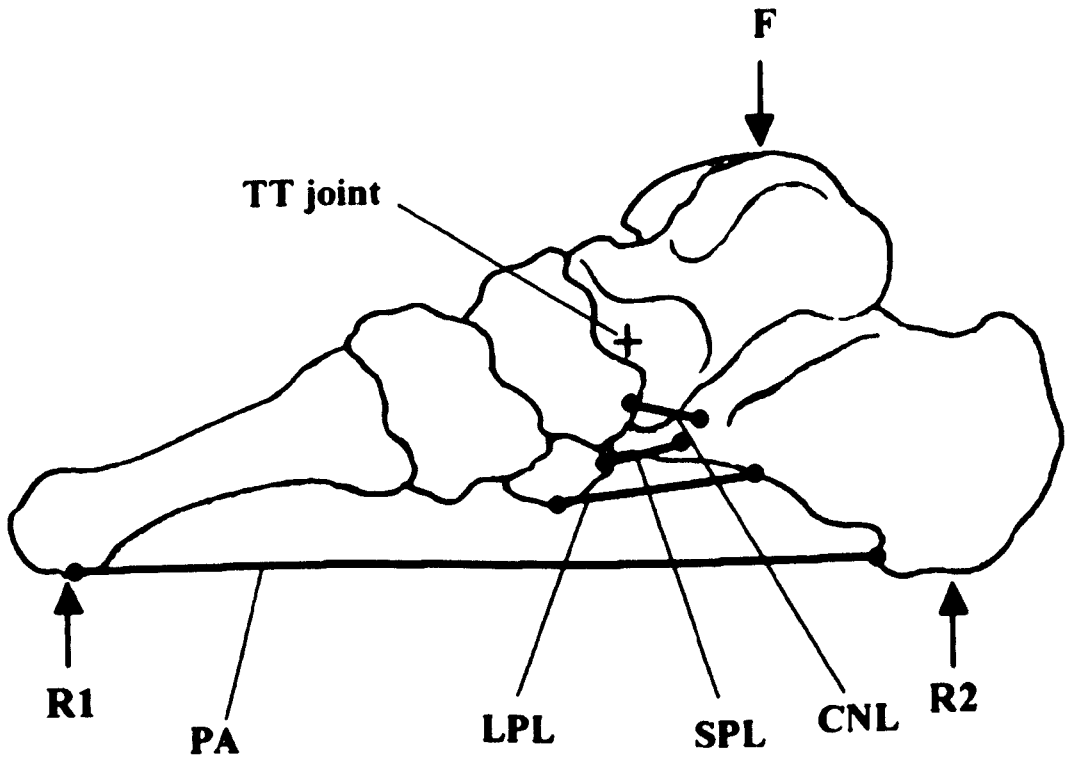


Figure 6.1 Schematic view of the foot model. Vertically applied force,  $F$ , is supported at the heel and metatarsal heads by ground reaction forces  $R_1$  and  $R_2$ . The ligaments supply the necessary forces required to produce equilibrium at the TT joint.

## **CHAPTER 6. MATHEMATICAL MODELLING OF THE FOOT**

### **6.1 INTRODUCTION**

Previous structural models of the foot have addressed some aspects of ligament mechanics but none have attempted a separate quantitative investigation of the deeper ligaments of the tarsus during simulated activity. This chapter describes the formulation, solving method and results of a two-dimensional model designed to yield quantitative data on the forces and strains in the foot ligaments during standing. The model provided data for comparison with the experimentally derived ligament forces and strains and also allowed the effects of ligament injury and a corrective surgical procedure to be assessed. The effects of extrinsic muscle force on ligament function were also investigated. The model used anatomical data derived directly from cadaveric specimens whilst the force-deflection data from tests on the same specimens provided the remaining information necessary to complete the mathematical analysis.

### **6.2 MODEL DESCRIPTION**

#### **6.2.1 Theory**

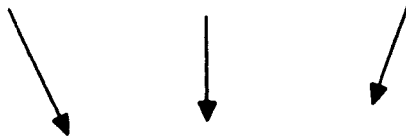
A two-dimensional representation of the foot was constructed from mechanical elements and solved using static rigid body mechanical analysis (mass of the foot and its components and their inertial properties were neglected). In its entirety the foot is an extremely complex structure and does not lend itself easily to mathematical modelling. Although some three dimensional models have been formulated the function of the separate ligaments was not included (Scott and Winter, 1993 and Salathe *et al*, 1986) or was simplified (Simkin, 1982, and Morlock, 1989). Two-dimensional treatment of the foot as a structure has been more common in the literature (Kim and Voloshin, 1995, Simkin and Leichter, 1990, Veres 1977 and Wright and Rennels, 1964) and was adopted in the present study. A diagrammatic representation of the model is shown in figure 6.1. The elements and forces used in the formulation of the model are listed in table 6.1. In the model the applied tibial forces, such as in standing, caused the bones to displace

**Inputs**

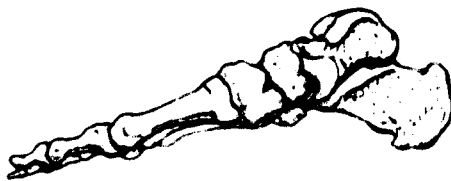
Experimental  
forces and  
deflections

Anatomical  
co-ordinate  
data

TT joint  
position



**The Foot Model**



**Outputs**

Strain

Force

TT angle

Moments

Figure 6.2 Diagrammatic representation of the flow of information into and out of the model.

relatively at the transtarsal (TT) joint resulting in strain and force in the ligaments acting across this joint. Inputs to the model included the force-deflection data for whole feet in which the ligaments were sectioned in sequence, and positional data relating to ligament insertions and force application points. The outputs from the model were ligament force, ligament strain, TT joint motion and the moment at the TT joint balanced by each ligament. A pictorial representation of the flow of information in and out of the model is given in figure 6.2

Element	No.	Description
Joints	2	Ankle (TC) and transtarsal (TT). Uniaxial by definition of 2D model.
Bones	2	Rigid elements comprising metatarsals, cuneiforms, cuboid and navicular (forefoot segment) and calcaneus and talus (rearfoot segment).
Ligaments	4	PA, LPL, SPL and CNL. Deformable elements defined by a single line between two insertion points located on rearfoot and forefoot segments.
Forces	5	Muscle force (TP). Tibial/ankle force F. Vertical reaction force under segments 1 and 2, $R_1$ and $R_2$ .

Table 6.1 Mechanical elements comprising the model of the foot.

### 6.2.2 Experimental Forces and Deflections

Experimental forces and deflection data were obtained for the foot by conducting loading tests in the Instron® load frame using similar procedures to those used in chapter 4. In order to eliminate the inherent indeterminacy of the model when undergoing deflection (more than one ligament crosses the TT joint) it was necessary to successively cut the test ligaments to produce a series of load-deflection curves. This type of test was essentially identical to those of Huang *et al* (1995), Ker *et al* (1987) and Walker (1991).

Three test specimens, Nos. 113L, 107L and 104R (now referred to as foot 1, 2 and 3 respectively) which had previously undergone testing as described in chapter 4, were used in this part of the investigation. Before testing the specimens were thawed overnight at room temperature. The skin and superficial fascia on the sole of each

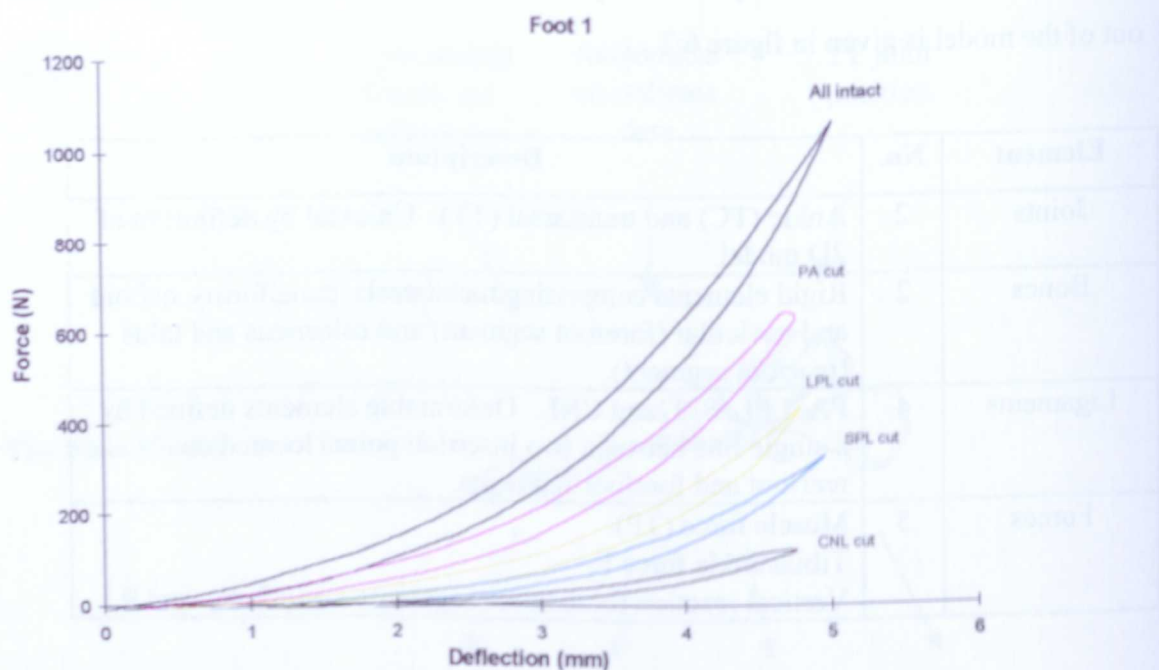


Figure 6.3 Force-deflection behaviour of the whole foot under applied vertical loading and unloading (foot 1). Successive curves show the changes in mechanical properties of the whole foot when the ligaments were cut.

specimen were removed and the tibia was remounted in the loading collar for introduction into the load frame. A modified polypropylene surface plate was used on the support platform to allow free excursion of the support points with low friction (heel and metatarsal heads) when the feet were loaded. A rigid load cell coupling was used which eliminated tibial torsion during loading and the feet were tested in the neutral position with no applied muscle forces.

A consistent and stable reference condition was required for the calculation of force at each deflection for inclusion into the model the Instron® was operated under displacement control). Each specimen was therefore subjected to a short load relaxation test, where a 20N vertical force was applied to the feet over a period of approximately 15 min. After this time the specimen was loaded cyclically from 20N to between 700 and 800 N until a stable reference load of 20N was attainable (to within 0.2N over 30s). The crosshead extension was then zeroed at this new displacement origin position. The feet were subsequently loaded at a constant extension rate of 100mm/min for 5 cycles to a deflection limit that produced a force of 700 to 800N with all the ligaments intact (Note: 700N vertical load was the upper limit applied in simulated standing in the intact tests). Each ligament was then cut (in the order PA, LPL, SPL, CNL) with the foot *in situ* on the Instron® and the tests repeated. The order in which the ligament structures are sectioned in this type of test, has been shown not to affect the force deflection behaviour of the foot in each specific state (Huang, *et al* 1993). Data were sampled at 20Hz using the Instron® control software (Instron®, SERIES XII), without the need for analogue conversion.

The resulting force-deflection curves showed the form expected from previous results i.e. non-linear relationship demonstrating hysteresis and a reduction in stiffness as more ligament structures were removed (Huang *et al*, 1995, Ker *et al*, 1987 and Walker, 1991). The load-deflection curve for foot 1 is shown in figure 6.3. The raw force-deflection data were processed for inclusion into the model. Only the loading data were considered since these produced the largest ligament forces. It was a prerequisite of the model that the force values for each ligament sectioning were input at the same levels of deflection. Linear interpolation of the raw data was performed to assign force levels at each of the deflection increments which were chosen at 10 regular intervals

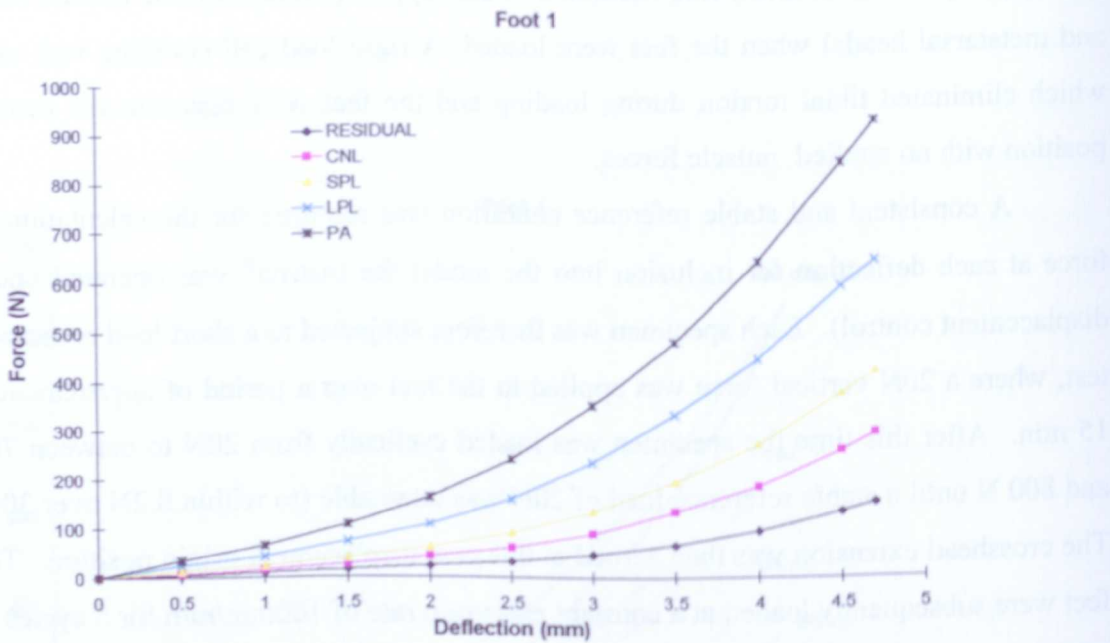


Figure 6.4 a Force-deflection input data for the model obtained from sectioning tests on foot 1 (loading parts of curves only for 1 cycle).

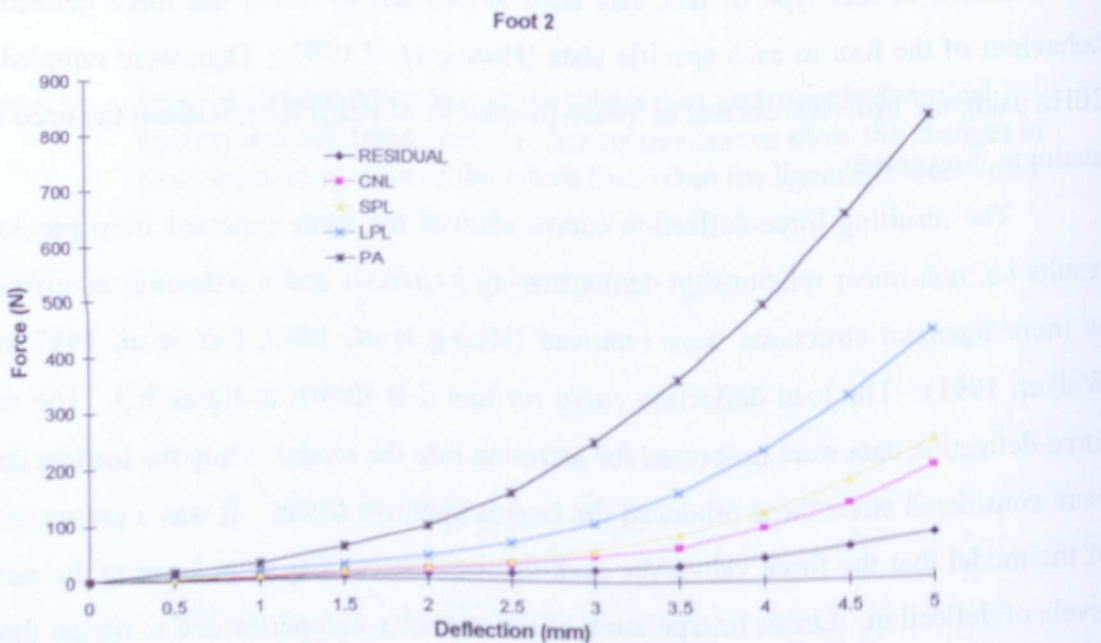


Figure 6.4 b Force-deflection input data for the model obtained from sectioning tests on foot 2 (loading parts of curves only for 1 cycle).

across the experimental range. The resulting force-deflection data, shown in figure 6.4 were then entered into the model.

The physiological support points were assumed to be under the heel and metatarsal heads as represented in the model and conditions of simple support (no shear forces or moments) were represented. Both of these assumptions are valid during standing since there are no net horizontal ground reaction force components acting on the foot and pressure measurements in living subjects have shown support forces to be concentrated at the heel and metatarsal heads (Walker, 1991).

### 6.2.3 Anatomy Variables

Positional input data required for the model were measured directly from the foot specimens. This information consisted of two-dimensional co-ordinates of the ligament insertions, force application points and joint centres. Since the structures had to remain intact at the time of testing a technique utilising X-rays was devised.

After the tests in chapter 4, access was possible to all the test ligament insertions with a small amount of further dissection. The anatomical points of interest were marked with lead shot, of diameter 1.5mm, which were inserted into small holes created in the bones at the required positions and cemented in place using cyanoacrylate adhesive. The markers implanted and their positions are shown in table 6.2. The specimens were then carefully refrozen in the neutral position

Points of interest	No. markers	Notes
Metatarsal heads	3	Met. heads 1, 2 and 5.
Calcaneus	2	Lowest point and PA insertion.
Ankle	2	Tips of lateral and medial malleoli.
Ligament insertions	8	Proximal and distal of PA, LPL, SPL and CNL
Muscle insertions	3	TACH, TP and TA

Table 6.2 Markers used to obtain positional data from X-ray exposures.

Foot 3

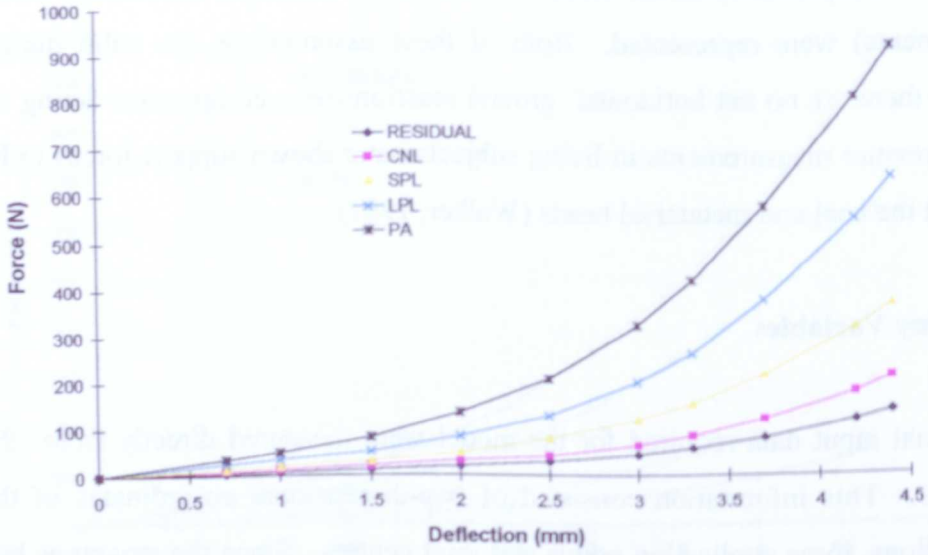


Figure 6.4 c Force-deflection input data for the model obtained from sectioning tests on foot 3 (loading parts of curves only for 1 cycle).

Force (N)	Deflection (mm)	RESIDUAL	CNL	SPL	LPL	PA
0	0	0	0	0	0	0
20	0.5	20	10	10	10	10
40	1.0	40	20	20	20	20
80	1.5	80	30	30	40	30
150	2.0	150	40	40	80	40
220	2.5	220	50	50	120	50
330	3.0	330	70	70	210	70
480	3.5	480	100	100	300	100
650	4.0	650	140	140	400	140
950	4.5	950	200	200	650	160

At a later date the specimens were photographed using X-rays in a Faxitron<sup>®</sup> cabinet (Hewlett Packard, Philadelphia, USA). Before exposure, the specimen was placed with the medial side uppermost with the lateral border resting on the film plate and the tibia parallel to the base of the cabinet. The heel of each specimen was also supported on polyethylene blocks so as to align the longitudinal axis of the foot with the film. The film to source distance was 648 mm with a maximum coverage at the film of 41.9 mm. An exposure of 7 minutes at 70 kV was used for all specimens. To assess the effects of parallax due to divergence of the X-rays from the source, a calibration object was also exposed onto the film. This consisted of two 100 mm long steel wires placed at right angles with a vertical 70 mm separation (one rested on the film). The centre of the beam target was aligned with the approximate TT joint centre to further reduce the distortion effects on the tarsal ligament insertion sites (close to the TT joint). The parallax calibration object was placed as near to the beam centre as possible, adjacent to the specimen (fig 6.5).

After exposure a positive contact print was taken from the developed films. The marker positions were then transferred onto acetate and measured to the nearest 1 mm using graph paper. Parallax error was assessed by measuring the difference in apparent length of the two rods on the exposures and was found to be between 1 and 5% for the three specimens. The X-ray for foot 1 is shown in figure 6.5. The measured anatomical co-ordinate data is presented in appendix 9.

The position of the TC joint centre was taken at the centre of the talar dome found by drawing normals to the curved surface, the mid-line of the tibia and taking the average intersection of these lines. The average position of malleolar tips was found to consistently place the TC joint centre too posteriorly. The metatarsal force application point was taken as the average of the first and second metatarsal markers. A first estimate of the TT joint centre was taken at the centre of the talar head found by taking the average insertion of 3 surface normals drawn perpendicular to the anterior spherical surface. The effect of position of the TT joint on the model results was investigated (see sections 6.3 and 6.4).



Figure 6.5 Lateral X-ray of foot 1 (specimen 113L). Anatomical landmarks were identified with spherical lead markers. The cross arrangement was used to assess magnification errors.

#### 6.2.4 Kinematic Constraints

In the model, deformation of the foot structure was limited to rotation and translation at the two joints (TT and TC) and horizontal translation at the two support points. The TT joint was assumed to be a unified joint describing the articulation of the forefoot with respect to the rearfoot, in this particular case in the sagittal plane only. Anatomically speaking the modelled articulation was designed to closely approximate the flexion/extension movements at the calcaneocuboid and talonavicular joints. Descriptions of such a composite joint have occurred previously in the literature (Manter, 1941, Hicks, 1953, Elftman, 1960, and Wright and Rennels, 1964) but its position has not been expressed quantitatively in terms of identifiable anatomical landmarks. By assuming such a joint in the model it was further surmised that the majority of motion in the foot takes place at this joint and that rigid elements were formed by the tarsals and calcaneus and by the tarsals and metatarsals. Justifications for assuming the talus and calcaneus as one unit were that no tibial rotation (and hence subtalar motion), or anteroposterior rotation were allowed during experimental loading. Additionally the large contact areas of the talocalcaneal joints, loaded in compression, ensured a close approximation to a single structure. Motion analysis of the mid and forefoot joints has shown that in the sagittal plane, applied forces produce the largest degree of movement at the talonavicular and calcaneocuboid joints (Lundberg, 1988, and Ouzounian and Sherref, 1989).

The defined kinematic constraints prescribed that the support points were always in contact with the ground. By definition also the forces acting at these points only had components in the vertical ( $Y_g$ ) plane. This was justified by the fact that during standing in the neutral position the contact forces in the two horizontal planes ( $X_g$ ,  $Z_g$ ) sum to zero. In addition the model assumed no movements or loading other than in the sagittal plane as already discussed.

In order to solve the model for ligament strains and forces it was assumed that the kinematics of deformation remained constant with each successive ligament cut, i.e., the deformation patterns remained the same whilst the overall stiffness of the foot was altered by removal of the ligaments. Video records taken from the medial aspect of a foot being tested revealed that changes in foot deformation, as measured between the

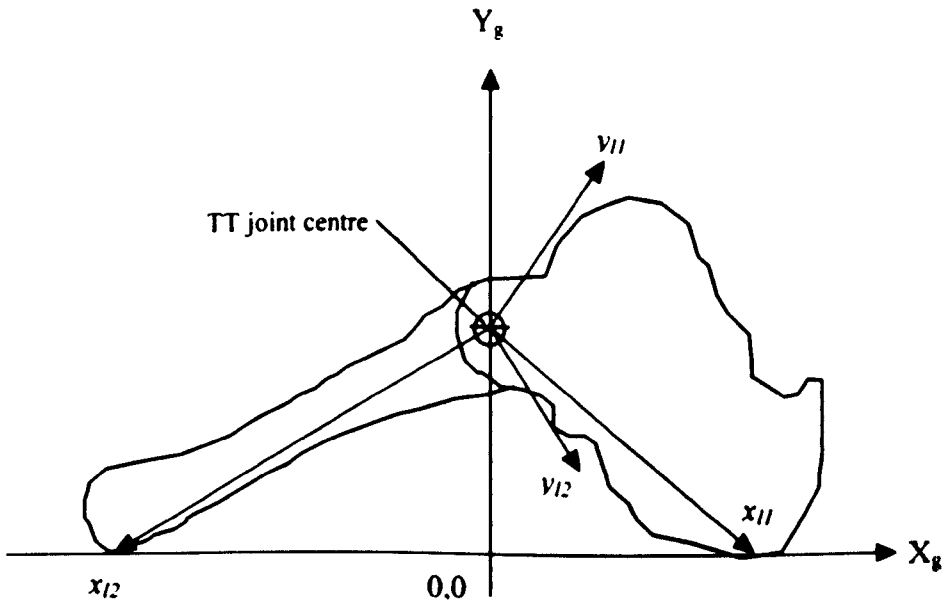


**Figure 6.6** Global and local co-ordinate systems used in the model. The kinematics were constrained such that vertical movement of the TT joint occurred along the global ( $Y_g$ ) axis. The local co-ordinate systems ( $x_{11}$ ,  $y_{11}$  and  $x_{12}$ ,  $y_{12}$ ) were fixed to the rearfoot and forefoot segments respectively and had their origins at the TT joint centre.

first metatarsal head and posterior point of the heel, did not change by more than 10% between the intact condition and when the four subject ligaments were cut. This assessment was based on manual measurements taken directly from the video images. Evidence for these small changes in foot shape with successive ligament cutting was witnessed in the load-deformation curves for the whole foot, where the pre-load of 20 N in the zero deflection condition reduced to near zero when all ligaments were cut. This implied that changes in foot stiffness, by definition, were caused by slight relaxation of the natural unloaded foot shape.

Applied deflections at the ankle joint, measured during the experimental loading, were transferred to the position of the TT joint by simple trigonometry. Global co-ordinates, used to calculate the deformed geometry and subsequently the model results, were defined as shown in figure 6.6. To calculate the ligament insertion co-ordinates at each deflection increment, two local co-ordinate systems were set up to describe the constant positions of the insertions relative to the two rigid skeletal elements of the model (forefoot and rearfoot). The local co-ordinates,  $\begin{bmatrix} x \\ y \end{bmatrix}_l$ , of the ligament insertions were calculated from the zero deflection geometry by the transformation:

$$\begin{bmatrix} x \\ y \end{bmatrix}_l = \begin{bmatrix} \cos\theta & \sin\theta \\ -\sin\theta & \cos\theta \end{bmatrix} \left[ \begin{bmatrix} x \\ y \end{bmatrix}_r - \begin{bmatrix} 0 \\ y \end{bmatrix}_0 \right] \quad (6.1)$$

Where  $\begin{bmatrix} x \\ y \end{bmatrix}_r$  are the global co-ordinates of the insertion,  $\begin{bmatrix} 0 \\ y \end{bmatrix}_0$  is the initial position vector of the TT joint in global co-ordinates and  $\theta$  is the inclination between the global and local co-ordinate systems found from the initial geometry. During solving of the model the global co-ordinates of the ligament insertions, and tibial force application point, were found by a reverse transformation at each deflection increment  $j$ .

$$\begin{bmatrix} x \\ y \end{bmatrix}_r = \begin{bmatrix} \cos\theta_j & -\sin\theta_j \\ \sin\theta_j & \cos\theta_j \end{bmatrix} \begin{bmatrix} x \\ y \end{bmatrix}_l + \begin{bmatrix} 0 \\ y \end{bmatrix}_j \quad (6.2)$$

where  $\begin{bmatrix} 0 \\ y \end{bmatrix}_j$  is the position vector of the TT joint at each deflection increment. The strain in each of the ligaments at each increment,  $\varepsilon_j$ , was calculated using the 2-D distance formula and the global co-ordinates of the insertion points, i.e.,

$$\varepsilon_j = \frac{\sqrt{(x_{2j} - x_{1j})^2 + (y_{2j} - y_{1j})^2}}{\sqrt{(x_{20} - x_{10})^2 + (y_{20} - y_{10})^2}} - 1 \quad (6.3)$$

Where  $x_{1j}$ ,  $y_{1j}$ ,  $x_{2j}$  and  $y_{2j}$  are the global co-ordinates of the forefoot and rearfoot insertion points at increment  $j$  and  $x_{10}$ ,  $y_{10}$ , etc., are the initial co-ordinates of the same points.

The angular deflection at the TT joint,  $\delta_j$  was calculated from the rotation of the bone segments such that:

$$\delta_j = \theta_{1j} + \theta_{2j} - (\theta_{11} + \theta_{22}) \quad (6.4)$$

$$\theta_{1j} = \arctan\left(-\frac{x_{R1j}}{y_{hj}}\right) \quad (6.5)$$

$$\theta_{2j} = \arctan\left(-\frac{x_{R2j}}{y_{hj}}\right) \quad (6.6)$$

Where  $\theta_{1j}$ ,  $\theta_{2j}$  are the angular deviations of each segment from the global  $y$  axis,  $x_{R1j}$ ,  $y_{R2j}$ , are the global co-ordinates of the support points  $R_1$  and  $R_2$  and  $y_{hj}$  is the  $y$  co-ordinate of the TT at increment  $j$ .

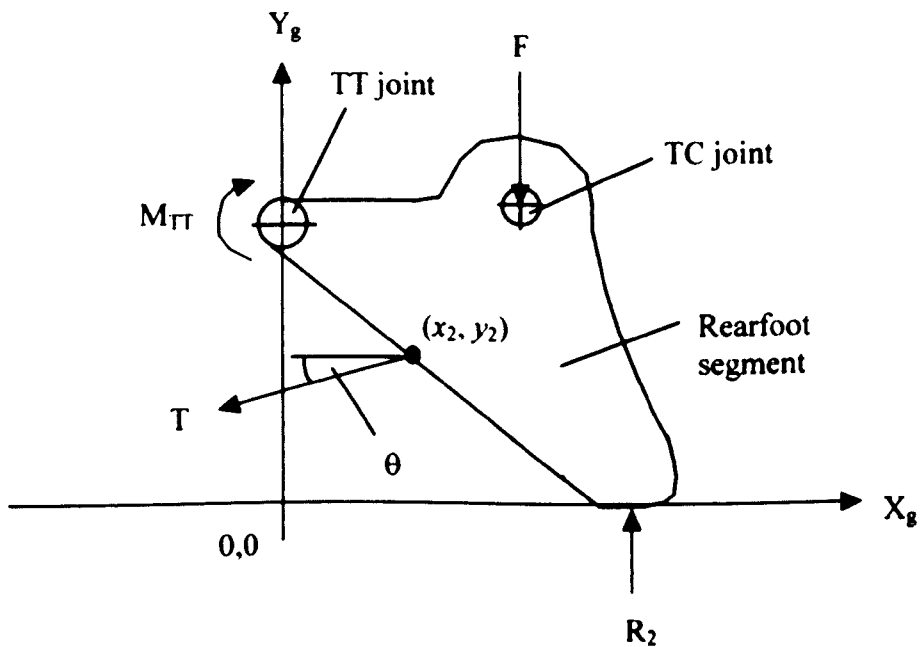


Figure 6.7 Free body diagram of the rearfoot model segment used to calculate ligament forces ( $T$  = ligament force,  $F$  = applied vertical force through TC joint,  $R_2$  = ground reaction force under the heel,  $M_{TT}$  = moment at TT joint balanced by ligament and  $\theta$  = ligament line of action). The global co-ordinate reference system ( $X_g, Y_g$ ) is shown as defined.

### 6.2.5 Ligament Force Calculations

The ligament forces were calculated by taking moments around the TT joint for the heel in isolation (figure 6.7). The tension, T, in the ligament during any foot deflection was found by:

$$M_{TT} = F x_F - R_2 x_{R_2} + T(x_l \sin\theta + (y_{TT} - y_l) \cos\theta) \quad (6.7)$$

$$M_{TT} = 0 \quad (6.8)$$

By rearrangement:

$$T = \frac{F x_F - R_2 x_{R_2}}{(x_l \sin\theta + (y_{TT} - y_l) \cos\theta)} \quad (6.9)$$

Where  $M_{TT}$  is the moment at the TT joint balanced by the ligament force, F is the applied force,  $R_2$  is the heel support reaction force,  $x_F$ ,  $x_{R_2}$ ,  $x_l$  and  $(y_{TT} - y_l)$  the moment arms of the applied forces and  $\theta$  is the ligament line of action to the horizontal:

$$\theta = \arctan \frac{(y_2 - y_1)}{(x_2 - x_1)} \quad (6.10)$$

$x_{1,2}$  and  $y_{1,2}$  are the global co-ordinates of the two insertion sites at any deflection increment.

In order to find the force carried by each successive ligament structure the moments at the TT joint balanced by each ligament was found by subtraction of the moments calculated from the experimentally applied forces during progressive sectioning. The moment carried by any particular structure  $M_{TT}$  was given by:

$$M_{TT} = M_i - M_{(i-1)} \quad (6.11)$$

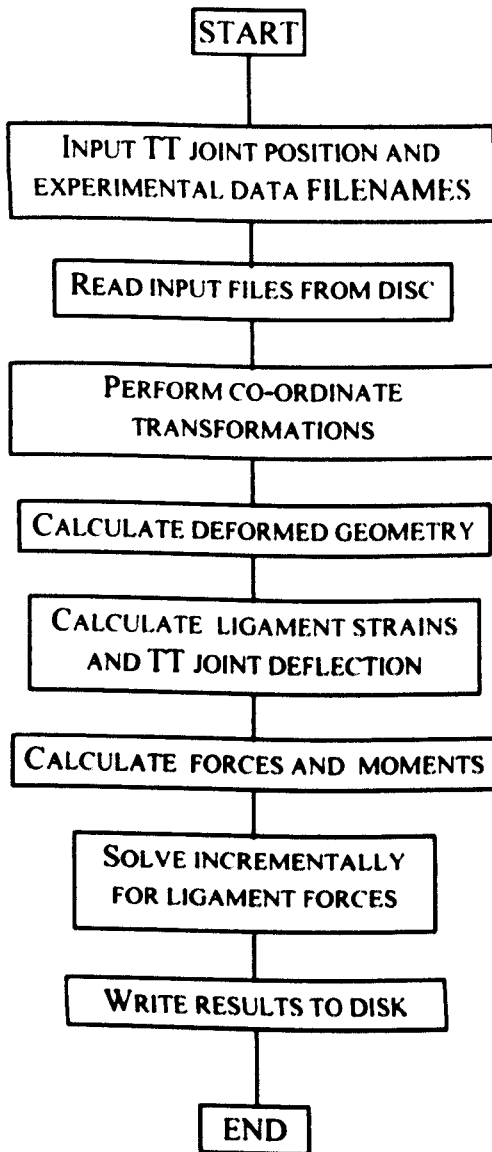


Figure 6.8 Solving routine used by the program foot2d.pas.

Where  $M_i$  = the moment with  $i$  structures intact and  $M_{(i-1)}$  is the moment with  $(i-1)$  structures intact. The solving process was repeated at each force increment in order to give a number of points from which to construct the force-strain curve for each ligament.

#### **6.2.6 Other Assumptions**

In order to ensure that the applied ankle deflection was transmitted directly to the skeletal structures, the skin and superficial fascia of the sole of each foot specimen was removed. Previous tests have shown that the effect of removal of the skin has a negligible effect on the force-deflection of the whole foot in the neutral position (Ker *et al*, 1983 and Walker, 1991).

Walker, 1991 did however note that during inversion/eversion skin removal produced medial and lateral load shifts. Neutral position loading only was applied to the specimens during the present analysis.

Strain of the PA was calculated over the length from the heel insertion to the metatarsal head markers. The true functional length of the PA may have extended into the forefoot thereby causing slight overestimation of strain in this structure.

The simplified movement in the model, in one plane, and the linear representation of the ligaments were not a fully accurate simulation of foot function but the assumptions were considered sufficiently accurate, to allow mathematical treatment of the foot as described above (i.e. small errors were introduced by simplifying the problem to two dimensions).

#### **6.2.7 Solving Routine**

The above mathematical relationships were expressed in the code of a computer program, 'foot2d.pas', specially written for this investigation in Turbo Pascal Version 7 (Borland International, Inc., California, USA ). This program solved equations 6.1 - 6.11 after first prompting the user to input the TT joint position. Other input data were read automatically by the program and output files containing the results were created.

The general solving routine is outlined in the flow chart in figure 6.8. The model program code is contained in appendix 10.

## 6.3 RESULTS

### 6.3.1 Introduction

Results from the modelling study consisted of ligament forces, ligament strains, TT joint motion and the moments balanced by the ligaments around the TT joint in a simulated stance condition. The initial position of the TT joint was estimated from previous biomechanical and anatomical analyses. Since no exact TT axis has been defined relative to the measurable anatomical landmarks, the joint position was varied and the effect of these changes on the model results were investigated (Note: It was likely that the true instantaneous centre of rotation was not constant throughout the range of motion). The results were presented within the context of a variable joint position. The following possible joint positions were used (all were located within the TCN or calcaneocuboid joint capsules).

Joint Position No.	Position
1	Centre of talar head
2	Perimeter of talar head directly inferior to centre
3	5 mm anterior to '2' along the margin of the talar head
4	5 mm posterior to '2' along the margin of the talar head
5	Superior margin of calcaneocuboid joint
6	Average of positions 1 and 2.

Table 6.3 Descriptions of the TT joint positions used in the foot model.

Due to the kinematics of deformation of the foot, mathematical optimisation of the joint position was not possible (minimisation of a defined function of strain would have resulted in convergence to an unrepresentative joint centre). Since the number of specimens modelled was small the entire results data set is presented.



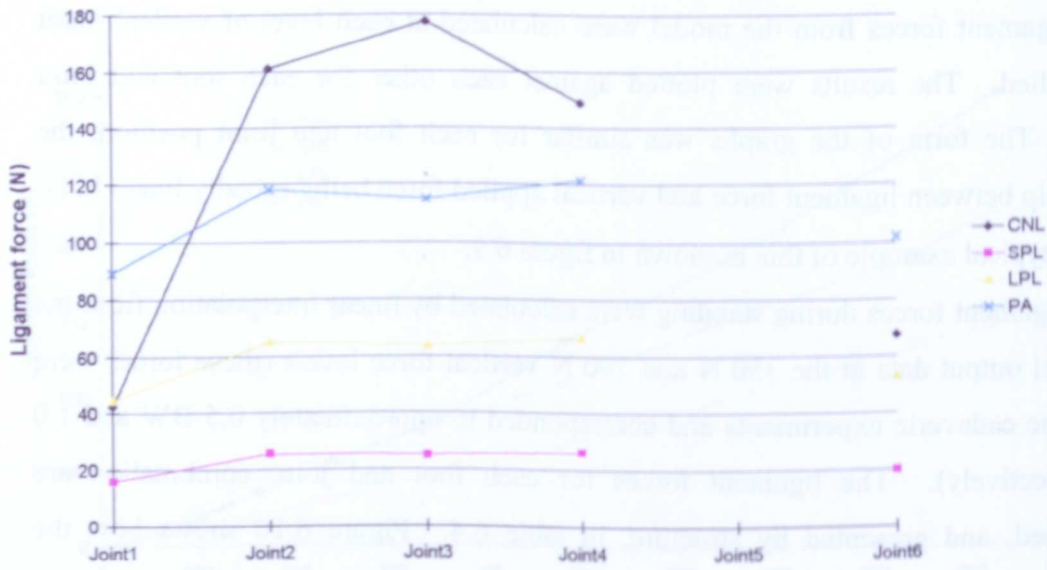
### 6.3.2 Ligament Forces

Ligament forces from the model were calculated at each level of vertical input force applied. The results were plotted against each other for each foot and joint position. The form of the graphs was similar for each foot and joint position, the relationship between ligament force and vertical applied force being broadly linear in all cases. A typical example of this is shown in figure 6.9.

Ligament forces during standing were calculated by linear interpolation from the raw model output data at the 350 N and 700 N vertical force levels (these forces were used in the cadaveric experiments and corresponded to approximately 0.5 BW and 1.0 BW respectively). The ligament forces for each foot and joint combination are summarised, and presented by structure, in table 6.4. Figure 6.10 shows how the ligament forces varied with joint position for feet 2 and 3 at the 0.5 BW loading level (the full set of force result graphs are presented in appendix 11). Joint 5 was not a valid condition for foot 2. The position of the joint in this case was in close proximity to the line of action of the CNL. This resulted in a very small moment arm and caused the program mathematics to return an unrealistically large ligament force. Results for this joint position were not presented for foot 2.

From figure 6.10 it was seen that the CNL was the ligament most sensitive to movements of joint position in the vertical ( $Y_g$ ) direction. This was due to the fact that the CNL was the closest ligament to the joint. Any change in joint position had the greatest relative effect on the moment arm of this ligament. In all feet the smallest ligament forces were calculated in the SPL, of approximately 60 N and 150 N at the 0.5 BW and BW levels respectively. For all feet the maximum forces were calculated in the CNL at the inferior joint positions (160 N and 460 N at 0.5 BW and 1.0 BW). The force values in the LPL, SPL and PA were considerably less variable than those of the CNL as seen from the graphs and standard deviations for the force data in table 6.4. Trends in the joint forces were identified for the PA, LPL and SPL with changing joint position in all feet.

Foot 2 (0.5BW)



Foot 3 (0.5BW)

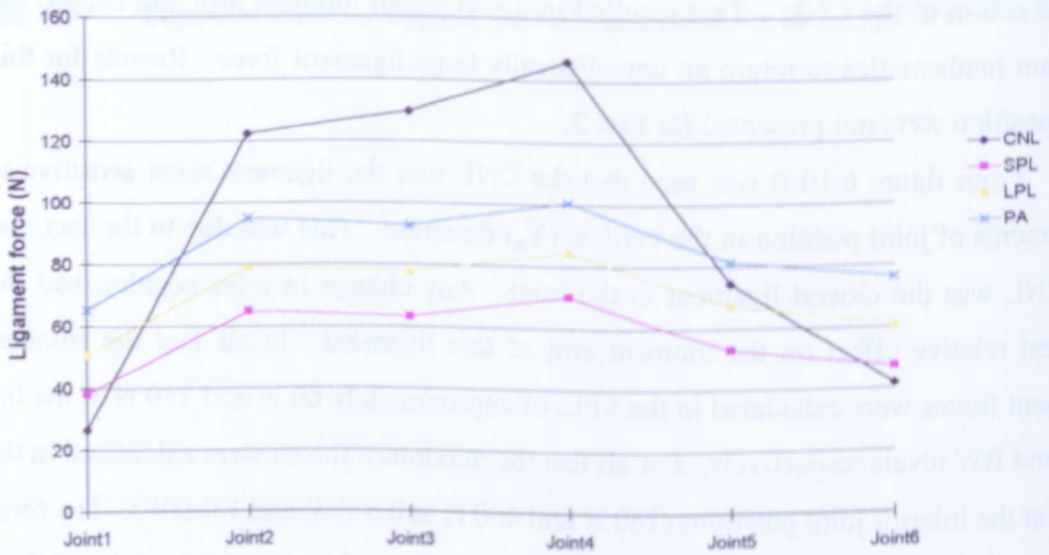


Figure 6.10 Ligament forces with varying joint position at 0.5BW applied load (feet 2 and 3).

Ligament	Applied load (N)	Foot	Ligament force (N)				
			Mean	SD	Max	Min	Range
CNL	350	1	89.9	35.8	160.2	58.4	101.8
		2	119.5	60.3	177.4	42.6	134.8
		3	90.2	49.7	146.2	26.6	119.5
	700	1	228.3	105.0	438.1	147.2	290.9
		2	392.9	207.7	617.2	134.8	482.4
		3	243.6	113.2	359.4	64.4	295.0
SPL	350	1	46.3	6.8	57.5	37.8	19.7
		2	22.5	4.4	26.2	16.0	10.1
		3	56.0	12.1	70.0	38.2	31.8
	700	1	102.7	16.5	132.4	85.3	47.1
		2	45.9	9.1	53.2	32.6	20.6
		3	122.4	24.5	149.5	81.4	68.0
LPL	350	1	87.6	10.3	103.9	74.1	29.8
		2	58.5	9.4	66.4	44.6	21.8
		3	69.9	12.7	84.3	50.6	33.6
	700	1	169.2	22.0	208.2	145.0	63.2
		2	139.2	22.9	157.1	105.4	51.7
		3	167.5	28.4	197.6	118.6	78.9
PA	350	1	80.0	7.2	89.8	70.2	19.6
		2	109.1	13.2	121.4	89.5	32.0
		3	85.2	13.2	100.7	65.3	35.4
	700	1	155.1	15.4	180.6	137.6	43.0
		2	210.6	26.3	233.8	171.4	62.4
		3	159.7	23.9	186.2	119.8	66.4

Table 6.4 Ligament forces calculated by the foot model at 0.5 BW and 1.0 BW.

### 6.3.3 Ligament Strains

For the raw strain results a non-linear relationship between input load and ligament strain was found as expressed in the shape of the force deflection graph of the whole foot. Figure 6.11 shows the typical form of the strain-applied load relationship for foot 3.

Ligament strains were calculated at 0.5 BW and 1.0 BW levels by linear interpolation as per the force results. The form of the results was similar for all feet modelled, the strains showing the same trends between different joints. The strains for each foot and joint combination are summarised in table 6.5, again grouped by structure.

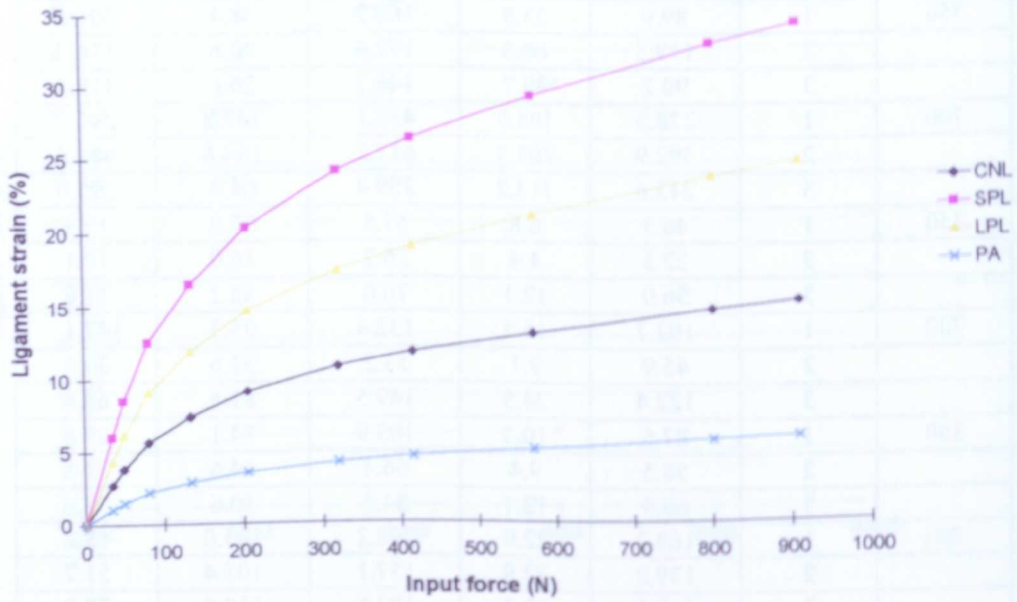


Figure 6.11 Ligament strain vs. applied vertical input force for foot 3, joint 6.

Figure 6.12 shows the variations of strain with joint force for feet 2 and 3 at the 0.5 BW level (the full set of strain results during stance is given in appendix 11).

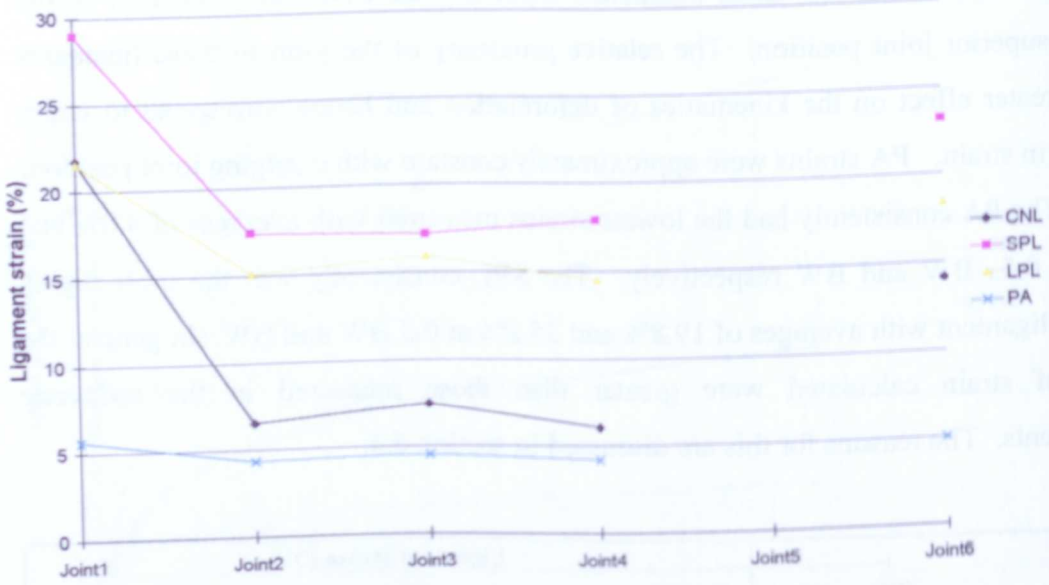
It was seen that the tarsal ligaments, especially the CNL, were sensitive to the inferior-superior joint position. The relative proximity of the joint to these ligaments had a greater effect on the kinematics of deformation and hence correspond to larger changes in strain. PA strains were approximately constant with changing joint position,

The PA consistently had the lowest strains measured with averages of 4.0% and 5.1% at 0.5 BW and BW respectively. The SPL consistently was the most highly strained ligament with averages of 19.8% and 25.2% at 0.5 BW and BW. In general the levels of strain calculated were greater than those measured in the cadaveric experiments. The reasons for this are discussed in section 6.4.

			Ligament strain (%)				
Ligament	Applied load (N)	Foot	Mean	SD	Max	Min	Range
CNL	350	1	14.5	4.0	20.5	9.7	10.8
		2	11.2	6.7	21.7	6.1	15.7
		3	7.1	6.2	18.0	2.4	15.6
	700	1	19.2	5.6	27.6	13.0	14.6
		2	14.4	8.7	28.1	7.8	20.3
		3	8.9	7.8	22.6	3.0	19.6
SPL	350	1	17.2	3.6	22.2	11.7	10.5
		2	20.9	5.2	29.0	17.1	11.9
		3	21.3	5.5	30.9	17.3	13.6
	700	1	21.8	5.0	29.9	15.7	14.2
		2	27.2	6.7	37.7	22.4	15.3
		3	26.8	6.9	38.9	21.7	17.2
LPL	350	1	12.0	1.7	14.5	9.9	4.7
		2	17.1	2.9	21.5	14.5	7.1
		3	16.2	3.2	21.3	12.8	8.5
	700	1	15.8	2.5	19.5	13.2	6.3
		2	22.1	3.8	27.9	18.7	9.2
		3	20.3	4.0	26.8	16.1	10.7
PA	350	1	3.3	0.4	3.8	2.9	0.9
		2	4.7	0.6	5.7	4.2	1.5
		3	4.0	0.6	5.0	3.3	1.7
	700	1	4.3	0.6	5.1	3.7	1.4
		2	6.1	0.8	7.2	5.4	1.9
		3	4.9	0.8	6.2	4.1	2.1

Table 6.5 Ligament strains calculated by the foot model at 0.5 BW and 1.0 BW.

Foot 2 (0.5BW)



Foot 3 (0.5BW)

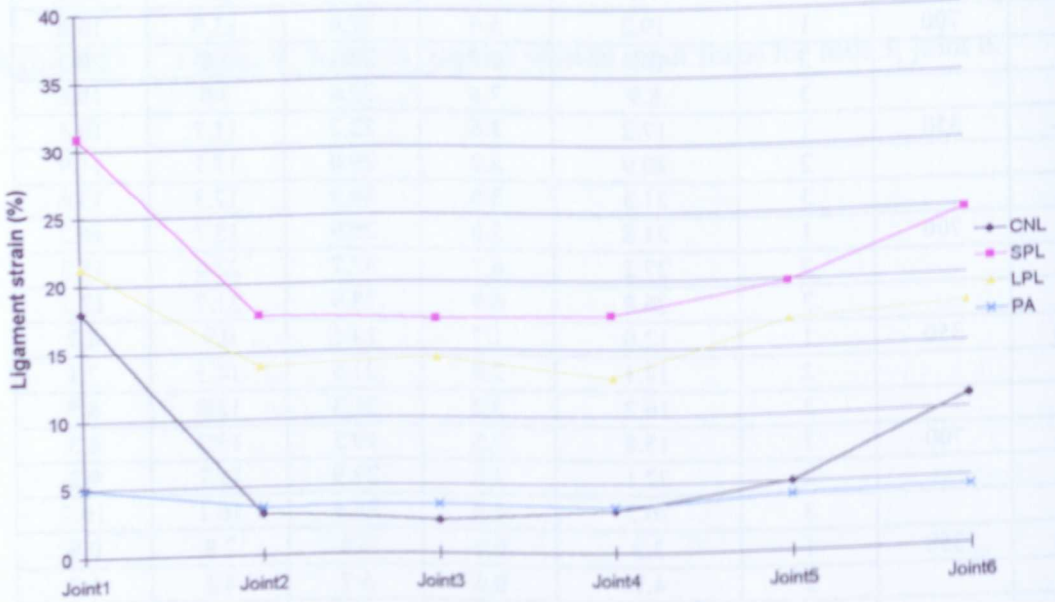


Figure 6.12 Ligament strain with varying joint position at 0.5BW applied load (feet 2 and 3).

The model correctly predicted the form of the ligament force/strain curves, i.e. non-linear progressively stiffening behaviour as shown in figure 6.13. Comparison to the cadaveric results could not be conducted since normalisation of this relationship was not performed. Stress/strain relationships for the ligaments were not derived since the sectioning technique did not readily allow accurate measurements of ligament cross-sectional area.

### 6.3.4 Joint Deflections

The values of TT joint flexion were calculated by the model and are presented below for each foot. The patterns of changing joint flexion were consistent with each joint position and loading level (again the values were calculated using linear interpolation). Figure 6.14 shows the typical variations of flexion angle with changing joint position. Average flexion angles of 2.8° and 3.6° were found at the 0.5 BW and 1.0 BW levels. The standard deviation values highlighted relatively small amount of variation between each joint position. The results of the analysis of joint flexion angle with joint position and varying applied load are summarised in table 6.6.

		TT joint motion (deg.)				
Applied load (N)	Foot	Mean	SD	Max	Min	Range
350	1	2.4	0.4	2.8	1.8	1.0
	2	2.9	0.3	3.3	2.5	0.8
	3	3.1	0.4	3.6	2.3	1.2
700	1	3.2	0.5	3.8	2.4	1.3
	2	3.7	0.4	4.2	3.2	1.1
	3	3.8	0.5	4.4	2.9	1.5

Table 6.6 TT joint flexion angles calculated by the foot model at 0.5 BW and BW.

### 6.3.5 Ligament Insufficiency

The model was formulated in such a way that the effects of ligament insufficiency could be explored. In this manner the implications on the ligament mechanics of two clinical situations were investigated.

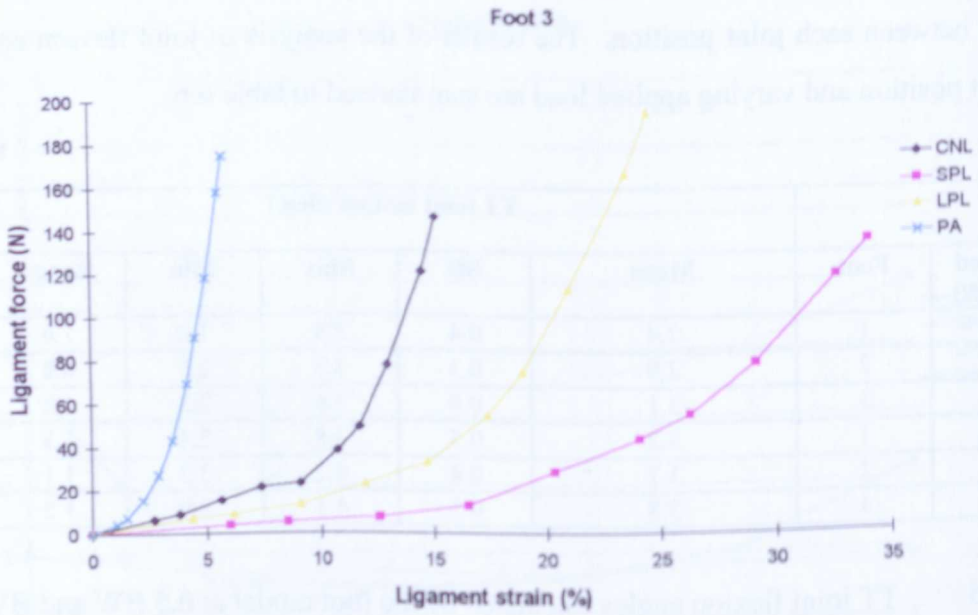
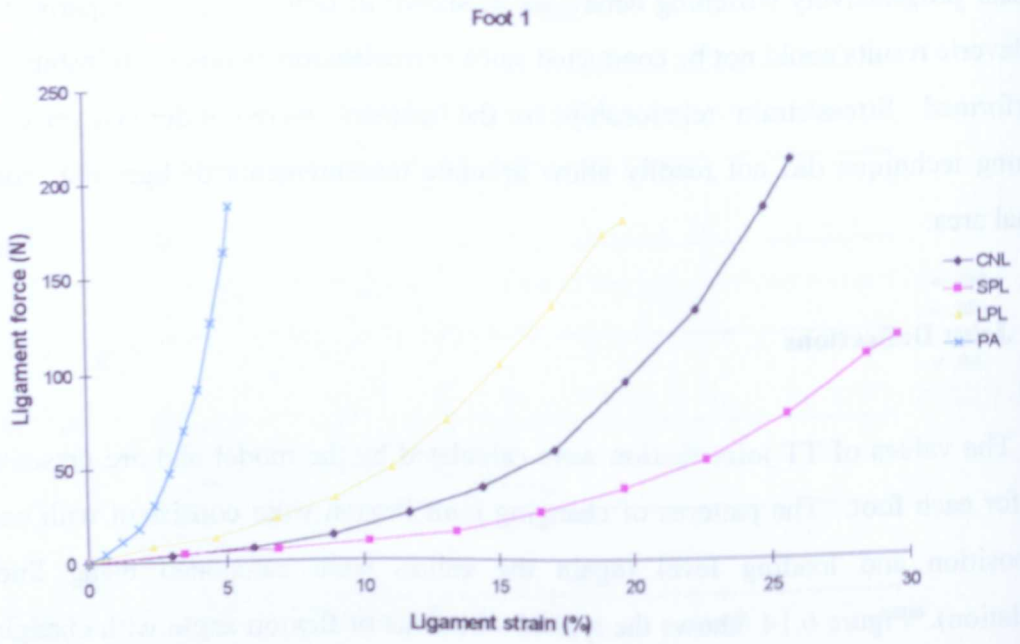


Figure 6.13 Force-strain relationships for the modelled ligaments of feet 1 and 3, at joint position 6.

In cases of intractable plantar-fasciitis, surgical release of the PA is often carried out to relieve symptoms when conservative treatments have proved unsuccessful. It has been noted that this procedure can lead to excessive loading in the remaining passive support structures and flattening of the arched foot shape (Daly *et al*, 1992). Rupture of the PA has also been reported in athletes as a result of trauma (Ahstrom, 1988 and Leach *et al*, 1978).

These two conditions, (i.e. an insufficient PA) were investigated by removing the contribution of the PA from the model and examining the effects of the strain and forces in the remaining ligaments (LPL, SPL and CNL). The strains and forces in the LPL, SPL and CNL were calculated and compared to those with the intact PA at the 0.5 BW loading level. The results presented were taken with joint position 6. It was considered that this joint gave a compromise between the outer limits of force and strain achieved by moving the joint position as previously described (the trends in force and strain were opposite with vertical shifting of the TT axis). The results of this analysis are summarised in table 6.7.

		Ligament force (N)		
Ligament	Foot	PA intact	PA divided	% Increase
CNL	1	58.4	100.8	73
	2	67.5	206.3	206
	3	41.8	71.9	72
SPL	1	37.8	56.9	50
	2	19.7	39.7	101
	3	47.2	73.7	56
LPL	1	74.1	108.8	47
	2	52.9	122.4	131
	3	60.8	104.8	72

Table 6.7 Increases in ligament force due to PA insufficiency (results for joint 6 at the 0.5 BW level).

As expected the strains and forces during stance in the remaining ligaments were increased when the PA was removed. The magnitude of the increases varied between feet, foot 2 recording the largest changes. Increases in ligament forces of between 72 and 206 % for the CNL, 50 and 100% for the SPL and 47 and 131% for the LPL were found. Increases in the ligament strains were of a lesser magnitude compared to the

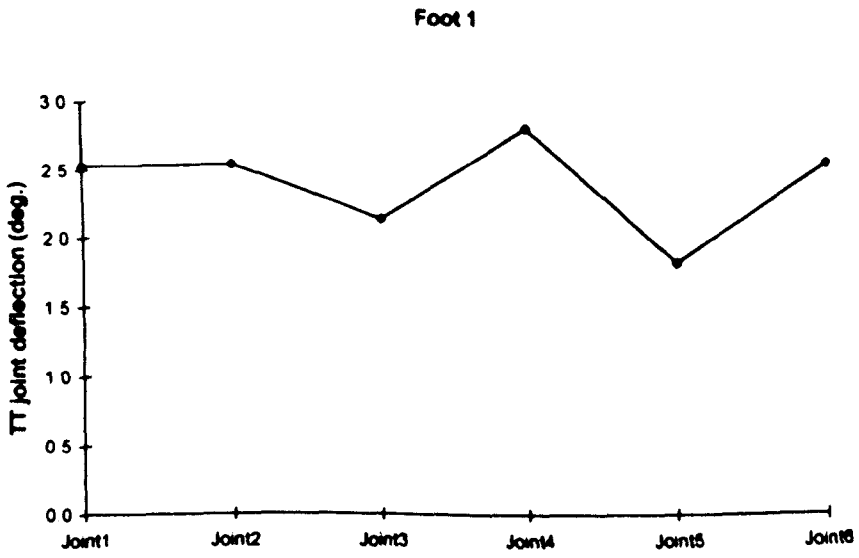


Figure 6.14 TT joint motion with varying joint position for foot 1.

force data. Due to the proportionality of the kinematics the increases in strain in all ligaments of the same foot were similar (table 6.8), the full implications of these increases are discussed in section 6.4.

		Ligament strain (%)		
Ligament	Foot	PA intact	PA divided	% Increase
CNL	1	17.1	20.2	18
	2	14.1	18.1	28
	3	11.0	12.7	15
SPL	1	19.7	23.2	18
	2	23.2	29.9	29
	3	24.8	28.6	15
LPL	1	13.1	15.4	18
	2	18.3	23.5	28
	3	17.9	20.6	15

Table 6.8 Increases in ligament strain due to PA insufficiency (results for joint 6 at the 0.5 BW level).

### 6.3.6 Effects of Muscle Force

It has been reported in the literature that traumatic rupture of the tibialis posterior tendon has been shown to cause progressive onset of flat-foot deformities and associated stretching of the plantar ligaments (Cozen, 1965; Mann, 1983; Mann and Thomson, 1985 and Funk *et al*, 1986). It was also shown in chapter 4 that the extrinsic muscles were able to reduce strain in the plantar foot ligaments.

The effects of muscle forces on the ligaments were explored through the model by comparing the moments at the TT balanced by each ligament to the moment of one muscle around the same joint. Of the 4 muscles loaded during the cadaveric experiments only one, the TP presented itself for study. The other muscles could not be included for the following reasons: (1) TA: the inverting action of this muscle could not be built into the model, (2) FDL: complex routing and insertions could not be modelled due to indeterminacy problems and (3) PL: as with the FDL. The moment arms of the TP were measured from the lateral X-rays as being the perpendicular distance of the joint to the line of action of the tendon (drawn from its insertion site to the tip of the medial malleolus where it entered the foot). The same levels of muscle force applied in

the cadaveric tests, 50 N and 100 N, were used to give the levels of moment used in this analysis (table 6.9). These moments were compared directly with those for the ligaments in table 6.10 to assess how effectively applied muscle forces could ‘off load’ the ligaments.

Details of the progressive recruitment patterns of the loaded ligaments could not be found from the model hence the moment comparisons were only measures of the hypothetical action of the muscles. In the actual case it is likely that applied muscle force would have reduced the force to some degree in all ligaments (this was the case as seen from the results of chapter 4, although the greatest effects were seen for the tarsal ligaments).

On inspection of the two sets of moment values it was found that the muscle action would, as previous observations have shown, have been more effective in reducing the force and strain in the ligaments of the tarsus, especially the CNL.

<b>Applied muscle force (N)</b>	<b>Foot</b>	<b>Tibialis posterior moment (Nm)</b>
50	1	0.48
	2	0.43
	3	0.40
100	1	0.95
	2	0.85
	3	0.80

Table 6.9 Moments at the TT joint as a result of applied TP muscle forces.

			Ligament moment (Nm)				
Ligament	Applied load (N)	Foot	Mean	SD	Max	Min	Range
<b>CNL</b>	350	1	1.1	0.1	1.2	1.0	0.2
		2	0.7	0.0	0.7	0.7	0.1
		3	0.5	0.0	0.5	0.5	0.1
	700	1	2.8	0.1	2.9	2.6	0.4
		2	2.2	0.1	2.3	2.1	0.2
		3	1.2	0.1	1.3	1.1	0.2
<b>SPL</b>	350	1	1.2	0.1	1.2	1.1	0.2
		2	0.5	0.0	0.5	0.5	0.0
		3	1.3	0.1	1.4	1.2	0.2
	700	1	2.6	0.1	2.8	2.4	0.3
		2	1.0	0.0	1.1	1.0	0.1
		3	2.8	0.1	3.0	2.6	0.4
<b>LPL</b>	350	1	2.7	0.1	2.8	2.5	0.4
		2	1.7	0.1	1.8	1.6	0.1
		3	2.0	0.1	2.2	1.9	0.3
	700	1	5.2	0.2	5.5	4.8	0.7
		2	4.0	0.1	4.2	3.8	0.3
		3	4.8	0.2	5.0	4.4	0.7
<b>PA</b>	350	1	3.1	0.1	3.3	2.8	0.4
		2	4.5	0.1	4.7	4.3	0.4
		3	3.0	0.1	3.2	2.8	0.4
	700	1	5.9	0.3	6.2	5.4	0.8
		2	8.3	0.3	8.7	8.0	0.7
		3	5.5	0.3	5.8	5.0	0.8

Table 6.10 Moments balanced by the ligaments calculated in the foot model at 0.5 BW (350N) and 1.0 BW (750N).

## 6.4 DISCUSSION

### 6.4.1 Ligament Forces

The position of the TT joint had a significant effect on the values of force produced by the model. It was immediately apparent, on inspection of the ligament force results at 0.5 BW and 1.0 BW, that the CNL was the structure most sensitive to movements of the TT joint, particularly in the superior/inferior direction (see appendix 11). The differing ligament forces at each joint position were due to the changes in moment arm in each case. The CNL, due to its proximity to the TT joint, had the

smallest moment arm and hence any change in joint position had a correspondingly larger effect on this ligament (as seen in the results). Indeed one particular position, joint 5 in foot 2, produced errors during execution of the program by attempting to divide by a very small moment arm thus nullifying this result. Force values in the other ligaments were less variable with joint position as seen from the graphically presented results in figure 6.10, appendix 11, and the standard deviations of the results as listed in table 6.4.

At the most inferior joint positions, joints 3 to 5, the levels of force in the CNL approached those of Davis *et al* (1996) who found the ultimate force of this ligament to be 477 N ( $\pm$  261 N). In view of this it is unlikely that the more inferior joint positions resulted in realistic values of CNL ligament force.

Investigation	Ligament	Force (N)	Activity	Method
Simkin (1982)	PA	260	Standing	Modelling
	LPL	67		
Morlock (1990)	PA	2200	Athletic Side-Step	Inverse dynamics
Kim & Voloshin (1995)	PA	50	Standing	Inverse dynamics
Wright & Rennels (1964)	PA	164	Standing	Modelling
Present Study Mean values (n = 2)	PA (Distal)	99	Standing	Instrumented cadaveric specimens
	PA (Prox.)	59		
	LPL	29		
	SPL	9		
	CNL	29		
Present Study Mean values (n = 3)	PA	91	Standing	Modelling
	LPL	72		
	SPL	42		
	CNL	100		

Table 6.11 Functional force estimates in the foot ligaments for the present and previous studies.

The values of force during standing calculated by the model were compared to those found in chapter five and other investigations (table 6.11). Whilst the two values of PA force for the cadaver and modelling experiments agree closely, the model tended

to give larger force results for the other three ligaments. Since the model results showed closer agreement between specimens and were not prone to local variations in strain measurements it was concluded that the force estimates from the model were more representative of the likely forces occurring *in vivo*. The forces occurring at the 700N level were approximately 2 times the values at the 350N applied load level, as expressed from the linear form of the ligament force/applied force relationships. The ligament forces at this level constituted upper limits before the onset of intrinsic muscle activity with additional external loading.

#### **6.4.2 Ligament Strains**

The ligament strains showed similar trends between feet with changing joint position as revealed by the shape of the graphs in figure 6.12 and appendix 11. In general the strains were greatest with superiorly placed joint positions. As in the force results the CNL was most sensitive to the inferior/superior movements in joint position. As discussed earlier this was due to the close proximity of the CNL to the TT joint centre thereby increasing the relative effects of changing joint position. The PA strains were noted to be both the smallest and least variable of the four test structures.

On inspection of the actual strains produced, at 0.5 BW and 1.0 BW, it was seen that the values were significantly greater than those measured during cadaver experiments (table 6.12). There may have been a number of possible reasons for this: The length of each ligament in the model was taken from the radiographic markers implanted during partial dissection. This length could perhaps have underestimated the true effective length of the ligament, given the complexity of the geometry of the insertion areas (e.g. the PA inserts in the forefoot distal to the metatarsal heads and the LPL has distal attachments to the metatarsal bases). The fact that the model calculated bulk strains based on estimated lengths, whereas the *in vivo* strains were local measurements, could have accounted for the differences in the two sets of values. The model assumed that all deformation of the foot skeleton under load occurred at the TT joint. This assumption would also have tended to cause over estimation of strains since some deformation would inevitably have been present elsewhere in the foot, e.g. at the

tarsometatarsal joints and intertarsal joints in addition to a small amount of metatarsal bending.

Ligament	Mean Strain (%)	Method
PA	4.0	Modelling
LPL	15.1	
SPL	19.8	
CNL	10.9	
PA (Distal)	1.1	Cadavers
PA (Proximal)	1.3	
LPL	2.4	
SPL	3.3	
CNL	4.6	
PA	2.62	Cadavers (Kogler et al (1995) at 450N vertical load)

Table 6.12 Comparison of ligament strains from modelling and cadaver experiments and previous studies.

As shown in chapter 5 the strain distribution along the length of the foot ligaments is not uniform, thus concentrations of strain not measured by the local instrumentation would have been lumped into the values calculated by the model. Finally, small rotations of the tibia, and subsequent TCN motion, were seen to have an influential effect on the strain values, especially in the tarsal ligaments. Slight tibial rotations during loading of the cadaveric feet may have reduced the overall levels of strain in the ligaments. Tibial rotations and their effects were not represented in the model.

The force and strain graphs revealed that the movements in joint position had opposite effects on these two quantities. Determination of a joint position by optimisation of either quantity in isolation would have produced a non-convergent solution. Optimisation of joint position by minimising the total strain energy of deformation may have been possible but was not performed. Alternatively a number of joint positions were investigated. Joint position number 6 produced strains and forces

in the mid-range of the values produced and was considered the most representative from this viewpoint.

The specific force-strain relationships of each ligament had the characteristic non-linear shape expected. In each foot the PA was the stiffest structure whilst the SPL was the most compliant.

### 6.4.3 Joint Angles

The mean ranges of motion of the TT joint predicted by the model were comparable to those previously measured *in vivo* (table 6.13)

Joint	Mean (deg.)	SD (deg.)	Method
TT	2.7	0.4	Modelling
TCN	7.0	4.7	Loaded cadaveric specimens (Ouzounian & Shereff (1989))
Calcaneocuboid	2.3	3.01	
Talonavicular	5.6	3.2	Loaded cadaveric specimens (Lundberg (1988))
Calcaneocuboid	3.1	1.9	

Table 6.13 Comparison of model and *in vitro* transtarsal joint motion.

Components of motion of the joints in the sagittal plane (dorsiflexion) were presented for the *in vitro* studies. The values of joint motion calculated by the model were of the same magnitude as those found *in vitro* within the ranges of the experimental data presented. The greater variation in the experimental results indicate that the kinematics of the foot were more complex than those represented in the model. The mean values of motion of the talocalcaneal joint were similar in magnitude to those of the model indicating that the inferior joint positions were more representative of the true kinematics of the foot. When comparing the joint motion at the 0.5 BW and 1.0 BW levels it was seen that the deformation of the foot was non-linear as expected (doubling the applied force did not give a similar increase in calculated joint angle).

In the absence of a previously strictly defined TT joint position the effect of this variable on the results of the model was examined in detail. Whilst the assumption of an idealised TT joint in the sagittal plane was an approximation to the true kinematics of the foot it was concluded, from the above comparison, that the model was sufficiently accurate in representing the deformation of the foot under applied vertical loading.

#### 6.4.4 Ligament Insufficiency

The aim of this part of the modelling exercise was to explore the biomechanics of the effects of PA rupture and surgical division and to predict the likely outcome of these clinical situations.

The analysis of the ligament forces was conducted at the 0.5 BW level since there was clear evidence that no muscle action was present in the foot at this level of loading (Basmajian and Stecko, 1963). When comparing the ligament forces before and after it was immediately apparent that PA sectioning caused increased loading of the remaining ligaments. The model assumed that PA sectioning did not invoke intrinsic muscle action as a reflex response to increased deformation of the foot. This may not have been the case *in vivo* but to date no indisputable evidence has been presented that has established that reflex control of this nature actually occurs. Although the values of strain produced by the model overestimated those values measured during the cadaver experiments, as discussed, the relative increases in strain are valid measurements of the effects of PA sectioning. Due to the nature of the defined kinematics the relative increases in strain were the same for all ligaments of each foot. The relative increases in strain were significantly less than those of the forces as expected from the non-linear behaviour of the ligamentous tissue.

Inspection of the forces in, and moments balanced by, each ligament revealed that although the PA carried the least force of all the structures, its moment at the TT was the largest of the ligaments studied, i.e. the PA had the largest moment arm about the TT joint. The fact that the PA had this strong mechanical advantage explains why, when cut, the forces in the remaining ligaments were increased by such a large amount (47 - 206%). In light of the above evidence it was concluded that surgical release of the PA in treatment of intractable plantar fasciitis should be avoided in favour of more conservative management regimes. Sectioning the PA in young active patients may be particularly detrimental in the long term if a return to sporting activities is made after treatment without the use of an orthosis (overuse syndrome). In the case of PA rupture, steps should be taken that will prevent long term overloading of the ligaments, e.g. arch support orthoses.

#### **6.4.5 Muscle Forces**

There has been significant evidence presented in the literature that extrinsic muscle dysfunction can lead to overloading and eventual pathology of the foot ligaments, e.g. rupture of the TP. These observations are supported by the results of the present study where applied TA and TP muscle forces were seen to reduce the strains in the ligaments of the weight bearing foot. The modelling exercise introduced a biomechanical analysis designed to examine whether these findings had a valid theoretical basis. The model confirmed that applied TP forces had an effect on the TT joint moment such that ligament forces were reduced in magnitude.

Although only the TP was included in the above analysis the results showed that muscle action was able to 'off-load' the ligaments. Comparison of the moments balanced at the TT joint showed that the muscle forces had a greater potential to reduce loading in the tarsal ligaments. Evidence from the cadaveric experiments supported this hypothesis.

## CHAPTER 7. DISCUSSION AND CONCLUSIONS

### 7.1 INTRODUCTION

The work presented in this thesis has investigated the biomechanics of the foot with special reference to the function of the ligamentous structures. The experimental program was divided into 3 main areas of investigation.

In chapter 4, results from tests on intact cadaveric feet were presented. Strain in the ligaments of 6 feet were measured under simulated functional conditions (standing and gait) applied in a loading apparatus. In particular the effects of foot position, extrinsic muscle force, toe extension and tibial rotation during standing were investigated. To aid interpretation the strain results were normalised and averaged to allow direct comparison between each set of applied conditions.

In chapter 5 the ligaments of 2 feet were tested in tension as isolated bone-ligament-bone preparations instrumented with strain transducers. This experimental procedure allowed forces in the intact foot to be estimated by cross matching against strain in the results of chapter 4. Measurements of ligament cross-sectional area were conducted in order to obtain results for functional ligament stress and to investigate the normalised tissue mechanics in simple tension.

In chapter 6 a 2D mathematical model of the foot was described. The *in vitro* load/deformation properties and measurements of intact anatomy were used as inputs to the model which calculated ligament strain, force, TT joint rotation and the moment at the TT joint balanced by each ligament during standing. The model was used to explore the effects of pathology in addition to verification of the experimental results.

While the results of each chapter have been previously discussed and compared to those of other investigators, the aim of this chapter is to review and discuss the findings of this thesis in a wider context relating to the load bearing function of the foot. A summary of the conclusions reached and recommendations for future work are also presented. Particular emphasis will, naturally, be placed on those aspects of foot biomechanics under direct investigation, i.e. normal foot function (standing and walking), ligament biomechanics and the pathological foot.

## 7.2 DISCUSSION

### 7.2.1 Standing

The foot is one of the most human of characteristics. In no other animal is the foot as specialised to a particular function to the degree of that in the human. The function of the foot is to provide sustained, adaptive support thus facilitating standing and bipedal locomotion. Debate has long existed over the precise roles and interaction of the component structures of the foot during support activities.

EMG analysis has shown that during quiet standing there is negligible muscle activity in the foot and lower limb implying ligaments alone are capable of providing support (Basmajian and Stecko, 1963, Mann and Inman, 1964 and Walker, 1991). *In vitro* analysis of loaded foot specimens has confirmed that the ligaments are indeed the primary means of maintenance of the arched shape of the foot (Huang *et al*, 1993, Ker *et al*, 1989 and Walker, 1991).

The results of the present study have confirmed that the plantar foot ligaments are utilised during standing and have quantified the strains and forces experienced in the major ligamentous structural elements. The present study found values of functional strain and force during standing of similar magnitudes to previous studies of the ligaments of the foot and other joints (Forces: PA = 90 N, LPL = 70 N, SPL = 40 N and CNL = 100 N). The general function of ligaments, related to their non-linear mechanical properties, is considered to be control of movement (kinematic function) and to limit extreme motion at joints (restraint function). The complex strain patterns observed in the tarsal ligaments during loading of the foot in various positions would seem to support this simple hypothesis, e.g. tarsal ligament strain was particularly sensitive to eversion and inversion positions. Further evidence for the involvement of the ligaments in limiting relative movement of the foot bones was found when rotation was applied to the tibiae of loaded foot specimens. Large variations in strain in the tarsal ligaments were witnessed during this activity implying that these structures have an important role in motion in the tarsal joints induced as a result of rotations around the TCN joint (main components of foot inversion and eversion).

In many biomechanical analyses, during the examination of gait in the laboratory for instance, the foot is treated for simplicity as a rigid body. In reality the foot, as a whole, does deform during standing. The deformation of the foot structures under load was investigated in the present study and was found to be similar to previous *in vitro* analyses (Ouzounian and Shereff, 1989 and Lundberg, 1988). The kinematics of foot deformation were found to be highly non-linear with applied vertical load giving approximately 3° of angular movement at the TT joint during standing (this result is entirely consistent with the non-linear mechanics of ligament deformation). The relationship between applied vertical force and foot ligament force was found to be approximately linear due to the small amounts of motion involved.

The ability of the foot to change shape and to achieve a large range of motion with respect to the lower limb, are a direct indication of its suitability to provide adaptive support. In support situations that are more demanding than quiet standing, the role of muscles becomes important. The work of Walker (1991) has shown that intrinsic musculature is more fatigue resistant and thus better adapted to sustained load support. While the function of intrinsic muscle force was not explored directly there is overriding EMG evidence that these muscles have an important function during increased loading of the foot, during locomotion for example (Basmajian and Stecko, 1963, Mann and Inman, 1964, Reeser *et al*, 1983 and Walker, 1991).

Quantitative exploration of the role of extrinsic musculature in support of the foot structure in the present study found that, in general, extrinsic muscle forces were able to reduce ligament loading. In the case of the TP and TA muscles the strain in the tarsal ligaments was reduced by between 39 - 100% due to their inverting action.

Adaptation in the forefoot is another important functional characteristic of the human foot (Hicks, 1953 and 1954, Jacob, 1989 and Reeser *et al*, 1983). The function of the PA has a close association to the forefoot due to its complex anatomical insertions in this region. It was noted that the loading distribution along the PA was influenced by changes in forefoot loading conditions.

In summary it was found that, after quantification, the load-bearing and deformation of the foot structure during standing is controlled by ligamentous mechanisms.

### 7.2.1 Gait

The human foot, in addition to providing a means of sustained standing, is notable in nature for its specialisation to facilitate bipedal locomotion. The muscle activity required to produce these motions have a recognisable pattern (Mann and Inman, 1964, Procter, 1980 and Walker, 1991). As mentioned in the previous section the intrinsic musculature is better adapted for sustained support but extrinsic muscles can also off-load the ligaments if required.

In simulating gait *in vitro* in the present study no intrinsic muscle forces could be represented for practical reasons. As such the loading conditions represented a worst case scenario for ligament loading (Mann and Inman (1964) and Walker (1991) have demonstrated that the intrinsic muscles are most active during the foot flat period of normal gait). It was believed that the loading patterns applied were sufficiently representative of gait to draw meaningful conclusions regarding potential ligament loading during this activity.

The greatest ligament loading levels of the entire study were found during the toe-off phase of gait (where strains of approximately four times those during standing for all ligaments were noted, giving a five fold increase in ligament force). Loading during mid-stance and heel strike gave increases in ligament strain by a factor of three and two respectively compared to the neutral standing condition. Given these large increases it is likely that the muscles do indeed provide a dynamic reserve called upon reflexively during excessive loading as previously suggested (Basmajian and Stecko, 1963 and Walker, 1991).

The existence of a reflex control mechanism linking ligament strain and intrinsic muscle force has not yet been unequivocally established, but the ligament loading patterns found in the present study augment the current evidence for this (Valenti, 1988).

In addition to any neuromuscular mechanisms operating during load bearing locomotion, there is at least one important mechanical mechanism of foot adaptation to weight bearing function. The 'windlass' mechanism, as first described by Hicks (1954), is particularly important during gait. When the toes are extended in the human foot tension in the PA is increased. Although not simulated to its full extent during the gait

experiments it was found that during standing 45° of toe extension increased the tension in the PA by a factor of four. The loading in the remaining ligaments was less predictable, however, indicating that the windlass mechanism does not simply unload the tarsal ligaments in every case. This was most likely due to secondary movements at the tarsus caused by the action of toe extension.

During locomotion it can be summarised that the underlying ligamentous support is augmented by muscular activity (extrinsic and intrinsic) and by additional specialised mechanical ligamentous mechanisms (namely the windlass mechanism).

### **7.2.3 Pathology**

The foot's complex anatomy and specialised function give rise to pathologies which are both common in occurrence and varied in nature. Ligamentous pathology may arise from injury, overuse-syndromes, neurological trauma and congenital deformities for example.

Of the specific ligament structures studied the most important, from a clinical perspective, is the PA. Injury to this structure either through traumatic rupture or via intractable plantar fasciitis, and subsequent surgical release, may give rise to insufficiency of this ligament. Previous investigation has shown that the likely mechanism of plantar fasciitis is one of repeated overloading of the PA (Andrews, 1983, Kogler *et al*, 1995b and Torg *et al*, 1987). PA insufficiency, modelled in the present study, was found to significantly increase the forces in the tarsal ligaments during standing (CNL: 72-206%, LPL: 47 - 131% and SPL: 50 - 100%). This was due to the large mechanical advantage of the PA at the TT articulation.

In the absence of increased intrinsic muscle activity it is likely that the sustained overloading of the tarsal ligaments would lead to progressive deformity and flattening of the arched foot structure. This result confirmed the clinically witnessed manifestation of this pathology following PA insufficiency (Daly *et al*, 1992).

As previously noted the PA and forefoot have an intimate inter-relationship due to the complex insertions between both structures. It is likely that PA insufficiency would have a detrimental effect on the biomechanics of the forefoot, perhaps by affecting the pressure distributions under the metatarsal heads during weight bearing.

Whilst PA sectioning for intractable plantar fasciitis may give good short term results in terms of pain relief, the results in the long term may be detrimental to foot function (Daly *et al*, 1972 and Kogler *et al*, 1995b). The results of this study confirm the underlying biomechanical mechanisms behind these observations and highlight that conservative measures of treatment should always be used in preference to surgical intervention.

Muscle dysfunction has been demonstrated as a cause of ligament pathology in the foot. TP tendon rupture for example can give rise to progressive flat foot deformity (Cozen, 1965; Mann, 1983; Mann and Thomson, 1985 and Funk *et al*, 1986). A simple biomechanical analysis of TP tendon function during standing confirmed that TP muscle forces were potentially able to off-load the plantar foot ligaments, particularly those in the tarsus. Although the analysis of muscle force was limited in scope, it was recommended that during surgical procedures affecting muscle function, e.g. tendon transfer procedures to correct congenital deformities, care should be taken not to further compromise the foot structure in the long term. Further investigation into the biomechanics of tendon transfer procedures is recommended.

In the design of athletic footwear, measurements of the rearfoot motion are often used to evaluate alternative designs. It is thought that excessive ‘rearfoot pronation’ (eversion of the foot) on heel strike during running is a cause of ankle ligament and tendon overuse disorders (Nigg, 1986). Some evidence for this hypothesis was found in the present investigation where the strain in the CNL (continuous with the medial ankle ligaments) was seen to be increased during plantar flexion and eversion. Whilst the results were obtained under a pseudo-static loading regime the increased strains witnessed are still relevant to the dynamic events occurring during repeated heel strike. Measures to control excessive eversion during heel strike may reduce the incidence of these problems.

The biomechanical mechanisms underlying clinically reported ligament pathology have been demonstrated and possible implications for treatment methods have been suggested.

#### **7.2.4 Ligament Mechanics**

The general non-linear, viscoelastic behaviour of parallel-fibred collagenous tissue has been amply demonstrated. The general properties of this type of tissue have also been shown to complement the adaptive support function provided by the human foot (in the present study).

The tensile testing studies of this investigation showed that the plantar foot ligaments had non-linear properties, with small amounts of hysteresis and viscoelasticity in the preconditioned state. Mathematical models formulated to explain the biomechanical basis for this behaviour revealed that the elastic response of the ligaments did not generally agree with those models previously suggested by QLV theory.

The elastic behaviour was found to be accurately described by a cubic polynomial relationship. It was concluded that linear representation of the tissue properties, although convenient, does not accurately express the behaviour of the ligaments in the physiological range of function (the levels of strain and force witnessed were predominantly in the 'toe' region of the force/extension relationship). Approximate values of the elastic modulus from the linear part of the tissue responses were in close agreement with previous studies ( $E_{PA} = 350$  MPa,  $E_{CNL} = 28$  MPa) (Davis *et al*, 1996 and Wright and Rennels, 1964).

The effects of age on the specimens tested must be taken into account when relating the results of this study to a younger population ( $n = 6$ , mean age = 70 years). Previous studies have shown that the elastic modulus and the ultimate stress and strain properties of ligaments all decrease with age by a factor of about two (Noyes and Grood, 1976). Bearing the above result in mind, this does not negate in any way the results of the present study which tested specimens from what is, on average, an increasingly more aged population. Additionally there may have been some benefit from testing specimens that were, although normal, from a donor age range where pathology would have been more prevalent.

The techniques used to measure ligament properties and function were verified when testing isolated ligament specimens. Comparison of bulk and local strain measurements revealed that observed changes in histology of the ligament had influenced the local strain measurements obtained, as in previous investigations (Butler *et al*, 1984 and 1990 and Woo *et al*, 1983). In addition the longitudinal strain

distribution along the PA was seen to vary, as a result of the intrinsic non-homogeneous substructure of the ligament tissue.

The mechanics of the foot ligaments were, in summary, found to be non-linear in the range of physiological function, and should be interpreted within the context of the age of the specimens tested. The verified methods of strain measurement highlighted some histologically related intraligament variations in the mechanical properties of the tissues.

### **7.3 CONCLUSIONS**

The arguments presented in this thesis have shown that the ligaments have a vital and complex role in the functioning of the normal foot. In addition the mechanisms and biomechanical bases of some aspects of ligament related foot pathology have been described. Finally the non-linear mechanics of the foot ligament tissues were investigated, and described mathematically and compared to contemporary physical models of soft tissue behaviour.

To summarise the major findings of this investigation the particular conclusions drawn are listed below:

#### **7.3.1 Standing**

- 1. The foot ligament strains during standing are of a similar magnitude to functional strains in the ligaments of other joints of the body.**
- 2. Complex patterns of tarsal ligament strain occur with varying foot position. Tarsal ligament strain is particularly variable during inversion and eversion movements.**
- 3. Inversion and eversion of the foot induced by external and internal rotation of the tibia cause significant decreases and increases in foot ligament loading respectively. The order of sensitivity of the ligaments to these movements is, in descending order; CNL, SPL, LPL and PA (variation in tarsal ligament strain is 2 to 4 times that in the PA).**

4. General reductions in ligament loading were noted with applied extrinsic muscle forces during standing. TA and TP muscle forces were able to reduce tarsal ligament strain by between 39 and 100% due to their inverting action.
5. PL forces reduced loading in the SPL and LPL and caused the strain distribution in the PA to change due to altered forefoot loading. CNL strains were increased due to the evertion action of this muscle.
6. The relationship between vertically applied force and foot ligament force during standing is approximately linear.
7. Non-linear deformation kinematics of the whole foot were found with angular deflections of approximately  $3^\circ$  in the sagittal plane at the TT joint during standing.
8. The strain distribution in the PA varies along its length with changes in forefoot loading. This was due to its complex insertions in the forefoot and with the longitudinal septa and the skin.
9. The force in the PA during standing is approximately 100 N (verified by experimental and modelling studies) in persons with a body mass of 70kg.
10. Tarsal ligament forces predicted by the modelling study were higher than those found by experimental analysis, but were more consistent between specimens, and as such were considered more representative (LPL = 72 N, SPL = 42 N and CNL = 100 N on average in persons with a body mass of 70kg).

### **7.3.2 Gait**

1. The largest strains were found during toe-off and were approximately 4 times those seen during quiet standing. In the absence of intrinsic muscle activity this result represents a maximum expected loading condition for the foot during walking.

2. The extrinsic muscles were able to reduce strain in the ligaments confirming the theory of the dynamic support role of these muscles (see 7.3.1 conclusion 4).
3. Toe extension of 45° increased the force in the PA to 4 times the value found during standing. As a result of this the windlass mechanism was able to off load the tarsal ligaments during walking.

### **7.3.3 Pathology**

1. Insufficiency of the PA either through injury or surgical intervention in the treatment of plantar fasciitis, results in increased loading in the remaining ligaments (increases of 72 - 206% in the CNL, 47 - 131% in the LPL and 50 - 100% in the SPL). This was due to the large mechanical advantage of the PA at the TT joint.
2. PA insufficiency causes approximately 15 - 30% increase in ligament strain in the tarsal ligaments.
3. PA insufficiency may lead to pathology in the forefoot (forefoot loading conditions have a direct effect in the strain distribution of the PA).
4. Release of the PA is not recommended in the treatment of intractable plantar fasciitis, particularly in young active subjects. PA sectioning, without the use of an orthosis, will predispose the foot to further progressive injury and deformity.
5. The TP muscle was found to be able to reduce strain in the foot ligaments during weight bearing. This result explains and confirms, from a mechanical perspective, the clinically reported incidence of progressive flat foot deformity following TP tendon rupture or the onset of muscle dysfunction.

6. Strain increases in the CNL during plantar flexion and eversion indicated a possible injury mechanism to this structure during excessive eversion, of the rear foot, during heel strike in running (so called excessive 'rearfoot pronation').

#### **7.3.4 Tissue Mechanics**

1. The mechanical behaviour of the foot ligaments in tension is characterised by a non-linear relationship with a small amount of strain rate dependency, viscoelasticity and hysteresis.
2. The elastic response of the foot ligaments was accurately represented by a cubic polynomial expression. A linear model of the ligament mechanics was not applicable to the functioning of the ligaments in the physiological range.
3. Elastic responses of the ligamentous tissues of the foot do not generally agree with tissue models suggested previously by QLV theory.
4. The elastic modulus and stiffness of the PA were found to be approximately 350 MPa and 225 N/mm respectively. An elastic modulus of 28 MPa was found for the CNL.
5. The longitudinal strain distributions in the foot ligaments were dependent on the histology of the ligament (fibre density and alignment). The direct (bulk) and local measurements of strain in the PA were equal in magnitude.

#### **7.4 RECOMMENDATIONS FOR FUTURE WORK**

The results of this investigation follow on from those of Walker (1991) and have satisfied some of his recommendations for future work. The experiments of the present study were carried out on all the specimens made available and judged to be free of pathology. Cadaveric specimens are, however, not readily obtainable and the results in the present study were based on tests performed on 6 specimens. In order to add to the

present data and to enable meaningful statistical analysis it is recommended that additional specimens be tested. Increased numbers of specimens would also allow the effects of specific pathologies to be examined, e.g. pes planus, hallux valgus, given sufficient numbers. The stress relaxation properties of the foot ligaments could be examined if a larger sample size was used although wastage of other ligament specimens would be inevitable. By obtaining the stress-relaxation relationships, in this manner, the full viscoelastic behaviour of the ligaments could be described.

Initially this study was planned with a more comprehensive modelling component. It was, however, found that the information necessary to validate a complex model of the foot was not available from the literature. The technical complexity of assembling an accurate 3D model of the whole foot was found to be too great and was not feasible in the time available. A possible area of future investigation would be to model the geometry of the ligament structures in 3D using solid modelling software and to explore the mechanics of the foot using finite element analysis. By creating a series of such models for each of the joints of the foot, a model of the whole structure could be assembled. At the present time the detailed quantitative anatomical information required to construct such a model does not exist, although extensive interrogation and processing of 3D CT and MRI data would yield the necessary material. The results of the present study have provided quantitative data which could be used to validate such a model.

The ligament strain techniques developed during this investigation could be taken further to explore the foot ligament mechanics. The use of multiple transducers on each ligament would reveal additional information on the recruitment patterns throughout the test structures. The transducers could also be used to explore additional aspects of ligament function such as the effectiveness of orthoses, in a similar fashion to Kogler *et al* (1995), the effects of various types of footwear and simulated injuries, e.g. lateral ankle ligament rupture during forced inversion. The ligament strain techniques developed may be applied to other joints of the body, e.g. the wrist, knee and spine, to further explore the biomechanics of the musculoskeletal system. Development and use of strain measurement systems to investigate the foot ligaments *in vivo* would constitute the ultimate extension of the work presented here.

The results of the present study have established and quantified many aspects of the ligament biomechanics of the human foot. Many characteristics of foot function, however, remain undiscovered or warrant further investigation. The results presented in this thesis may facilitate ongoing investigations into the mechanics of the human foot and serve as a record of foot ligament function.

## REFERENCES

- Ahstrom, J.P. Jr. (1988), Spontaneous rupture of the plantar fascia. *Am. J. Sports Med.*, 16, 306-307.
- Albert, J., Rieman, P., Njus, G., Kay, D.B. and Theken, R. (1992), Ligament strain and ankle joint opening during ankle distraction. *Arthroscopy*, 8, 469-473.
- Alexander, R. McNeill (1992), *The Human Machine*, Natural History Museum Publications, London, UK.
- Allard, P., Thiry, P.S. and Duhaime, M. (1985), Estimation of the ligaments' role in maintaining foot stability using a kinematic model. *Med. & Biol. Eng. & Comput.*, 23, 237-242.
- An, K-N., Berglund, L., Cooney, W.P., Chao, E.Y.S. and Kovacevic, N. (1990), Technical note: Direct *in vivo* tendon force measurement system. *J. Biomechanics*, 23, 1269-1271.
- Andrews, J.R. (1983), Overuse syndromes of the lower extremity. *Clin. Sports Med.*, 2, 137-148.
- Arms, S., Boyle, J., Johnson, R. and Pope, M. (1983), Strain measurement in the medial collateral ligament of the human knee: An autopsy study. *J. Biomechanics*, 16, 491-496.
- Attarian, D.E., McCrackin, H.J., DeVito, D.P., McElhaney, J.H. and Garrett, W.E.Jr. (1985), Biomechanical characteristics of human ankle ligaments. *Foot & Ankle*, 6, 54-58.
- Ateshian, G.A., Kwak, S.D., Soslowky, L.J., Mow, V.C. (1994), A stereophotogrammetric method for determining *in situ* contact areas in diarthrodial joints, and a comparison with other methods. *J. Biomechanics*, 27, 111-124.
- Barbenel, J.C., Evans, J.H. and Finlay, J.B. (1973), Stress-strain-time relations for soft connective tissues, in "Perspectives in Biomedical Engineering", Ed. RM Kenedi, McMillan, London, pp 165-172.
- Barnes, G.R.G. and Pinder, D.N. (1974), *In vivo* tendon and bone strain measurement and correlation. *J. Biomechanics*, 7, 35-42.
- Barry, D. and Ahmed, A.M. (1986), Design and performance of a modified buckle transducer for the measurement of ligament tension. *J. Biomech., Engng.*, 108, 149-152.
- Basmajian, J.V. and Stecko, G. (1963), The role of the muscles in arch support of the foot. *J. Bone Joint Surg.*, 45A, 1184-1190.

- Beynon, B., Howe, J.G., Pope, M.H., Johnson, R.J. and Fleming, B.C. (1992), The measurement of anterior cruciate ligament strain *in vivo*. *International Orthopaedics (SICOT)*, 16, 1-12.
- Beynon, B.D., Johnson, R.J., Fleming, B.C., Renström, P., Nichols, C.E., Pope, M.H. and Haugh, L.D. (1994), The measurement of elongation of anterior cruciate-ligament grafts *in vivo*. *J. Bone Joint Surg.*, 76-A, 520-531.
- Beynon, B.D., Pope, M.H., Wertheimer, C.M., Johnson, R.J., Fleming, B.C., Nichols, C.E. and Howe, J.G. (1992), The effect of functional knee-braces on strain in the anterior cruciate ligament *in vivo*. *J. Bone Joint Surg.*, 74-A, 1298-1312.
- Blanton, P.L. and Biggs, N.L., (1970), Ultimate tensile strength of fetal and adult human tendons. *J. Biomechanics*, 3, 181-189.
- Bojsen-Møller, F. and Flagstad, K.E. (1976), Plantar aponeurosis and internal architecture of the ball of the foot. *J. Anat.*, 121, 599-611.
- Brooks, M. and Warwick, R. (1989), *Nomina Anatomica*, 6th edition, Churchill Livingstone, Edinburgh, UK.
- Brown, T.D., Sigal, L., Njust G.O., Njus, N.M., Singerman, R.J. and Brand, R.A. (1986), Dynamic performance characteristics of the liquid metal strain gage. *J. Biomechanics*, 19, 165-173.
- Butler, D.L., Grood, E.S., Noyes, F.R., Zernicke, R.F. and Brackett, K. (1984), Effects of structure and strain measurement techniques on the material properties of young human tendons and fascia. *J. Biomechanics*, 17, 579-596.
- Butler, D.L., Noyes, F.R. and Grood, E.S. (1978), Measurement of the mechanical properties of ligaments, in "CRC Handbook of Engineering in Medicine and Biology, Section B: Instrument and Measurements, Vol. 1", eds. B.N. Feinberg and D.G. Fleming, CRC Press, Palm Beach, Florida, USA, pp 279-314.
- Butler, D.L., Sheh, M.Y., Stouffer, D.C., Samaranayake, V.A. and Levy, M.S. (1990), Surface strain variation in human patellar tendon and knee cruciate ligaments. *J. Biomech. Engng.*, 112, 38-45.
- Calhoun, J.H., Li, F., Ledbetter, B.R. and Viegas, S.F. (1994), A comprehensive study of pressure distribution in the ankle joint with inversion and eversion. *Foot & Ankle*, 15, 125-133.
- Campbell, J.W. and Inman, V.T. (1974), Treatment of plantar fasciitis and calcaneal spurs with the UC-BL shoe insert. *Clinical Orthopaedics & Related Research*, 103, 57-62.
- Carlsöö, S. and Wetzenstein, H. (1968), Change of form of the foot and the foot skeleton upon momentary weight-bearing. *Acta. Orthop. Scand.*, 39, 413-423.

Cavanagh, P.R. and Rodgers, M.M. (1987), The arch index: A useful measure from footprints. *J. Biomechanics*, 20, 547-551.

Cawley, P.W. and France, E.P. (1991), Biomechanics of the lateral ligaments of the ankle: An evaluation of the effects of axial load and single plane motions on ligament strain patterns. *Foot & Ankle*, 12, 92-99.

Chao, E.Y.S., Lynch, J.D., and Vanderploeg, M.J. (1993), Simulation and animation of muscoskeletal joint system. *J. Biomech. Engng.*, 115, 563-568.

Cobbold, R.S.C., (1974), *Transducers for biomedical measurements: Principles and applications*, Wiley-Interscience, New York, USA.

Colville, M.R., Marder, R.A., Boyle, J.J. and Zarins, B. (1990), Strain measurement in lateral ankle ligaments. *Am J. Sports Med.*, 18, 196-200.

Cozen, L. (1965), Posterior tibial tenosynovitis secondary to foot strain. *Clin. Orthop.*, 42, 101-102.

Cronkite, A.E., (1936), The tensile strength of human tendons. *Anat. Rec.*, 64, 173-186.

Daly, P.J., Kitaoka, H.B. and Chao, E.Y.S. (1992), Plantar fasciotomy for intractable plantar fasciitis: Clinical results and biomechanical evaluation. *Foot & Ankle*, 13, 188-195.

Davis, W.H., Sobel, M., DiCarlo, E.F., Torzilli, P.A., Deng, X., Geppert, M.J., Patel, M.B. and Deland, J. (1996), Gross, histological, and microvascular anatomy and biomechanical testing of the spring ligament complex. *Foot & Ankle*, 17, 95-102.

Delp, S.L., Loan, .P.J., Hoy, M.G., Zajac, F.E., Topp, E.L., and Rosen, J.M. (1990), An interactive graphics-based model of the lower extremity to study orthopaedic surgical procedures. *IEEE Trans. Biomed. Engng.*, 37, 757-766.

Derwin, K.A., Soslowsky, L.J., Green, W.D.K. and Elder, S.H. (1994), Technical note. A new optical system for the determination of deformations and strains: calibration characteristics and experimental results. *J. Biomechanics*, 27, 1277-1285.

Donn, A.W. (1992), *Dynamic loading and shock absorption in the lower limb*. IEP Project Report, Department of Mechanical Engineering, The University of Leeds, Leeds.

Edwards, R.G., Lafferty, J.F. and Lange, K.O (1970), Ligament strain in the human knee joint. *J. Basic Eng.*, March 1970, 131-136.

Elftman, H. (1960), The transverse tarsal joint and its control. *Clin. Orthop.*, 16, 41-45.

- Ellis, D.G., (1969), Cross-sectional area measurements for tendon specimens: A comparison of several methods. *J. Biomechanics*, 2, 175-186.
- Fleming, B.C., Beynnon, B.D., Nichols, C.E., Renström, P., Johnson, R.J., and Pope, M.H. (1994a), An *in vivo* comparison between intra-operative isometric measurement and local elongation of the graft after reconstruction of the anterior cruciate ligament. *J. Bone Joint Surg.*, 76A, 511-519.
- Fleming, B.C., Beynnon, B.D., Tohyama, H., Johnson, R.J., Nichols, C.E., Renström, P. and Pope, M.H. (1994b), Determination of a zero strain reference for the anteromedial band of the anterior cruciate ligament. *J. Orthop. Res.*, 12, 789-795.
- France, E.P., Daniels, .U., Goble, E.M. and Dunn, H.K. (1983), Simultaneous quantitation of knee ligament forces. *J. Biomechanics*, 16, 553-564.
- Freeman, M..A.R (1965), Co-ordination exercises in the treatment of functional instability of the foot. *Physiotherapy*, 51, 393-395.
- Freeman, M..A.R, Dean, M.R.E. and Hanham, I.W.F (1965), The etiology and prevention of functional instability of the foot. *J. Bone Joint Surg.*, 47-B, 678-685.
- Frisén, M., Mägi, M., Sonnerup, L. and Viidik, A. (1969), Rheological analysis of soft collagenous tissue. Part I: Theoretical considerations. *J. Biomechanics*, 2, 13-20.
- Fujie, H., Livesay, G.A., Woo, S.L-Y., Kashiwaguchi, S. and Blomstrom, G. (1995), The use of a universal force-moment sensor to determine in situ forces in ligaments: A new methodology. *J. Biomech. Engng.*, 117, 1-7.
- Fukashiro, S., Komi, P.V., Järvinen, M. and Miyashita, M. (1992), Comparison between the directly measured achilles tendon force and the tendon force calculated from the ankle joint moment during vertical jumps. *Clin. Biomech.*, 8, 25-30.
- Fung, Y.C. (1993), Bioviscoelastic solids, in "Biomechanics. Mechanical Properties of Living Tissue, Second Edition", Springer-Verlag, London, pp 242-320.
- Fung, Y.C.B. (1967), Elasticity of soft tissues in simple elongation. *Am J. Physiol.* 213, 1532-1544.
- Fung, Y.C.B. (1972), Stress-strain-history relations of soft tissues in simple elongation, in "Biomechanics. Its foundations and objectives", eds. Y.C. Fung, N. Perrone and M. Anliker, Prentice-Hall, Inc., New Jersey, pp 181-208.
- Funk, D.A., Cass, J.R. and Johnson, K.A. (1986), Acquired adult flat foot secondary to posterior tibial-tendon pathology. *J. Bone & Joint Surg.*, 68-A, 95-102.
- Galante, J.O. (1967), Tensile properties of the human annulus fibrosus. *Acta. Orthop. Scandinav.*, Suppl . No. 100, 75-83.

- Goel, V.K., Kong, W., Han, J.S., Weinstein, J.N., and Gilbertson, L.G. (1993), A combined finite element and optimisation investigation of lumbar spine mechanics with and without muscles. *Spine*, 18, 1531-1541.
- Good, E.S. and Noyes, F.R. (1976), Cruciate ligament prosthesis: Strength, creep, and fatigue properties. *J. Bone Joint Surg.*, 58-A, 1083-1088.
- Hawes, M.R., Nachbauer, W., Sovak, D. and Nigg, B.M. (1992), Footprint parameters as a measure of arch height. *Foot & Ankle*, 13, 22-26.
- Haut, R.C. and Little, R.W. (1972), A constitutive equation for collagen fibres. *J. Biomechanics*, 5, 423-430.
- Hennig, E.M. and Cavanagh, P.R. (1985), Ultrasonic quantification of the arch of the weight-bearing foot, in "International Series on Biomechanics, Vol. 5A, Biomechanics IX-A", ed. D.A. Winter, Human Kinetics Publishers Inc., Illinois, US, pp 211-216.
- Hicks, J.H. (1953), The mechanics of the foot: I The joints. *J. Anat.*, 87, 345-357.
- Hicks, J.H. (1954), The mechanics of the foot: II The plantar aponeurosis and the arch. *J. Anat.*, 88, 25-30.
- Hicks, J.H. (1955), The foot as a support. *Acta. Anat.*, 25, 34-45.
- Holden, J.P., Grood, E.S, Korvik, D.L., Cummins, J.F., Butler, D.L. and Bylski-Austrow, D.I. (1994), *In vitro* forces in the anterior cruciate ligament: Direct measurements during walking and trotting in a quadruped. *J. Biomechanics*, 27, 517-526.
- Hølmer, P., Søndergaard, L., Nielson, P.T. and Jørgensen, L.N. (1994), Epidemiology of sprains in the lateral ankle and foot. *Foot & Ankle*, 15, 72-74.
- Howe, J.G., Wertheimer, C., Johnson, R.J., Nichols, C.E, Pope, M.H. and Beynon, B. (1990). Arthroscopic strain gauge measurement of the normal anterior cruciate ligament. *Arthroscopy: J Arthroscopic & Related Surg.*, 6, 198-204.
- Huang, C.K., Kitaoka, H.B., An, K.N., and Chao, E.Y.S. (1993), Biomechanical evaluation of the longitudinal arch stability. *Foot & Ankle*, 14, 353-357.
- Humphry, G.M. (1867), Reply to Prof. Hancock concerning the arches of the foot. *J. Anat. Physiol.*, 1, 187-188.
- Inman, V.T. (1976), *The joints of the ankle*, Williams and Wilkins, Baltimore, USA.
- Isman, R.E. and Inman, V.T. (1969), Anthropometric studies of the human foot and ankle. *Bul. Prosthet. Res.*, 11, 97-129.

Jackson, P. (1988), Ankle injuries, in "The Foot, Volume 2", eds. B. Helal, and D. Wilson, Churchill Livingstone, London, UK, pp 868-893.

Jacob, H.A.C. (1989), Biomechanics of the fore foot, PhD Thesis, Bioengineering Unit, The University of Strathclyde, Glasgow, Scotland.

Jansen, M. (1994), Personal communication.

Jansen, M. (1995), Tendon strain, force and function in equine locomotion. PhD thesis, University of Utrecht, Netherlands.

Janssen, M.L. and Walter, J.D. (1971), Rubber strain measurements in bias, belted-bias and radial ply tires. *J. Coated Fibrous Materials*, 1, 102-117.

Jenkins, R.B. and Little, R.W. (1974), A constitutive equation for parallel-fibered elastic tissue. *J. Biomechanics*, 7, 397-402.

Jones, R.L. (1941), The human foot. An experimental study of its mechanics, and the role of its muscles and ligaments in the support of the arch. *Am. J. Anat.*, 68, 1-39.

Karlsson, J., Löfvenberg, R. and Eriksson, B.I. (1995), Ligament injuries of the ankle. *Current Opinion in Orthopedics*, 6, 40-46.

Kayano, J., Norimatsu, T., Fujita, M., Matsusaka, N., Teramoto, N., Yang, S., and Suzuki, R. (1978), Dynamic changes of the medial arch of the foot during walking, in "International Series on Biomechanics, Vol. 6A, Biomechanics X-A", ed. Bengt Jonsson and Kurt Jorgensen, University Park Press, Baltimore, pp 409-412.

Kaye, R.A. and Jahss, M.H. (1991), Tibialis posterior: A review of anatomy and biomechanics in relation to support of the medial longitudinal arch. *Foot & Ankle*, 11, 244-247.

Kennedy, J.C., Hawkins, R.J., Willis, R.B. (1977), Strain gauge analysis of knee ligaments. *Clinical Orthopaedics and Related Research*, 129, 225-229.

Kennedy, J.C., Hawkins, R.J., Willis, R.B. and Danylchuk, K.D., (1976) Tension studies of human knee ligaments. Yield points, ultimate failure, and disruption of the cruciate and tibial collateral ligaments. *J. Bone Joint Surg.*, 58-A, 350-355.

Kepple, T.M., Arnold, A.S., Stanhope, S.J., Siegel, K.L. (1994), Assessment of a method to estimate muscle attachments from the surface landmarks: A 3D computer graphics approach. *J. Biomechanics* 27, 365-371.

Ker, R.F., Bennet, M.B., Alexander, R.McN., and Kester, R.C. (1989), Foot strike and the properties of the heel pad. *Proc. Instn. Mech. Engrs.*, 203, Part H: *J Eng. Med.* 191-196.

- Ker, R.F., Bennet, M.B., Bibby, S.R., Kester, R.C. and Alexander, R.McN. (1987), The spring in the arch of the human foot. *Nature*, 325, 147-149.
- Kim, W. and Voloshin, A.S. (1995), Role of plantar fascia in the load bearing capacity of the human foot. *J. Biomechanics*, 28, 1025-1033.
- Kim, W. and Voloshin, A.S. and Johnson, S.H. (1994), Modelling of heel strike transients during running. *Human Movement Science*, 13, 221-244.
- Kitaoka, H.B., Lou, Z.P., Growney, E.S., Berglund, L.J., An, K-N. (1994), Material Properties of the plantar aponeurosis. *Foot & Ankle*, 15, 557-560.
- Kogler, G.F., Solomonidis, S.E. and Paul, J.P. (1995a), *In vitro* method for quantifying the effectiveness of the longitudinal arch support mechanism of a foot orthosis. *Clin. Biomech.*, 10, 245-252.
- Kogler, G.F., Solomonidis, S.E. and Paul, J.P. (1995b), The biomechanics of longitudinal arch support mechanisms in foot orthoses and their effect on plantar aponeurosis strain, "Conference Proceedings. Nineteenth Annual Meeting of the American Society of Biomechanics" Stanford University, Stanford, California, pp 91-92.
- Komi, P.V. (1990), Relevance of *in vivo* force measurements to human biomechanics. *J. Biomechanics*, 23, Suppl. 1, 23-34.
- Komi, P.V., Fukashiro, S. and Järvinen, M. (1992), Biomechanical loading of achilles tendon during normal locomotion. *Clin. Sports Med.*, 11, 521-531.
- Kurosawa, H., Yamakoshi, K-I., Yasuda, K. and Sasaki, T. (1991), Simultaneous measurement of changes in length of the cruciate ligament during knee motion. *Clinical Orthopaedics and Related Research*, 265, 233-240.
- Lam, P.C., Downing, M., and Reddy, N.P. (1987), One more step in redesigning the ankle-foot orthotic. *SOMA*, April 87, 36-39.
- Lamontagne, M., Doré, R., Drouin, G. and Meunier, A. (1987), Mechanical properties of tendons measured by strain gauges for different loading angles, in "International Series on Biomechanics, Volume 6B, Biomechanics X-B", Ed. B. Jonsson, Human Kinetics Publishers Inc., Illinois, USA, pp 955-960.
- Lamontagne, M., Németh, G. and Wretenberg, P. (1993), A new approach to validate a musculo-skeletal human knee joint model, in "Book of Abstracts, International Society of Biomechanics", XIV Congress, Paris.
- Langelaan, E.J. van (1983), A kinematical analysis of the tarsal joints. PhD thesis, University of Leiden, The Netherlands.

- Lanir, Y. (1980), A microstructure model for the rheology of mammalian tendon. *J. Biomech. Engng.*, 102, 332-339.
- Lanir, Y. and Fung, Y.C. (1974), Two-dimensional mechanical properties of rabbit skin-1. Experimental system. *J. Biomechanics*, 7, 29-34.
- Lapidus, P.W. (1943), Mechanics of the arch of the foot. *Arch. Surg.*, 46, 410-421.
- Leach, R., Jones, R., and Silva, T., (1978), Rupture of the plantar fascia in athletes. *J. Bone & Joint Surg.*, 60-A, 537-539.
- LeMelle, D.P., Kisilewicz, P. and Janis, L.R. (1990), Chronic plantar fascial inflammation and fibrosis. *Clinics in Podiatric Medicine & Surgery*, 7, 385-389.
- Lewis, J.L., Lew, W.D. and Schmidt, J. (1982), A note on the application and evaluation of the buckle transducer for knee ligament force measurement. *J. Biomech. Engng.*, 104, 125-128.
- Li, P. and Ladin, Z. (1992), Mathematical modelling of the effect of sole elasticity distribution on pronation. *J. Biomechanics*, 25, 501-510.
- Lundberg, A. (1988), Patterns of motion of the ankle/foot complex. PhD thesis, Department of Orthopaedics, Karolinska, Sweden.
- McMinn, R.M.H., Hutchings R.T. and Logan, B.M. (1982), A colour atlas of foot and ankle anatomy, Wolfe Medical Publications Ltd, London, UK.
- Mann, R.A. (1983), Acquired flatfoot in adults. *Clinical Orthopaedics & Related Research*, 181, 47-51.
- Mann, R. and Inman, V.T. (1964), Phasic activity of intrinsic muscles of the foot. *J. Bone Joint Surg.*, 46-A, 469-483.
- Mann, R.A. and Plattner, P.F. (1988), Principles and practices of tendon transfers, in "The Foot, Volume 1", eds. B. Helal, and D. Wilson, Churchill Livingstone, London, UK, pp 378-384.
- Mann, R.A. and Thompson, F.M. (1985), Rupture of the posterior tibial tendon causing flat foot. *J. Bone Joint Surg.*, 67-A, 556-561.
- Manter, J.T. (1941), Movements of the subtalar and transverse tarsal joint. *Anat. Rec.*, 80, 97-410.
- Manter, J.T. (1946), Distribution of compressive forces in the joints of the human foot. *Anat. Rec.*, 96, 313-321.
- Meglan, D., Berme, N. and Zuelzer, W. (1988), Technical note. On the construction, circuitry and properties of liquid metal strain gages. *J. Biomechanics*, 21, 681-685.

- Meyer, S.A., Callaghan, J.J., Albright, J.P., Crowley, E.T. and Powell, J.W. (1994), Midfoot sprains in collegiate football. *Am. J. Sports Med.*, 22, 392-401.
- Michelson, J.D. and Hutchins, C. (1995), Mechanoreceptors in human ankle ligaments. *J. Bone Joint Surg.*, 77-B, 219-224.
- Momersteeg, T.J.A., Blankevoort, L., Huiskes, R., Kooloos, J.G..M., Kauer, J.M.G. and Hendriks, J.C.M., (1995), Technical Note. The effect of variable relative insertion orientation of human knee bone-ligament-bone complexes on the tensile stiffness. *J. Biomechanics*, 28, 745-752.
- Monahan, J.J., Grigg, P., Pappas, A.M., Leclair, W.J., Marks, T., Fowler, D.P. and Sullivan, T.J. (1984), *In vivo* strain patterns in the four major canine knee ligaments. *J. Orthop. Res.*, 2, 408-418.
- Morlock, M. (1989), A generalised three-dimensional six-segment model of the ankle and the foot, PhD Thesis, Department of Medical Science, The University of Calgary, Alberta, Canada.
- Morlock, M. and Nigg, B.M. (1991), Theoretical considerations and practical results on the influence of the representation of the foot for the estimation of internal forces with models. *Clin. Biomech.*, 6, 3-13.
- Nachbauer, W. and Nigg, B.M. (1992), Effects of arch height of the foot on ground reaction forces in running. *Med. Sci. Sports Exerc.*, 24, 1264-1269.
- Nakamura, S., Crowninshield, R.D. and Cooper, R.R. (1981), An analysis of soft tissue loading in the foot - a preliminary report. *Bulletin of Prosthetics Research*, 18, 27-34.
- Newell, S.G. and Miller, S.J. (1977), Conservative treatment of plantar fascial strain. *Phys. Sports Med.*, 5, 68-73.
- Nigg, B.M., (1986), *Biomechanics of running shoes*, Human Kinetics Publishers, Inc., Champaign, IL 61820, USA.
- Nigg, B.M., Cole, G.K. and Nachbauer, W. (1993), Effects of arch height of the foot on angular motion of the lower extremities in running. *J. Biomechanics*, 26, 909-916.
- Nigg, B.M., Skarvan, G., Frank, C.B. and Yeadon, M.R. (1990), Elongation and forces of ankle ligaments in a physiological range of motion. *Foot & Ankle*, 11, 30-40.
- Noyes, F.R., Butler, D.L., Grood, E.S., Zernicke, R.F. and Hefzy, M.S. (1984), Biomechanical analysis of human ligament grafts used in knee-ligament repairs and reconstructions. *J. Bone Joint Surg.*, 66-A, 334-352.

Noyes, F.R. and Grood, E.S. (1976), The strength of the anterior cruciate ligament in humans and rhesus monkeys. Age related and species related changes. *J. Bone Joint Surg.*, 58-A, 1074-1082.

Ottevanger, E.J.C., Spoor, C.W., van Leeuwen, J.L., Sauren, A.A.H.J., Janssen, J.D. and Huson, A. (1989), An experimental set-up for the measurement of forces on a human foot during inversion. *J. Biomechanics*, 22, 957-962.

Ouzounian, T.J. and Shereff, M.J. (1989), In vitro determination of midfoot motion. *Foot & Ankle*, 10, 140-146.

Patil, K.M., Braak, L.H., and Huson, A. (1993), Stresses in a simplified two dimensional model of a normal foot - a preliminary analysis. *Mechanics Research Communications*, 20, 1-7.

Phillips, G. (1989), ACQUIRE, Data acquisition software and manual, Bioengineering Unit, The University of Strathclyde, Glasgow, UK.

Platt, D., Wilson, A.M., Timbs, A., Wright, I.M. and Goodship, A.E. (1994), Technical Note: Novel force transducer for the measurement of tendon force *in vivo*. *J. Biomechanics*, 27, 1489-1493.

Pradas, M.M. and Calleja, R.D. (1990), Non-linear viscoelastic behaviour of the flexor tendon of the human hand. *J. Biomechanics*, 23, 773-781.

Procter, P. (1980), Ankle joint biomechanics, PhD Thesis, Bioengineering Unit, The University of Strathclyde, Glasgow, Scotland.

Race, A. and Amis, A.A. (1994), The mechanical properties of the two bundles of the human posterior cruciate ligament. *J. Biomechanics*, 27, 13-24.

Reeser, L.A., Susman, R.L. and Stern, J.T. Jr. (1983), Electromagnetic studies of the human foot: Experimental approaches to hominid evolution. *Foot & Ankle*, 3, 391-407.

Renstrom, P., Wertz, M., Incavo, S., Pope, M., Ostgaard, H.C., Arms, S. and Haugh, L. (1988), Strain in the lateral ligaments of the ankle. *Foot & Ankle*, 9, 59-63.

Riemersma, D.J. and Lammertink, J.L.M. (1988), Calibration of the mercury-in-silastic strain gauge in tendon load experiments. *J. Biomechanics*, 21, 469-476.

Rigby, B.J., Hirai, N., Spikes, J.D. and Eyring, H. (1959), The mechanical properties of rat tail tendon. *J. Gen. Physiol.*, 43, 265-283.

Romanes, G.J. (1987), Cunningham's manual of practical anatomy, 13th edition, Oxford University Press, Oxford, UK.

Roy, S (1983), How I manage plantar fasciitis. *Phys. Sports. Med.*, 11, 127-131.

Salathe, E.P. Jr., Arangio, G.A. and Salathe, E.P. (1986), A biomechanical model of the foot. *J. Biomechanics*, 19, 989-1001.

Salathe, E.P. Jr., Arangio, G.A. and Salathe, E.P. (1990), The foot as a shock absorber. *J. Biomechanics*, 23, 655-659.

Sarrafian, S.K. (1983), *Anatomy of the foot and ankle*, J.B. Lippincott Co, Philadelphia, USA.

Sarrafian, S.K. (1987), Functional characteristics of the foot and plantar aponeurosis under tibiotalar loading. *Foot & Ankle*, 8, 4-18.

Savelberg, H.H.C.M., Kooloos, J.G.M., Delange, A., Huijskes, R. and Kauer, J.M.G. (1991), Human carpal ligament recruitment and three-dimensional carpal motion. *J. Orthop. Res.*, 9, 693-704.

Savelberg, H.H.C.M., Kooloos, J.G.M., Huijskes, R. and Kauer, J.M.G. (1993), Technical note. An indirect method to assess wrist ligament forces with particular regard to the effect of preconditioning. *J. Biomechanics*, 26, 1347-1351.

Scott, S.H. and Winter, D.A. (1993), Biomechanical model of the human foot: Kinematics and kinetics during the stance phase of walking. *J. Biomechanics*, 26, 1091-1104.

Shapiro, M.S., Wascher, D.C. and Finerman, G.A. (1994), Rupture of Lisfranc's ligament in athletes. *Am. J. Sports Med.*, 22, 687-691.

Shereff, M.J., DiGiovanni, L., Bejjani, F.J., Hersh, A. and Kummer, F.J. (1990), A comparison of nonweight-bearing and weight-bearing radiographs of the foot. *Foot & Ankle*, 10, 306-311.

Siegler, S., Block, J. and Schneck, C.D. (1988), The mechanical characteristics of the collateral ligaments of the human ankle joint. *Foot & Ankle*, 8, 234-242.

Simkin, A. (1982), *Structural analysis of the human foot in standing posture*, PhD Thesis, Tel-Aviv University, Tel-Aviv, Israel.

Simkin, A. and Leichter, I. (1990), Role of the calcaneal inclination in the energy storage capacity of the human foot - a biomechanical model. *Med. & Biol. Eng. & Comput.*, 28, 149-152.

Simkin, A., Leichter, I., Giladi, M., Stein, M. and Milgrom, C. (1989), Combined effect of foot arch structure and an orthotic device on stress fractures. *Foot & Ankle*, 10, 25-29.

- Stokes, I.A.F., Hutton, W.C., and Stott, J.R.R. (1979), Forces acting on the metatarsals during normal walking. *J. Anat.*, 129, 579-590.
- Stone, J.E., Madsen, N.H., Milton, J.L., Swinson, W.F. and Turner, J.L. (1983), Developments in the design and use of liquid metal strain gages. *Exp. Mech.* 23, 129-139.
- Suzuki, N. (1972), An electromyographic study of the role of muscles in arch support of the normal and flat foot. *Nagoya Med. J.*, 17, 57-79.
- Torg, J.S., Pavlov, H. and Torg, E. (1987), Overuse injuries in sport: The foot. *Clin. Sports Med.*, 6, 291-320.
- Veres, G. (1977), Graphic analysis of forces acting upon a simplified model of the foot. *Prosthetics and Orthotics International*, 1, 161-172.
- Valenti, V. (1988), Proprioception, in "The Foot, Volume 1", eds. B. Helal, and D. Wilson, Churchill Livingstone, London, UK, pp 87-95.
- Viidik, A. (1966), Biomechanics and functional adaptation of tendons and joint ligaments, in "Studies on the anatomy and function of bone and joints", ed. F.G. Evans, Springer Verlag, pp 17-39.
- Viidik, A. (1980a), Mechanical properties of parallel-fibred collagenous tissues, in "Biology of Collagen" eds. A. Viidik and J. Vuust, Academic Press Inc. (London) Ltd., London, pp 237-255.
- Viidik, A. (1980b), Interdependence between structure and function in collagenous tissues, in "Biology of Collagen" eds. A. Viidik and J. Vuust, Academic Press Inc. (London) Ltd., London, pp 257-280.
- Viidik, A. (1982), Age-related changes in connective tissues, in "Lectures on Gerontology, Vol. 1, Part A", ed. A. Viidik, Academic Press Inc. (London) Ltd., London, pp 173-211.
- Viidik, A. (1987), Properties of Tendons and Ligaments, in "Handbook of Bioengineering", Eds. R. Skalak and S. Chien, McGraw-Hill Book Company, New York, pp 6.2-6.19.
- Viidik, A. and Lewin, (1966), Changes in tensile strength characteristics and histology of rabbit ligaments induced by different modes of postmortal storage. *Acta. Orthop. Scandinav.*, 37, 141-155.
- Vogel, H.G. (1983), Age dependence of mechanical properties of rat tail tendons (hysteresis experiments). *Akt. Gerontol.*, 13, 22-27.
- Walker, L.T. (1991), The biomechanics of the human foot. PhD thesis, University of Strathclyde, Glasgow, UK.

- Wang, C.L., Cheng, C.K., Chen, C.W., Lu, C.M., Hang, Y.S. and Liu, T.K. (1995), Contact areas and pressure distributions in the subtalar joint. *J. Biomechanics*, 28, 269-279.
- Williams, P.L., Warwick, R., Dyson, M. and Bannister, L.H. (1989), *Gray's Anatomy*, 37th edition, Churchill Livingstone, Edinburgh, UK.
- Winson, I.G., Lundberg, A. and Bylund, C. (1994), The pattern of motion of the longitudinal arch of the foot. *The Foot*, 4, 151-154.
- Woo, S.L-Y., Gomez, M.A. and Akeson, W.H. (1981), The time and history-dependent viscoelastic properties of the canine medial collateral ligament. *J. Biomech. Engng.*, 103, 293-298.
- Woo, S.L-Y., Gomez, M.A., Seguchi, Y., Endo, C.M. and Akeson, W.H. (1983), Measurement of mechanical properties of ligament substance from a bone-ligament-bone preparation. *J. Orthop. Res.*, 1, 22-29.
- Woo, S.L-Y., Johnson, G.A. and Smith, B.A. (1993), Mathematical modelling of ligaments and tendons. *J. Biomech. Engng.*, 115, 468-473.
- Woo, S.L-Y., Orlando, C.A., Camp, J.F. and Akeson, W.H. (1986)a, Effects of post-mortem storage by freezing on ligament tensile behaviour. *J. Biomechanics*, 19, 399-404.
- Woo, S.L-Y., Orlando, C.A., Gomez, M.A., Frank, C.B. and Akeson, W.H. (1986)b, Tensile properties of the medial collateral ligament as a function of age. *J. Orthop. Res.*, 4, 133-141.
- Woo, S.L-Y., Ritter, M.A., Amiel, D., Sanders, T.M., Gomez, M.A., Kuei, S.C., Garfin, S.R. and Akeson, W.H. (1980), The biomechanical and biochemical properties of swine tendons - long term effects of exercise on the digital extensors. *Connective Tissue Research*, 7, 177-183.
- Wright, D.G. and Rennels, D.C. (1964), A study of the elastic properties of plantar fascia. *J. Bone Joint Surg.*, 46-A, 482-492.
- Xu, W.S., Butler, D.L., Stouffer, D.C., Grood, E.S. and Glos, D.L. (1992), Theoretical analysis of an implantable force transducer for tendon and ligament structures. *J. Biomech. Engng.*, 114, 170-177.
- Yang, S.M., Kayamo, J., Norimatsu, T., Fujita, M., Matsusaka, N., Suzuki, R. and Okumura, H. (1985), Dynamic changes of the arches of the foot during walking, in "International Series on Biomechanics, Vol 5A, Biomechanics IX-A", ed. D.A. Winter, Human Kinetics Publishers Inc., Illinois, US, pp 417-422.

Yettram, A.L., and Camilleri, N.N. (1992), The forces acting on the human calcaneus. *J. Biomed. Eng.* 15, 46-50.

Youdin, M. and Reich, T. (1976), Mercury-in-rubber (Whitney) strain gauge. Temperature compensation and analysis of error caused by temperature drift. *Annals Biomed. Eng.*, 4, 220-231.

Zitzlperger, S. (1960), The mechanics of the foot based on the concept of the skeleton as a statically indetermined space framework. *Clinical Orthopaedics & Related Research*, 16, 47-63.

## APPENDIX 1. TRANSDUCER CALIBRATIONS

Test No.	Mean R <sup>2</sup>	Calib. Factor
1	0.999	0.8654
2	0.995	0.8618
3	0.988	0.8724
4	0.988	0.8728
5	0.988	0.8847
6	1	1.6873

Table A1.1 TACH cell calibration factors.

Test No.	LMSG No.	G.L./mm	Structure	Mean Gradient	Mean R <sup>2</sup>	Mean R <sub>q</sub> <sup>2</sup>	Calib. Factor	Temp./°C
1	5	14	PA(Distal)	0.9184	0.999	0.999	79.194	22.8
	9	14	PA(Prox.)	0.8134	0.999	0.999	70.139	22.6
	8	9	LPL	1.1786	0.999	0.999	91.471	22.9
	7	6	SPL	0.7027	1	1	60.594	22.9
	6	4	CNL	1.0965	0.984	0.987	94.551	22.2
2	16	14	PA(Distal)	0.9113	0.988	0.989	78.581	20.8
	17	14	PA(Prox.)	0.8041	0.995	0.995	69.338	20.9
	18	9	LPL	1.1254	0.991	0.992	87.342	21
	21	6	SPL	0.5712	0.999	1	49.255	20.9
	20	4	CNL	0.6626	0.968	0.973	57.136	21.2
3	24	14	PA(Distal)	0.7758	0.994	0.995	66.897	20.4
	25	14	PA(Prox.)	0.5889	0.999	0.999	50.781	20.5
	26	9	LPL	0.9104	0.994	0.994	70.656	20.9
	27	6	SPL	0.7004	1	1	60.395	20.9
	23	4	CNL	0.959	0.946	0.956	82.695	20.9
4	32	14	PA(Distal)	1.0256	0.991	0.992	88.437	21.7
	33	14	PA(Prox.)	0.7264	0.996	0.996	62.637	22.2
	34	9	LPL	0.8859	0.998	0.998	68.755	21.9
	35	6	SPL	0.6746	0.999	1	58.171	21.9
	36	4	CNL	0.8664	0.987	0.989	74.710	22.1
5	37	14	PA(Distal)	0.7171	0.998	0.998	61.836	20.6
	38	14	PA(Prox.)	0.5761	0.999	0.999	49.677	21
	39	9	LPL	1.1347	0.996	0.997	88.064	21
	40	6	SPL	0.6831	1	1	58.904	21.1
	41	4	CNL	1.2739	0.999	0.999	109.848	21
6	55	14	PA(Distal)	1.537	0.999	1	132.536	21.8
	56	14	PA(Prox.)	1.5984	0.999	1	137.830	21.9
	57	9	LPL	1.0515	0.998	0.999	81.607	22.2
	58	6	SPL	0.6632	0.999	1	57.188	22.2
	59	4	CNL	0.239	0.999	0.999	20.609	22.4

Table A1.2 LMSG calibration data for intact foot tests.

Specimen	LMSG No.	G.L./mm	Structure	Mean Gradient	Mean R <sup>2</sup>	Mean R <sub>q</sub> <sup>2</sup>	Calib. Factor	Temp. <sup>o</sup> C
107R	60	14	PA(Distal)	1.4203	0.999	1.000	122.472	21.0
	61	14	PA(Prox.)	1.5452	0.999	1.000	133.243	20.0
	62	9	LPL	1.1124	0.999	1.000	86.333	21.2
	63	6	SPL	0.6834	0.999	1.000	58.930	20.8
	64	4	CNL	0.4169	0.999	0.999	35.949	21.3
113L	68	14	PA(Distal)	1.5088	0.999	1.000	130.104	23.0
	69	14	PA(Prox.)	1.4645	0.999	1.000	126.284	22.9
	70	9	LPL	1.1185	0.999	1.000	86.807	22.9
	71	6	SPL	0.6264	0.999	1.000	54.014	23.0
	72	4	CNL	0.3870	0.995	0.997	33.371	23.1

Table A1.3 LMSG calibration data for the isolated ligament tests.

## APPENDIX 2. LMSG PERFORMANCE ASSESSMENT

### A2.1 TEMPERATURE SENSITIVITY AND COMPENSATION OF LMSG OUTPUT

The relationship between LMSG output and temperature has been found to be dominated by thermally induced changes in the resistivity of mercury (Jansen, 1994; Meglan *et al*, 1988; Riemersma and Lammertink, 1988 and Youdin and Reich, 1976). Recalling from Chapter 4:

$$\Delta V = C_c \varepsilon [1 + \alpha(T_i - T_0)] \quad (\text{A2.1})$$

Where  $\Delta V$  = LMSG output,  $C_c$  = calibration factor,  $\varepsilon$  = strain applied to LMSG,  $\alpha = 0.00089^\circ\text{C}^{-1}$ ,  $T_i$  = temperature and  $T_0$  = temperature at calibration. The effective gradient of the calibration curve is altered by temperature such that,

$$\Delta V = C_i \varepsilon, \quad \text{for } T_i \neq T_0 \quad (\text{A2.2})$$

where  $C_i$  is the temperature corrected calibration factor. For every  $1^\circ\text{C}$  temperature rise the value of  $C_c$  increases by 0.089%. Changes in temperature during a test would have caused shifts in LMSG output. LMSG resistance,  $R$ , may be written:

$$R = R_0 [1 + \alpha(T_i - T_0)] \quad (\text{A2.3})$$

The resistance change due to temperature,  $\Delta R$  is, thus,

$$\Delta R = R - R_0 = R_0 \alpha (T_i - T_0) \quad (\text{A2.4})$$

Substituting  $\Delta R$  in equation 4.2, thus

$$\frac{\Delta R}{R_0} = 2 \left( \frac{\Delta L}{L_0} \right) \quad (\text{A2.5})$$

and rearranging yields:

$$\varepsilon = \frac{\Delta L}{L_0} = \frac{\alpha(T_i - T_0)}{2} \quad (\text{A2.6})$$

Thus for an LMSG of any length every  $1^\circ\text{C}$  temperature shift results in an apparent strain of 0.045%. This theoretical value has been verified by experiment by Jansen (1994) and Riemersma and Lammertink (1988) who found a temperature strain artefact of 0.051%.

An attempt was made to verify the above observations. Three LMSGs 14, 9, and 8 mm in length, were calibrated in a temperature controlled water bath. A small jig was designed to extend the LMSG. Displacement was measured with an LVDT (Schlumberger, AG-5). Due to noise in the LVDT signal and laxity in the sliding parts of the rig a poorer linear fit to the data was obtained, i.e. smaller  $R^2$  values. From plots of the regression lines, and on inspection of the regression constants, consistent patterns in the change of  $C_c$  were not identifiable within the accuracy of the equipment used. Plots of the regression lines for the raw test data are shown in figures A2.1 to A2.3. Shifts in gauge response were identified, however, again due to reduced efficiency and reproducibility of the linear regression procedures, quantification of temperature induced changes in these specific experiments was not feasible. In the absence of effective demonstration of the small changes in LMSG behaviour with temperature the previously verified compensation values described above were used to correct the ligament strain results for changes in temperature.

During testing the laboratory temperature was controlled and did not vary more than  $2^\circ\text{C}$  over the duration of the whole test. Relative zero references were taken at regular intervals and temperature was approximately constant within these measuring periods ( $\pm 0.2^\circ\text{C}$ ). In view of these facts the only temperature compensation conducted was that given in equation A2.1.

LMSG No.	Pre-test		Post-test		Ratio (Pre/Post)
	Mean $R^2$	Calib. Factor	Mean $R^2$	Calib. Factor	
32	0.991	88.437	0.999	90.308	0.9793
33	0.996	62.637	0.999	65.854	0.9512
36	0.987	74.710	0.999	76.539	0.9761
37	0.998	61.836	0.998	67.303	0.9188
38	0.999	49.677	0.999	53.154	0.9346
39	0.996	88.064	0.999	91.083	0.9669
40	1	58.904	0.999	62.991	0.9351

Table A2.1: Post-test LMSG calibration comparisons.

## A2.2 STABILITY OF GAUGE RESPONSE WITH TIME

The stability of the LMSG calibration factors with time was verified by calibrating a selection of LMSGs on successive days. No detectable changes in LMSG response could be measured on consecutive days outwith the accuracy of the calibration procedures. Although LMSGs were not routinely recalibrated after testing, a small number of transducers that were undamaged after removal were calibrated a second time. Each of the LMSGs was decontaminated in ethanol and any misshapen adhesive residue was carefully removed from the end electrodes.

On recalibration, between 6 and 8 weeks after testing, the gauge response was found to have remained stable and highly linear. An increase of approximately 5% in  $C_c$  was found after 50 days. Assuming a linear change of  $C_c$  with time due to effects such

as amalgamation, oxidation and creep of the silicone rubber tube material. A change of 0.1%  $C_c$  per day was calculated. Pre- and post- test LMSG calibration data is presented in table A2.1.

### A2.3 LMSG FORCE/EXTENSION BEHAVIOUR

It is essential for accurate measurement of ligament strain that the transducer, when implanted, should not significantly alter the normal structure or force deflection relationship. To achieve this the force required to deform the transducer should be a very small proportion of the force being transmitted by the ligament. During routine LMSG calibration the force required to deform the gauges was measured with a 100 N capacity load cell. The extension force was found to vary slightly from gauge to gauge and was approximately 0.16 N at 20% applied strain. This value is small compared to the forces likely to occur in the test ligaments (Simkin (1982) estimated forces in the PA and LPL of 260 N and 62 N respectively during standing). It was concluded that implantation of LMSG's into the subject ligaments had a minimal effect on the natural mechanical properties. Force extension curves for 14 mm and 4 mm LMSG's are shown in figures A2.4 and A2.5. Note that although the LMSG output was very reproducible during loading and unloading the force/deflection plots show a large degree of hysteresis.

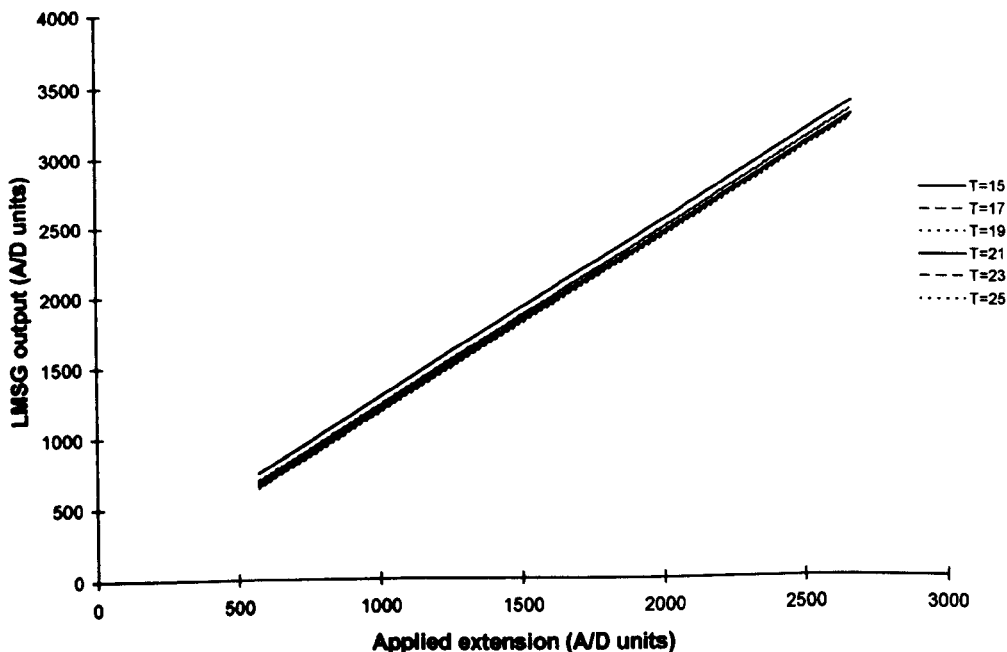


Figure A2.1 Regression lines for calibration of 14mm LMSG (No. 42) between 15°C and 25°C.

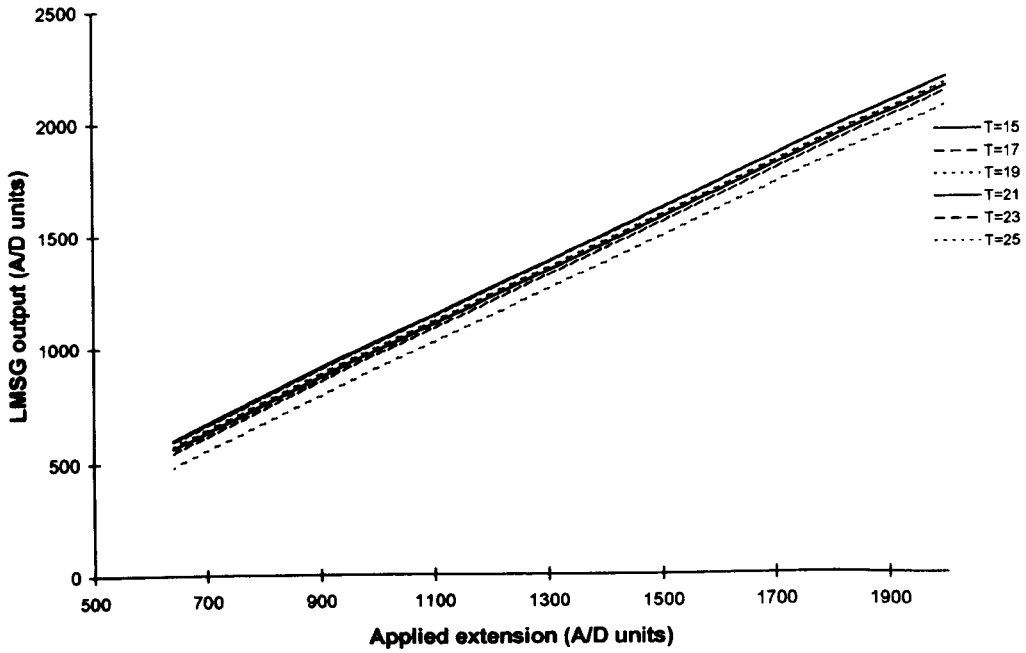


Figure A2.2 Regression lines for calibration of 9mm LMSG (No. 43) between 15°C and 25°C.

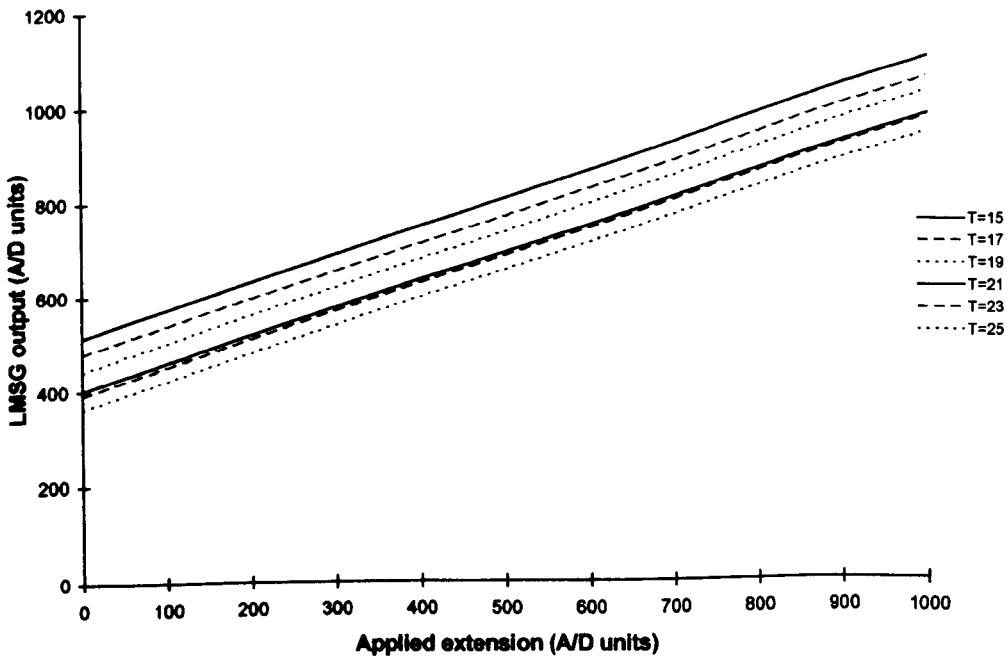
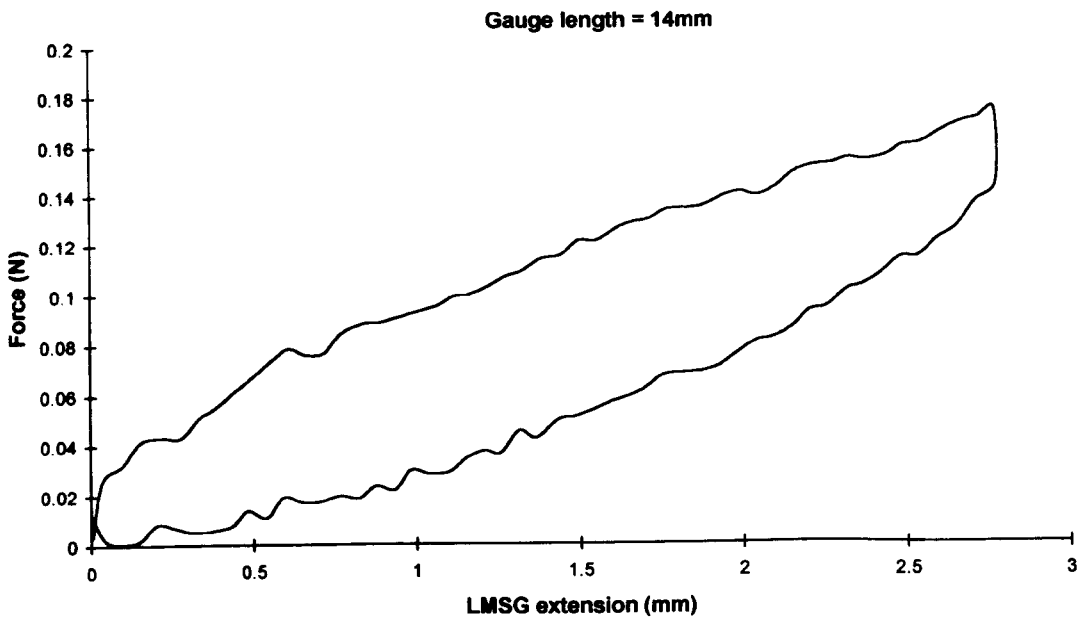
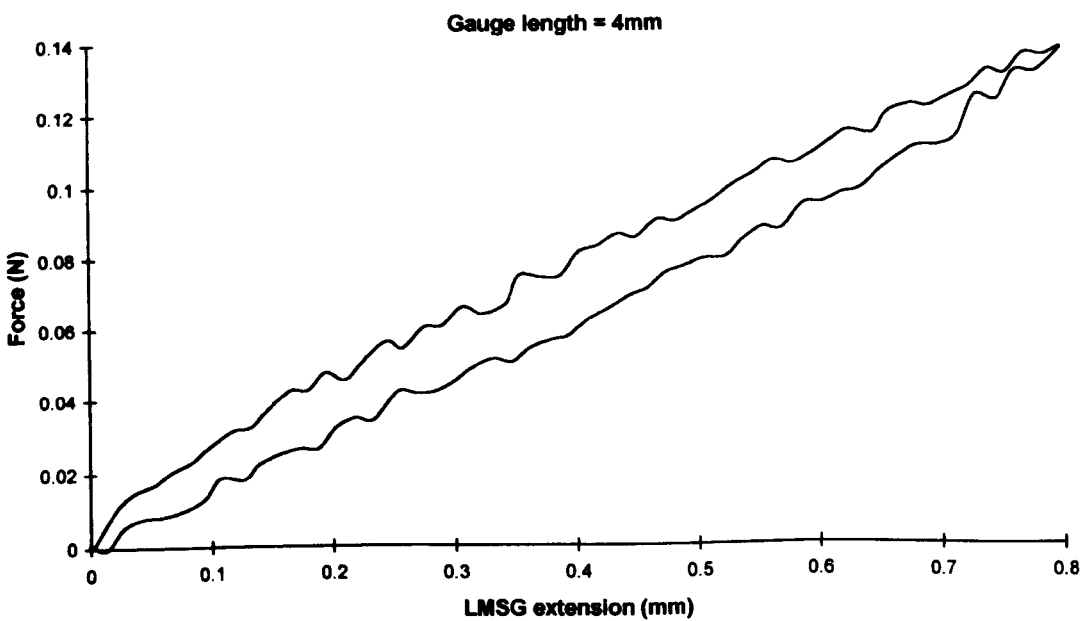


Figure A2.3 Regression lines for calibration of 6mm LMSG (No. 45) between 15°C and 25°C.



**Figure A2.4** Force extension curve for a 14mm LMSG (No.25) for one loading/unloading cycle (strain rate =  $4\%s^{-1}$ , extension rate =  $0.56\text{mm}s^{-1}$ ).



**Figure A2.5** Force extension curve for a 4mm LMSG (No.36) for one loading/unloading cycle (strain rate =  $4\%s^{-1}$ , extension rate =  $0.16\text{mm}s^{-1}$ ).

### **APPENDIX 3. LMSG PLACEMENT PARAMETERS**

The parameters used to calculate the size, position and orientation of the implanted LMSG's relative to the ligament structure were derived from observations and measurements on 3 embalmed cadaveric feet. The feet were selected from the available specimens to cover the range of sizes expected during testing, i.e., small, medium and large. The LPL, SPL and CNL were all of a similar form, i.e., approximately trapezoidal in shape, small thickness to length ratio with patch insertions. In order to aid the derivation of the placement parameters two measurement concepts were derived for the ligaments. The Mid Inter Insertion Line (MIIL) was defined as a line joining the centroids of the areas of insertion on each bone. The dominant fibre direction (DFD) at any point on the ligament was defined as the direction of the majority of ligament fibres at that point. In some ligaments the fibre direction was parallel to the edges along the ligament borders and continuously variable across the width of the ligament. This was termed 'edge variability'. In the LPL and SPL, the ligament structure was fasciculated (ligament fibres in bundles) and the MIIL and DFD were seen to correspond closely. The structure and fibre direction of the CNL and PA were more complex and were examined in more detail.

CNL and PA specimens were removed from an embalmed cadaveric specimen and dissected in layers to examine the fibre direction through the thickness of the ligaments. Photographs were taken at regular intervals. On inspection of the plantar structure of the CNL a 'rising sun' pattern of fibres emanating from the proximal/medial corner was seen. The medial portion of the ligament was fibro-cartilagenous with faint fibres running as described above. On dissection it was found that the lateral portion was more fasciculated with the DFD approximately parallel to the MIIL (fig A3.1).

The PA fibre direction was assessed along the length from the proximal insertion to where it divided into the toe slips (Note: The length of the PA from the insertion to where the toe slips started was called the 'Solid Length'). The orientation of the fibres in the mid solid length were angled to the longitudinal axis of the foot at approximately 10° running slightly laterally when moving distally. At the distal end the fibres diverge into the toe slips and also slight divergence was noticed in the region of the calcaneal insertion (fig A3.2).

The ligament fibre direction was constant through the thickness, the toe slips becoming more pronounced towards the superior surface of the ligament. It was required that the placement parameters specified the length of the transducer (relative to the ligament dimensions), position of placement on ligament (relative to insertions) and orientation (along MIIL or DFD). It was necessary to manufacture the LMSG's before the tests, hence, the size of the transducer was the most approximate of the three criteria. Approximate sizes of gauges used were derived from the average measurements of the MIIL or solid length of the ligaments. Each ligament was measured before final selection of the gauge size to be used during testing.

### **LPL:**

- Size:** Approximately 50% of MIIL (Mean MIIL = 40 mm, gauge size  $\approx$  20 mm)
- Orientation:** Along the MIIL or its closest approximating DFD
- Position:** Along MIIL, or DFD, at mid free section, i.e. between ends of insertion patches.

### **SPL:**

- Size:** Approximately 75% of MIIL (Mean MIIL = 18 mm, gauge size = 13 mm)
- Orientation:** Along MIIL or its closest approximating DFD
- Position:** Along MIIL, or DFD at mid MIIL.

### **CNL:**

Because of the irregularities in the fibre structure of the CNL it was decided to implant the LMSG for this ligament relative to the insertion sites, i.e., the MIIL. It was felt that this arrangement would be more repeatable than implanting relative to fibre direction. A small LMSG had to be used due to the size of the CNL hence the gauge length to ligament length was increased.

- Size:** Approximately 85% of MIIL (Mean MIIL = 12 mm, gauge size = 10 mm)
- Orientation:** Along the MIIL
- Position:** Along MIIL at mid-MIIL.

### **PA:**

Since the PA was not fully exposed during LMSG implantation the placement positions had to be derived from measurements of the whole foot. It was found that the solid length of the PA was approximately 0.34 X's the length of the foot and the calcaneal insertion was located approximately 45 mm from the nearest point of the heel.

- Size:** Approximately 20% of solid length (Mean MIIL = 84 mm, gauge size = 18 mm)
- Orientation:** Along the apex and mid-line of the PA, or its closest approximately DFD
- Position:** Along the axis described above, equi-spaced along the solid length as shown in figure A3.2.

**NOTE:** The positions of the PA gauges were located in the region of the arch of the footprint and thus were not adversely affected during weight bearing. The edges of the PA were located during implantation by dissection subcutaneously to either side of the window in the fascia. The centre of the PA could then be found.

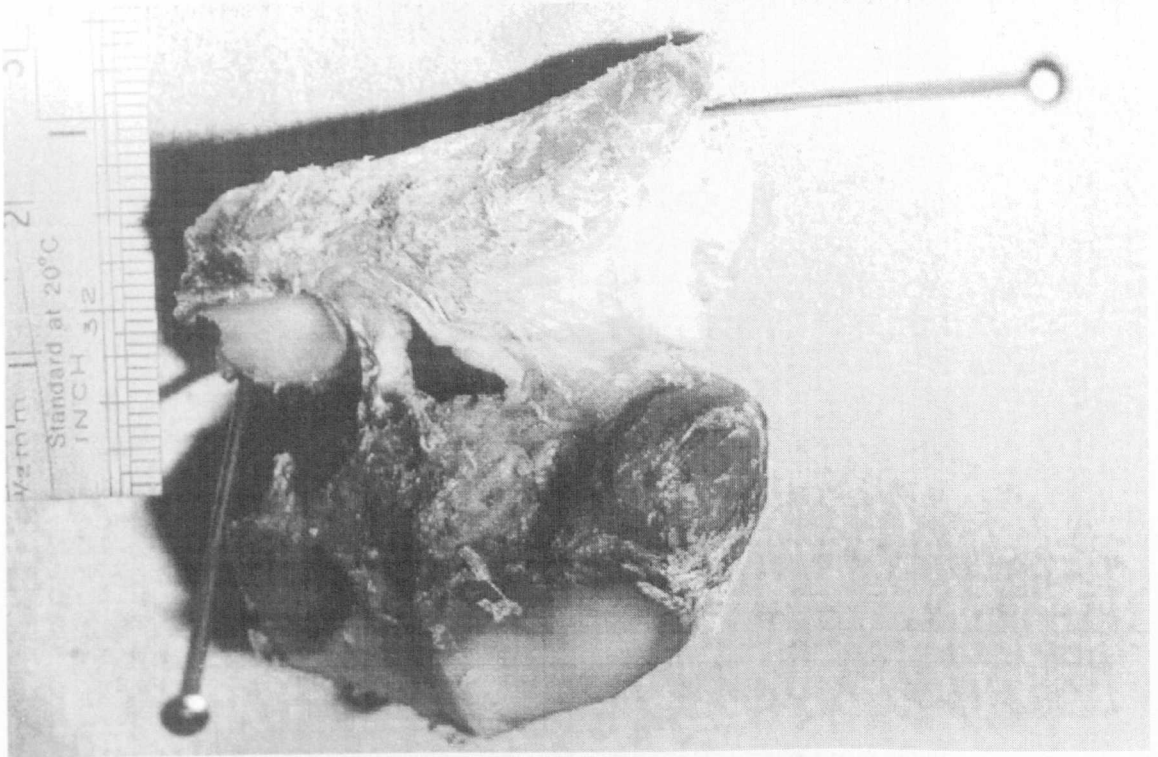


Figure A3.1 Dissected CNL specimen. A separate lateral division can be seen on the left of the picture. In the main part of the ligament the structure becomes progressively more fibrous towards the medial border (on the right of the picture).

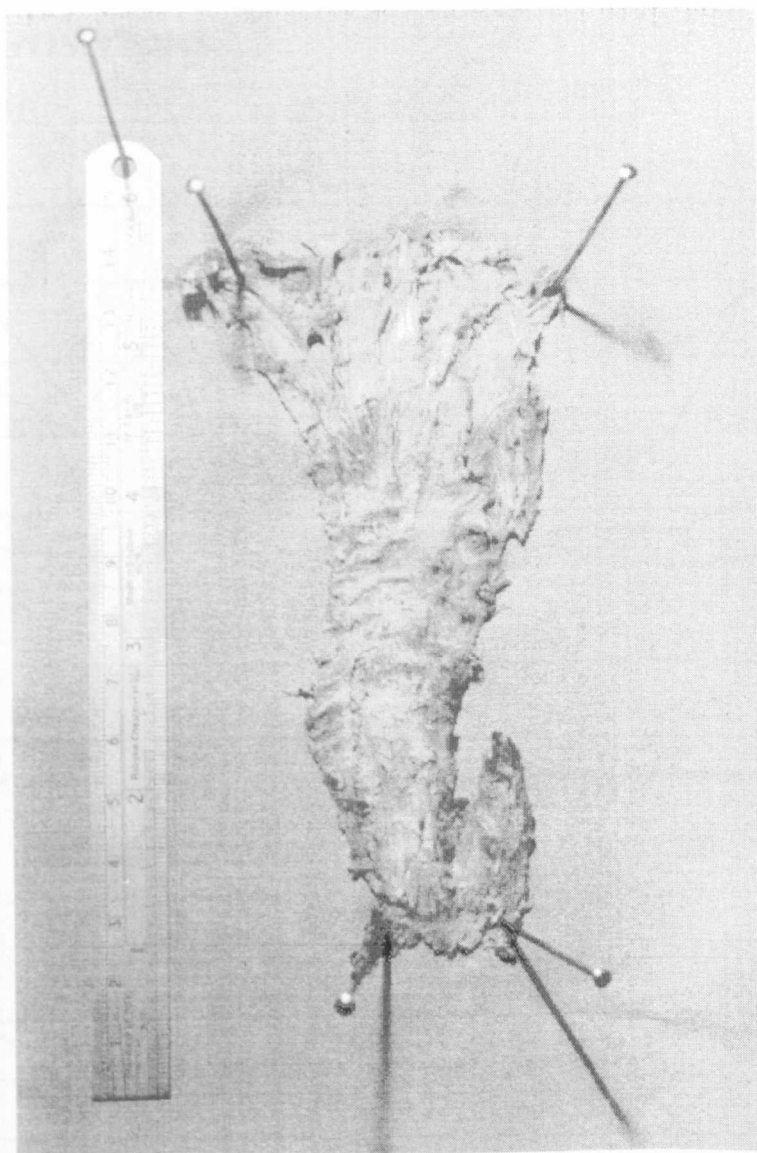


Figure A3.2 Dissected PA specimen. The fibre direction was confirmed as being constant through the thickness of the ligament. The divergence of the distal fibres into the separate toe slips can be seen at the top of the picture.

# APPENDIX 4. LIGAMENT STRAIN DATA FOR INTACT FOOT TESTS

## A4.1 FOOT POSITIONS

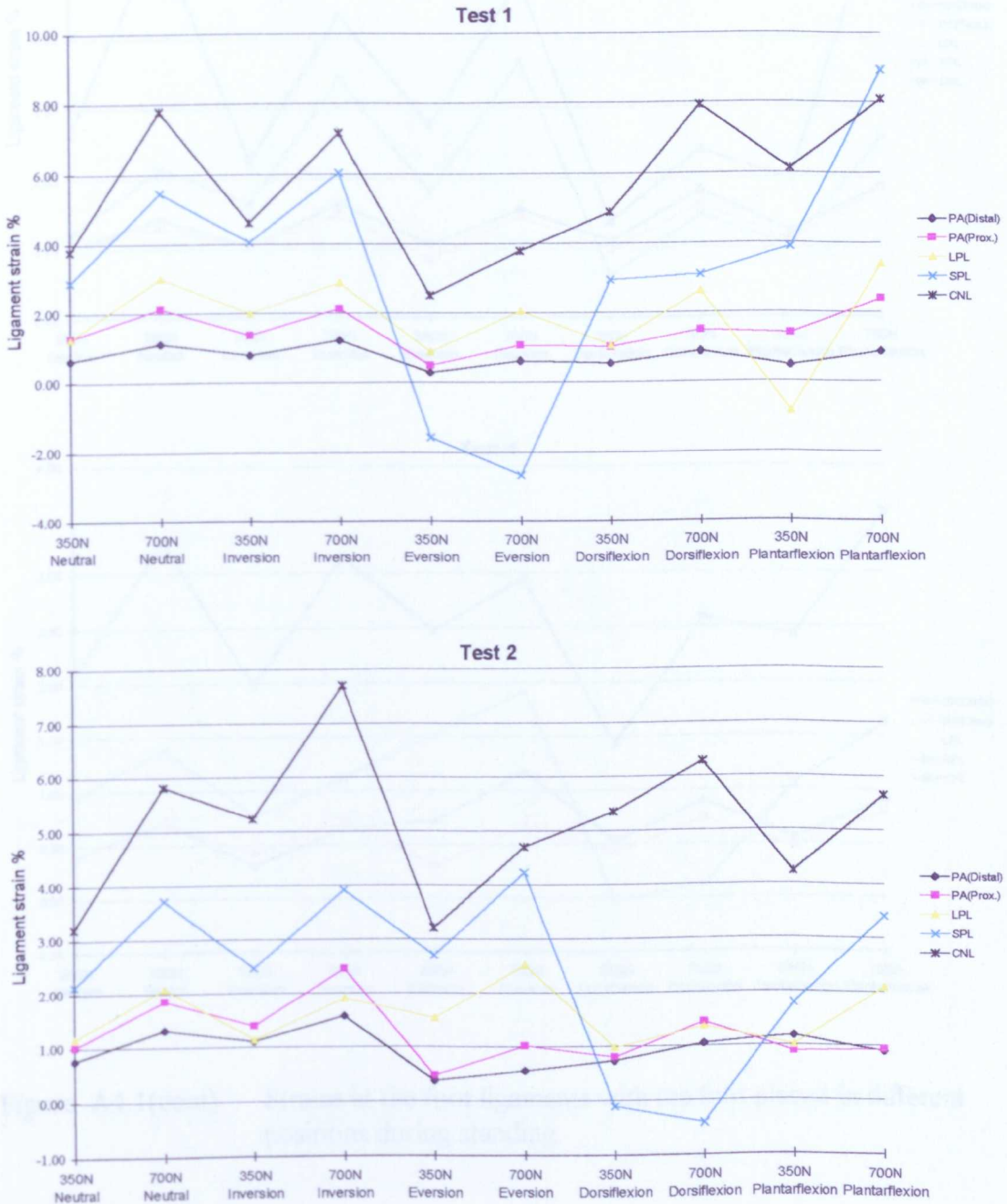


Figure A4.1 Strains in the foot ligaments with the foot placed in different positions during standing.

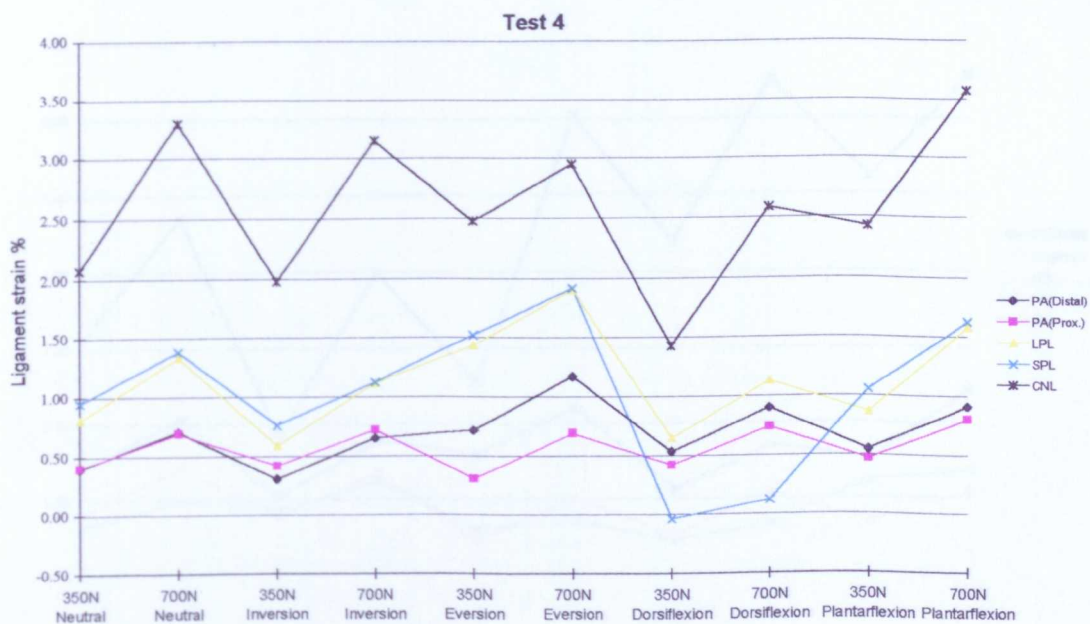
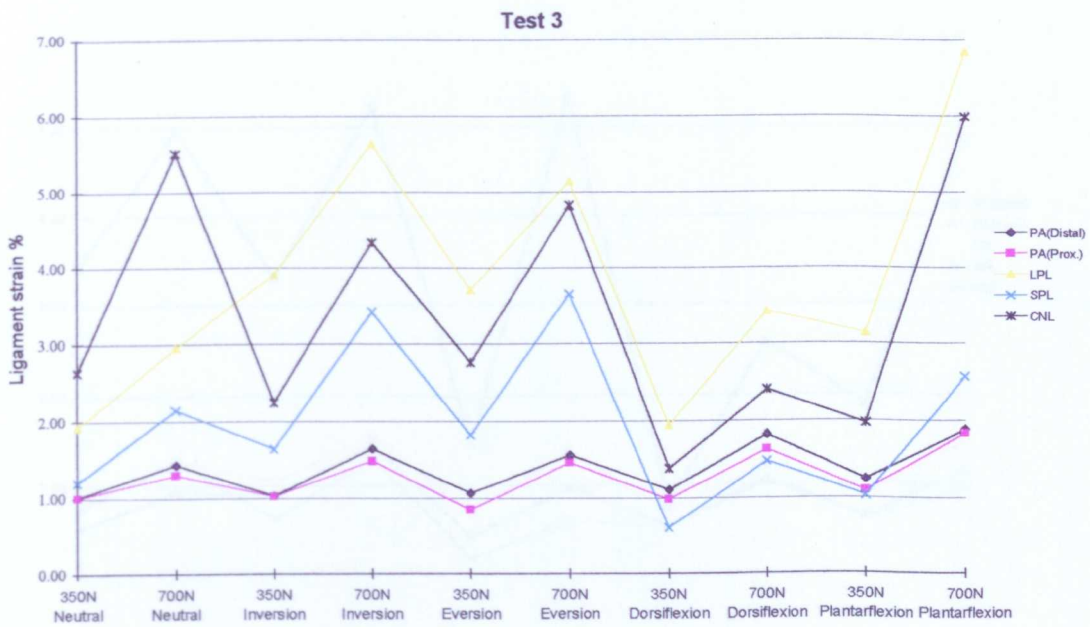


Figure A4.1(cont) Strains in the foot ligaments with the foot placed in different positions during standing.

# A4.2 TIBIAL TORSION

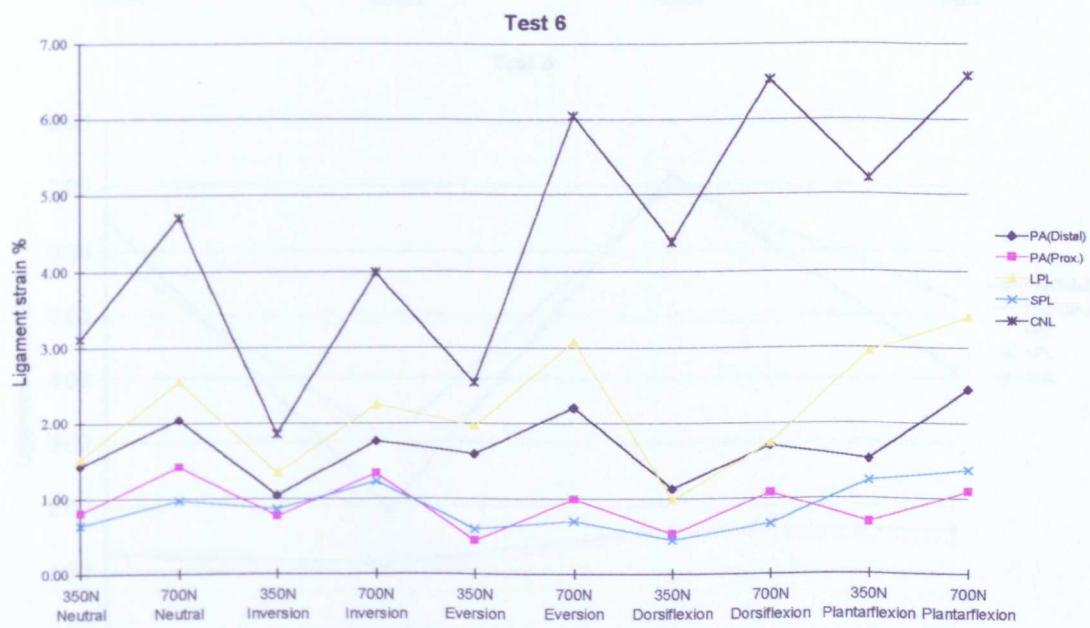
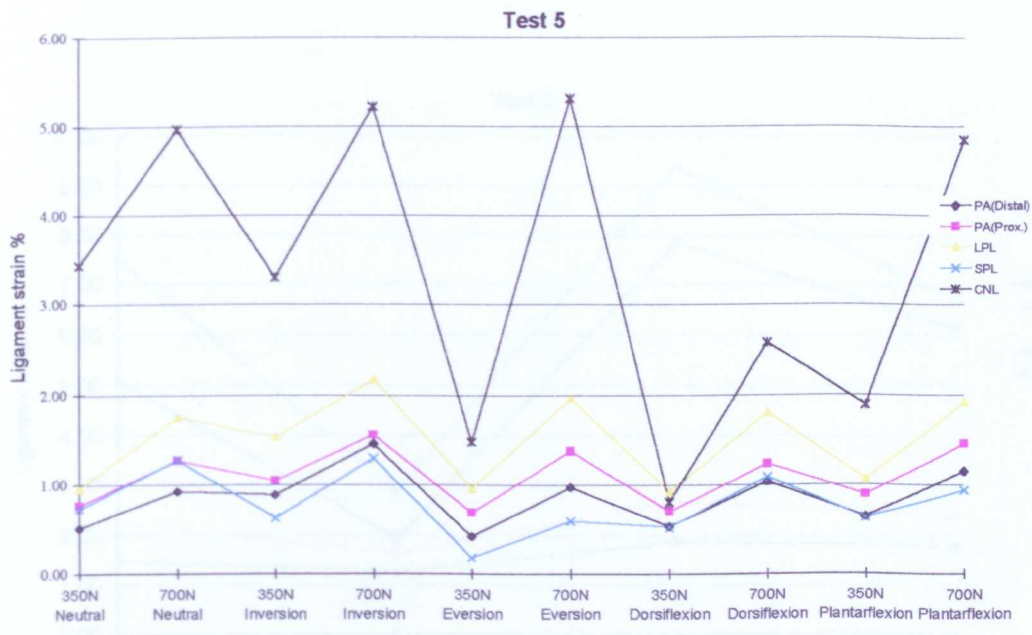


Figure A4.1(cont) Strains in the foot ligaments with the foot placed in different positions during standing.

## A4.2 TIBIAL TORSION

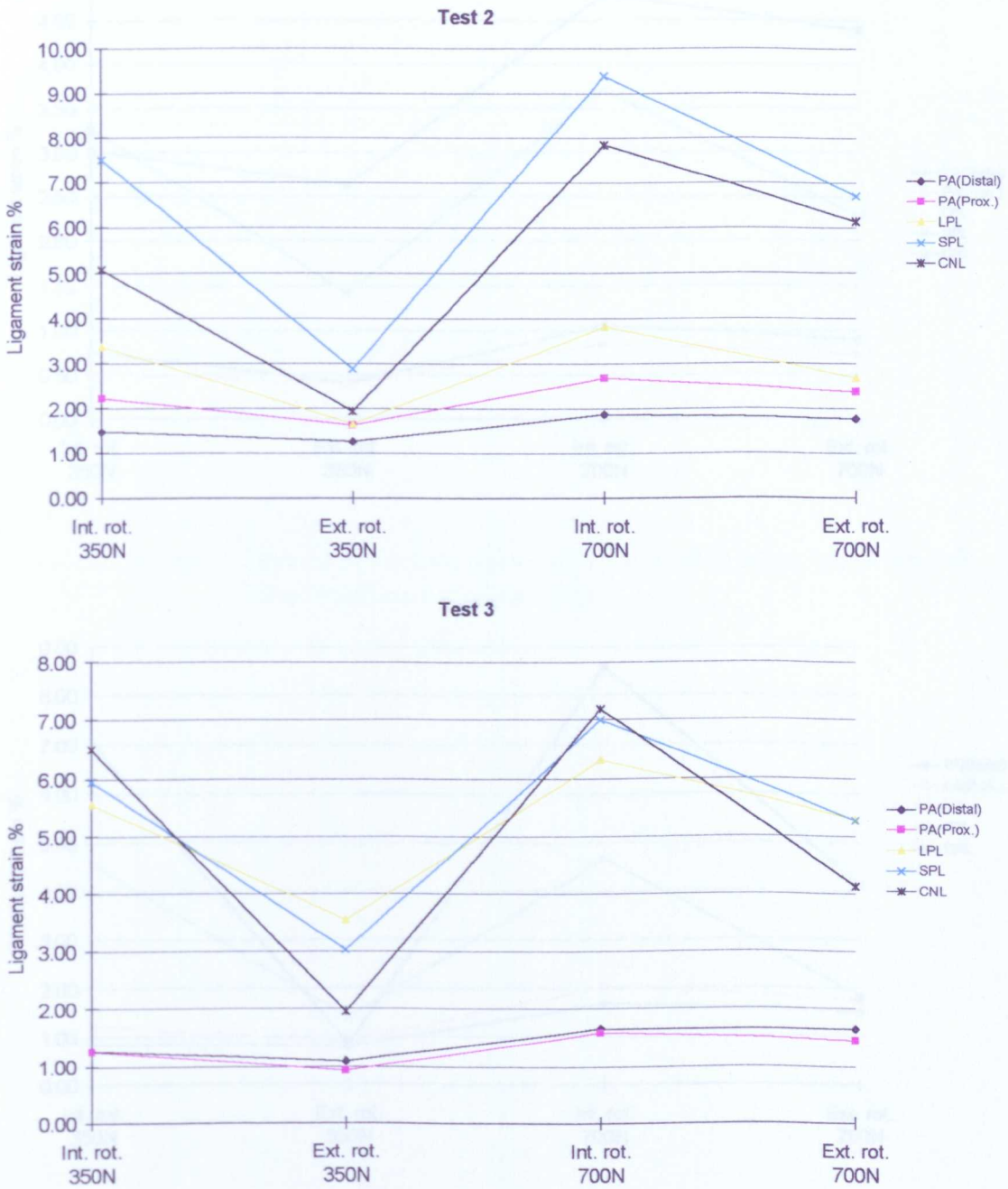


Figure A4.2 Strains in the foot ligaments with the foot subjected to applied tibial rotation during standing.

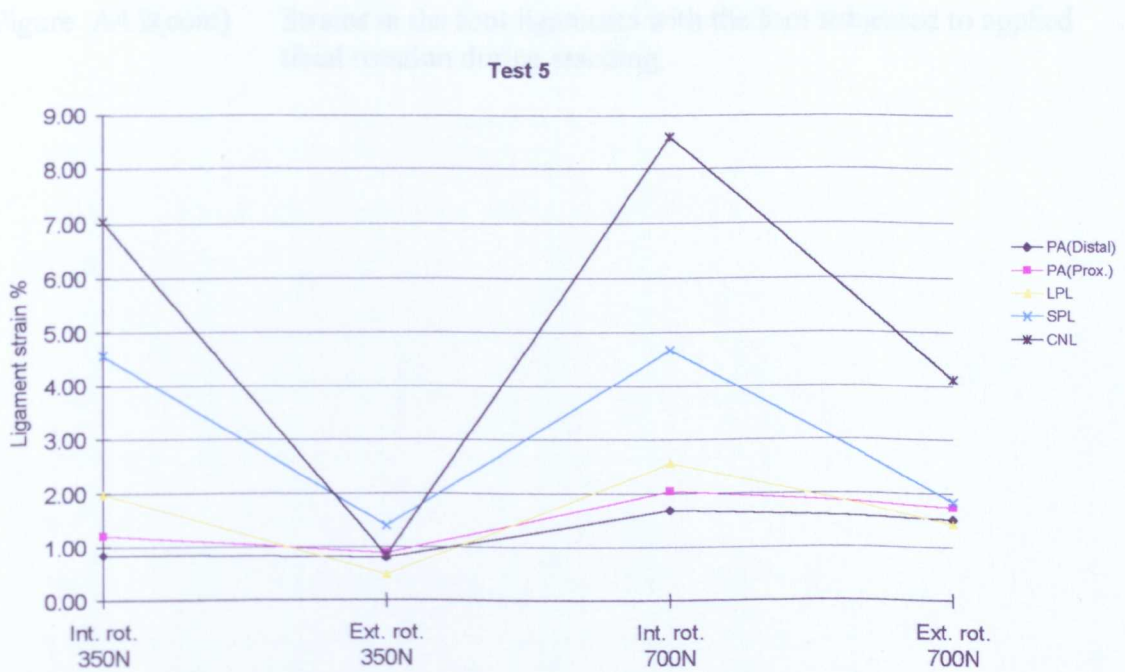
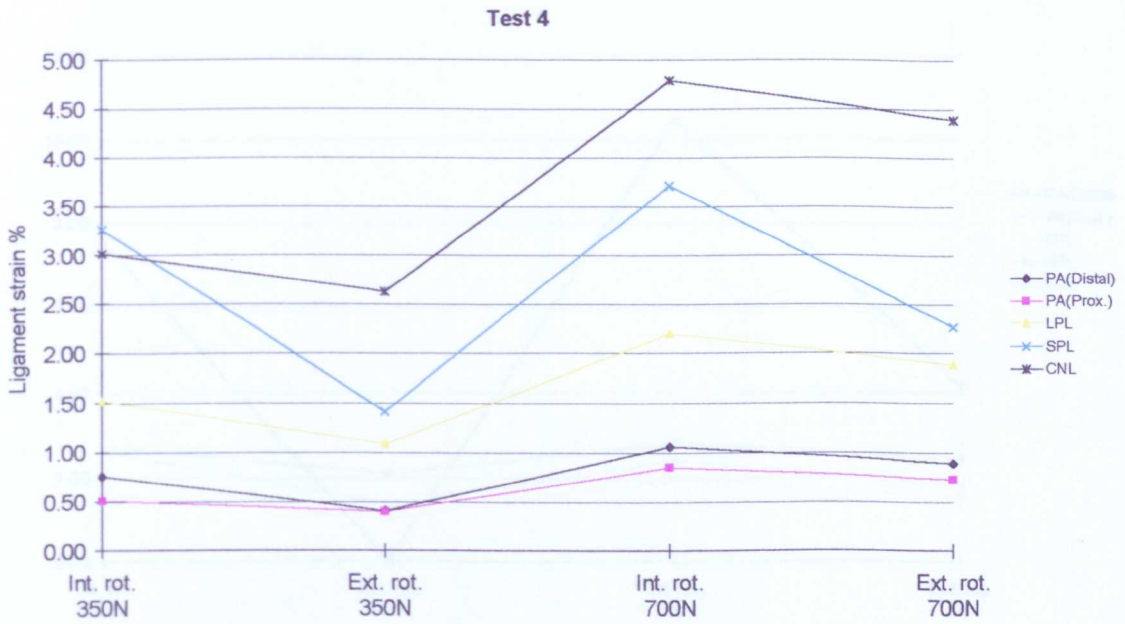


Figure A4.2(cont) Strains in the foot ligaments with the foot subjected to applied tibial rotation during standing.

4.3 MUSCLE FORCES

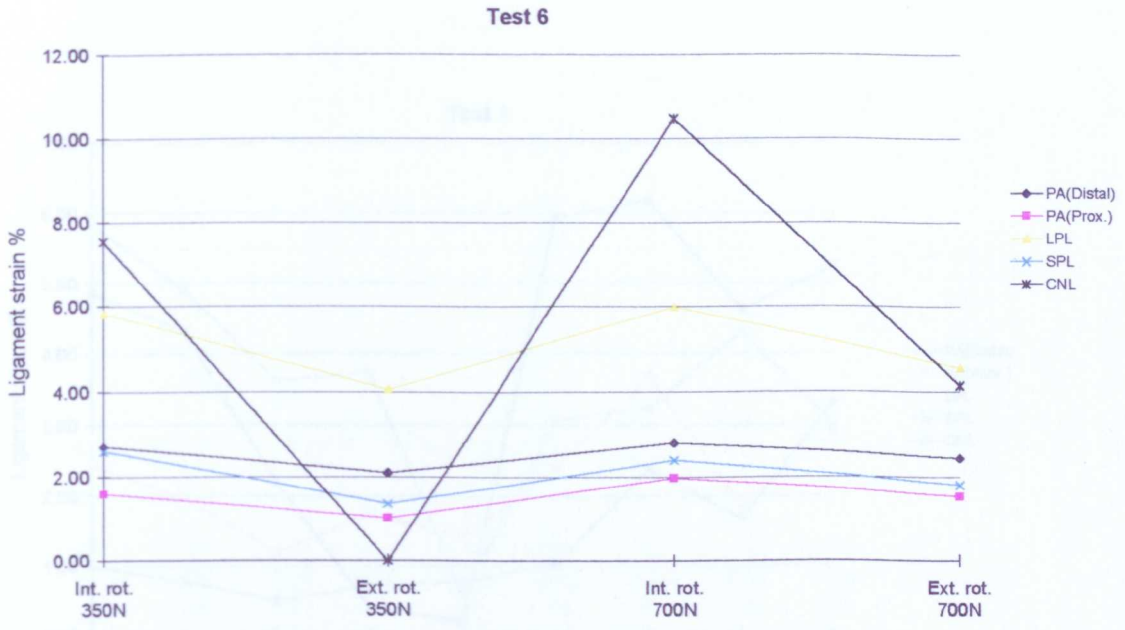


Figure A4.2(cont) Strains in the foot ligaments with the foot subjected to applied tibial rotation during standing.



Figure A4.3 Strains in the foot ligaments with applied dynamic muscle forces during standing.

### A4.3 MUSCLE FORCES

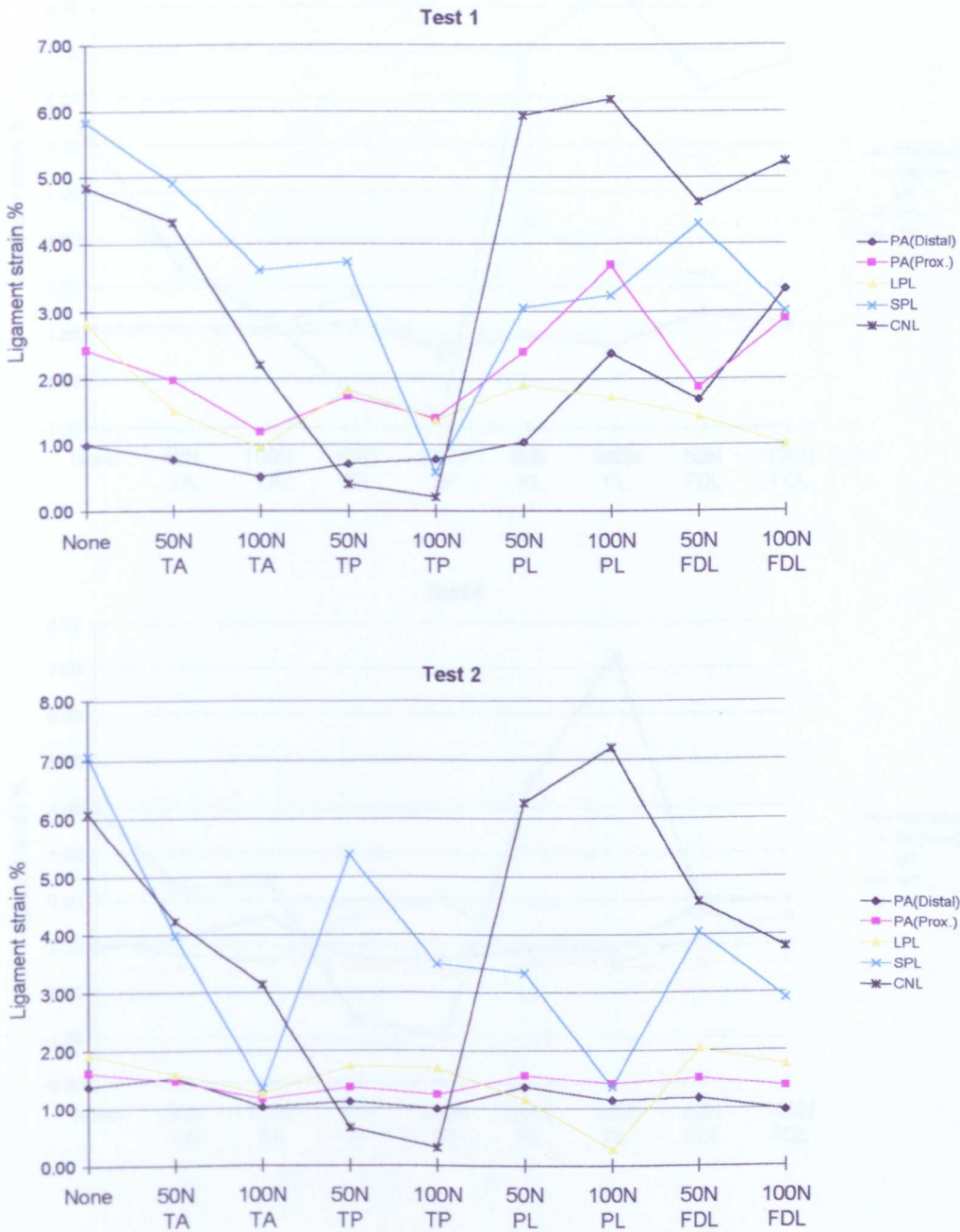


Figure A4.3 Strains in the foot ligaments with applied extrinsic muscle forces during standing.

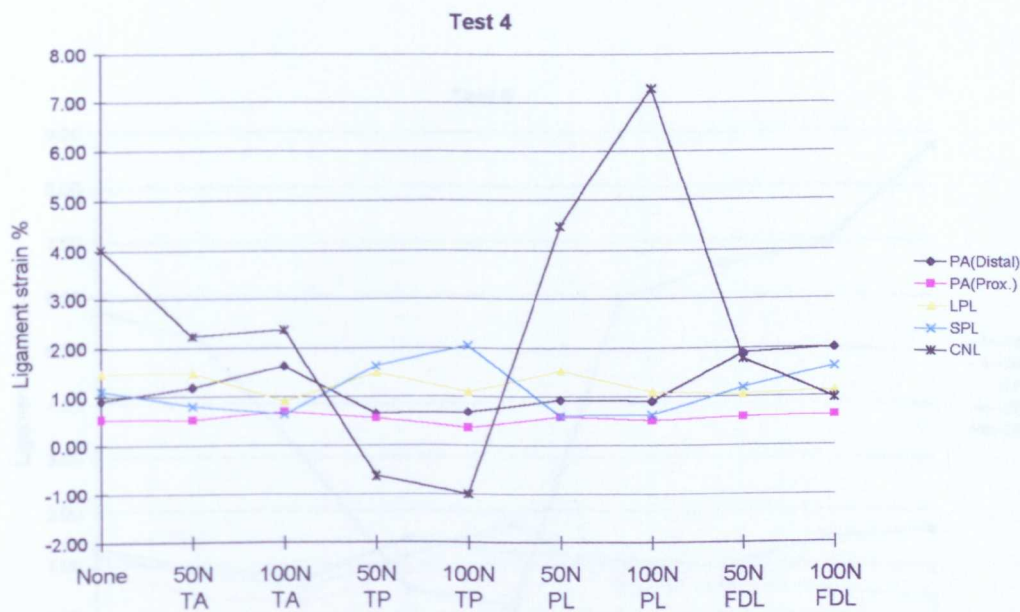
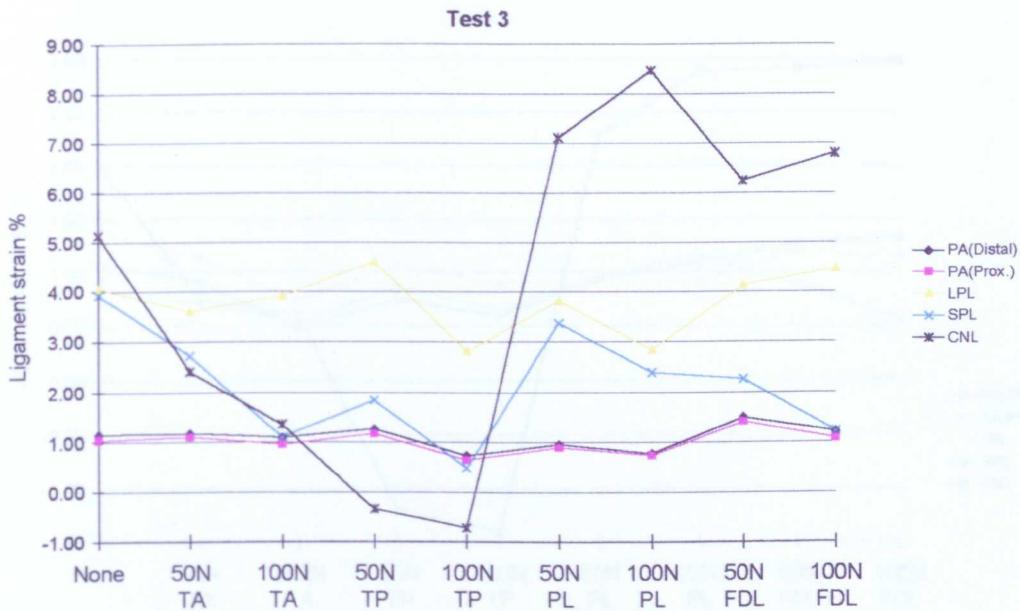


Figure A4.3(cont) Strains in the foot ligaments with applied extrinsic muscle forces during standing.

# ALL TOE EXTENSION

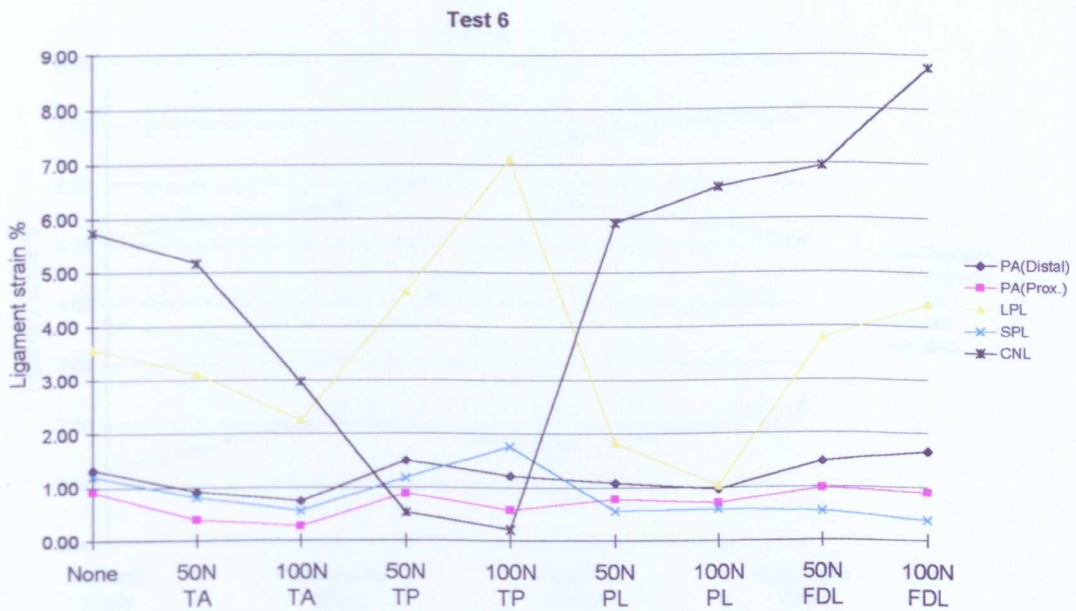
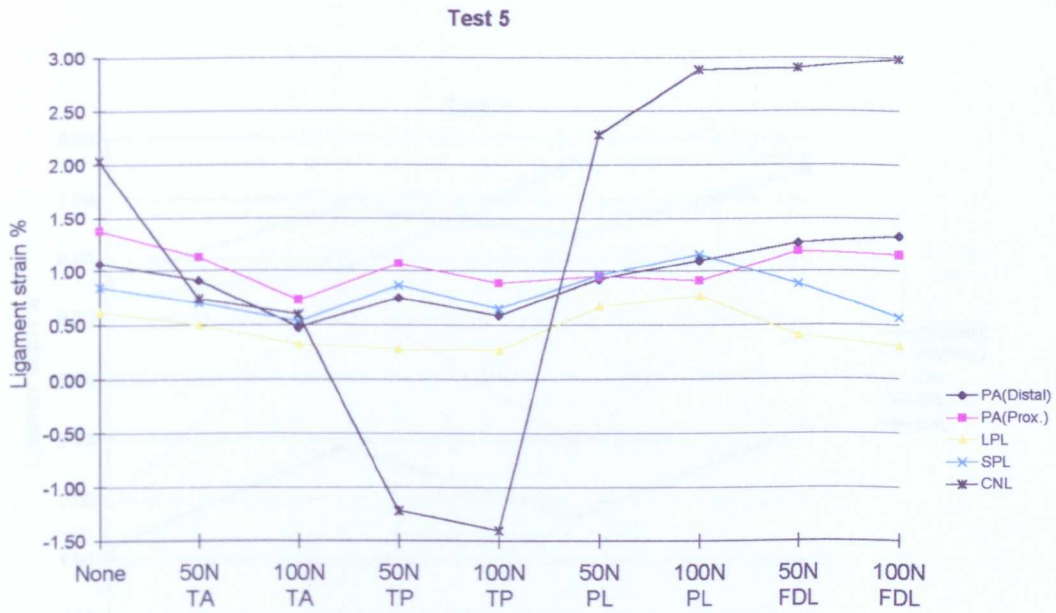


Figure A4.3(cont) Strains in the foot ligaments with applied extrinsic muscle forces during standing.

## A4.4 TOE EXTENSION

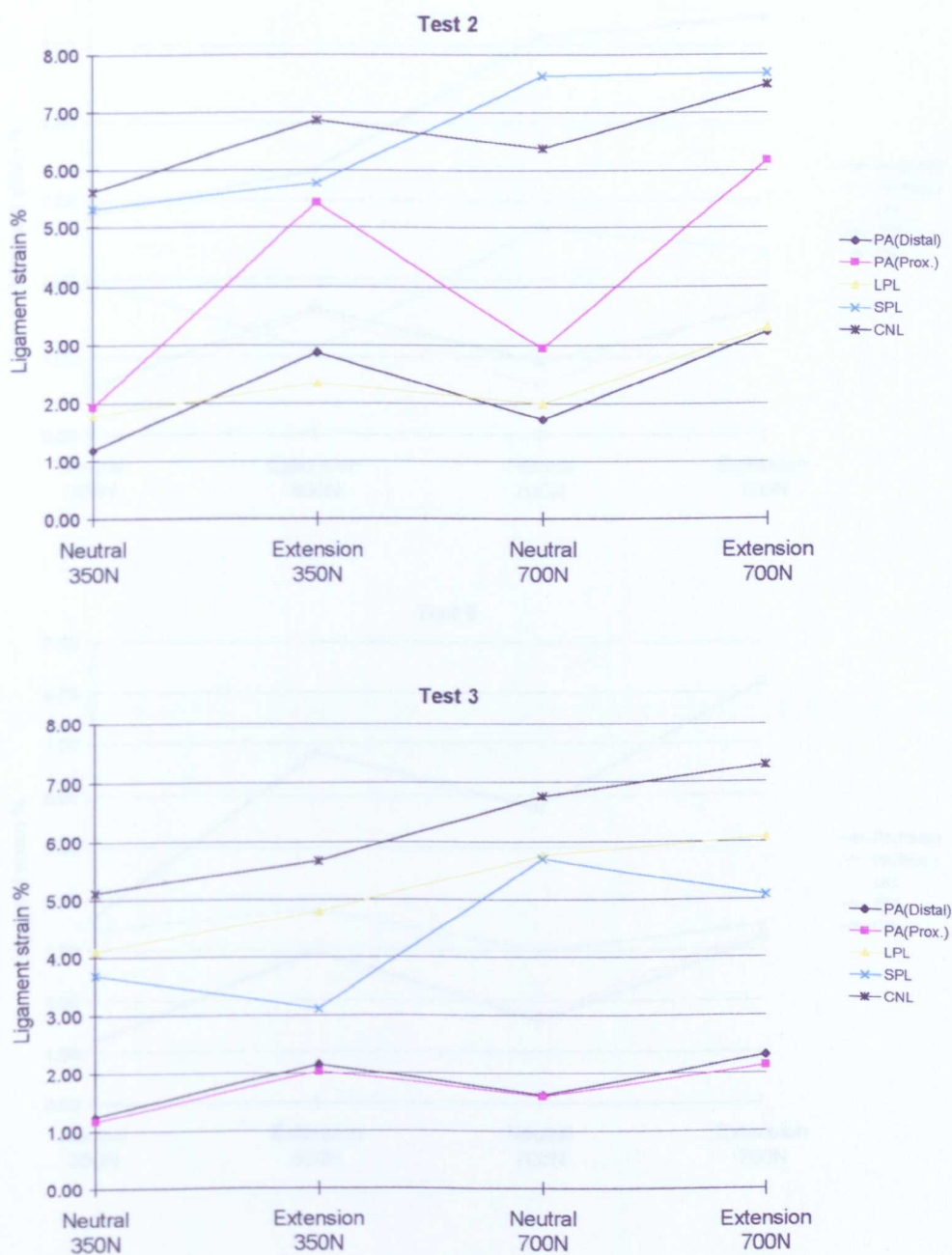


Figure A4.4 (cont) Strains in the foot ligaments with the foot subjected to toe extension during standing.

Figure A4.4 Strains in the foot ligaments with the foot subjected to toe extension during standing.

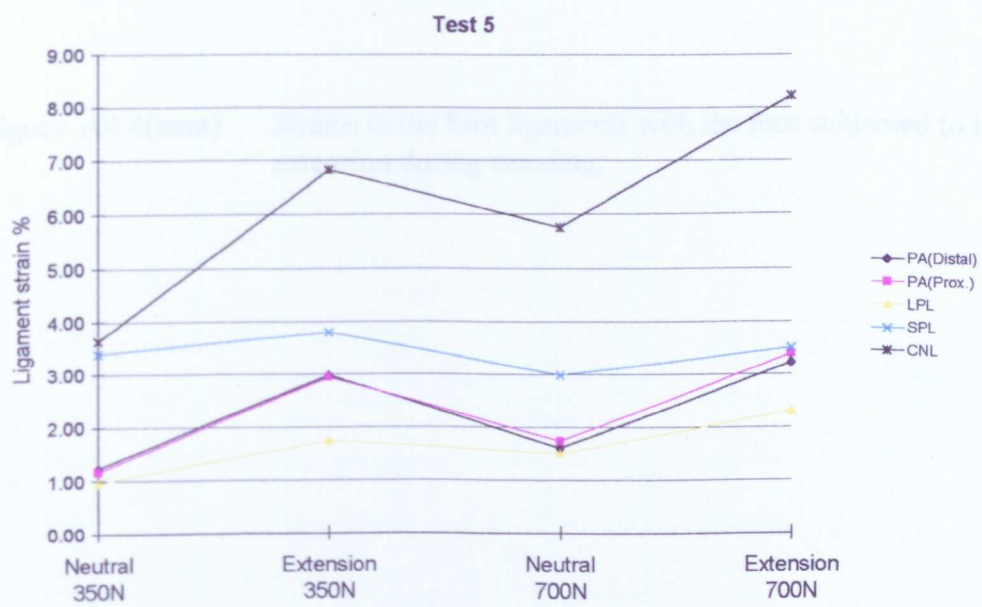
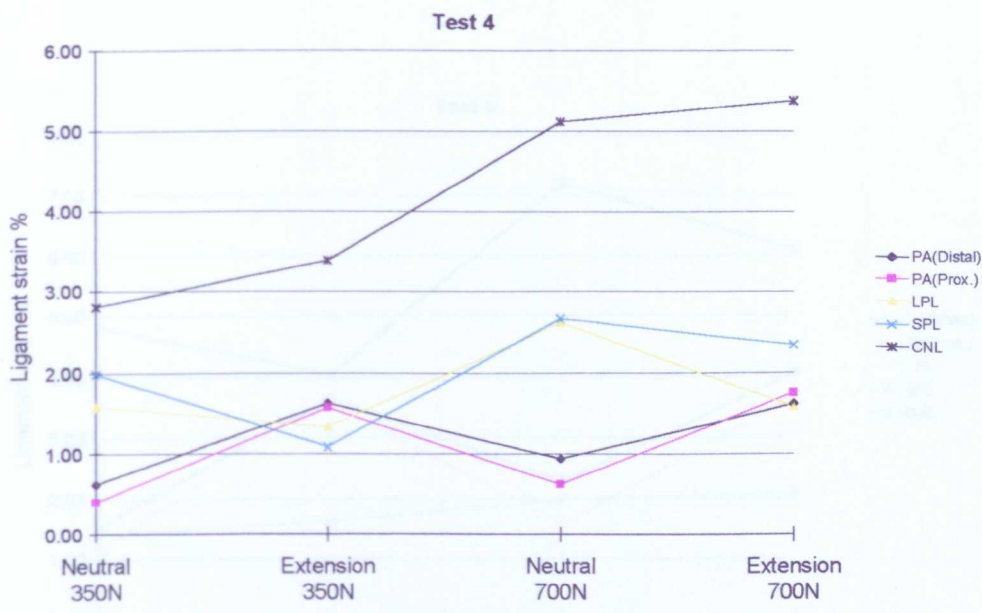


Figure A4.4(cont) Strains in the foot ligaments with the foot subjected to toe extension during standing.

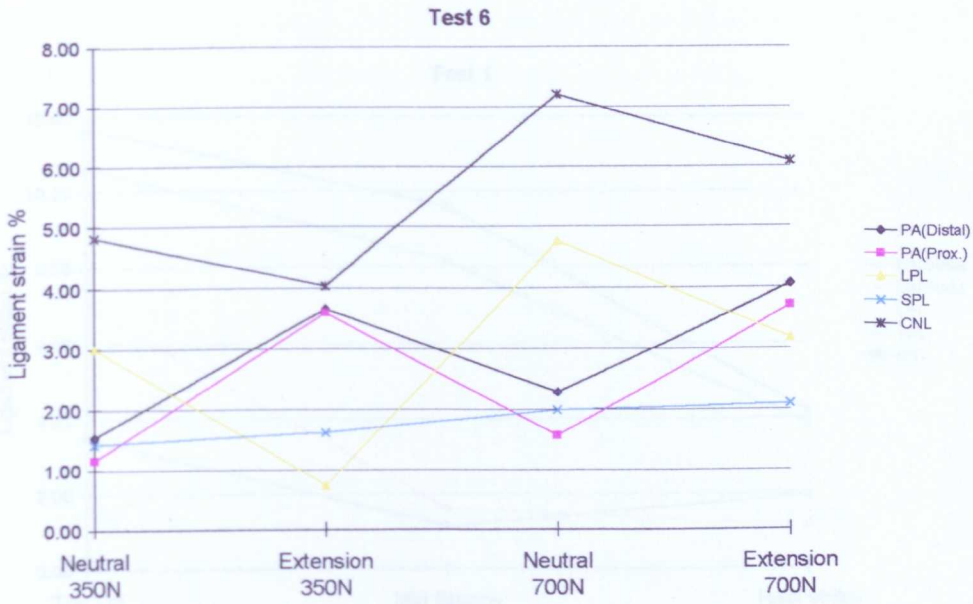


Figure A4.4(cont) Strains in the foot ligaments with the foot subjected to toe extension during standing.



Figure A4.5 Strains in the foot ligaments during 3 stages of simulated gait.

## A4.5 GAIT

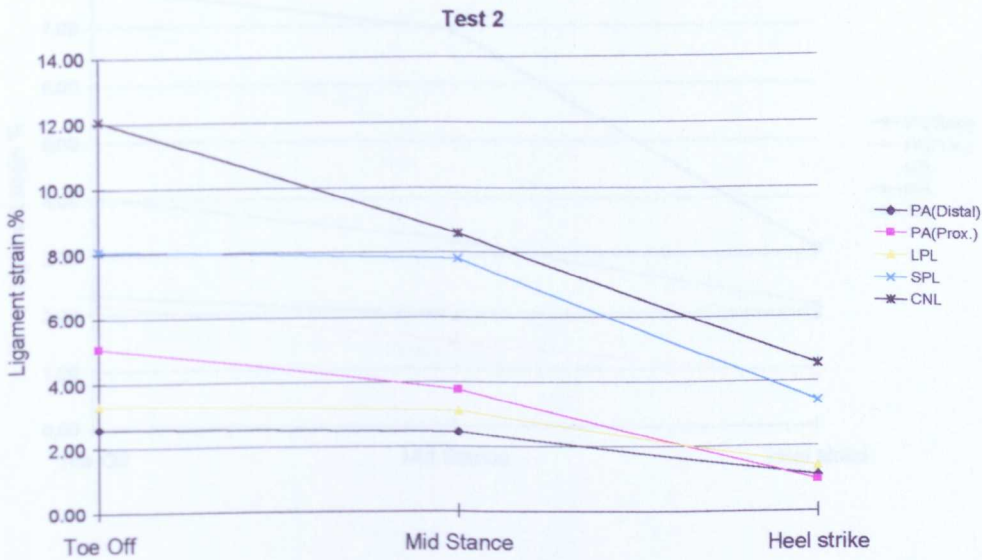
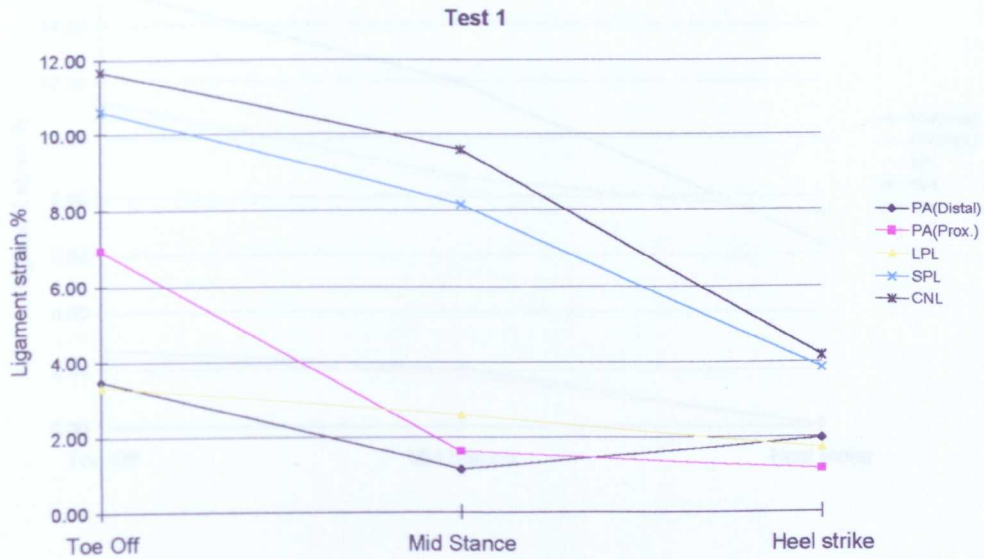


Figure A4.5(a) Strains in the foot ligaments during 3 stages of simulated gait.

Figure A4.5 Strains in the foot ligaments during 3 stages of simulated gait.

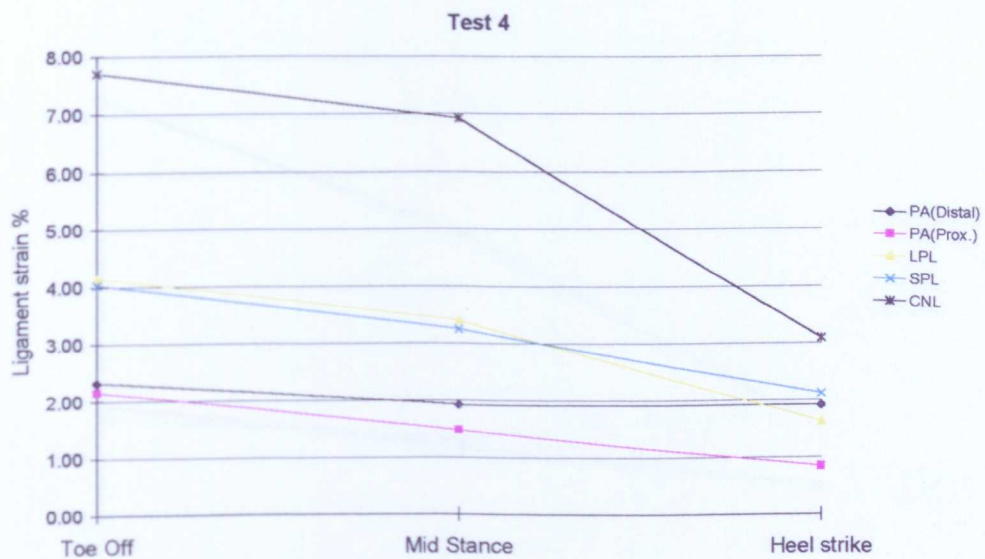
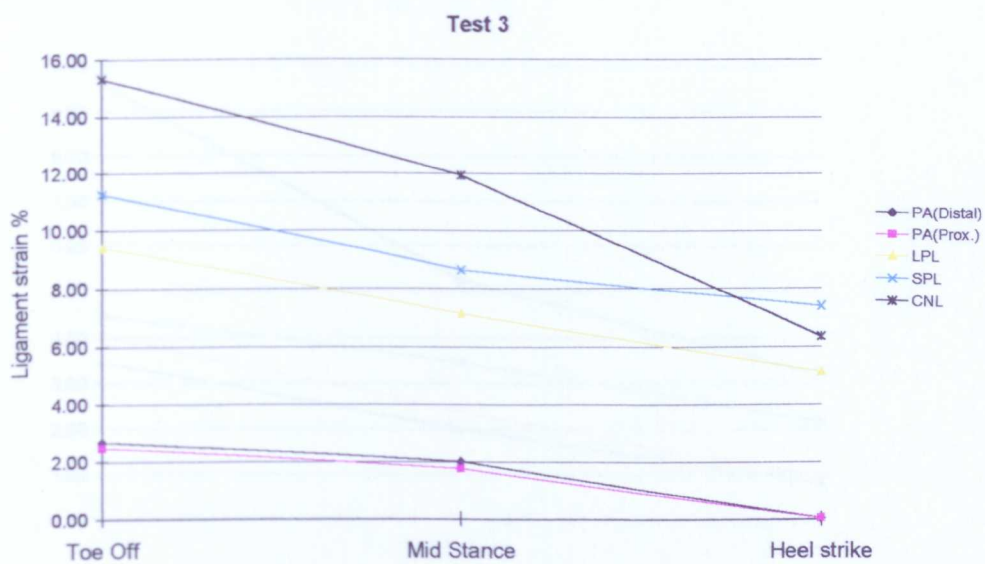
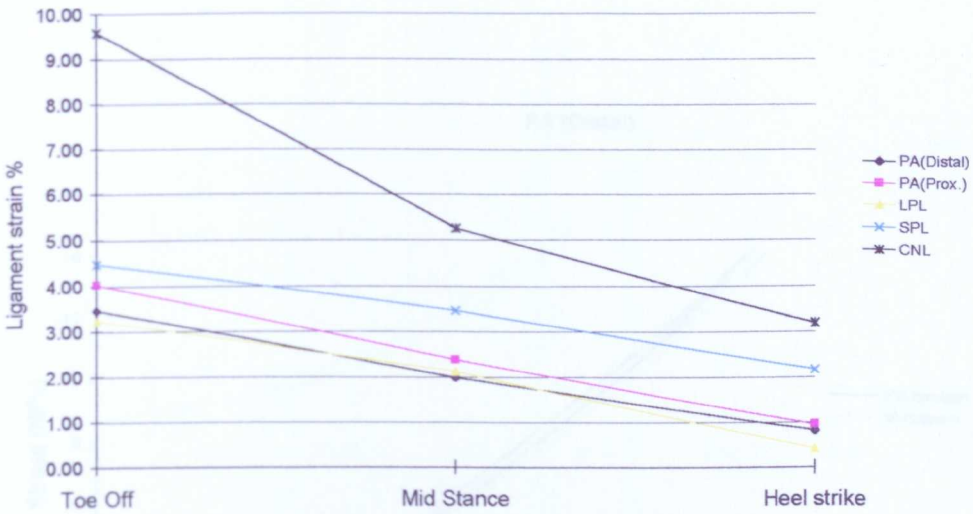


Figure A4.5(cont) Strains in the foot ligaments during 3 stages of simulated gait.

A4.5 STRESS-STRAIN RESULTS

Test 5



Test 6

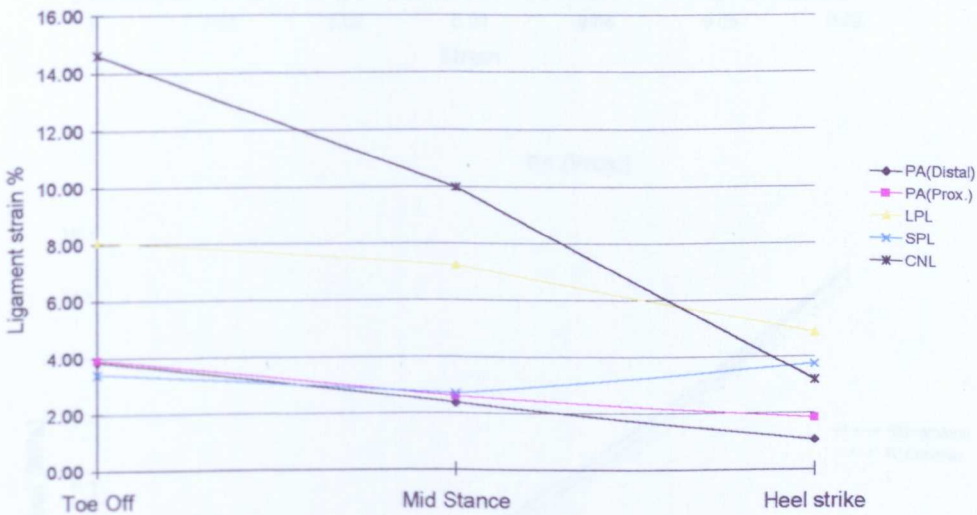


Figure A4.5(cont) Strains in the foot ligaments during 3 stages of simulated gait.

Figure A4.1 Stress-strain relationships in the foot ligaments (specimen 1311).

# APPENDIX 5. STRESS-STRAIN AND LOAD-STRAIN RELATIONSHIPS IN THE FOOT LIGAMENTS

## A5.1 STRESS-STRAIN RESULTS

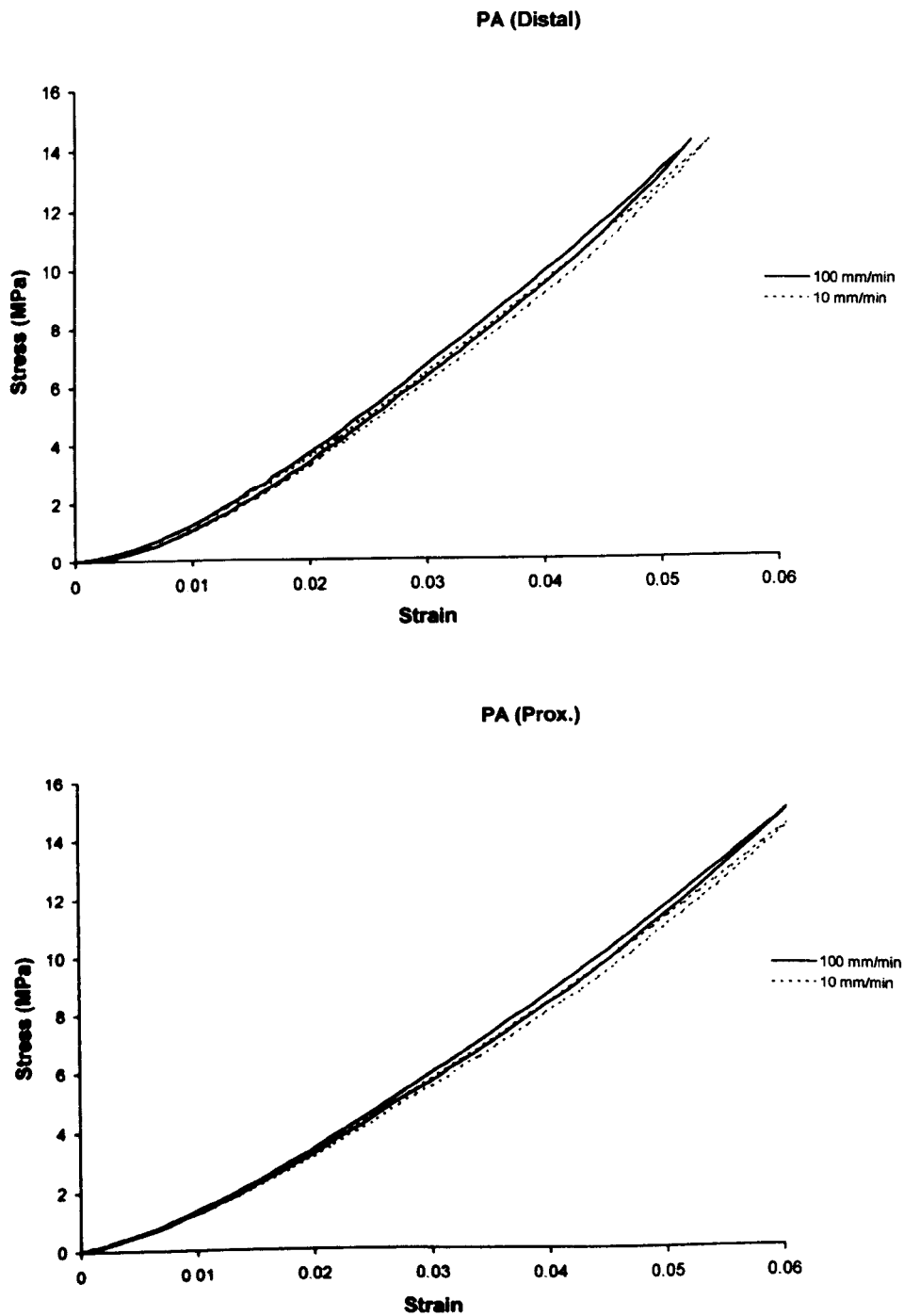


Figure A5.1 Stress-strain relationships in the foot ligaments (specimen 131L).

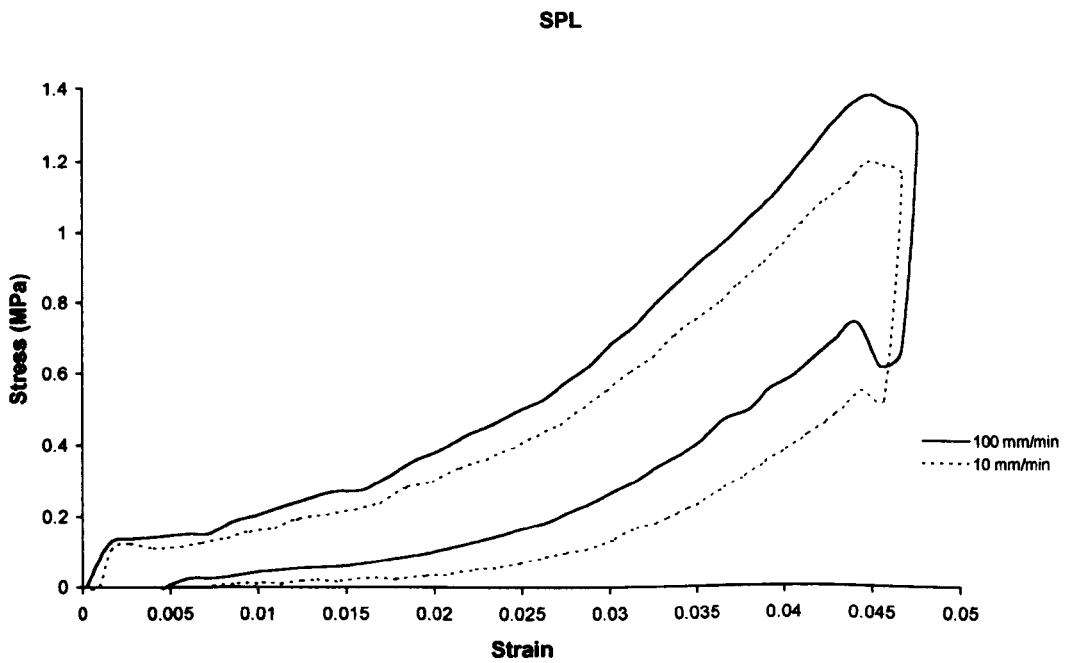
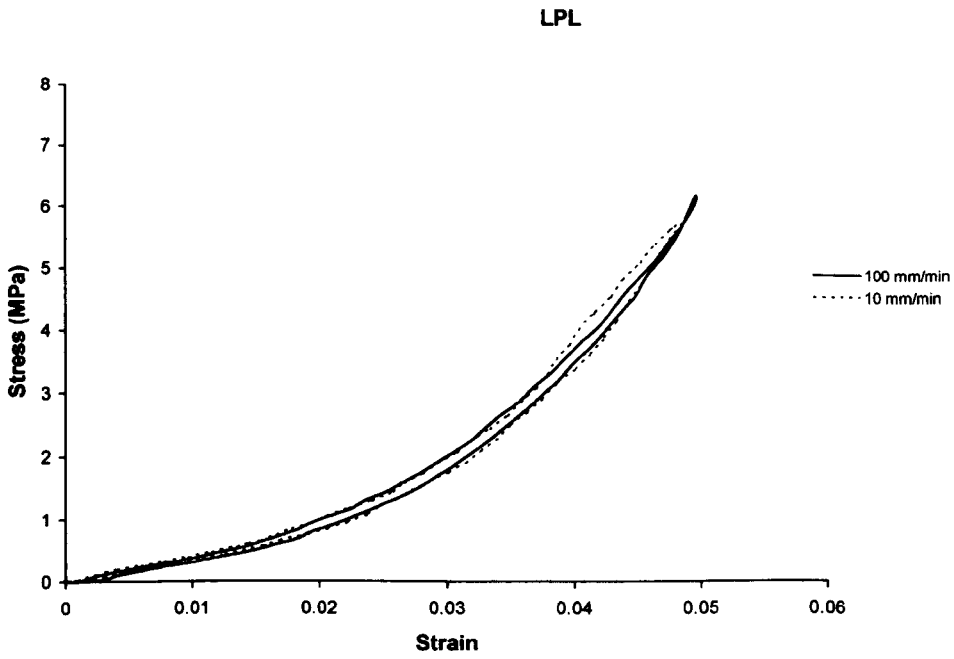


Figure A5.1(cont.) Stress-strain relationships in the foot ligaments (specimen 131L).

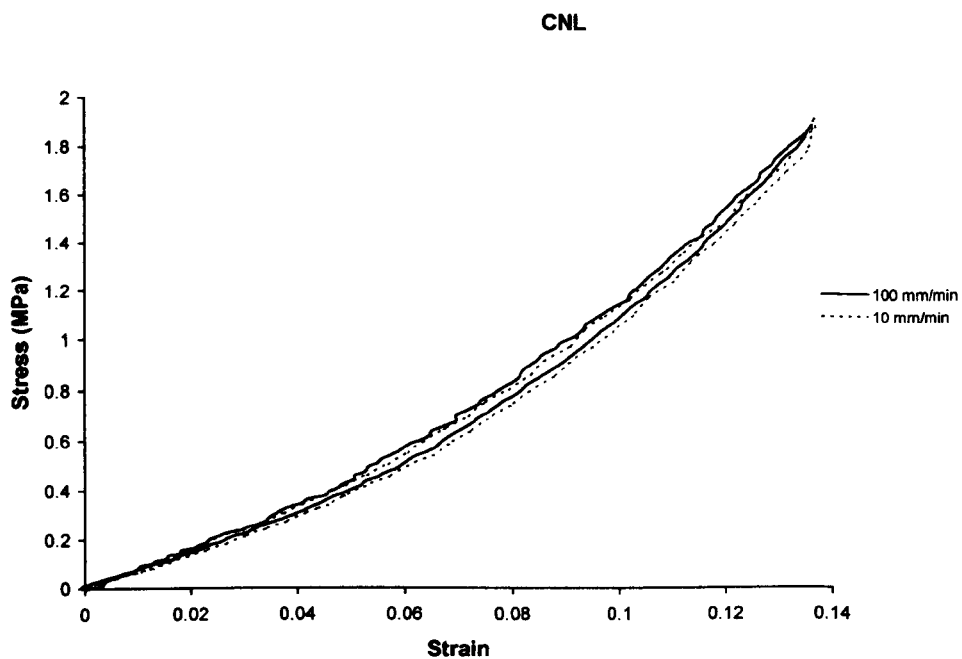


Figure A5.1(cont.) Stress-strain relationships in the foot ligaments (specimen 131L).

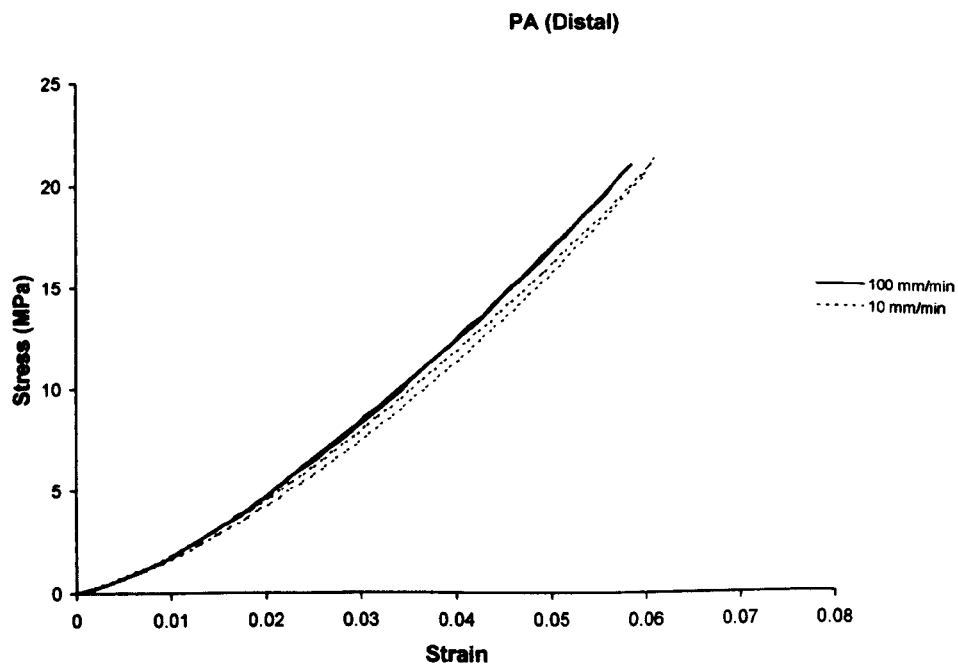
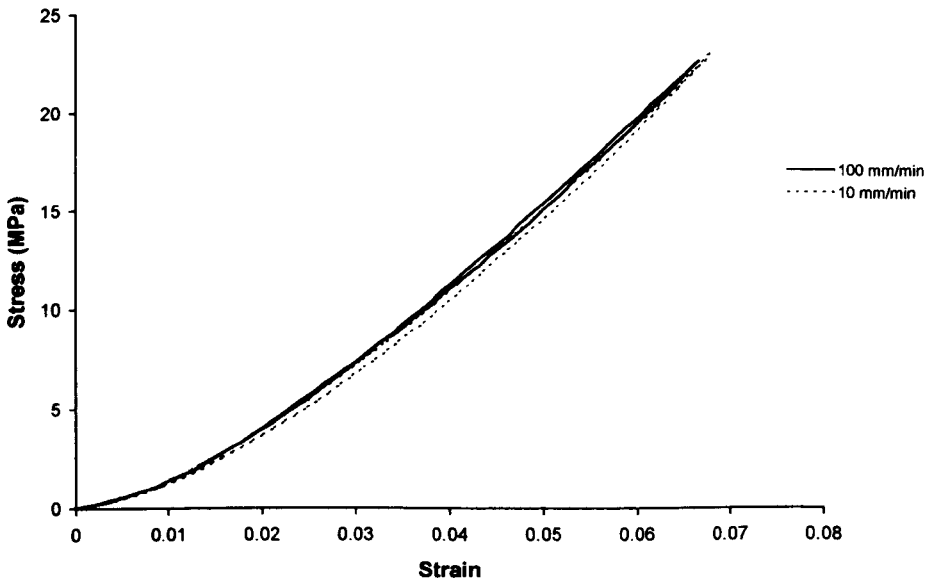


Figure A5.2 Stress-strain relationships in the foot ligaments (specimen 107R).

PA (Prox.)



LPL

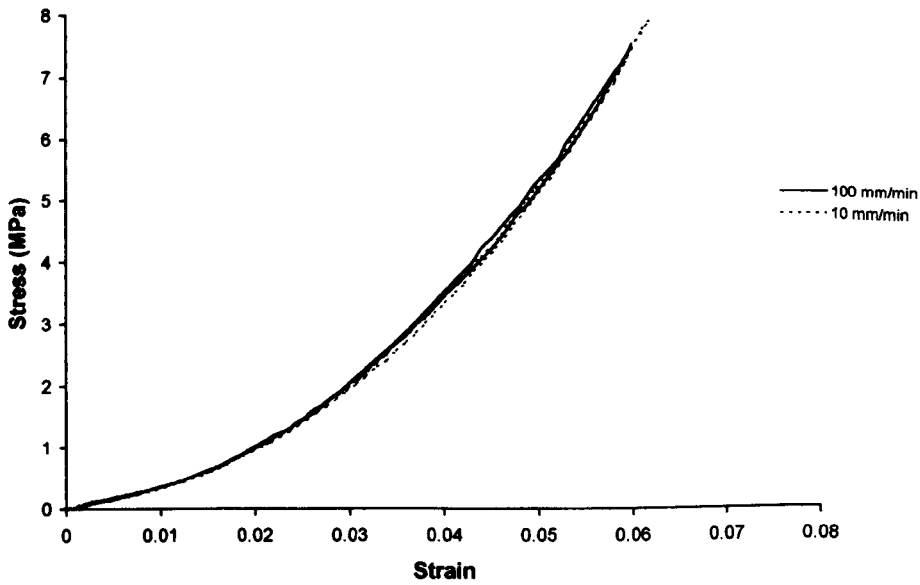


Figure A5.2(cont.) Stress-strain relationships in the foot ligaments (specimen 107R).

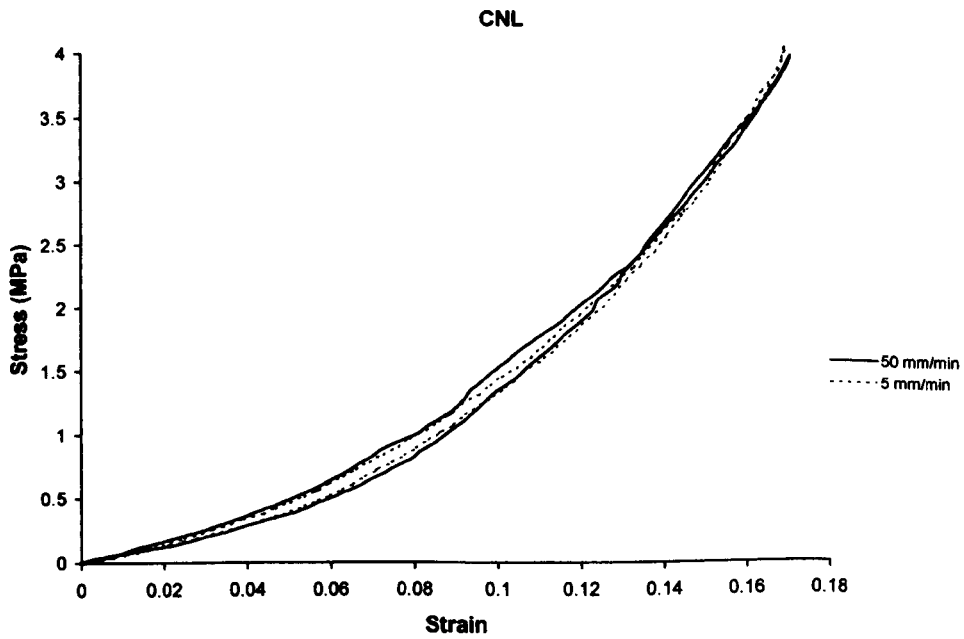
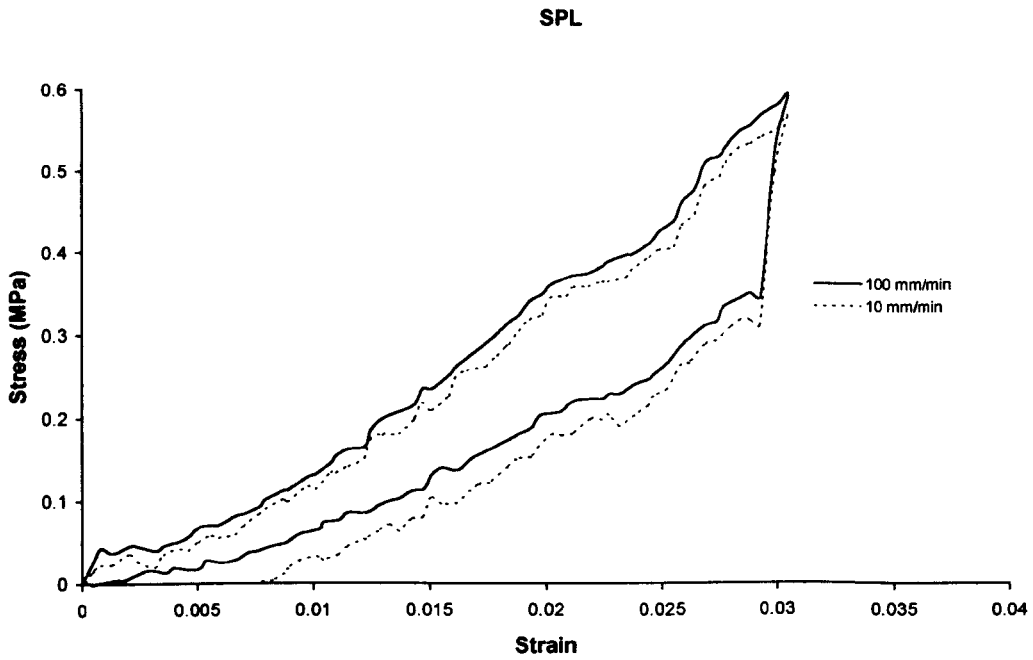


Figure A5.2(cont.) Stress-strain relationships in the foot ligaments (specimen 107R).

## A5.2 FORCE-STRAIN RESULTS

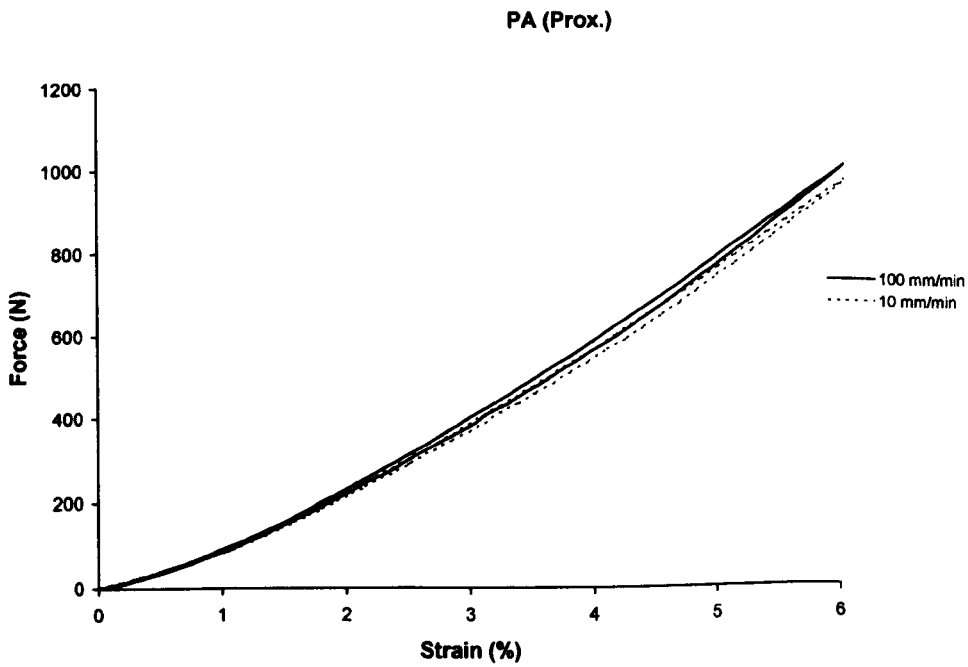
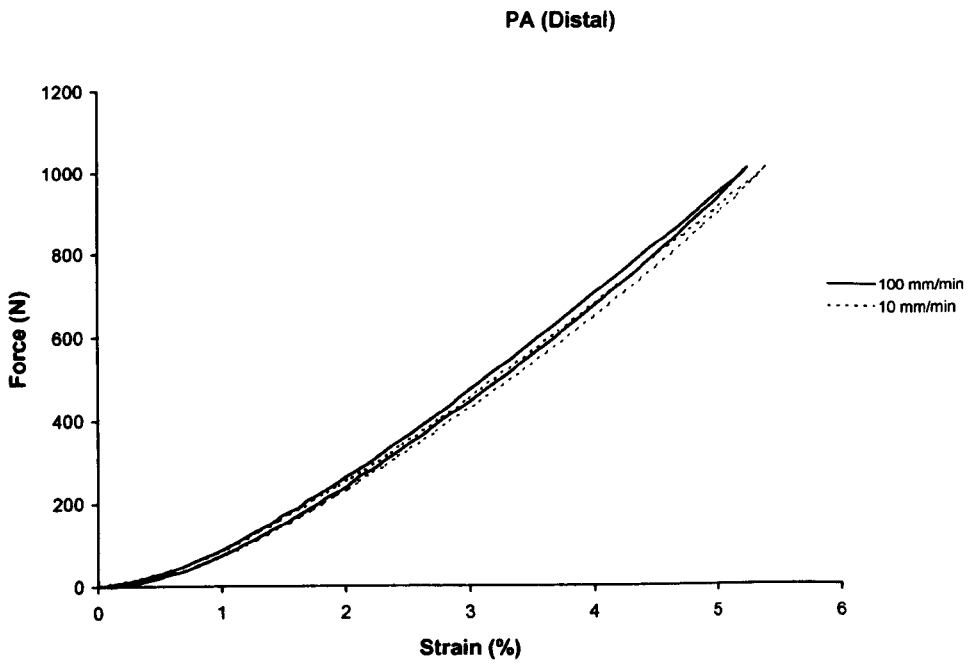
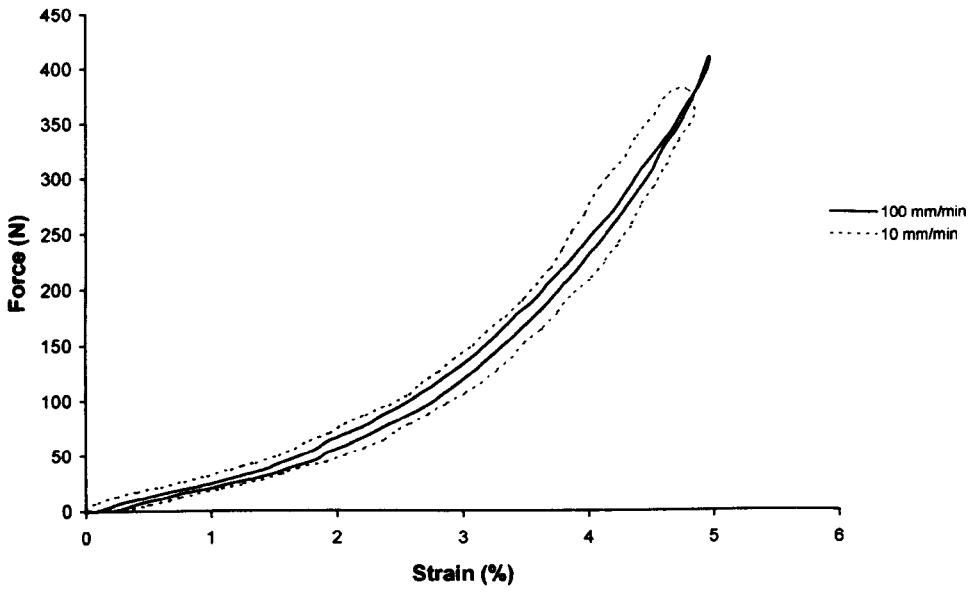


Figure A5.3 Force-strain relationships in the foot ligaments (specimen 131L).

LPL



SPL

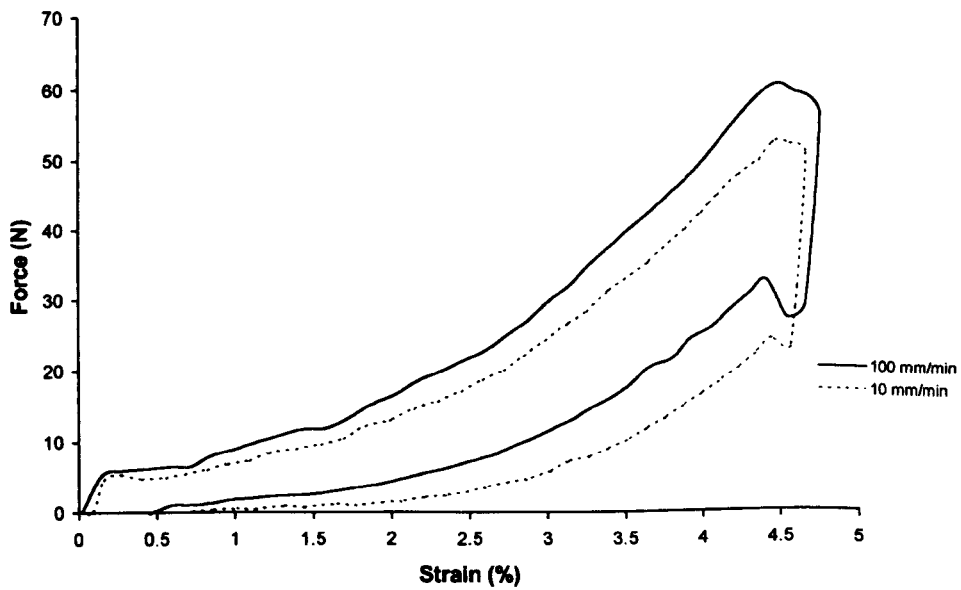


Figure A5.3(cont.) Force-strain relationships in the foot ligaments (specimen 131L).

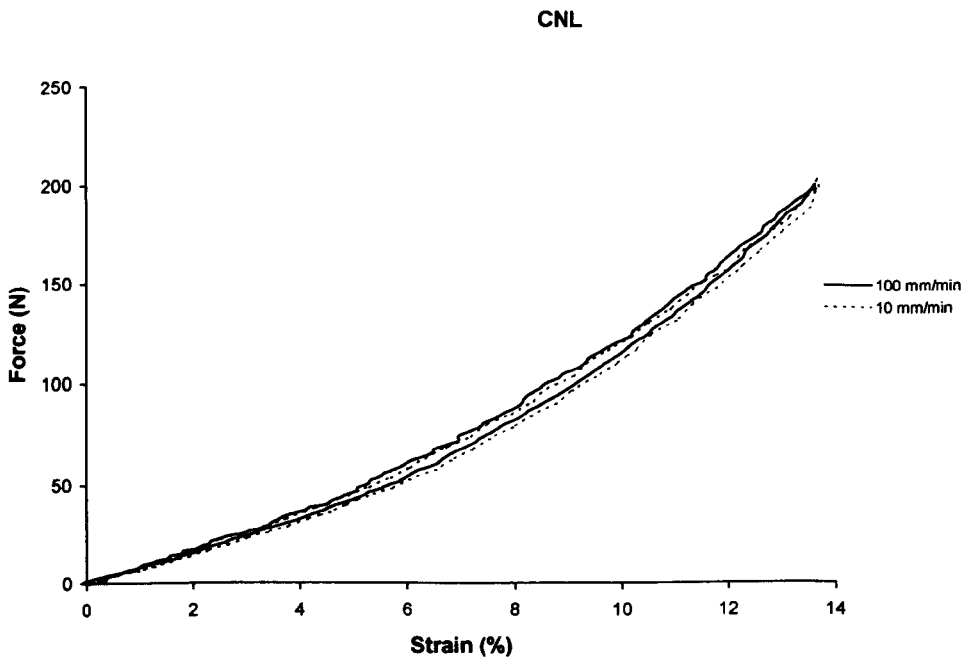


Figure A5.3(cont.) Force-strain relationships in the foot ligaments (specimen 131L).

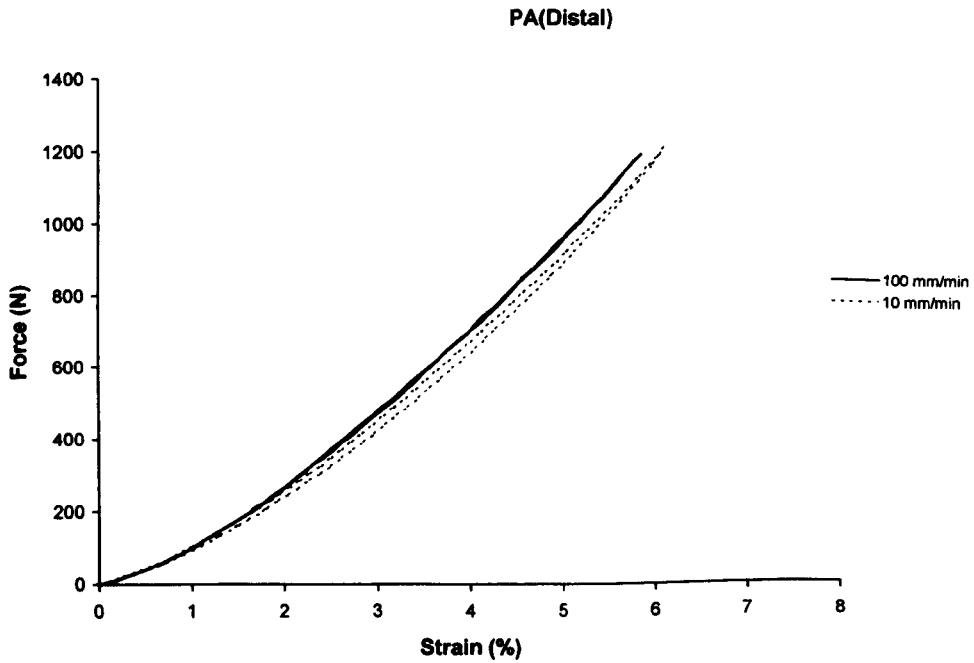
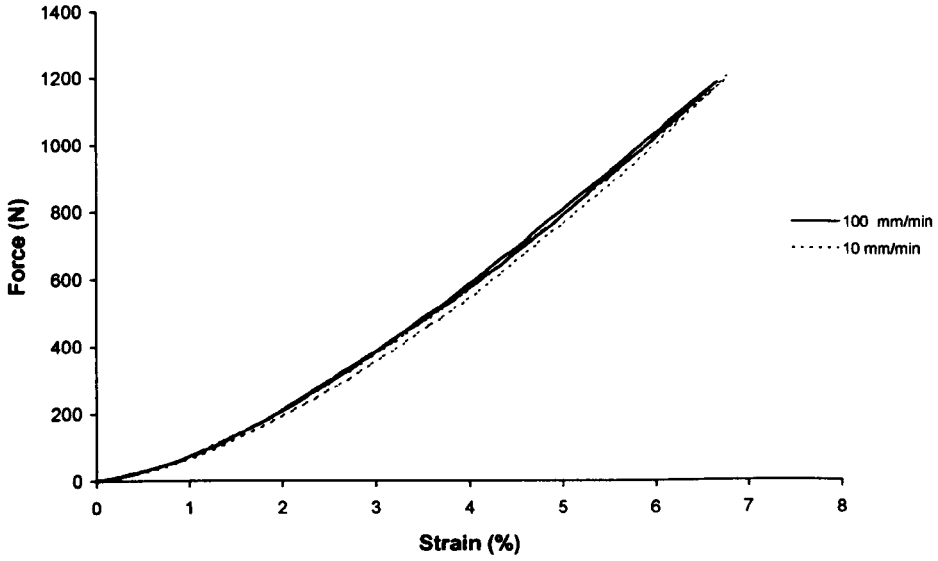


Figure A5.4 Force-strain relationships in the foot ligaments (specimen 107R).

PA(Prox.)



LPL

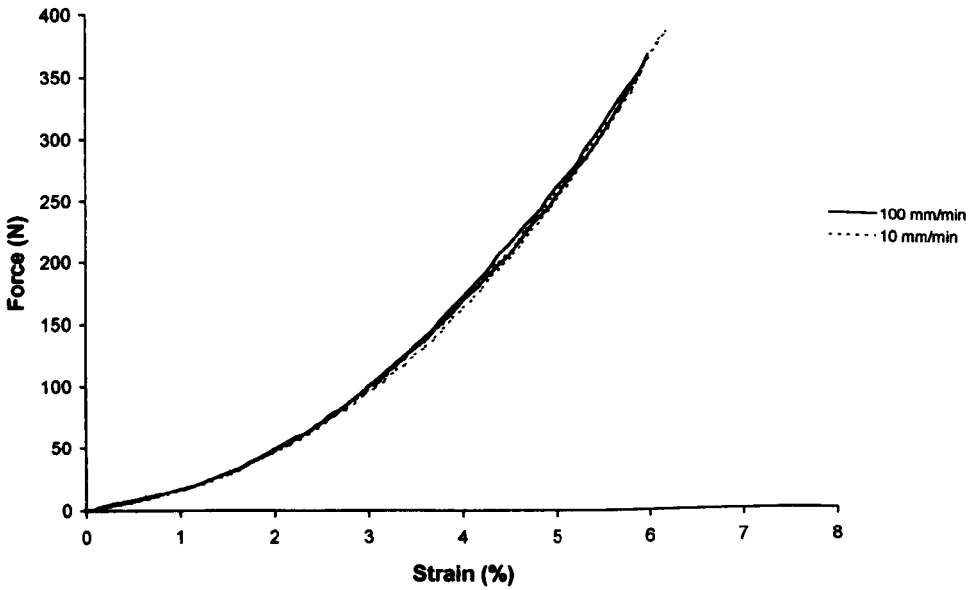


Figure A5.4(cont.) Force-strain relationships in the foot ligaments (specimen 107R).

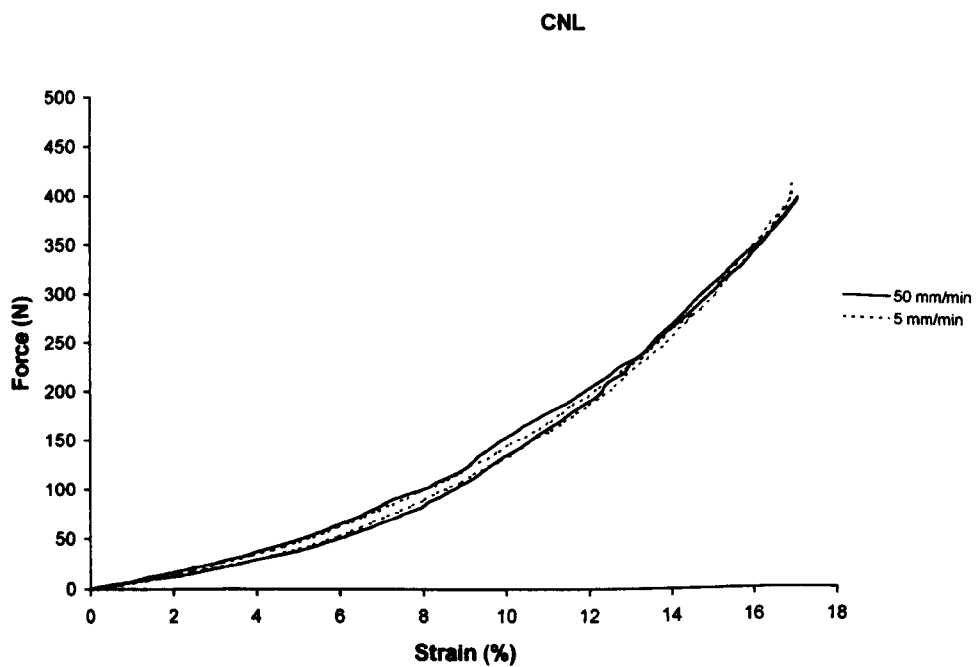
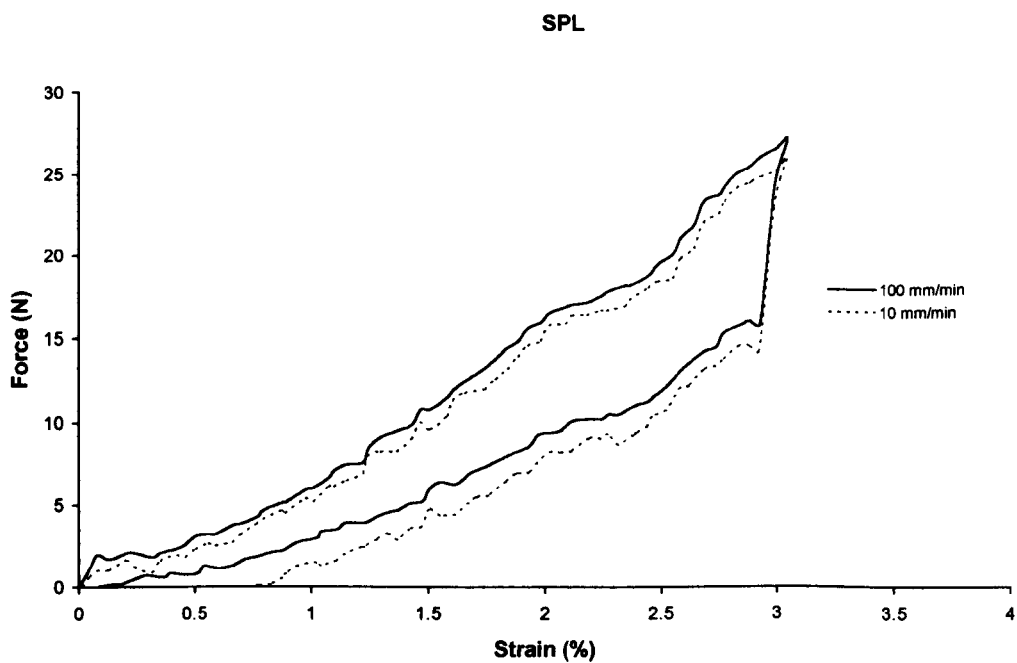


Figure A5.4(cont.) Force-strain relationships in the foot ligaments (specimen 107R).

# APPENDIX 6. FUNCTIONAL FORCES IN THE FOOT LIGAMENTS

## A6.1 FOOT POSITIONS

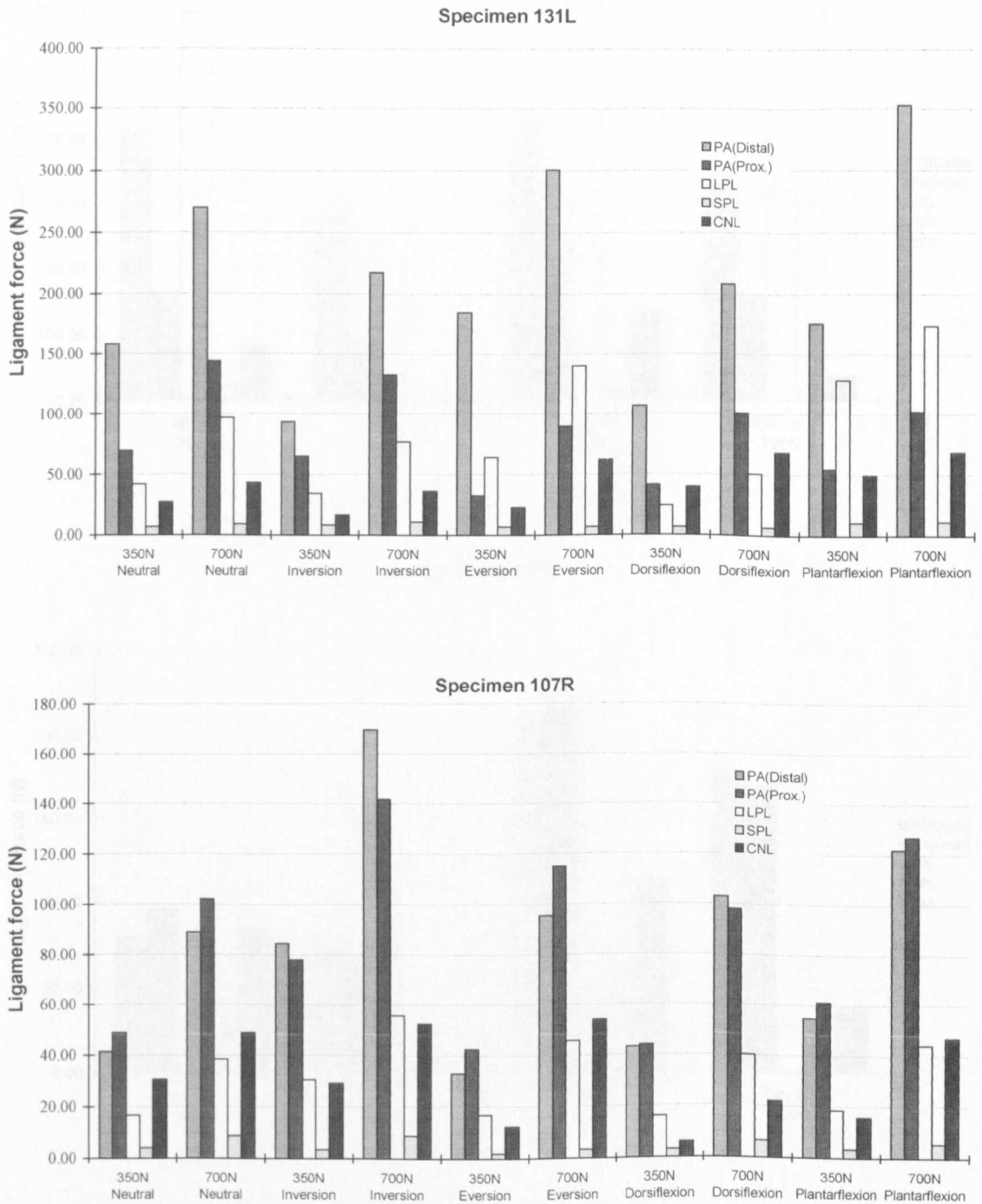


Figure A6.1 Functional forces in the foot ligaments with the foot placed in different positions during standing.

## A6.2 TIBIAL TORSION

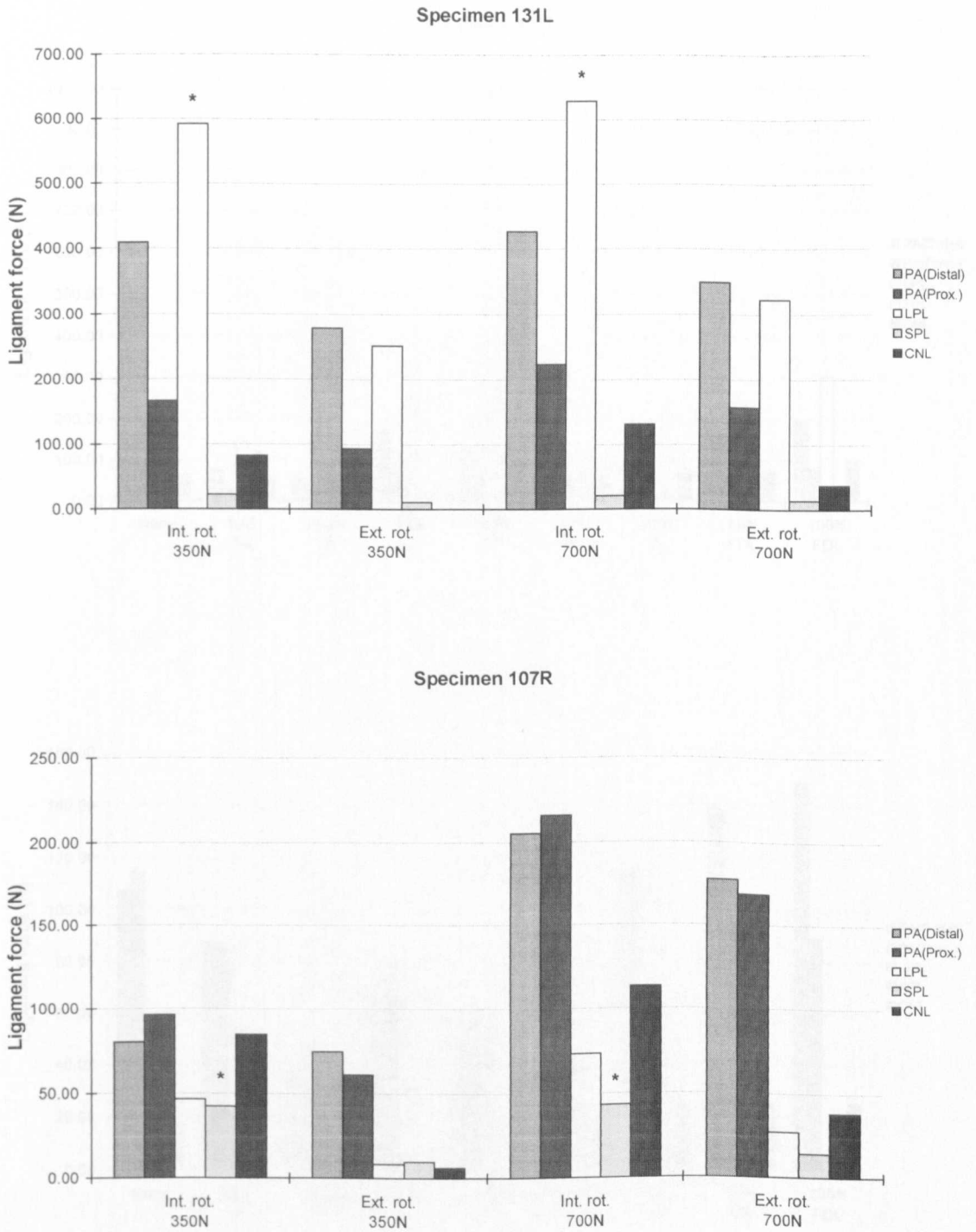


Figure A6.2 Functional forces in the foot ligaments with the foot subjected to applied tibial rotation during standing.

### A6.3 MUSCLE FORCES

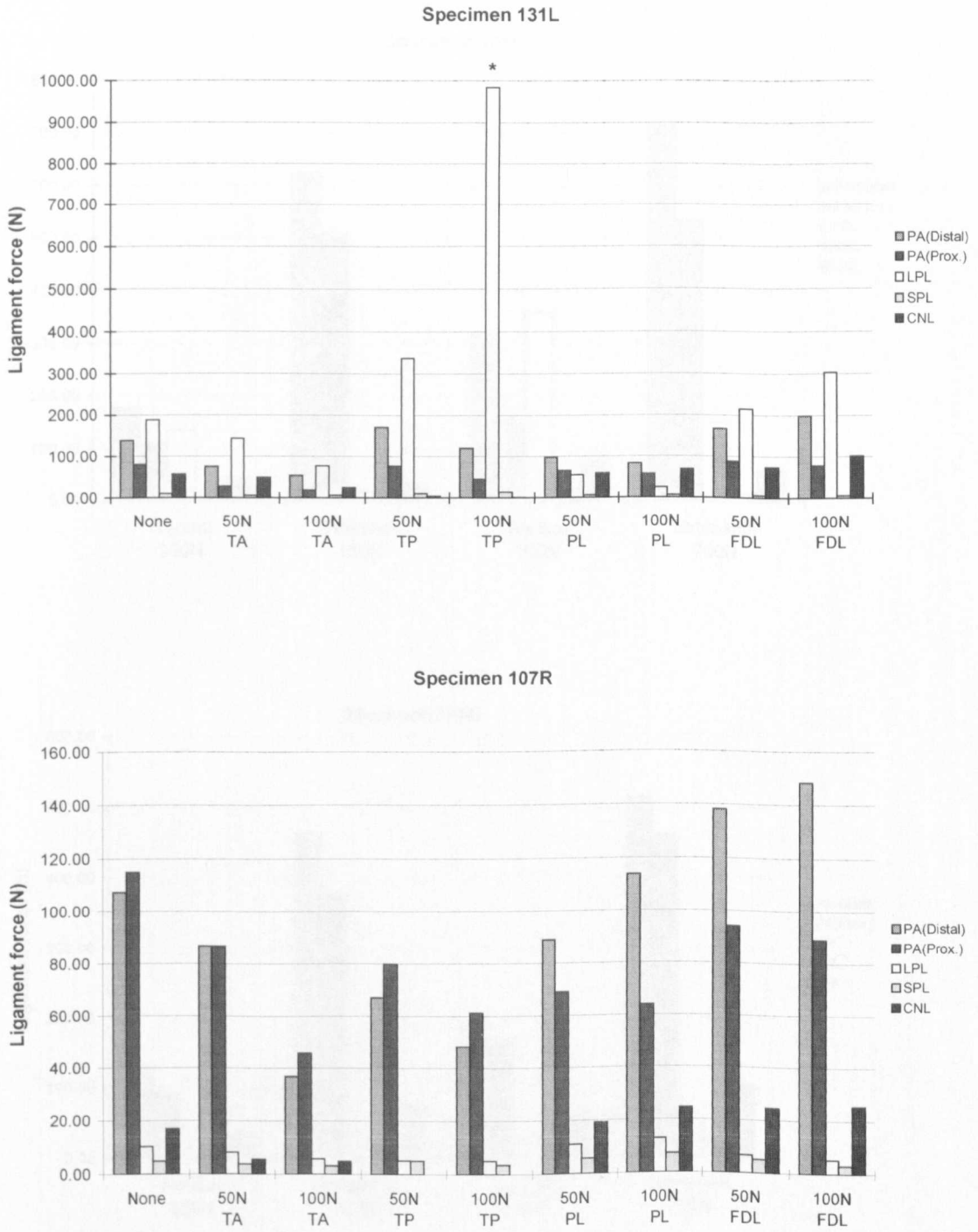


Figure A6.3 Functional forces in the foot ligaments with applied extrinsic muscle forces during standing.

## A6.4 TOE EXTENSION

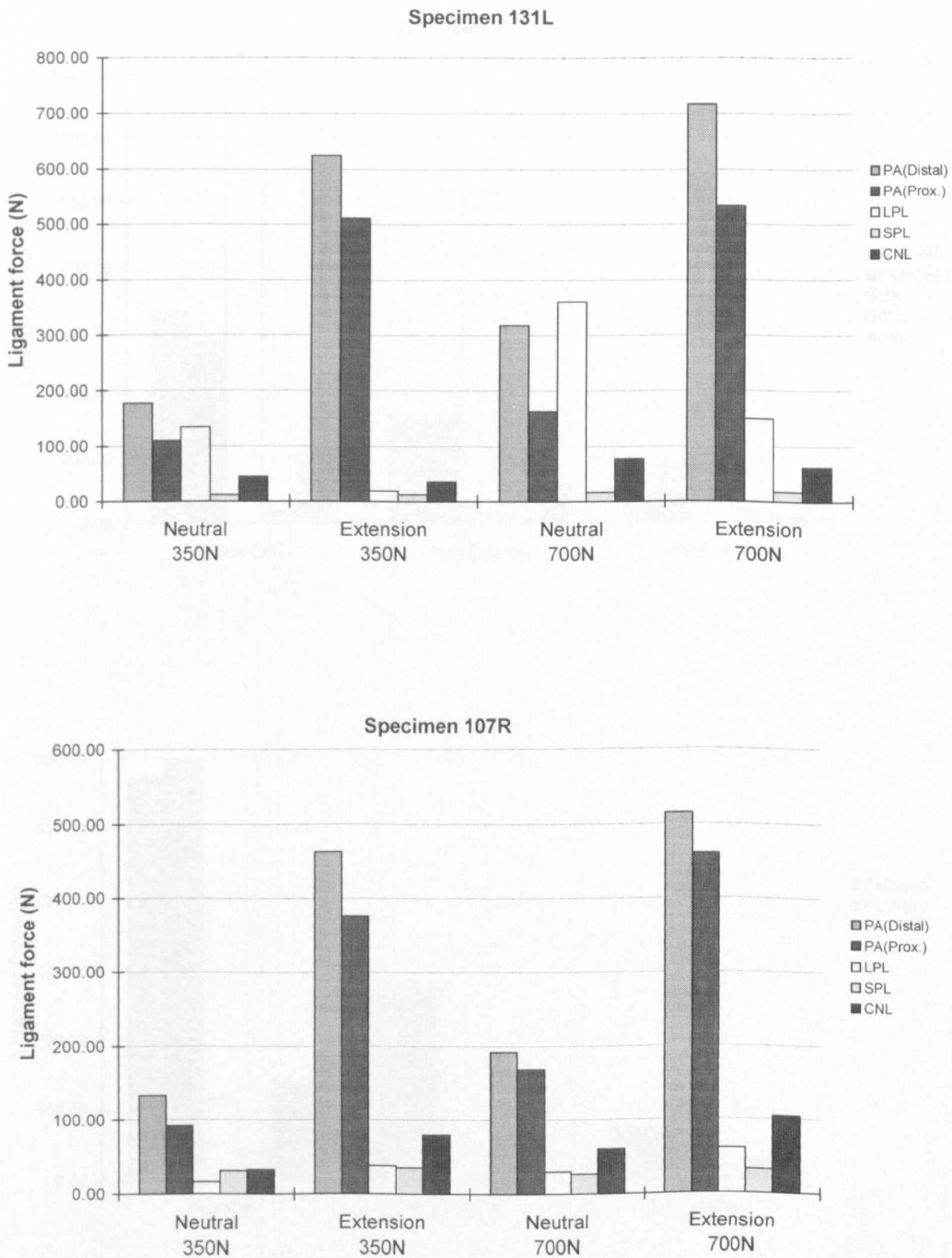


Figure A6.4 Functional forces in the foot ligaments with the foot subjected to toe extension during standing.

A6.5 GAIT

FUNCTIONAL FORCES IN THE FOOT

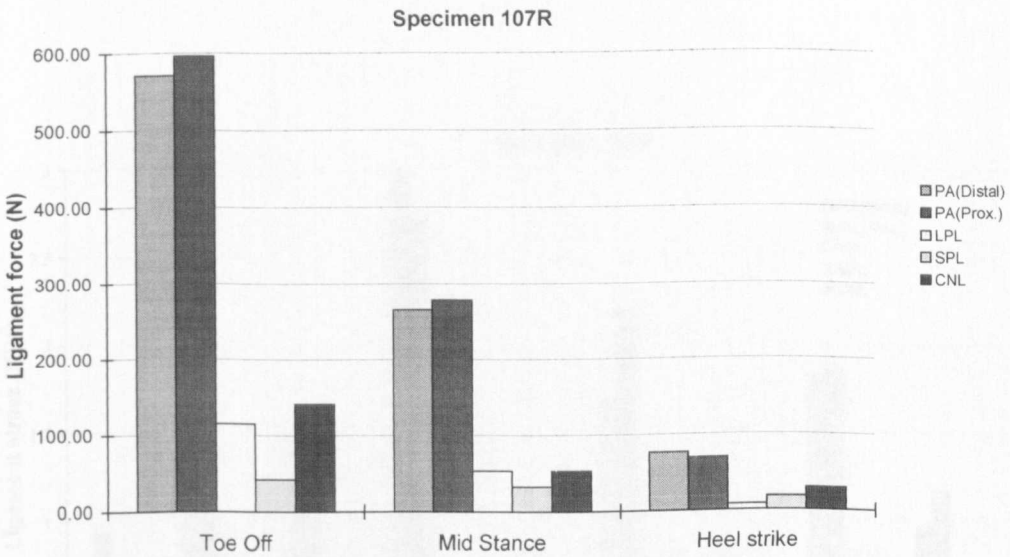
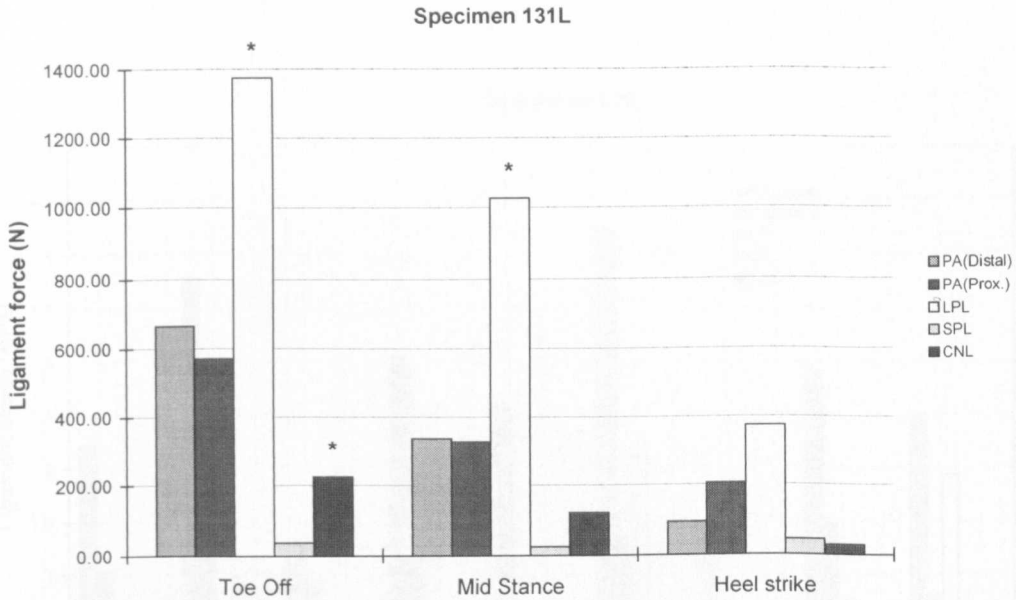


Figure A6.5 Functional forces in the foot ligaments during 3 stages of simulated gait.

# APPENDIX 7. FUNCTIONAL STRESSES IN THE FOOT LIGAMENTS

## A7.1 FOOT POSITIONS

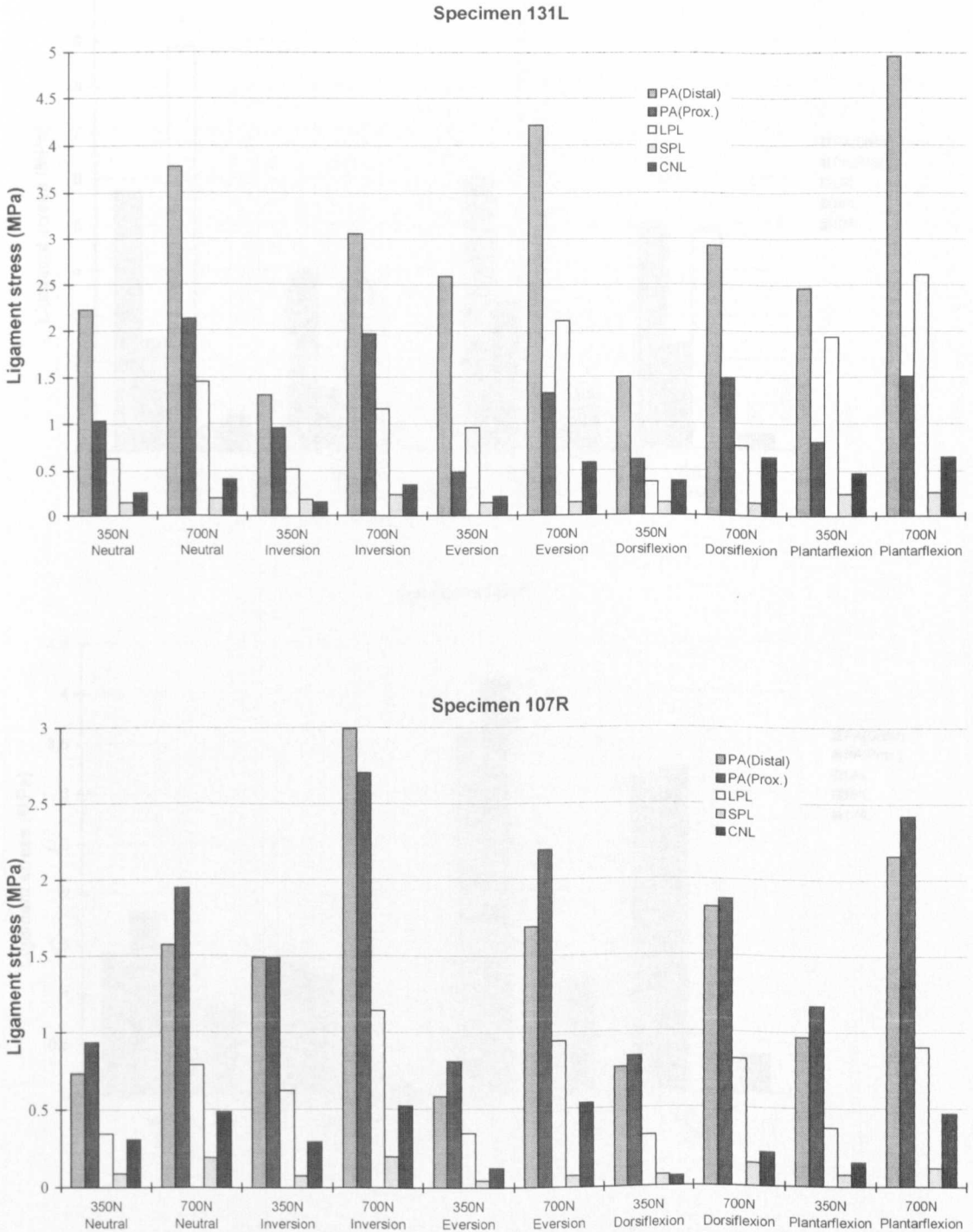


Figure A7.1 Functional stresses in the foot ligaments with the foot placed in different positions during standing.

## A7.2 TIBIAL TORSION

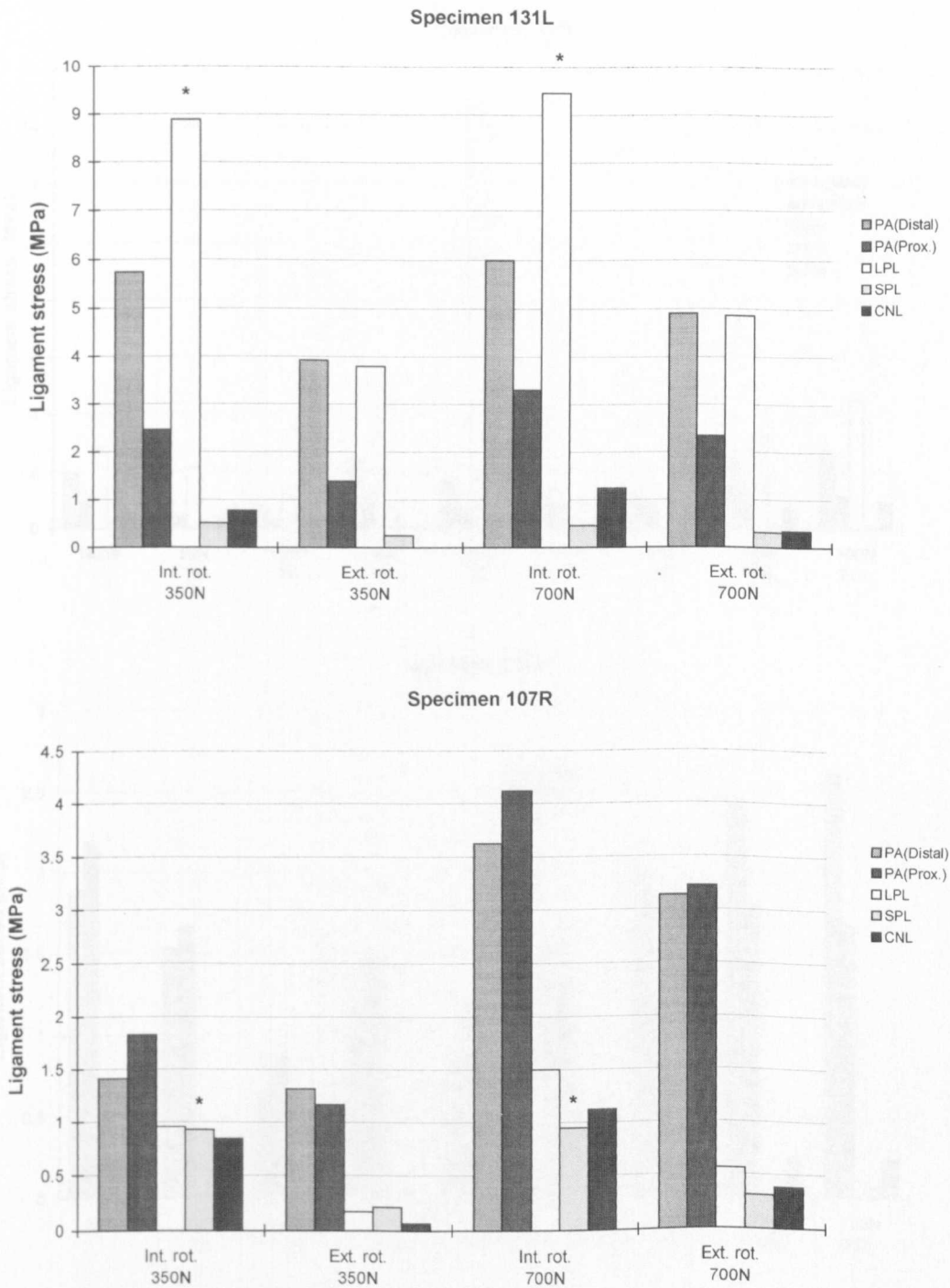


Figure A7.2 Functional stresses in the foot ligaments with the foot subjected to applied tibial rotation during standing.

### A7.3 MUSCLE FORCES

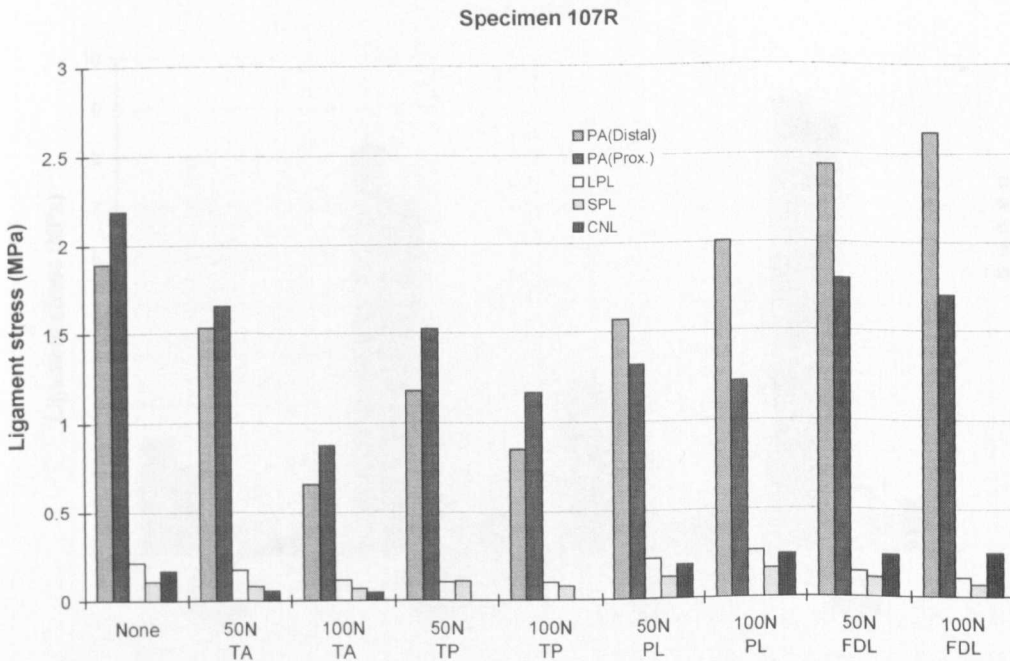
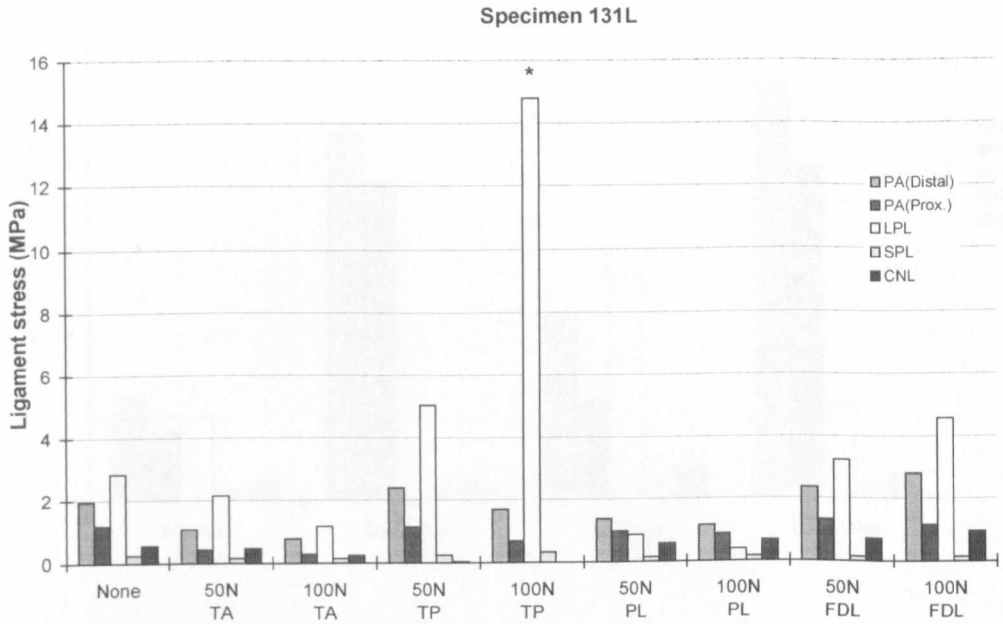


Figure A7.3 Functional stresses in the foot ligaments with applied extrinsic muscle forces during standing.

## A7.4 TOE EXTENSION

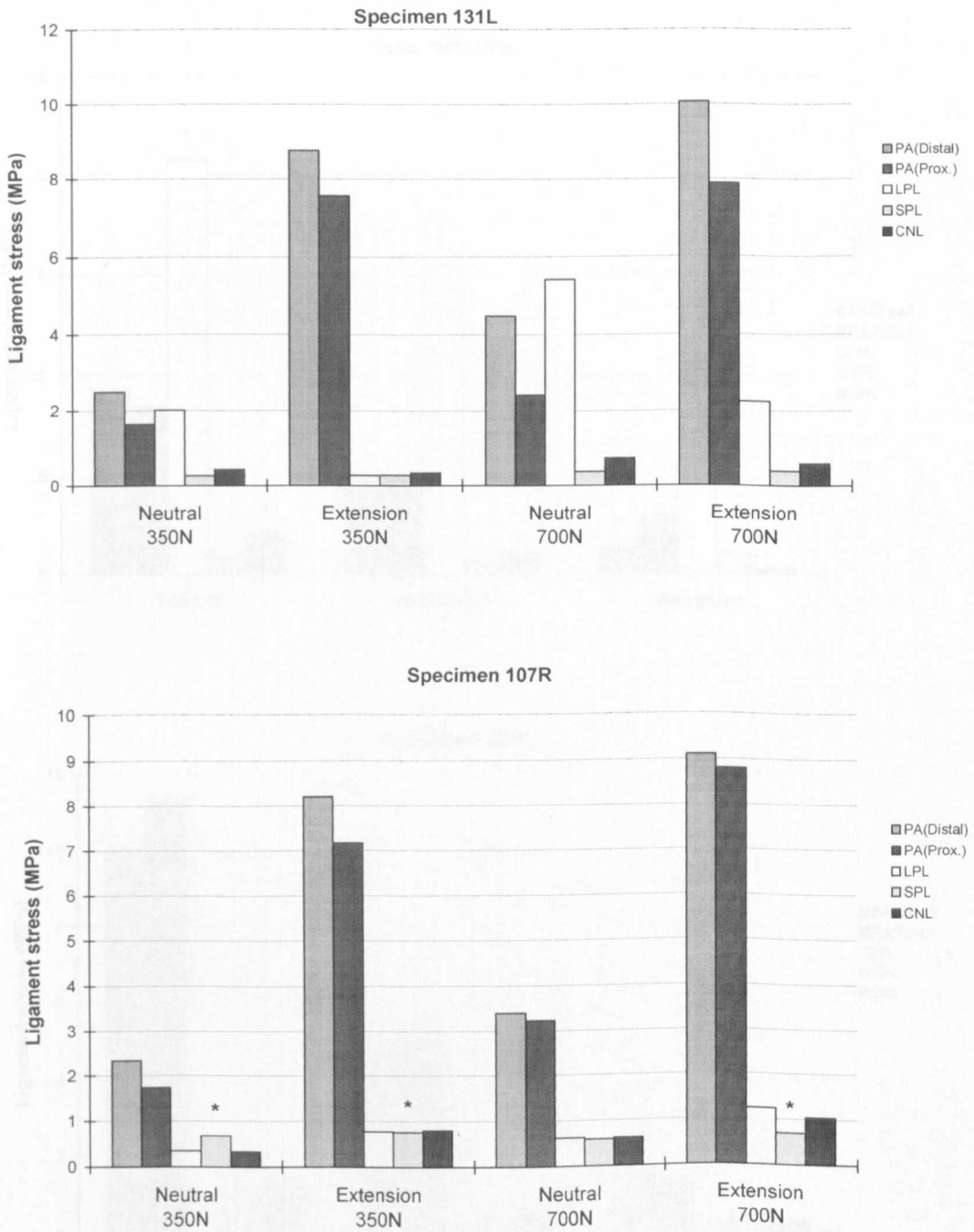
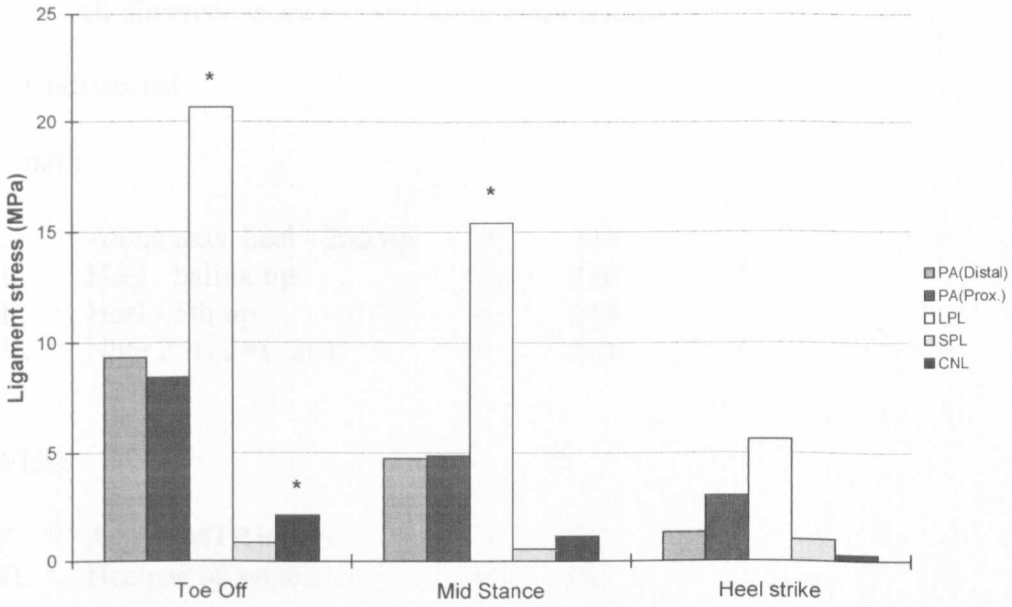


Figure A7.4 Functional stresses in the foot ligaments with the foot subjected to toe extension during standing.

A7.5 GAIT

Specimen 131L



Specimen 107R

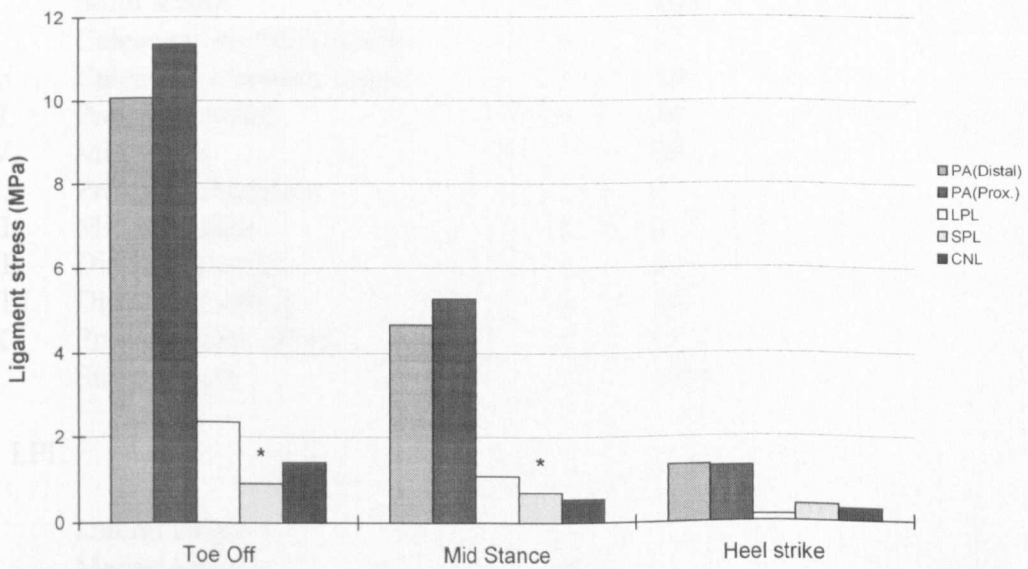


Figure A7.5 Functional stresses in the foot ligaments during 3 stages of simulated gait.

## APPENDIX 8. ISOLATED LIGAMENT TEST SPECIMEN DIMENSIONS

### A8.1 SPECIMEN 107R

Note: All dimensions are in mm (to the nearest mm)

#### 1. Undissected

##### Length

I.	Along axis, heel - 2nd tip	=	239
II.	Heel - hallux tip	=	236
III.	Heel - 5th tip	=	214
IV.	Note 2>1, 2=1, 2<1	=	2<1

##### Width

V.	Across MTP joints	=	89
VI.	Heelpad @ widest	=	49

#### 2. PA

I.	Solid length	=	105
II.	Calcaneal insertion width	=	22
IIa.	Calcaneal insertion length	=	19
III.	Proximal width	=	34
IV.	Mid width	=	20
V.	Proximal thickness	=	3
VI.	Mid thickness	=	2
VII.	Distal thickness	=	2
VIII.	Distal axis offset	=	18
IX.	Proximal axis offset	=	9
X.	Strain length	=	150

#### 3. LPL

I.	Lateral length	=	55
II.	Medial length	=	69
III.	Proximal width	=	23
IV.	Distal width	=	24
V.	Minimum width	=	17
VI.	Calcaneus insertion length	=	18
VII.	Cuboid insertion length	=	6

VIII.	MIIL (along closest DFD)	=	42
IX.	Mid thickness	=	2

#### 4. SPL

I.	Lateral length	=	25
II.	Medial length	=	24
III.	Proximal width	=	14
IV.	Distal width	=	19
V.	Proximal uncovered length	=	3
VI.	Distal uncovered length	=	14

#### 5. CNL

I.	Lateral length	=	21
II.	Medial length	=	27
III.	Proximal width	=	29
IV.	Distal width	=	21
V.	Calcaneus insertion width	=	4
VI.	Navicular insertion width	=	4
VII.	MIIL (not along DFD see placement param's)	=	26
VIII.	Mid width $\perp$ to MIIL @ mid MIIL	=	22
IX.	Mid thickness	=	3
X.	Note of existence of beak band	=	✓

## A8.2 SPECIMEN 131L

Note: All dimensions are in mm (to the nearest mm)

### 1. Undissected

#### Length

I.	Along axis, heel - 2nd tip	=	257
II.	Heel - hallux tip	=	259
III.	Heel - 5th tip	=	221
IV.	Note $2>1, 2=1, 2<1$	=	$2>1$

#### Width

V.	Across MTP joints	=	103
VI.	Heelpad @ widest	=	63

## 2. PA

I.	Solid length	=	110
II.	Calcaneal insertion width	=	19
IIa.	Calcaneal insertion length	=	16
III.	Proximal width	=	80
IV.	Mid width	=	25
V.	Proximal thickness	=	2
VI.	Mid thickness	=	3
VII.	Distal thickness	=	3
VIII.	Distal axis offset	=	18
IX.	Proximal axis offset	=	6
X.	Strain length	=	165

## 3. LPL

I.	Lateral length	=	47
II.	Medial length	=	63
III.	Proximal width	=	17
IV.	Distal width	=	34
V.	Minimum width	=	14
VI.	Calcaneus insertion length	=	29
VII.	Cuboid insertion length	=	7
VIII.	MIIL (along closest DFD)	=	32
IX.	Mid thickness	=	2

## 4. SPL

I.	Lateral length	=	21
II.	Medial length	=	33
III.	Proximal width	=	16
IV.	Distal width	=	20
V.	Proximal uncovered length	=	16
VI.	Distal uncovered length	=	15

## 5. CNL

I.	Lateral length	=	13
II.	Medial length	=	22
III.	Proximal width	=	21
IV.	Distal width	=	21
V.	Calcaneus insertion width	=	3
VI.	Navicular insertion width	=	3
VII.	MIIL (not along DFD see placement param's)	=	20
VIII.	Mid width $\perp$ to MIIL @ mid MIIL	=	24
IX.	Mid thickness	=	3
X.	Note of existence of beak band	=	✓

## APPENDIX 9      MODEL POSITIONAL DATA

<b>Ligament insertions</b>		<b>x co-ord.</b>	<b>y co-ord.</b>
CNL	Navicular	0.113	0.035
	Calcaneus	0.127	0.037
SPL	Cuboid	0.106	0.029
	Calcaneus	0.124	0.025
LPL	Cuboid	0.101	0.019
	Calcaneus	0.135	0.019
PA	Metatarsals	0.002	0.004
	Calcaneus	0.162	0.009
<b>Muscle insertions</b>			
TA		0.070	0.036
TP		0.105	0.032
TACH		0.196	0.036
<b>Force application points</b>			
R1		0.000	0.000
R2		0.176	0.000
F		0.142	0.070
<b>TT joint centres</b>			
Joint 1		0.122	0.061
Joint 2		0.122	0.052
Joint 3		0.115	0.053
Joint 4		0.127	0.051
Joint 5		0.110	0.045
Joint 6		0.122	0.057

Table A9.1      Positional data for foot 1 measured from a lateral x-ray (dimensions in metres, and expressed in the base co-ordinate system).

<b>Ligament insertions</b>		<b>x co-ord.</b>	<b>y co-ord.</b>
CNL	Navicular	0.104	0.042
	Calcaneus	0.117	0.043
SPL	Cuboid	0.106	0.031
	Calcaneus	0.122	0.026
LPL	Cuboid	0.101	0.019
	Calcaneus	0.132	0.019
PA	Metatarsals	0.000	0.004
	Calcaneus	0.154	0.005
<b>Muscle insertions</b>			
TA		0.063	0.038
TP		0.100	0.037
TACH		0.190	0.040
<b>Force application points</b>			
R1		0.000	0.000
R2		0.168	0.000
F		0.140	0.074
<b>TT joint centres</b>			
Joint 1		0.111	0.060
Joint 2		0.111	0.048
Joint 3		0.106	0.048
Joint 4		0.116	0.048
Joint 5		Void	Void
Joint 6		0.111	0.054

Table A9.2 Positional data for foot 2 measured from a lateral x-ray (dimensions in metres, and expressed in the base co-ordinate system).

<b>Ligament insertions</b>		<b>x co-ord.</b>	<b>y co-ord.</b>
CNL	Navicular	0.101	0.039
	Calcaneus	0.115	0.036
SPL	Cuboid	0.096	0.024
	Calcaneus	0.111	0.019
LPL	Cuboid	0.086	0.013
	Calcaneus	0.114	0.014
PA	Metatarsals	0.020	0.005
	Calcaneus	0.141	0.005
<b>Muscle insertions</b>			
TA		0.054	0.033
TP		0.095	0.031
TACH		0.169	0.028
<b>Force application points</b>			
R1		0.000	0.000
R2		0.153	0.000
F		0.125	0.059
<b>TT joint centres</b>			
Joint 1		0.109	0.056
Joint 2		0.107	0.041
Joint 3		0.103	0.041
Joint 4		0.112	0.040
Joint 5		0.097	0.044
Joint 6		0.108	0.049

Table A9.3 Positional data for foot 3 measured from a lateral x-ray (dimensions in metres, and expressed in the base co-ordinate system).

## APPENDIX 10 FOOT2D PROGRAM CODE

```
Program Foot2d;

uses crt;

type
  arraytype = array[1..12] of real;
  array2type = array[1..12,1..24] of real;
  ident = string[10];
var
  { deflin,arch,jtangle: arraytype;
  tens:array2type;}
  xjt,yjt:real;
  dim1,dim2,dim3,dim4,dim5,dim6,ninc,nstruct,nfapp,code:integer;
  runid,outtext:ident;

  (* Procedure declarations *)

procedure getlod(dim,ninc:integer; var numarray:array2type);

var
  i,j,code: integer;
  filespec: string[40];
  thefile: text;

begin
  writeln(' Enter filespec for load input file, or');
  writeln(' press enter to cancel. ');
  readln(filespec);
  if length(filespec) = 0 then
    begin
      code := -1;
      exit
    end;
  filespec := ('c:\model2d\data' + filespec + '.lod');
  assign(thefile , filespec);
  {$I-}
  reset(thefile);
  code := ioresult;
  if code <> 0 then begin
    writeln(chr(7));
    writeln(' I/O error number', code,'(decimal)');
    writeln(' from reset in getlod. Aborted. ');
    exit
  end;
  for i := 1 to dim do begin
    for j:=1 to ninc do begin
      read(thefile, numarray[i,j]);
      code := ioresult;
      if code <> 0 then begin
        writeln(chr(7));
        writeln('I/O error number', code,'(decimal)');
        writeln(' from read in getlod. Aborted');
        exit
      end;
    end;
  end;
end;
```

```

        end
    end;
end;
close(thefile);
code := ioreult;
if code <> 0 then begin
    writeln(chr(7));
    writeln('I/O error number', code,'(decimal)');
    writeln('from close in getlod. Aborted');
    exit
end;
{$I+}
writeln;
writeln('Elements now in array load !');
writeln;
end;

```

```

procedure getdef(dim:integer; var numarray:arraytype);

```

```

var
    i,code: integer;
    filespec: string[40];
    thefile: text;

begin
    writeln(' Enter filespec for deflection input file, or');
    writeln(' press enter to cancel. ');
    readln(filespec);
    if length(filespec) = 0 then
        begin
            code := -1;
            exit
        end;
    filespec := ('c:\model2d\data\' + filespec + '.def');
    assign(thefile , filespec);
    {$I-}
    reset(thefile);
    code := ioreult;
    if code <> 0 then begin
        writeln(chr(7));
        writeln(' I/O error number', code,'(decimal)');
        writeln(' from reset in getdef. Aborted. ');
        exit
    end;
    for i := 1 to dim do begin
        read(thefile,numarray[i]);
        code := ioreult;
        if code <> 0 then begin
            writeln(chr(7));
            writeln('I/O error number', code,'(decimal)');
            writeln(' from read in getdef. Aborted');
            exit
        end
    end;
end;
close(thefile);
code := ioreult;
if code <> 0 then begin
    writeln(chr(7));

```

```

        writeln('I/O error number', code,'(decimal)');
        writeln('from close in getdef. Aborted');
        exit
    end;
    {$I+}
    writeln;
    writeln('Elements now in array def !');
    writeln
end;

procedure getfapp(dim,ninc:integer; var numarray:array2type);

var
    i,j,code: integer;
    filespec: string[40];
    thefile: text;

begin
    writeln(' Enter filespec for force application input file, or');
    writeln(' press enter to cancel. ');
    readln(filespec);
    if length(filespec) = 0 then
        begin
            code := -1;
            exit
        end;
    filespec := ('c:\model2d\data\' + filespec + '.fap');
    assign(thefile , filespec);
    {$I-}
    reset(thefile);
    code := ioresult;
    if code < 0 then begin
        writeln(chr(7));
        writeln(' I/O error number', code,'(decimal)');
        writeln(' from reset in getfap. Aborted. ');
        exit
    end;
    for i := 1 to dim do begin
        for j:=1 to ninc do begin
            read(thefile, numarray[i,j]);
            code := ioresult;
            if code < 0 then begin
                writeln(chr(7));
                writeln('I/O error number', code,'(decimal)');
                writeln(' from read in getins. Aborted');
                exit
            end
        end;
    end;
    end;
    close(thefile);
    code := ioresult;
    if code < 0 then begin
        writeln(chr(7));
        writeln('I/O error number', code,'(decimal)');
        writeln('from close in getfap. Aborted');
        exit
    end;
    {$I+}

```

```

    writeln;
    writeln('Elements now in array fapp !');
    writeln
end;

procedure getins(dim,ninc:integer; var numarray:array2type);

var
    i,j,code: integer;
    filespec: string[40];
    thefile: text;

begin
    writeln(' Enter filespec for ligament insertion input file, or');
    writeln(' press enter to cancel. ');
    readln(filespec);
    if length(filespec) = 0 then
        begin
            code := -1;
            exit
        end;
    filespec := ('c:\model2d\data\' + filespec + '.ins');
    assign(thefile , filespec);
    {$I-}
    reset(thefile);
    code := ioresult;
    if code <> 0 then begin
        writeln(chr(7));
        writeln(' I/O error number', code,'(decimal)');
        writeln(' from reset in getins. Aborted. ');
        exit
    end;
    for i := 1 to dim do begin
        for j:=1 to ninc do begin
            read(thefile, numarray[i,j]);
            code := ioresult;
            if code <> 0 then begin
                writeln(chr(7));
                writeln('I/O error number', code,'(decimal)');
                writeln(' from read in getins. Aborted');
                exit
            end
        end;
    end;
    close(thefile);
    code := ioresult;
    if code <> 0 then begin
        writeln(chr(7));
        writeln('I/O error number', code,'(decimal)');
        writeln('from close in getins. Aborted');
        exit
    end;
    {$I+}
    writeln;
    writeln('Elements now in array ins !');
    writeln
end;

```

```
procedure dout (numarray:arraytype; runid:ident;
               numcols:integer);
```

```
var
```

```
  i,code: integer;
  filespec:string[40];
  thefile: text;
```

```
begin
```

```
  filespec := ('c:\model2d\data\' + runid);
  assign(thefile , filespec);
  {$I-}
  rewrite(thefile);
  code := ioreult;
  if code <> 0 then begin
    writeln(chr(7));
    writeln(' I/O error number', code,'(decimal)');
    writeln(' from rewrite of ',filespec, '. Aborted. ');
    exit
  end;
  for i := 1 to numcols do begin
    write(thefile, numarray[i]);
    code := ioreult;
    if code <> 0 then begin
      writeln(chr(7));
      writeln('I/O error number', code,'(decimal)');
      writeln(' from write of ',filespec, '. Aborted');
      exit
    end
  end;
  writeln(thefile);
  close(thefile);
  code := ioreult;
  if code <> 0 then begin
    writeln(chr(7));
    writeln('I/O error number', code,'(decimal)');
    writeln('from close of ',filespec, '. Aborted');
    exit
  end;
  {$I+}
  writeln(filespec, ' written to disk.')
```

```
end;
```

```
procedure dout2 (numarray:array2type; runid:ident;
                 numcols,numrows:integer);
```

```
var
```

```
  i,j,code: integer;
  filespec:string[80];
  thefile: text;
```

```
begin
```

```
  filespec := ('c:\model2d\data\' + runid);
  assign(thefile , filespec);
  {$I-}
  rewrite(thefile);
  code := ioreult;
  if code <> 0 then begin
```

```

        writeln(chr(7));
        writeln(' I/O error number', code,'(decimal)');
        writeln(' from rewrite of ',filespec,'. Aborted. ');
        exit
    end;
for i := 1 to numRows do begin
    for j:=1 to numcols do begin
        write(thefile, numarray[i,j]:12:9,' ');
        code := ioresult;
        if code <> 0 then begin
            writeln(chr(7));
            writeln('I/O error number', code,'(decimal)');
            writeln(' from write of ',filespec,'. Aborted');
            exit
        end
    end;
    writeln(thefile);
end;
close(thefile);
code := ioresult;
if code <> 0 then begin
    writeln(chr(7));
    writeln('I/O error number', code,'(decimal)');
    writeln('from close of ',filespec,'. Aborted');
    exit
end;
{$I+}
writeln(filespec,' written to disk.')
end;

```

```

procedure din (var numarray:arraytype; runid:ident;
               numcols:integer);

```

```

var

```

```

    i,code: integer;
    filespec:string[40];
    thefile: text;

```

```

begin

```

```

    filespec := ('c:\model2d\data' + runid);
    assign(thefile , filespec);
    {$I-}
    reset(thefile);
    code := ioresult;
    if code <> 0 then begin
        writeln(chr(7));
        writeln(' I/O error number', code,'(decimal)');
        writeln(' from rewrite of ',filespec,'. Aborted. ');
        exit
    end;
    for i := 1 to numcols do begin
        read(thefile, numarray[i]);
        code := ioresult;
        if code <> 0 then begin
            writeln(chr(7));
            writeln('I/O error number', code,'(decimal)');
            writeln(' from write of ',filespec,'. Aborted');
            exit
        end;
    end;
end;

```

```

        end
        end;
    readln(thefile);
    close(thefile);
    code := ioreult;
    if code <> 0 then begin
        writeln(chr(7));
        writeln('I/O error number', code,'(decimal)');
        writeln('from close of ',filespec,'. Aborted');
        exit
        end;
    {$I+}
    writeln(filespec,' read from disk.')
end;

procedure din2 (var numarray:array2type; runid:ident;
                numcols,numrows:integer);

var
    i,j,code: integer;
    filespec:string[80];
    thefile: text;

begin
    filespec := ('c:\model2d\data\' + runid);
    assign(thefile , filespec);
    {$I-}
    reset(thefile);
    code := ioreult;
    if code <> 0 then begin
        writeln(chr(7));
        writeln(' I/O error number', code,'(decimal)');
        writeln(' from rewrite of ',filespec,'. Aborted.');
```

```

        exit
        end;
    for i := 1 to numrows do begin
        for j:=1 to numcols do begin
            read(thefile, numarray[i,j]);
            code := ioreult;
            if code <> 0 then begin
                writeln(chr(7));
                writeln('I/O error number', code,'(decimal)');
                writeln(' from write of ',filespec,'. Aborted');
```

```

            exit
            end
        end;
        readln(thefile);
    end;
    close(thefile);
    code := ioreult;
    if code <> 0 then begin
        writeln(chr(7));
        writeln('I/O error number', code,'(decimal)');
        writeln('from close of ',filespec,'. Aborted');
```

```

        exit
        end;
    {$I+}
    writeln(filespec,' read from disk.')
```

```

end;

procedure res (numarray:arraytype; runid,ext:ident;
              numcols:integer);

var
  i,code: integer;
  filespec:string[40];
  thefile: text;

begin
  filespec := ('c:\model2d\res\' + runid + '.' + ext);
  assign(thefile , filespec);
  {$I-}
  rewrite(thefile);
  code := ioreult;
  if code < 0 then begin
    writeln(chr(7));
    writeln(' I/O error number', code,'(decimal)');
    writeln(' from rewrite of ',filespec,'. Aborted.');
```

```

    exit
    end;
  for i := 1 to numcols do begin
    write(thefile, numarray[i]:12:4);
    code := ioreult;
    if code < 0 then begin
      writeln(chr(7));
      writeln('I/O error number', code,'(decimal)');
      writeln(' from write of ',filespec,'. Aborted');
```

```

      exit
      end
    end;
    writeln(thefile);
    close(thefile);
    code := ioreult;
    if code < 0 then begin
      writeln(chr(7));
      writeln('I/O error number', code,'(decimal)');
      writeln('from close of ',filespec,'. Aborted');
```

```

      exit
      end;
    {$I+}
    writeln(filespec,' written to disk.')
```

```

end;
```

```

procedure res2 (numarray:array2type; runid,ext:ident;
               numcols,numrows:integer);
```

```

var
  i,j,code: integer;
  filespec:string[80];
  thefile: text;
```

```

begin
  filespec := ('c:\model2d\res\' + runid + '.' + ext);
  assign(thefile , filespec);
  {$I-}
  rewrite(thefile);
```

```

code := ioreult;
if code <> 0 then begin
  writeln(chr(7));
  writeln(' I/O error number', code,'(decimal)');
  writeln(' from rewrite of ',filespec,'. Aborted. ');
  exit
end;
for i := 1 to numRows do begin
  for j:=1 to numcols do begin
    write(thefile, numarray[i,j]:12:4);
    code := ioreult;
    if code <> 0 then begin
      writeln(chr(7));
      writeln('I/O error number', code,'(decimal)');
      writeln(' from write of ',filespec,'. Aborted');
      exit
    end
  end;
  writeln(thefile);
end;
close(thefile);
code := ioreult;
if code <> 0 then begin
  writeln(chr(7));
  writeln('I/O error number', code,'(decimal)');
  writeln('from close of ',filespec,'. Aborted');
  exit
end;
{$I+}
writeln(filespec,' written to disk.')
end;

procedure geometry (xjt,yjt:real;dim1,dim5,dim6,nfapp,ninc:integer);

var
  i,j:integer;
  l1,l2,h10,h20,d1,d2,gamma,xfloc,yfloc,ankle:real;
  arch,def:arraytype;
  ins,fcor,fapp,geom,local,angle:array2type;

begin
  (*Read in experimental data *)

  getins(dim5,2,ins);
  getdef(ninc,def);
  getfapp(nfapp,2,fapp);

  (* Convert force applications to global co-ords*)

  fapp[1,1]:= fapp[1,1] - xjt;
  fapp[1,2]:= 0;
  fapp[2,1]:= fapp[2,1] - xjt;
  fapp[2,2]:= 0;
  fapp[3,1]:= fapp[3,1] - xjt;

  (* Calculate arch heights from ankle deflectons *)

  h10:= yjt;

```

```

d1:= fapp[2,1];
h20:= fapp[3,2];
d2:= fapp[2,1] - fapp[3,1];
l1:= sqrt((h10*h10)+(d1*d1));
l2:= sqrt((h20*h20)+(d2*d2));
gamma:= arctan(h20/d2) - arctan(h10/d1);

```

```

for i:=1 to ninc do begin
  ankle:= (h20 - def[i]);
  arch[i]:= l1*sin(arctan(ankle/sqrt((l2*l2)
    -(ankle*ankle)))- gamma);
end;

```

(\* Calculate reaction force co-ordinates for [fcor] rows 1-2 \*)

```

for i:=1 to ninc do begin
  fcor[1,(2*i)-1]:= -sqrt((arch[1]*arch[1]) +
    (fapp[1,1]*fapp[1,1]) -
    (arch[i]*arch[i]));
  fcor[1,(2*i)]:= 0;
  fcor[2,(2*i)-1]:= sqrt((arch[1]*arch[1]) +
    (fapp[2,1]*fapp[2,1]) -
    (arch[i]*arch[i]));
  fcor[2,(2*i)]:= 0;
end;

```

(\* Calculate angles for local co-ordinate calculations \*)

```

for i:=1 to ninc do begin
  angle[1,i]:= arctan(-arch[i]/fcor[1,(2*i)-1]) + pi; (* changed to minus arch*)
  angle[2,i]:= arctan(-arch[i]/fcor[2,(2*i)-1]);
end;
dout2(angle,'locang',ninc,2);

```

(\* Calculate local co-ords of ligament insertions \*)

```

for i:=1 to nstruct do begin
  local[(2*i)-1,1]:= ((ins[(2*i)-1,1]-xjt)*cos(angle[1,1])) +
    ((ins[(2*i)-1,2]-yjt)*sin(angle[1,1]));
  local[(2*i)-1,2]:= (-ins[(2*i)-1,1]-xjt)*sin(angle[1,1]) +
    ((ins[(2*i)-1,2]-yjt)*cos(angle[1,1]));
  local[(2*i),1]:= ((ins[(2*i),1]-xjt)*cos(angle[2,1])) +
    ((ins[(2*i),2]-yjt)*sin(angle[2,1]));
  local[(2*i),2]:= (-ins[(2*i),1]-xjt)*sin(angle[2,1]) +
    ((ins[(2*i),2]-yjt)*cos(angle[2,1]));
end;
dout2(local,'local',2,dim5);

```

(\* Calculate deformed geometry in global co-ordinates \*)

```

for i:=1 to nstruct do begin
  for j:=1 to ninc do begin
    geom[(i*2)-1,(j*2)-1]:= (local[(i*2)-1,1]*cos(angle[1,j]))-
      (local[(i*2)-1,2]*sin(angle[1,j]));
    geom[(i*2)-1,(j*2)]:= (local[(i*2)-1,1]*sin(angle[1,j]) +
      (local[(i*2)-1,2]*cos(angle[1,j]) +
      arch[j]);
    geom[(i*2),(j*2)-1]:= (local[(i*2),1]*cos(angle[2,j]))-

```

```

                (local[(i*2),2]*sin(angle[2,j]));
geom[(i*2),(j*2)]:= (local[(i*2),1]*sin(angle[2,j])) +
                (local[(i*2),2]*cos(angle[2,j]) +
                arch[j]);
    end
end;

(* Calculate co-ords of tibial force application, last row
of fcor matrix *)

xfloc:= fapp[3,1]*cos(angle[2,1]) +
        ((fapp[3,2]-yjt)*sin(angle[2,1]));
yfloc:= -(fapp[3,1]*sin(angle[2,1])) +
        ((fapp[3,2]-yjt)*cos(angle[2,1]));
for i:=1 to ninc do begin
    fcor[3,(i*2)-1]:= (xfloc*cos(angle[2,i])) -
                    (yfloc*sin(angle[2,i]));
    fcor[3,(i*2)]:= (xfloc*sin(angle[2,i])) +
                    (yfloc*cos(angle[2,i])) +
                    arch[i];
end;

(* Write arch heights, geometry and force application
global co-ords to disk *)

dout(arch,'arch',ninc);
dout2(geom,'geom',dim6,dim5);
dout2(fcor,'fcor',dim6,3)
end;

procedure angles (dim5,dim6,nstruct,ninc:integer);
var
    i,j:integer;
    x,y:real;
    angle,geom:array2type;

begin

    din2(geom,'geom',dim6,dim5);

    for i:=1 to nstruct do begin
        for j:=1 to ninc do begin
            y:=(geom[(2*i),(2*j)]-geom[(2*i)-1,(2*j)]);
            x:=(geom[(2*i),(2*j)-1]-geom[(i*2)-1,(2*j)-1]);
            angle[i,j]:= arctan(y/x);
            if angle[i,j] >(pi/2) then
                angle[i,j]:= (angle[i,j]-pi);
            end
        end;
        writeln('Calculating ligament lines of action!');
        dout2(angle,'angle',ninc,nstruct)
    end;

end;

procedure jangles (dim6,ninc:integer;runid:ident);

var
    i:integer;
    angle,arch,jtangle:arraytype;

```

```

fcor:array2type;

begin

  din2(fcor,'fcor',dim6,3);
  din(arch,'arch',ninc);

  for i:=1 to ninc do begin
    angle[i]:= ((arctan(fcor[1,(2*i)-1]/arch[i]))+
      (arctan(fcor[2,(2*i)-1]/arch[i])))-
      ((arctan(fcor[1,1]/arch[1]))+
      (arctan(fcor[2,1]/arch[1]))));
    angle[i]:= angle[i]*(180/pi)
  end;
  writeln('Calculating deformation angles!');
  res(angle,runid,'jan',ninc)
end;

procedure ligstr (dim5,dim6,ninc,nstruct:integer; runid:ident);

var
  i,j:integer;
  geom,straings:array2type;

begin
  din2(geom,'geom',dim6,dim5);

  for i:=1 to nstruct do begin
    for j:=1 to ninc do
      strains[i,j]:= 100*((sqrt(sqrt(geom[(2*i)-1,(j*2)-1])-geom[(2*i),(j*2)-1]) +
        sqrt(geom[(2*i)-1,(j*2)]-geom[(2*i),(j*2)])))/
        sqrt(sqrt(geom[(2*i)-1,1]-geom[(2*i),1]) +
        sqrt(geom[(2*i)-1,2]-geom[(2*i),2])))
        -1);
    end;
    writeln('Calculating ligament strains!');
    res2(strains,runid,'str',ninc,nstruct)
  end;
end;

procedure support (dim6,dim3,dim4,ninc,nstruct:integer; runid:ident);

var
  i,j:integer;
  fcor,force,react:array2type;
begin

  din2(fcor,'fcor',dim6,3);
  getlod(dim4,ninc,force);

  for i:=1 to dim4 do begin
    for j:=1 to ninc do begin
      react[((i*2)-1),j]:= (force[i,j]*(fcor[2,(2*j)-1]-fcor[3,(2*j)-1]))/
        (fcor[2,(2*j)-1]-fcor[1,(2*j)-1]);
      react[(i*2),j]:= force[i,j]-react[((i*2)-1),j]
    end;
  end;
  writeln('Calculating ground reaction loads!');
  dout2(react,'react',ninc,dim3);

```

```

    res2(react,runid,'sup',ninc,dim3);
    dout2(force,'force',ninc,dim4)
end;

procedure moments (dim4,dim3,dim6,ninc:integer;runid:ident);

var
    i,j:integer;
    mom,force,fcor,react:array2type;

begin

    din2(force,'force',ninc,dim4);
    din2(react,'react',ninc,dim3);
    din2(fcor,'fcor',dim6,3);

    for i:=1 to dim4 do begin
        for j:=1 to ninc do
            mom[i,j]:={ -(react[i,(j*2)-1])*fcor[i,(j*2)-1]) +}
                (force[i,j]*fcor[3,(j*2)-1]) -
                (react[(i*2),j])*fcor[2,(j*2)-1]);
        end;
        writeln('Calculating moment matrix');
        dout2(mom,'mom',ninc,dim4);
        res2(mom,runid,'mom',ninc,dim4)
    end;

procedure tension (dim4,dim5,dim6,nstruct,ninc:integer;runid:ident);

var
    i,j:integer;
    mom,geom,angle,tens:array2type;
    arch:arraytype;

begin

    din2(geom,'geom',dim6,dim5);
    din2(mom,'mom',ninc,dim4);
    din2(angle,'angle',ninc,nstruct);
    din(arch,'arch',ninc);

    for i:=1 to nstruct do begin
        for j:=1 to ninc do
            tens[i,j]:= {(mom[(i+1),j]-mom[i,j])/
                (((arch[j]-geom[(i*2)-1,(j*2)])*cos(angle[i,j])) +
                (geom[(i*2)-1,(j*2)-1]*sin(angle[i,j])) -
                ((arch[j]-geom[(i*2),(j*2)])*cos(angle[i,j])) -
                (geom[(i*2),(j*2)-1]*sin(angle[i,j]))));}
                -(mom[(i+1),j]-mom[i,j])/
                ((arch[j]-geom[(i*2),(j*2)])*cos(angle[i,j])) +
                (geom[(i*2),(j*2)-1]*sin(angle[i,j])));
        end;
        writeln('Calculating ligament tensions!');
        dout2(tens,'tens',ninc,nstruct);
        res2(tens,runid,'tens',ninc,nstruct)
    end;

BEGIN (* Main program*)

```

(\* This section gets runid and gets no.strucyures and increments\*)

```
clrscr;
write('Enter No. of structures in model: ');
readln(nstruct);{nstruct:=4;writeln;}
write('Enter No. of analysis increments: ');
readln(ninc);{ninc:=11}writeln;
write('Enter No. of force application points: ');
readln(nfapp){nfapp:=3}writeln;
write('Enter base co-ordinates of TT joint: ');
read(xjt,yjt);readln;writeln;
write('Enter run identifier: ');
readln(runid);writeln;writeln;
writeln;
```

(\* This section defines the solution matrix dimensions\*)

```
dim1:=nstruct;
dim2:=4*nstruct;
dim3:=2*(nstruct+1);
dim4:=nstruct+1;
dim5:=2*nstruct;
dim6:=2*ninc;
```

(\* Procedure calls for solving subroutines\*)

```
geometry(xjt,yjt,dim1,dim5,dim6,nfapp,ninc);
angles(dim5,dim6,nstruct,ninc);
jangles(dim6,ninc,runid);
ligstr(dim5,dim6,ninc,nstruct,runid);
support(dim6,dim3,dim4,ninc,nstruct,runid);
moments(dim4,dim3,dim6,ninc,runid);
tension(dim4,dim5,dim6,nstruct,ninc,runid);
```

(\* End of program \*)

```
writeln('*****');
writeln('***** END OF RUN *****');
writeln('*****');
```

```
repeat
until keypressed;
```

END.

# APPENDIX 11. LIGAMENT FORCES AND STRAINS PREDICTED BY MATHEMATICAL MODELLING

## A11.1 LIGAMENT FORCES

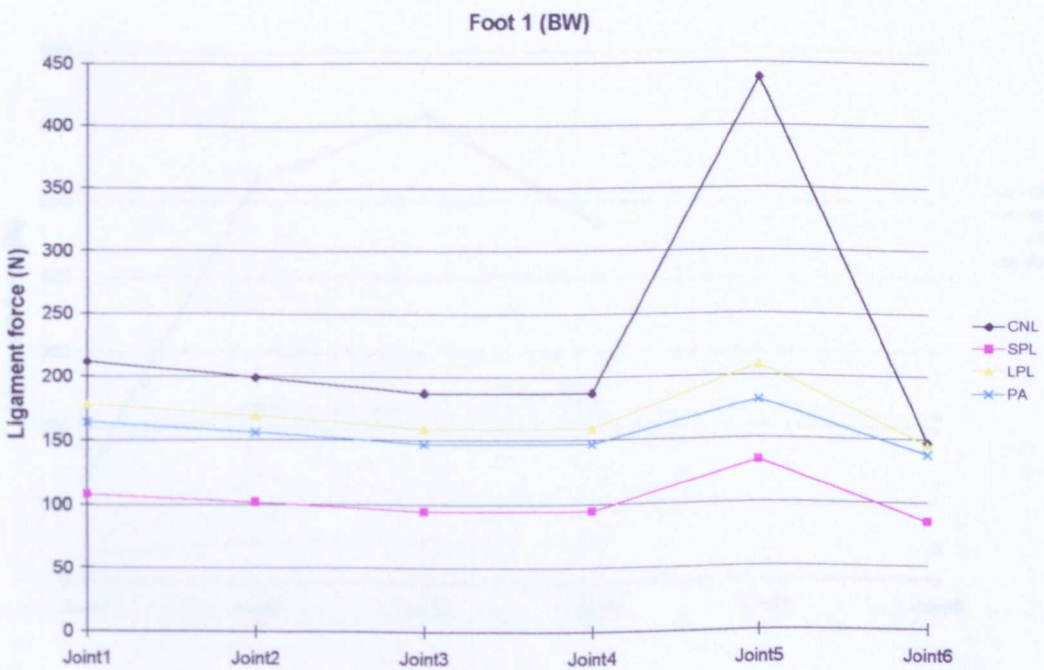
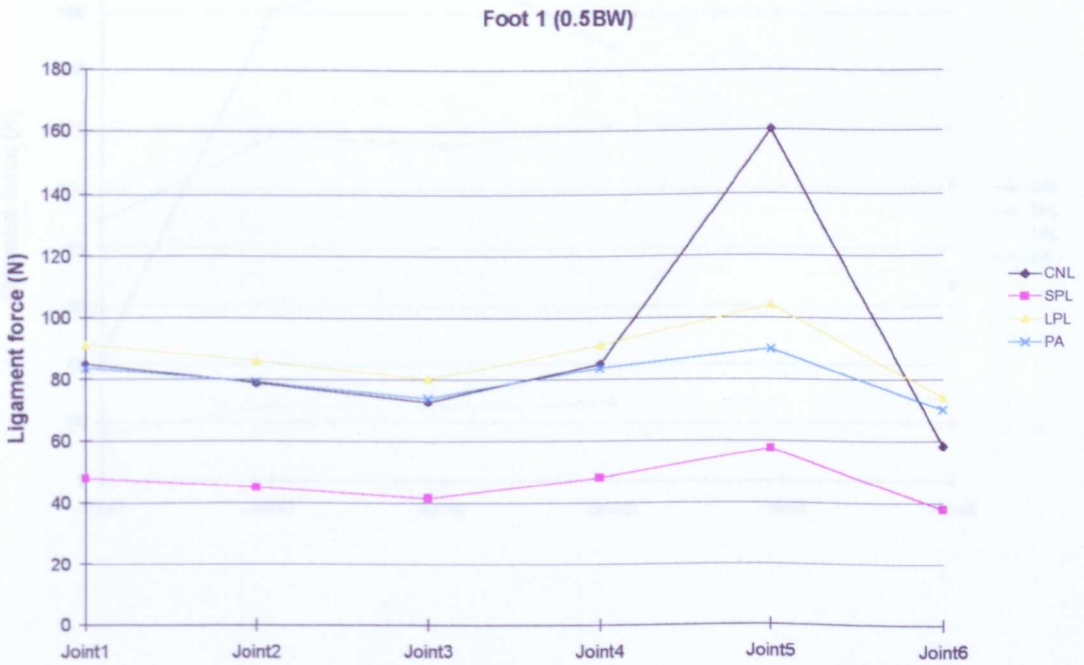
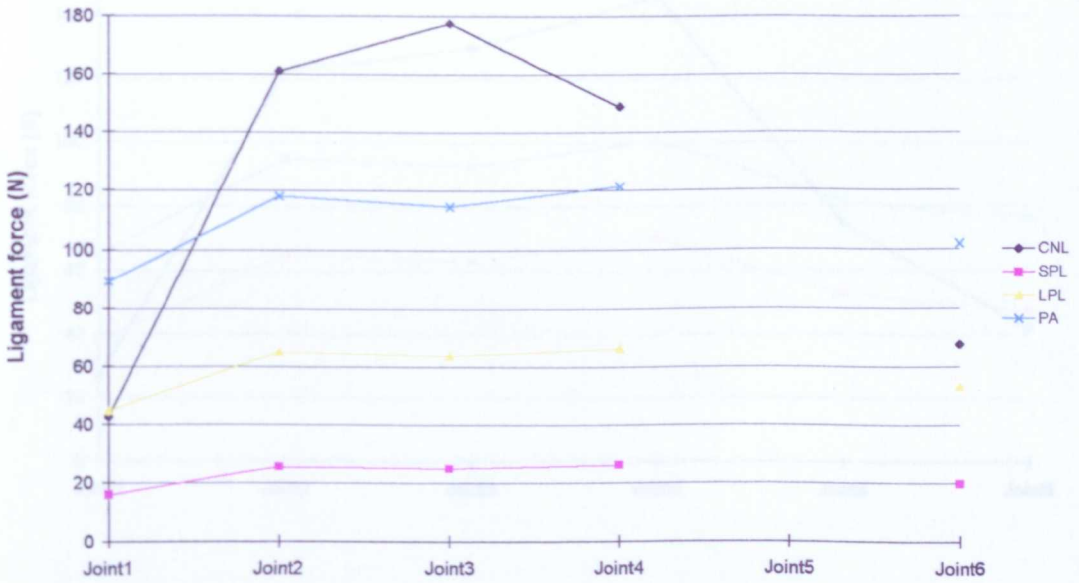


Figure A11.1 Ligament forces calculated in the foot model at 0.5BW and BW for foot 1.

Foot 2 (0.5BW)



Foot 2 (BW)

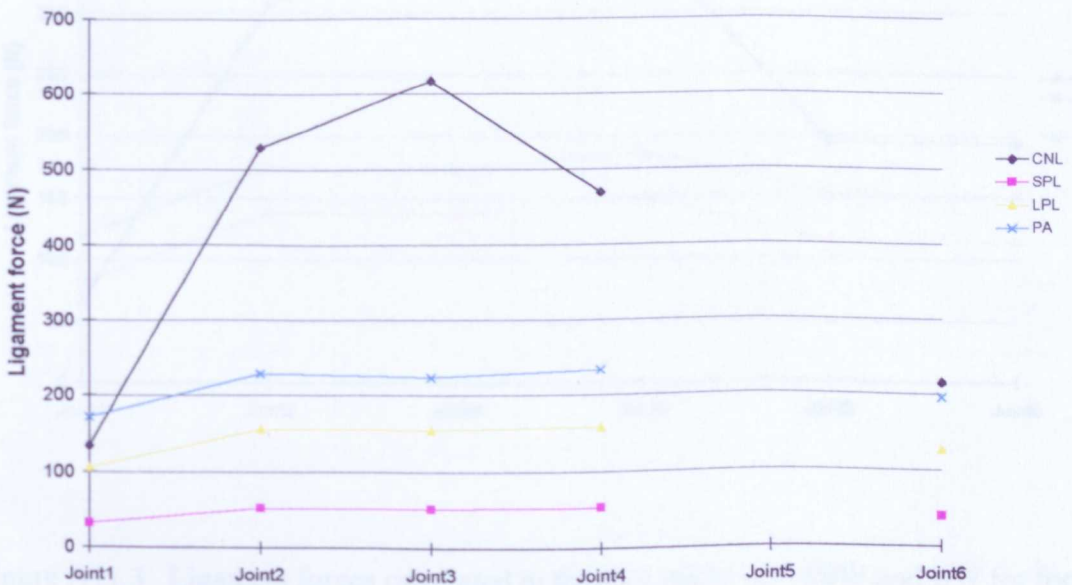
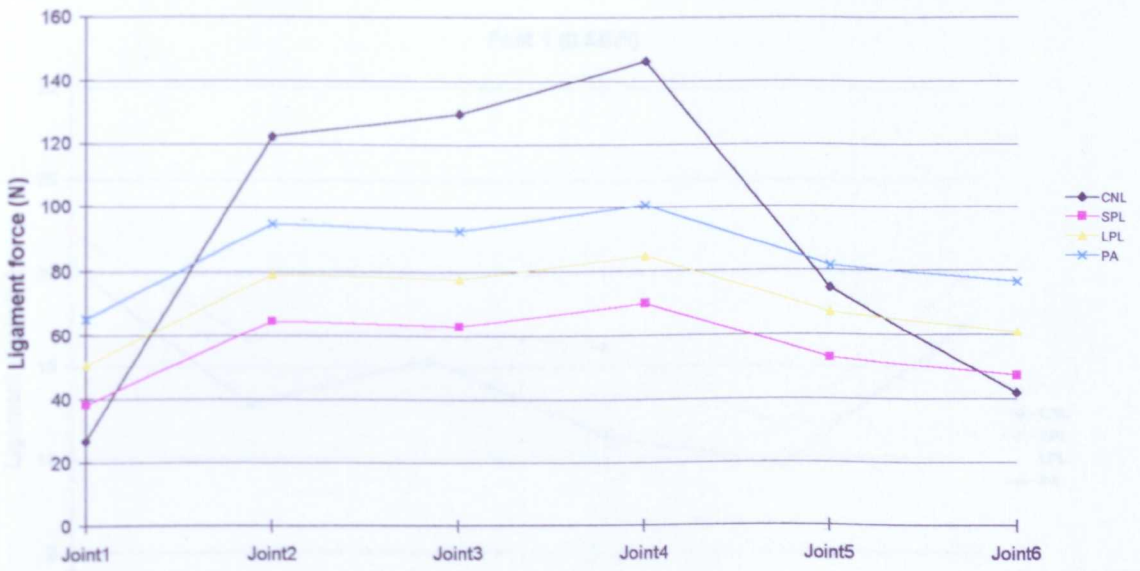


Figure A11.2 Ligament forces calculated in the foot model at 0.5BW and BW for foot 2.

Foot 3 (0.5BW)



Foot 3 (BW)

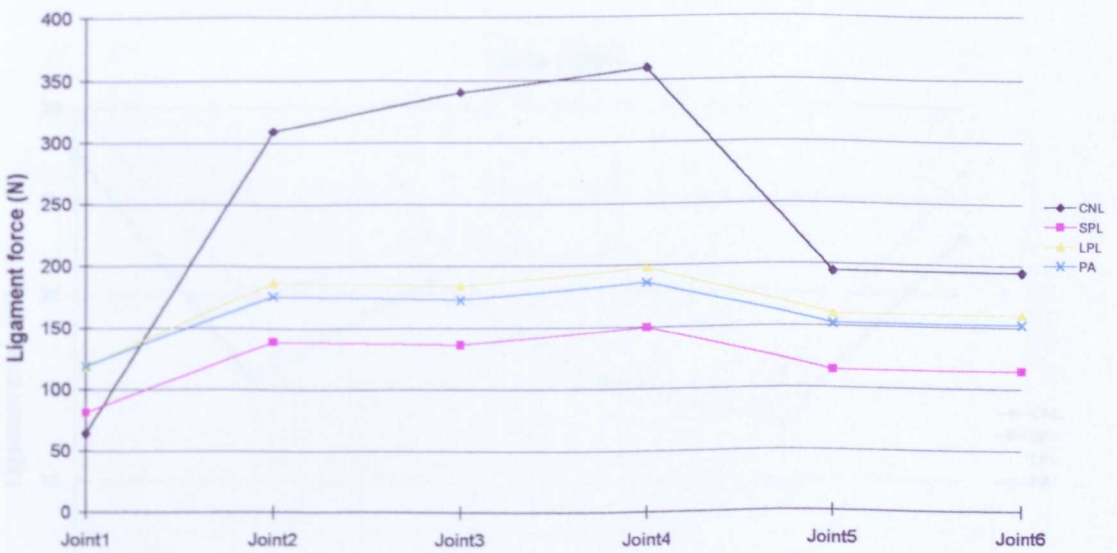


Figure A11.3 Ligament forces calculated in the foot model at 0.5BW and BW for foot 3.

## A11.2 LIGAMENT STRAINS

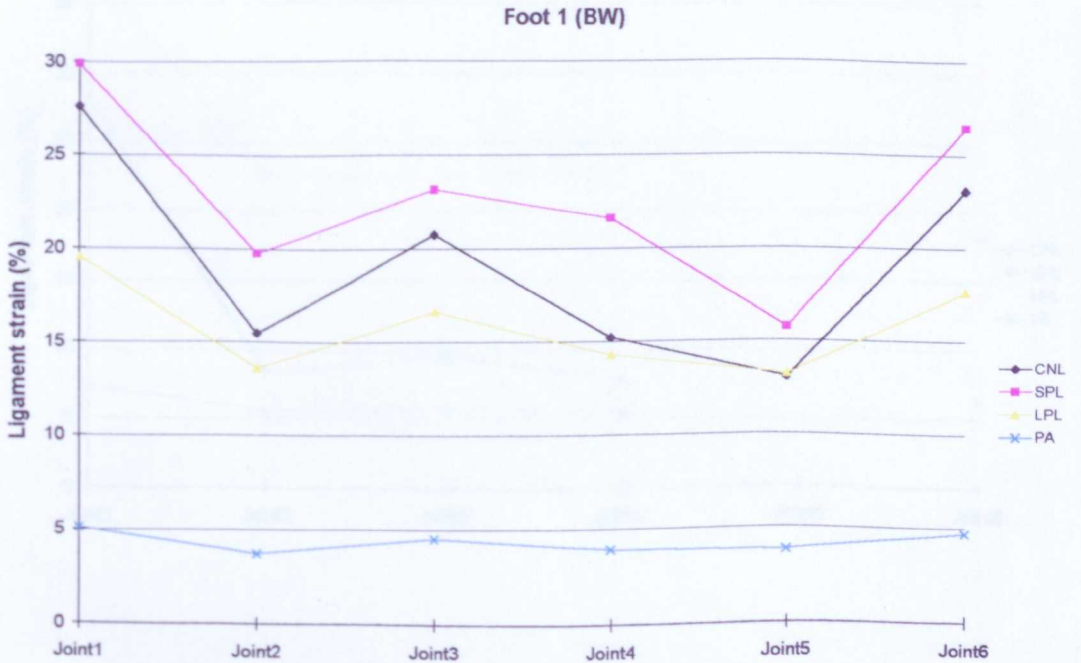
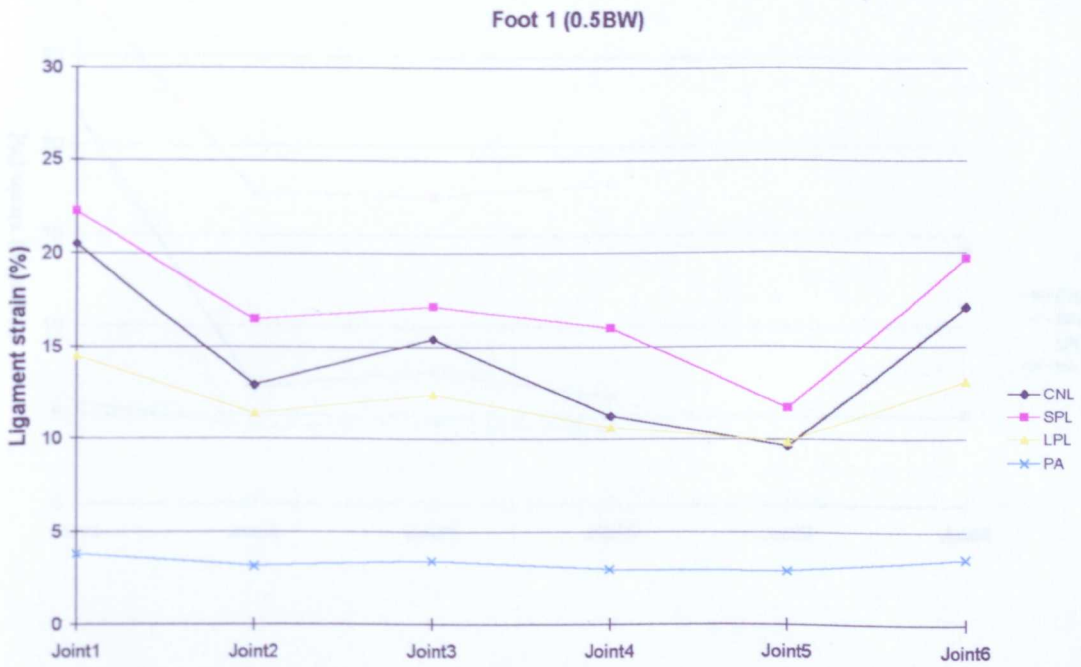


Figure A11.4 Ligament strains calculated in the foot model at 0.5BW and BW for foot 1.

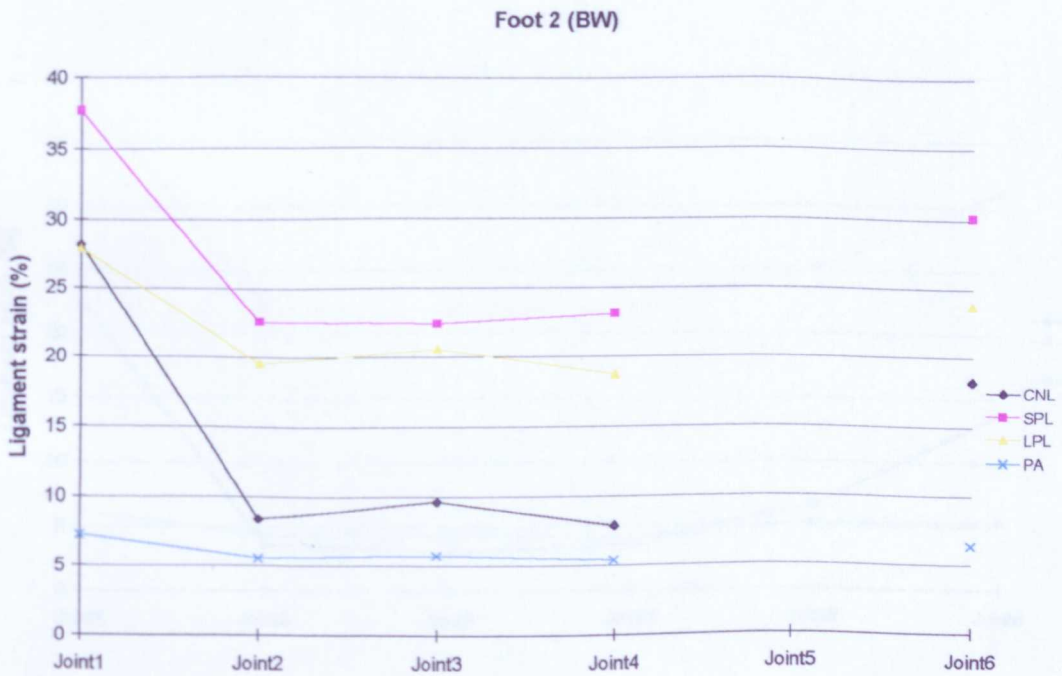
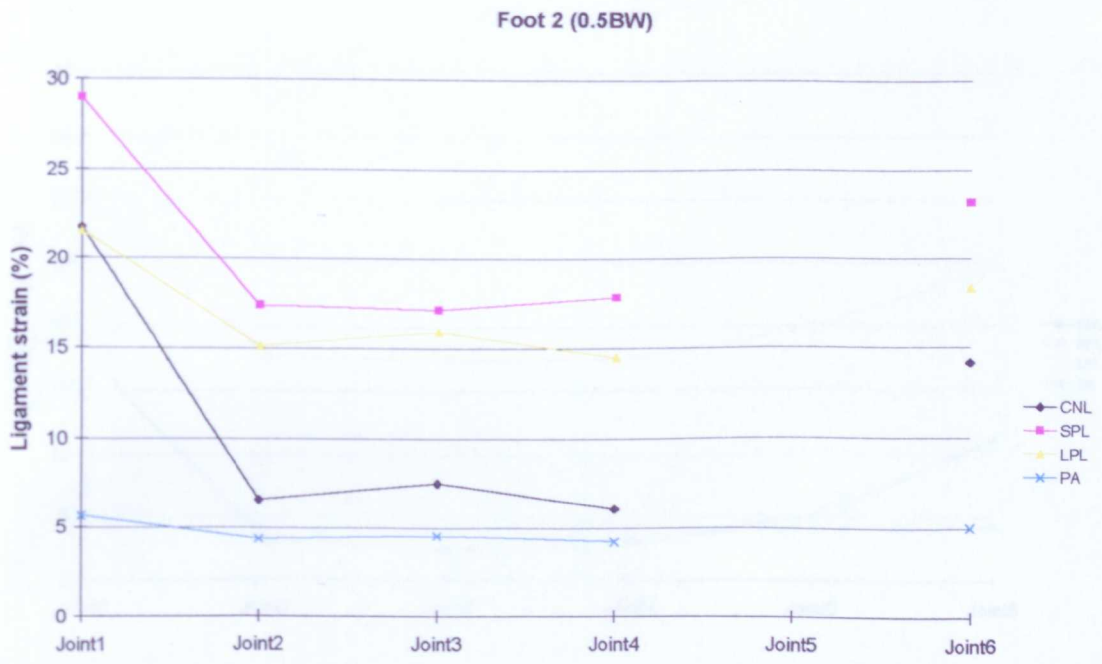
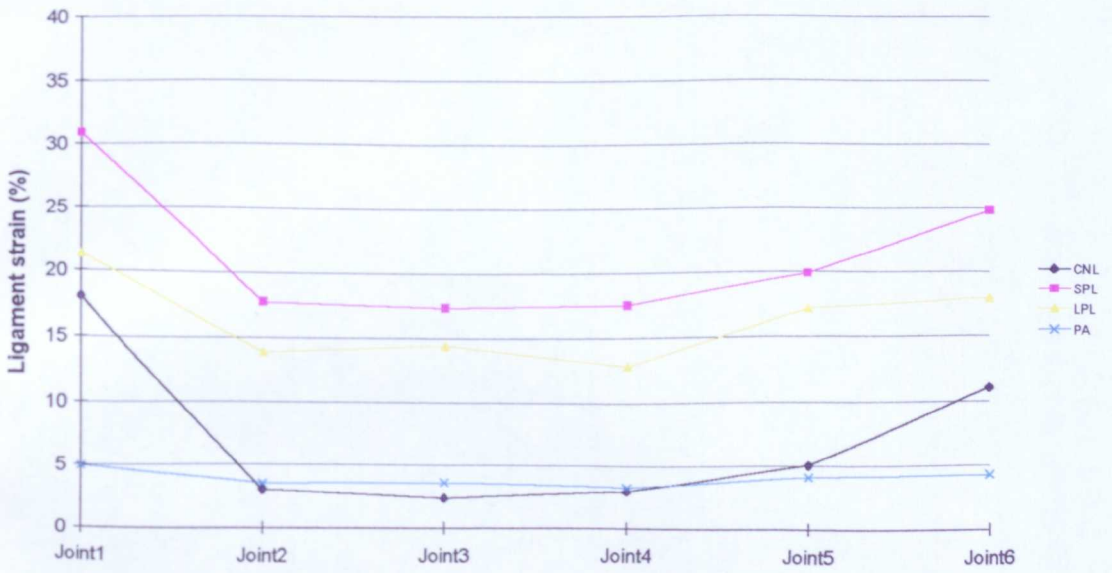


Figure A11.5 Ligament strains calculated in the foot model at 0.5BW and BW for foot 2.

Foot 3 (0.5BW)



Foot 3 (BW)

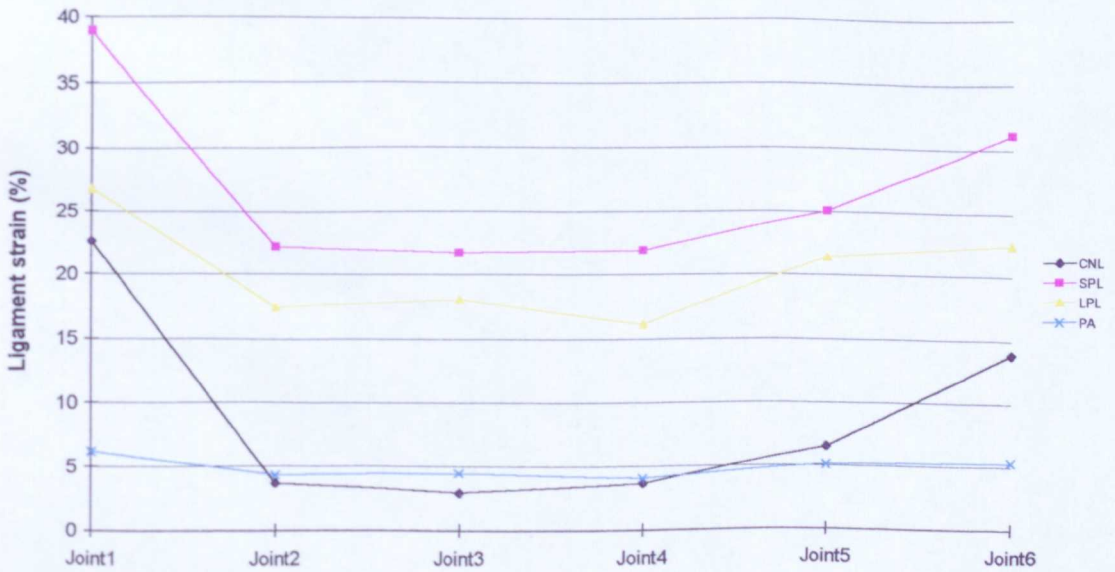


Figure A11.6 Ligament strains calculated in the foot model at 0.5BW and BW for foot 3.